Process Development for Fabrication of Silicon Semiconductor Devices in a Low Gravity, High Vacuum, Space Environment

by

Nicholas Pfeiffer

B.A.Sc. University of British Columbia, 1988

A THESIS SUBMITTED IN PARTIAL FULFILLMENT
OF THE REQUIREMENTS FOR THE DEGREE OF
MASTER OF APPLIED SCIENCE
IN THE SCHOOL OF ENGINEERING SCIENCE

SIMON FRASER UNIVERSITY

December 2000

Approval

Name: Nicholas Pfeiffer

Degree: Master of Applied Science

Title of thesis: Process Development for Fabrication of Silicon Semiconductor Devices in a Low Gravity, High Vacuum, Space Environment

Examining Committee:

Dr. Shahram Payandeh, Chairperson

Dr. Glenn Chapman, Senior Supervisor

Dr. John Jones, Supervisor

Dr. Ash Parameswaran, Examiner

Date Approved: December 11, 2000

Abstract

Semiconductor microchips are high value per mass products whose fabrication requires many of the resources available in low-Earth orbit. It is hypothesized that orbital fabrication of silicon microchip devices may be more economically attractive than traditional Earth-based fabrication based upon the inherent advantages of the space environment: vacuum, cleanliness, and microgravity.

This thesis examines the feasibility of fabricating semiconductor devices in near-Earth orbit through the use of process and economic models. The semiconductor fabrication processes are represented in a detailed, step-by-step, numerical model which uses mass flow, thermodynamics and other operational calculations to create models of important process operational parameters. Wherever possible, these calculations are verified either with measurements or published literature data on existing systems. Advantages of this approach are the ability to easily add new processes and to determine energy, consumable, time, and equipment requirements for each process step. As a confirmation of accuracy, the process flow for a standard 12 level CMOS device is modeled and the generated results are comparable to published literature values.

Handling of 37 gram, 200 mm diameter by 0.5 mm thick silicon wafers cannot be accomplished in a high vacuum environment with the vacuum suction method used on Earth. A system for the transport and fixturing of wafers in the orbital environment, in which non-contact forces are exerted on the wafer in six degrees of freedom through magnetic levitation, is modeled in this thesis.

It is found that by developing new, dry processes that are vacuum compatible, fabricating semiconductor devices in orbit is both technically and economically feasible. The outcome is a synergistic, orbital-based methodology for micro-

fabrication capable of building and delivering commercially marketable microfabricated structures. The base case modeled, production of 5,000 ASIC wafers per month, indicates that orbital fabrication is 103% more expensive than existing commercial facilities. However, optimization of process parameters and consumable requirements is shown to decrease the cost of orbital fabrication dramatically. Modeling indicates that the cost of orbital fabrication can be decreased to 58% that of an advanced, future Earth-based facility when trends of increasing process equipment costs and decreasing orbital transport costs are considered.

Acknowledgements

The author would like to thank Dr. Glenn Chapman of Simon Fraser University for his encouragement and support during this project and Jeff Johnson of Boeing Advanced Space & Communications for the reviews by him and his associates of many of the concepts developed in this project.

This work was supported in part by the Natural Sciences and Engineering Research Council of Canada and Simon Fraser University.

Table of Contents

List of Figures

List of Tables

List of Symbols

Symbol	Description	Defining Section
a	radius of circular current loop	4.4.1
A	surface area	4.5.1
$\mathbf{a}$	acceleration	4.8
$\bar{a}_r$	average radial acceleration	4.8
$\bar{a}_z$	average axial acceleration	4.8
$\mathbf{B}$	magnetic field	4.4.1
b	radius of eddy current loop	4.5
$\mathbf{B_0}$	magnetic field due to solenoid current loops	4.5.1
$\mathbf{B_{0end}}$	magnetic field due to magnetic charge on a single solenoid end	4.6.1
B_{0z}	axial component of magnetic field due to solenoid current loops	4.6.1
$\mathbf{B_c}$	magnetic field for circular solenoid array	4.6.1
B_{cr}	radial component of magnetic field for circular solenoid array	4.6.2
B_{cz}	axial component of magnetic field for circular solenoid array	4.6.2
$\mathbf{B_l}$	magnetic field for linear solenoid array	4.7.1
$\mathbf{B_m}$	magnetic field due to magnetization of solenoid ferromagnetic core	4.5.1
$\mathbf{B_{mend}}$	magnetic field for solenoid end	4.5.1
B_r	radial component of the magnetic field	4.4.1
$\mathbf{B_s}$	solenoid external magnetic field	4.5.1
B_z	axial component of the magnetic field	4.4.1
c	radius of solenoid circle in circular solenoid array	4.6.2
C	piping conductance	5.7.1.7

Symbol	Description	Defining Section
C_2	pipe conductance between the outlet of turbo molecular pump and inlet of roughing pump	5.7.1.7
C_c	consumable cost	8.2
$C_{capsule}$	capsule cost	8.9
C_d	depreciation cost	8.2
C_{down}	cost to return goods to Earth	8.9
$C_{equipfacility}$	capital cost of equipment and facility	8.10.1
C_{fixed}	fixed cost of equipment and facilities	8.2
$C_{fixeddown}$	fixed cost to retrieve a single return capsule	8.9
$C_{fixedup}$	fixed cost to perform a single launch	8.9
c_{gas}	cost of consumable gas per unit mass	8.10.4
c_h	heat rejection operating cost	8.10.2
C_i	specific heat of consumable *i*	5.7.2
c_{liquid}	cost of consumable liquid per unit mass	8.10.4
C_m	maintenance cost	8.2
C_{mask}	cost of single mask	8.10.4
C_o	operating cost	8.2
$_o$	operating cost per unit wafer	8.2
$C_{ownership}$	cost-of-ownership per wafer produced	8.2
c_p	power generation operating cost	8.10.2
$C_{roughpump}$	cost of roughing pump	5.7.1.4
$c_{roundtriptotal}$	round trip transportation cost per unit mass of finished goods	8.9
C_s	shipping cost	8.2
c_{solid}	cost of consumable solid per unit mass	8.10.4
$C_{totalequipfacility}$	total installed capital cost of equipment and facility	8.10.1
$C_{turbopump}$	cost of turbomolecular pump	5.7.1.4
C_u	utilities cost	8.2
C_{up}	cost to launch goods to orbit	8.9

Symbol	Description	Defining Section
c_{up}	incremental launch cost per unit mass	8.9
$C_{variable}$	variable cost to operate facility	8.2
C_{wafer}	wafer specific heat	5.7.2
C_{wafer}	cost of single wafer	8.10.4
$C_{yieldloss}$	cost due to yield loss	8.2
d	distance between current filament loops in solenoid, diameter of conductor in solenoid	4.5.1
d	pipe diameter	5.7.1.7
$Dose$	implant dose per unit area	5.7.2
dt	time step	5.7.1.7
dV	volume of gas removed from the vacuum chamber in timestep dt	5.7.1.7
E	energy	5.7
E_{doping}	energy required to dope wafer using ion implantation	5.7
ΔE_{doping}	incremental energy (energy per wafer) required to dope wafer using ion implantation	5.7
E_{ion}	energy of single ion	5.7.2
$E_{material}$	energy required to raise consumables to process temperature	5.7
$\Delta E_{material}$	incremental energy (energy per wafer) required to raise consumables to process temperature	5.7
$E_{processing}$	energy required for processing	5.7
$\Delta E_{processing}$	incremental energy (energy per wafer) required for processing	5.7
$E_{processstep}$	energy for single process step	5.7
$E_{pumpdown}$	energy required to pumpdown chamber	5.7
$\Delta E_{pumpdown}$	incremental energy (energy per wafer) required to pumpdown chamber	5.7
E_{wafer}	energy required to raise wafers to process temperature	5.7

Symbol	Description	Defining Section
ΔE_{wafer}	incremental energy (energy per wafer) required to raise wafers to process temperature	5.7
$\mathbf{F}$	force	4.4.1
f	solenoid waveform frequency	4.5
$f_{capsule}$	fractional capsule cost rate	8.9
f_{dep}	annual depreciation rate	8.10.1
$f_{downmatl}$	mass fraction of raw materials that are finished goods	8.9
f_{fixed}	ratio of fixed cost to retrieve a single return capsule to the fixed cost to perform a single launch	8.9
$f_{install}$	installation cost fraction (% of first cost)	8.10.1
f_{launch}	launch fraction	8.9
f_{maint}	annual maintenance cost fraction (% of total installed capital cost)	8.10.3
$\mathbf{F_p}$	instantaneous force at a point on eddy current loop due to the external magnetic field	4.7.1
$f_{payload}$	return capsule payload ability (mass fraction of the total return mass that consists of payload)	8.9
$\overline{F}_r$	average radial force	4.6.3
f_{updown}	non-dimensional fraction of fixed launch costs	8.9
F_x	x component of instantaneous force	4.7.1
$\overline{F}_x$	x component of average force	4.7.1
F_{xp}	x component of F_p	4.7.1
F_y	y component of instantaneous force	4.7.1
$\overline{F}_y$	y component of average force	4.7.1
F_{yp}	y component of F_p	4.7.1
F_z	instantaneous axial force	4.7.1
$\overline{F}_z$	average axial force	4.7.1
F_{zp}	z component of F_p	4.7.1

Symbol	Description	Defining Section
$\mathbf{H}$	magnetic field	4.4.1
H	heat rejection	8.10.2
i	current	4.4.1
i	index for consumable	5.7
i	index for equipment	8.5
i_e	induced current	4.5.2
i_s	solenoid current	4.5.2
i_{si}	current of inner solenoid in solenoid array	4.6.2
i_{smax}	maximum solenoid current	4.5.2
i_{so}	current of outer solenoid in solenoid array	4.6.2
j	number of outer solenoids in circular solenoid array	4.6.2
K_1	loss coefficient for pump orifice	5.7.1.6
K_2	pump power loss factor	5.7.1.6
$\mathbf{l}$	length	4.4.1
L	inductance	4.4.1
l	solenoid length	4.5.2
l	pipe length	5.7.1.7
l	number of layers used to fabricate wafer	8.3
L_s	solenoid inductance	4.5.2
$\mathbf{M}$	magnetization	4.4.1
m	mass	4.8
m_{down}	mass returned to Earth	8.9
$m_{equipfacility}$	mass of equipment and facility	8.10.1
m_{gas}	mass of consumable mass per level per wafer	8.10.4
m_i	mass of consumable i	5.7
Δm_i	incremental mass (mass per wafer) of consumable i	5.7
$\dot{m}_i$	mass flow of consumable i during processing	5.7.3.1
m_{liquid}	mass of consumable liquid per level per wafer	8.10.4

Symbol	Description	Defining Section
m_{mask}	mass of single mask	8.10.4
$m_{payload}$	mass of capsule payload	8.9
$m_{processstep}$	mass of consumables for single process step	5.7
$m_{roughpump}$	mass of roughing pump	5.7.1.4
m_{solid}	mass of consumable solid per level per wafer	8.10.4
$m_{turbopump}$	mass of turbomolecular pump	5.7.1.4
m_{up}	mass launched to orbit	8.9
m_{wafer}	wafer mass	5.7.2
$m_{wafermatl}$	raw material mass per wafer	10.4.1
MW_i	molecular weight of consumable *i*	5.7.3.2
N	number of turns of conductor in solenoid	4.5.1
n	number of moles in chamber	5.7.1.7
Δn	change in number of moles of consumables	5.7.3.2
n_{down}	number of wafers produced in return period	10.4.7
n_{equip}	number of pieces of critical (non-redundant) equipment	10.4.6
n_i	quantity of equipment of type *i*	5.7.3.2
Δn_i	change in number of moles of consumable *i*	5.7.3.2
$n_{maskset}$	number of wafers produced per mask set	8.3
$n_{processstep}$	number of wafers in process batch	5.7
n_{uses}	number of times that capsule can be reused	8.9
n_w	number of wafers produced by the facility within specified period	8.2
p	time period	4.5.2
P	pressure	5.7.1.2
$\overline{P}$	average pressure	5.7.1.7
P	power	8.10.2
$\mathbf{P_0}$	point on conductor	4.4.1

Symbol	Description	Defining Section
P_0	starting pressure	5.7.1.2
P_0	pump exit pressure	5.7.1.6
$\mathbf{P_1}$	point in magnetic field	4.4.1
P_1	ending pressure	5.7.1.2
P_2	pump inlet pressure	5.7.1.6
P_3	pump internal pressure	5.7.1.6
P_{base}	base pressure for a process	5.7.3.2
P_c	instantaneous circular solenoid array power	4.6.3
$\overline{P}_c$	average circular solenoid array power	4.6.3
p_{down}	period between finished goods returns	8.9
P_{end}	ending pressure	5.7.1.7
P_l	instantaneous recto-linear solenoid array power	4.7.3
$\overline{P}_l$	average recto-linear solenoid array power	4.7.3
p_{maint}	predicted maintenance period	10.4.6
$p_{mtbfequip}$	period between equipment failures (mean time between failure)	10.4.6
$P_{process}$	pressure at which process occurs	5.7.3.2
P_s	instantaneous solenoid power	4.5.2
$\overline{P}_s$	average solenoid power	4.5.2
P_{start}	starting pressure	5.7.1.7
p_{up}	period between launches	8.9
q	charge	4.4.1
q	unit charge of electron	5.7.2
Q	outgassing rate	5.7.1.2
q_m	magnetic charge	4.5.1
q_{m0end}	magnetic charge due to B_{0z}	4.6.1
q_{mend}	lumped magnetic charge at end of solenoid	4.6.1
R	resistance	4.4.1

Symbol	Description	Defining Section
$\mathbf{r}$	distance vector from point on conductor to point in magnetic field	4.4.1
r	distance from solenoid longitudinal (z) axis	4.4.1
R	universal gas constant	5.7.1.7
R_1	non-dimensional ratio that represents incremental space transport costs	8.9
R_2	non-dimensional ratio that represents fixed space transport costs	8.9
r_{down}	mass rate at which finished goods are required	8.9
R_s	solenoid resistance	4.5.2
$R_{throughput}$	production rate (throughput)	8.2
r_w	production rate (wafers per time period)	8.3
$\mathbf{S}$	Surface	4.4.1
S	pump speed	5.7.1.2
S_{eff}	effective pump speed	5.7.1.7
S_{norm}	normalized pump speed	5.7.1.5
S_{rated}	rated pump speed	5.7.1.5
t	Time	5.7.1.2
$\Delta\bar{t}_i$	normalized process time for equipment of type i, (single layer average)	8.5
$\mathbf{T}$	Torque	4.7.1
T	Temperature	5.7
$T_{process}$	process temperature	5.7
$t_{processing}$	time for processing	5.7
$t_{processstep}$	time for single process step	5.7
$\Delta t_{processstep}$	incremental process time (time per wafer) for process step	5.7
$\Delta t_{processstep,i}$	incremental process time for equipment of type i	8.5
$t_{pumpdown}$	time to pumpdown vacuum chamber	5.7

Symbol	Description	Defining Section
T_{start}	starting temperature	5.7.2
T_{xy}	instantaneous torque in x-y plane	4.7.1
$\overline{T}_{xy}$	average torque in x-y plane	4.7.1
T_{xz}	instantaneous torque in x-z plane	4.7.1
$\overline{T}_{xz}$	average torque in x-z plane	4.7.1
T_{yz}	instantaneous torque in y-z plane	4.7.1
$\overline{T}_{yz}$	average torque in y-z plane	4.7.1
U	utilization of equipment	8.2
$\mathbf{v}$	velocity	4.4.1
V	chamber volume	5.7.1.2
vf_i	ratio of volume of consumable *i* to volume of all consumables	5.7.3.2
$V_{roughpump}$	volume of roughing pump	5.7.1.4
$V_{turbopump}$	volume of turbomolecular pump	5.7.1.4
$\dot{W}_{compression}$	power for compression	5.7.1.6
$\dot{W}_{mechloss}$	power for mechanical losses	5.7.1.6
$\dot{W}_{processing}$	power for processing	5.7.1.6
$\dot{W}_{roughpump}$	power for roughing pump	5.7.1.6
$\dot{W}_{turbopump}$	power for turbo pump	5.7.1.6
x	x coordinate	4.7.1
y	y coordinate	4.7.1
Y	average yield of the entire process	8.2
$Y_{mechloss}$	yield due to mechanical losses during production	8.2
z	z coordinate	4.7.1
e	emf	4.4
e_{sr}	error fraction of radial component of magnetic field	4.6.1

Symbol	Description	Defining Section
e_{sz}	error fraction of axial components of magnetic field	4.6.1
h_{motor}	motor efficiency	5.7.1.6
m	magnetic permeability	4.4.1
m_0	magnetic permeability of vacuum	4.5
r	gas density	5.7.1.6
Φ_B	magnetic flux	4.4.1
χ	magnetic susceptibility	4.4.1

Foreword

This thesis is intended for two types of readers: those with a background in semiconductor fabrication who wish to explore the feasibility of producing semiconductor devices in orbit, and those with an aerospace background who wish to examine the possibility of implementing semiconductor processes in space. Thus, some of the material in this thesis is of an introductory nature, intended to provide the reader with basic concepts, in advance of the detailed work that follows.

Chapter 1
Introduction

1.1 General

This thesis is a first-pass feasibility analysis of fabricating semiconductor devices in near-Earth orbit. It is intended to find the obvious advantages and disadvantages of such manufacturing, as well as detecting current problems and determining possible solutions.

Both technical and economic factors are examined to determine the viability of a space-based semiconductor fabrication facility. It is postulated that orbital fabrication of silicon devices may be more economically attractive than traditional Earth-based fabrication based upon the inherent advantages of the space environment. However, thus far, space-based manufacturing has not proven competitive due to the high cost of material transport. It is hypothesized that the best case for space-based manufacturing can be made when the intrinsic processing cost is high and the mass of material low. Such is the case for semiconductor fabrication where fabricated 40 gram silicon wafers can reach values in excess of $5,000[i].

This chapter will introduce the twin topics of semiconductor fabrication and space-based manufacturing; subsequent chapters will cover these subjects in detail. The chapter will conclude with an outline of the remainder of the thesis chapters.

1.2 Background

The electronics industry is the world's largest manufacturer with $222 billion forecast for 2001[1]. The equipment utilized in semiconductor fabrication is expensive,

[i] all amounts shown in US dollars (USD)

requiring large capital investments up to $2 billion per new facility. This large capital requirement leads to ongoing operational costs due to equipment depreciation, forming a significant fraction of semiconductor wafer processing costs.

Starting material for microfabrication is usually a silicon wafer, a flat thin disk or other substrate, typically 150 to 300 mm in diameter by 0.5 to 0.6 mm thick. Microfabricated devices are created by the deposition and patterning of typically between 4 and 30 layers of thin films on these substrates. Smaller feature geometries and advances in state-of-the-art wafer fabrication techniques are leading to greater use of high vacuum processes and to requirements for improved cleanliness in wafer fabrication facilities, both of which increase fabrication costs.

Traditionally, semiconductor fabrication has been performed in dedicated, specialized facilities. These facilities provide clean environments for the wafer fabrication, process equipment, as well as support equipment and administrative facilities. The capital cost of modern fabrication facilities is now approaching $2 billion and growing at 20% per year.

The high cost of such facilities is prompting a review of the processes traditionally employed in wafer fabrication. The large, single clean room is giving way to equipment that integrates a built-in clean environment, and batch processing is being replaced by clusters of single wafer processing equipment[2]. In addition, increasingly stringent environmental regulations are causing the use of water for wafer cleaning to be curtailed, while concerns over global warming and pollution are restricting the use of many types of consumables[3].

Many semiconductor fabrication processes operate in a rarified vacuum environment, with gas pressures significantly below that of the atmosphere[4]. A space environment, such as that found in orbit around the Earth, can provide the high vacuum, clean environment needed for semiconductor fabrication. The ambient vacuum in low Earth orbit exceeds nearly all of the routine requirements for

semiconductor wafer processing and the low particle count provides an exceptionally clean environment for wafer fabrication and storage. Much of the support equipment, such as vacuum pumping systems, required for terrestrial fabrication is not required for space-based fabrication. Similarly, the inherently clean nature of the environment reduces the need for cleaning steps between separate wafer fabrication processes.

Wafer fabrication in a vacuum environment, such as found in Earth orbit, is inherently clean but requires changes in some basic processes. Liquid chemical-based cleaning processes, such as commonly employed in traditional semiconductor fabrication facilities, can not be used in a vacuum environment and must be replaced by vacuum-based, dry processes such as ion milling and plasma etching. The use of vacuum pickups and gravity assist for wafer handling and transport can not be used in space and an alternative magnetic levitation system, based upon inducing wafer eddy currents, is being researched. Spin-on coatings of volatile, organic photoresist, used in optical lithography for pattern definition on the wafer, can not be used in a vacuum environment, but sputter deposited coatings of inorganic materials for vacuum based, high resolution, thermal lithography appear to be a feasible alternative. Furthermore, the mass of material used for wafer fabrication must be minimized in orbital processing.

This thesis creates a computer model that enables the researcher to look at various proposed process flows for semiconductor fabrication, both on Earth and in space, and calculate such important parameters as consumable material masses, power, time, equipment, and costs. Proposed vacuum-based, dry process flows are developed specifically for space-based processing. Using this model, semiconductor fabrication flows are modeled for several devices (e.g. a 12 level, 2 metal CMOS) with both current Earth-based and space-based procedures. This model is providing supporting details in a preliminary exploration of a space-based semiconductor processing facility by Boeing that is being done in conjunction with this work.

Wafers must be moved from process to process during fabrication. As part of this thesis research, a system has been developed to allow the handling of large silicon wafers in a low gravity, vacuum environment using magnetically induced eddy currents. In this system, a pre-processing step is used to create circuit loops on the back side of the wafer. A time varying external magnetic field, applied by electromagnets embedded in wafer pickup and transport devices, is used to induce eddy currents in the circuit loops on the wafer. The strength and direction of these eddy currents is in direct relation to the rate of change and intensity of the external magnetic field. The eddy currents generate a counter magnetic field that is phase shifted with respect to the external field. The two magnetic fields cause a force to be exerted on the wafer at the location of the circuit loop. Control of the intensity and rate of change of the external magnetic field allow both attractive and repulsive forces to be generated. The use of multiple circuit loops located on the backside of the wafer allow for forces generated at individual circuit loops to be combined to create translational and rotational forces on the wafer, allowing six degrees of freedom of movement. Such a system can be used for both wafer transport between processes and fixturing of the wafer within process equipment.

Silicides are an excellent candidate for use as conductors to form the eddy current circuit loops on the back side of silicon wafers. Most silicides are low resistance conductors that are unaffected by the high temperatures found in downstream wafer processing steps. These silicides can be formed using a variety of processes such as laser induced chemical vapor deposition and sputtering with annealing and, once formed, do not affect the properties of the wafer for subsequent processing. A laser induced chemical vapor deposition system may be able simultaneously deposit and anneal tungsten silicides to form thick conductors. Such a system would have the ability to direct-write the circuit patterns on the wafer in a single pre-processing step and would be compatible with a low gravity, high vacuum

environment. The detailed laser deposition work, however, is beyond the scope of this thesis and will be carried on in a subsequent doctoral thesis continuing this work.

In current Earth-based fabrication facilities the depreciation of capital equipment accounts for a large fraction of the total wafer production cost. Projected equipment first costs for semiconductor fabrication in orbit may be lower than Earth-based equipment costs as many support systems such as vacuum pumps and associated systems are not required and many of the processes require less equipment in space. However, the transportation and installation costs for space-based equipment are significantly higher than those on Earth due to the high cost of launching equipment and supplies into orbit. These higher installed equipment costs lead to higher depreciation and higher operating costs for semiconductor fabrication in space.

The National Aeronautics and Space Administration (NASA) has determined that the infrastructure for transportation to and from Earth orbit must be improved if commercial utilization of space for production purposes is to take place. There are a number of initiatives aimed at reducing both the launch costs and the turnaround times. This is expected to directly reduce the projected cost of wafer fabrication in orbit. This thesis does a preliminary analysis of the implications of these previously seldom studied transportation needs, combined with the process modeling estimates on consumables and equipment, to create a first pass economic analysis of the operating costs of a space-based semiconductor fabrication facility.

The mode of transportation to and from an orbital semiconductor fabrication facility directly affects the wafer production costs. Semiconductor fabrication is relatively unique in that the mass and volume of the finished products is small compared with the product value. The amount of raw materials required to produce the finished products is also small. However, for many wafer customers, such as those producing devices using application specific integrated circuits, turnaround time

from design to finished wafer is critical. Thus, a semiconductor fabrication facility that has the capability to accept customer designs in electronic format and create the finished wafer from stockpiled materials will have differing transportation requirements to and from orbit. In such a situation, infrequent, high mass payload launches of raw materials, equipment, and return capsules from Earth to orbit and frequent, low mass payload, returns from orbit to Earth may be required.

Orbital transportation costs are projected to decrease while the cost of vacuum and cleaning equipment per processed wafer continues to increase.

1.3 Thesis Scope

This thesis studies the orbital fabrication of silicon semiconductor devices. Problems in traditional semiconductor wafer processing are identified and solutions presented. Concepts for alternative processes and equipment suited for a high vacuum, low gravity environment are developed. Wafer transport and fixturing is examined in detail and a system is developed that is based upon magnetic levitation of the wafer itself. This magnetic levitation system is modeled numerically and two main variants explored. An analytic economic model is constructed for both terrestrial and space-based semiconductor fabrication to account for capital, material, transport, infrastructure, and operating costs so that meaningful comparisons can be made.

1.4 Thesis Outline

Chapter 2 presents an overview of semiconductor processing in traditional, Earth-based fabrication facilities.

Chapter 3 describes space-based processing in an orbital facility and briefly covers issues related to all space-based production processes. The chapter continues

on to focus on semiconductor fabrication in space and identifies many of the advantages and disadvantages of fabricating silicon wafers in Earth orbit.

Chapter 4 describes a scheme for transport and fixturing of silicon wafers using magnetic levitation. The basic theory is reviewed and a numerical model developed. The results of that model are examined for two cases: fixturing of the wafer to an end effector, and non-contact wafer transport and fixturing using a two-dimensional linear motor.

Chapter 5 models many of the common processes found in semiconductor fabrication. For each process, the equipment and operating requirements are defined and competing process methodologies, such as single wafer versus batch processing, are implemented. These process models form the basis for process comparison between terrestrial and space-based semiconductor fabrication.

Chapter 6 examines the optimization of both terrestrial and space-based fabrication equipment and facilities under identical conditions. The key assumptions used in performing the optimization are presented and sample cases examined. The concept of functional breakdown for both equipment and facility is explained and the relationship between mass, volume, and first cost is considered.

Chapter 7 completes the work of the two prior chapters by presenting the results of process simulation models for a terrestrial semiconductor fabrication facility and an orbital semiconductor fabrication facility. The results of the models include process time, consumable use, and energy use for the process flow, as well as the equipment and facility requirements.

Chapter 8 develops an economic model for terrestrial and space-based semiconductor fabrication based upon the preceding requirements. The components of operating cost are reviewed and incorporated in the final economic model. The output of the model is the operating cost per wafer during the life of the facility.

These costs are subdivided into capital, shipping, depreciation, and operating costs so that comparisons can be performed.

Chapter 9 presents the results of the operating cost model developed in Chapter 8. Comparisons between Earth-based and space-based processing are conducted and the concept of operating cost ratio is introduced.

Chapter 10 examines issues surrounding the required infrastructure for routine space-based semiconductor fabrication. The impact of launch availability and the transportation mode is considered, as is servicing and support of an orbital production facility. The issue of transportation insurance is examined and found to be related to risk and market maturity. The requirement for new processing equipment that is more than an evolutionary extension of existing equipment and the cost of developing that equipment is evaluated.

Chapter 11 presents the conclusions and suggests further work.

Chapter 2
Semiconductor Processing

2.1 Introduction

This chapter will briefly summarize the basic processes used in the fabrication of semiconductor devices on silicon wafers.

Semiconductor fabrication, commonly referred to as microfabrication, involves the repeated application of process steps to a semiconductor wafer, generally silicon. The main types of processes used in commercial fabrication facilities will be presented along with the types of electronic devices produced by such processes.

The chapter will conclude with an overview of a commercial semiconductor fabrication facility including a functional breakdown of the main components.

2.2 Background

Electronic devices are commonly fabricated on thin wafers (200 mm by 0.5 mm thick disks typically) of semiconductor material in specialized facilities. Many electronic devices can be fabricated at the same time on a single wafer. Silicon is the most common material used to fabricate such devices and a global industry has developed to support the fabrication of silicon semiconductor devices. The most widespread device technology is silicon-based complementary metal oxide semiconductor (CMOS) and this is forecast to continue for the foreseeable future[5].

A silicon device is constructed from many thin layers of material, each with particular characteristics, that are deposited or formed on the silicon wafer. These layers form the conductors, gates, n and p doped regions, and insulators that make up the electronic device. A two transistor CMOS inverter, typical of the basic unit of the

types of devices constructed, is shown in Figure 2.1. Finished devices currently contain 10 to 100's of millions of transistors.

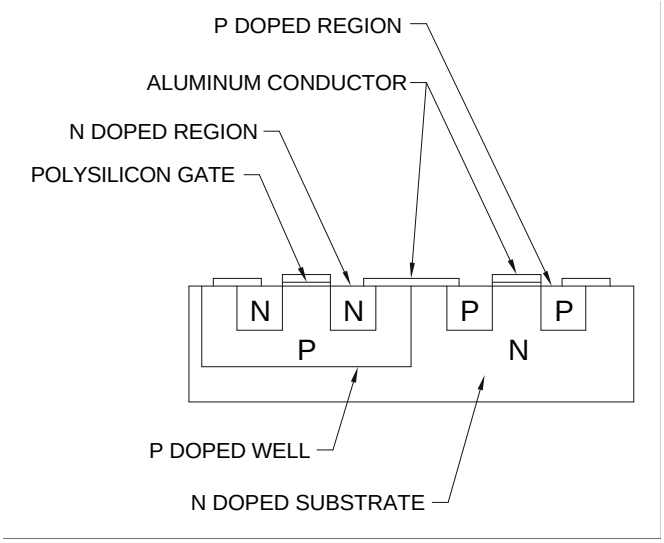

Figure 2.1 – Cross-section of CMOS Inverter

Each step in the construction of a silicon device is done by a specific process in sequence. Processes are performed by specialized pieces of equipment in dedicated semiconductor fabrication facilities and may be done in parallel for many wafers, or individually for a single wafer. The type of electronic device desired determines the number and types of processes used to construct the device.

There are three phases to the production of semiconductor devices: manufacture of the wafer itself, fabrication of the electronic device on the wafer, and packaging of the device into carriers suitable for electronic assembly. The central phase is commonly referred to as semiconductor fabrication.

2.3 Processes

All types of electronic devices are fabricated on silicon wafers using the same basic processes:

- Material Deposition
- Patterning
- Material Removal
- Doping
- Heating

In addition to the basic process, all wafers undergo ancillary processes:

- Interprocess Transportation
- Cleaning
- Testing/Inspection

Together, these eight processes are applied in sequence to produce the finished wafer. Each process may be repeated with variations many times in fabricating a wafer. For example, an advanced 0.25 μm logic chip is produced on 40 different workstations using 215 steps[6].

Figure 2.2 shows the typical sequence of steps to deposit and pattern a single layer on a wafer. Complex devices, such as microprocessors, may be fabricated from up to 30 individual layers.

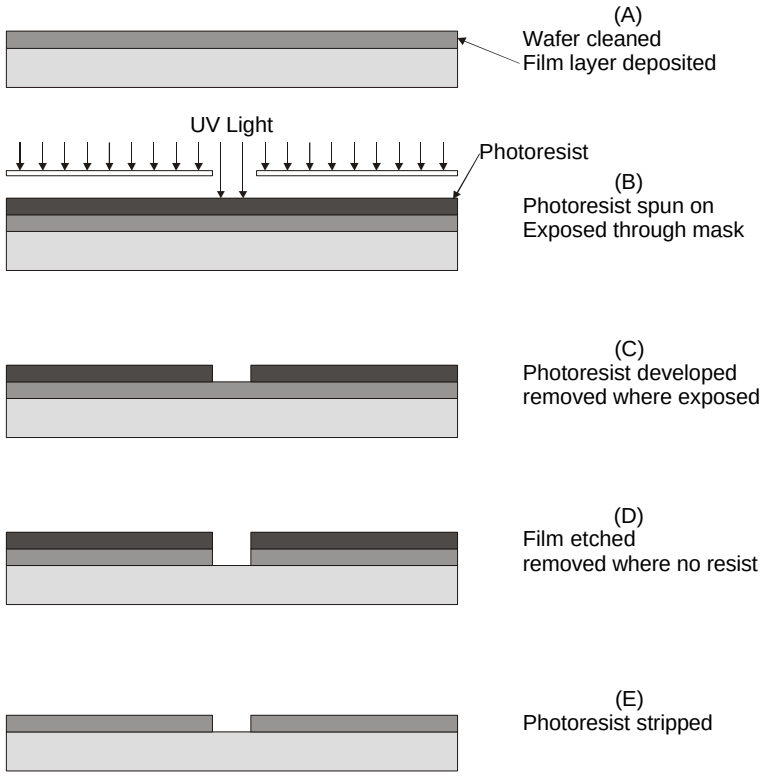

Figure 2.2 – Microfabrication Processes: Deposition and Patterning

2.3.1 Material Deposition

Deposition of thin films is the basis upon which all semiconductor devices are based and, as shown in Figure 2.2, is usually the first step in creating a new layer. These thin films are used to form conductors, insulators, or masks. The materials that make up the films are deposited on the substrate through a number of methods to ensure that the films have the desired characteristics. Chemical vapor deposition (CVD) is the most widely used method to deposit many materials in current fabrication facilities. Sputter deposition is commonly used to deposit metal conductors, although evaporation processes are also used to a lesser extent for metal

deposition. Thick silicon oxides, used as insulators, are grown on silicon through a thermal deposition process.

2.3.1.1 Chemical Vapor Deposition

Chemical vapor deposition is able to fill small, high aspect ratio gaps as well as uniformly coat a surface with a wide variety of films[7]. In the chemical vapor deposition process, the material to be deposited is contained within a carrier fluid (usually a gas) that is flowed over the wafer substrate. An energy source (heat, microwaves) forces a chemical reaction at the wafer surface causing the material to be deposited. The material is deposited on the substrate as the carrier gas flows past the substrate surface which is often heated to promote the deposition of the thin film material.

Low pressure chemical vapor deposition (LPCVD) is a popular method for CVD and is used for depositing a wide range of materials, particularly for polycrystalline silicon and dielectrics. The LPCVD system uses low pressures (0.1 to 1.0 torr) to reduce gas phase nucleation. The uniformity of the deposited material is highly dependent on the uniformity of the gas flow.

Plasma enhanced chemical vapor deposition (PECVD) uses microwaves to create a plasma in a moderate vacuum (1 - 100 mtorr) with a chemical atmosphere. This plasma breaks the CVD reactant into fragments that can react at substantially reduced temperatures. PECVD is a reduced pressure CVD, since the plasma can be sustained only in a low pressure environment. The three basic PECVD systems are cold wall parallel plate reactors, hot wall batch systems, and cold wall systems[8] and, to deposit high quality films at low temperatures, remote plasmas have recently been introduced. A typical PECVD system can operate at throughputs of up to 65 wafers per hour[9].

2.3.1.2 Sputter Deposition

In the sputter deposition process, accelerated ions are used to knock atoms and molecules from a source containing the material to be deposited. These free atoms and molecules are deposited by impingement on the target wafer, forming the thin film. Sputter deposition is most widely used to deposit metal thin films on semiconductor wafers and is the primary method currently utilized in the silicon industry. Its primary alternative is evaporation. Sputtering has better step coverage than plain evaporation and creates less damage than electron beam evaporation.

2.3.1.3 Evaporation

Used to deposit thin metal films, evaporation has been largely supplanted by sputter deposition in the semiconductor industry. Evaporated metal films have difficulty with step coverage on devices with small feature sizes. Evaporation processes require a good vacuum.

2.3.1.4 Oxide Growth

One of the reasons that silicon has become the preferred material for most semiconductor devices, is the ease at which oxides can be grown to form insulators. Silicon oxide (SiO_2) is readily formed when silicon reacts with oxygen. A thin layer is spontaneously formed at the silicon substrate surface immediately upon exposure to oxygen, and the thickness, density, and uniformity of this layer can be closely controlled by the time, temperature, and composition of the gas containing the oxygen. Dense silicon oxides are traditionally formed in a furnace at temperatures of 1000 to 1150 °C using a gas mixture of nitrogen, oxygen, and steam.

2.3.2 Patterning

Patterning is used to define the pattern of the top surface of the wafer. Lithographic systems are almost universally used for patterning in existing commercial silicon wafer fabrication processes.

The patterns produced are used for removal of deposited materials and to form masks for subsequent processes such as doping.

2.3.2.1 Optical Lithography with Conventional Photoresist

Almost all existing patterning systems use a photo sensitive liquid polymer (photoresist) that is applied to the surface of the wafer. The thin coating (1 μm typical) of photoresist is dried and exposed to a light source (such as ultraviolet) through a predefined mask as shown in Figure 2.2. The photoresist is transformed by the light in such a manner so that when the wafer and photoresist coating are placed in a chemical developer solution, selected portions of the photoresist are removed. Depending on the type of photoresist, the removed portions are either those that have been exposed to the light, or those that have not been exposed to the light. To provide the high resolution images necessary for small feature size, the masks must be carefully constructed and are usually at a larger scale than the final image to minimize diffraction effects. A special machine, called a step and repeat lithographic aligner, is used to expose the same mask in multiple locations on a single wafer, at throughput rates of 50 to 70 wafers per hour[10].

2.3.2.2 Electron Beam Direct Write

Usually used to generate the high precision masks, the electron beam direct write process creates a pattern by directing high energy electrons (25 – 50 kEV[11]) at the photoresist. Interactions between the electrons and the photoresist transform the photoresist so that selected portions can be removed in a developer solution. The

advantage of the electron beam direct write process is the high pattern accuracy that can be achieved. The main disadvantage is the slow speed with which the pattern is formed. Whereas the optical lithography process forms an entire pattern at a single time, the electron beam direct write process requires scanning of the electron beam over the pattern area to form the features.

2.3.2.3 X-Ray Lithography

The x-ray lithography process uses high energy photons (0.1 – 10 kEV[12]) to interact with the photoresist so that selected portions can be removed in a developer solution. The very short wavelength of the beam allows very high accuracy in pattern transfer from the mask as diffraction effects are insignificant. The generation of x-rays and the fabrication of x-ray masks in the x-ray lithographic process is much more difficult than in either the optical lithographic or electron beam direct write process. A number of groups are working on resolving these issues with the goal of making x-ray lithography a viable commercial process for semiconductor fabrication.

2.3.2.4 Thermal Lithography with Dry Resist

A promising new technique for patterning involves the use of thermal lithography with a dry (non-polymer), thermally activated resist[13]. In such a process, a bi-layer resist material is deposited on the surface of the wafer using sputter deposition. This resist is then patterned by a combination of thermal exposure and etching to creating an inorganic pattern on the wafer. Following conventional deposition, etching, or doping, the resist is removed by plasma cleaning and ion milling.

2.3.3 Material Removal

Much of the material deposited as thin films must be removed in order to create the desired feature geometry, as shown in Figure 2.2. Materials such as metals and polysilicon are removed to define conductors. Materials such as silicon oxide, when used to create mask layers, are removed to define the mask for subsequent processes such as doping. Materials including nitrides and oxides are removed to form insulators and gates.

The methods by which material is removed from the wafer vary depending on the geometry feature size, the amount of material to be removed, the thickness of the material, and the level of uniformity and anisotropy required. The four common methods are wet etching, plasma etching, ion milling, and reactive ion etching (RIE).

2.3.3.1 Wet Etching

Wet etching uses chemical reactions between liquid reactants and the wafer surface to remove material. It is the most common method used in semiconductor processing today. In a wet etch process, the liquid reactant reacts with the material at the surface of the wafer to form a product that is soluble in the liquid. The temperature of the solution, the molar strength of the reactants in solution, and the length of time over which the wafer is immersed in the solution all affect the amount and uniformity of material removed.

Wet etching may be used for isotropic material removal (uniform removal in all directions) or anisotropic material removal (more material is removed from some directions than others) depending on the etchant and the substrate film. Advantages of wet etching include high selectivity between the material to be etched and other materials on the wafer, and minimal substrate damage. However, wet etching does pose problems for uniformity, anisotropy, and process control.

2.3.3.2 Plasma Etching

Plasma etching is dry process. In this process, the etching occurs in a plasma environment through chemical reactions between the plasma and the wafer surface. Plasma etching requires a vacuum chamber and a radio frequency (RF) generator, making it more complex and expensive than wet etching. The high energy plasma species used in plasma etching are less discriminating in their reactions and selectivity is reduced over wet etching. However, a reactive plasma can be generated from many inert gases and avoids the need for volumes of dangerous reactors of liquid chemicals. The primary advantage of plasma is that it is able to provide anisotropic etching, necessary as feature size shrinks.

2.3.3.3 Reactive Ion Etching

Reactive ion etching uses a process in which ions assist a plasma etching process. Chlorine, fluorine, and bromine chemistries are typically used in the RIE process due to the high selectivity between doped and undoped areas. In the RIE process, ions impinging near vertically on the wafer surface are used to dope the surface so that the plasma chemistry can etch the doped areas. Very little doping occurs on vertical sidewalls, leading to highly anisotropic etching. Reactive ion etching provides both high selectivity and high anisotropy but requires highly corrosive precursor gases and precise process control.

2.3.3.4 Ion Milling

Similar to reverse sputtering, ion milling is a low temperature process for etching a variety of materials. In this process an ion beam is used to knock atoms and molecules from the wafer surface. These free atoms and molecules are deposited by impingement on a disposable target.

Ion milling offers two advantages that make it popular in certain applications: directionality and applicability. It is able to provide near vertical ion beams and it is able to pattern materials that for which there are no available etchants. However, ion milling has poor selectivity and requires a medium vacuum.

2.3.4 Doping

Semiconductors are so named because they are able to function as conductors or insulators based upon the concentration of charge carriers. Doping is the process of creating an excess of positive or negative majority carriers in a semiconductor. In commercial silicon fabrication processes, ion implantation has become the standard method by which the n and p doped regions are formed.

2.3.4.1 Ion Implantation

In the ion implantation process, a beam of ions is accelerated through an electrostatic field and scanned over the surface of the wafer. These ions penetrate into the surface of the wafer and, depending on ion type, dope the exposed surface of the semiconductor either positively or negatively. The dose of ions can be closely controlled through monitoring of the ion current, and ion beams with energy levels of 10 - 200 kEV[14] are common. Medium current implanters (0.5 – 1.7 mA) are generally single wafer machines, while high current implanters (10 mA or more) are most often batch processing systems[15].

Ion implantation allows fine control over the doping distribution of the substrate. It does require relatively expensive equipment and a high vacuum level[16], but provides precise control over the doping process. Despite the fact that ion implantation does damage to the silicon lattice that must be corrected through subsequent annealing, this process has nevertheless become the predominant method of doping silicon.

2.3.5 Thermal Processes

Many of the above processes require elevated temperatures for best results. Examples include growth of silicon oxide and some CVD processes. In addition, annealing of the wafer substrate at high temperatures is often required to correct damage in the crystal lattice, to promote growth of grain size in deposited materials such as polysilicon, and to convert materials such as silicides to a low resistivity phase.

Two types of thermal processes are commonly used to provide these elevated temperatures: furnaces and rapid thermal annealing.

2.3.5.1 Furnace Processes

A furnace process heats the wafer through a combination of conduction and convection. In this process, a batch of wafers is placed in an elongated furnace tube, constructed from a high temperature ceramic such as quartz. The temperature and atmosphere in the tube is controlled such that the wafer is exposed to a precise temperature profile with time. The quartz tube is heated externally and heat transfer to the wafer occurs primarily through conduction, with secondary effects from the convection of gases that flow longitudinally through the furnace tube. Advantages of furnace processing include the ability to simultaneously process batches of wafers and the low cost of the equipment. Disadvantages include the length of time required to heat and cool the wafer and the lack of control over uniformity of temperature profile across the wafer.

2.3.5.2 Rapid Thermal Processes

A rapid thermal process achieves heat transfer to the wafer primarily through direct radiation. In such a process, a single wafer is exposed to a radiant source, such as a flash lamp, for a brief period of time. The energy from the radiant source is

primarily absorbed by the wafer with an attendant rise in wafer temperature. Rapid thermal processes are used for annealing of wafers to remove implant damage as well as some CVD processes. A characteristic of rapid thermal processing is the short time required for the complete thermal cycle. Rapid thermal processing occurs in discrete chambers on single wafers and is not suited to batch processing.

2.3.6 Wafer Transport

Each of the above processes occurs in discrete pieces of equipment at different locations in the fabrication facility. Whether wafers are processed individually (single wafer processing) or in batches, the wafers need to be transported from place to place within the plant. Such interprocess transportation is provided by a variety of systems.

Batch processes have traditionally used wafer cassettes for storage and manual transportation of the cassette from process to process. Newer fabrication facilities use automated systems of robotic transfer vehicles or overhead rails for cassette transfer[17]. A number of groups are exploring the use of magnetic levitation or suspension for carrier transport.

Single wafer processing is becoming more common as fabrication facilities strive to reduce costs and cycle times. In single wafer processing environments, single wafer tools are often co-located in a single work station to provide a cluster tool. Wafer transport between individual tools within a cluster tool is accomplished by robotic pick and place arms. Wafer transport between cluster tools is accomplished using either batch or single wafer carriers.

In order to provide increased automation in new fabrication facilities, a number of standards have emerged that specify wafer carrier physical, mechanical, and electrical specifications so that common carrier transport systems can be developed.

2.3.7 Cleaning

The success of individual processes utilized in semiconductor fabrication is highly dependent on the cleanliness of the wafer surface and the materials used in the process. Even though wafer fabrication occurs under stringent conditions of cleanliness in a clean room, the wafer surface is still routinely contaminated during processing, transport, and storage. Dust particles in the air may lodge on the wafer surface, oxide spontaneously grows on exposed silicon, and organics and metals may be transferred to the wafer surface during processing or transport. To overcome these problems, many processes are immediately preceded by a cleaning step.

Cleaning with liquid-based chemicals is the prevalent method currently used. Plasma is used primarily for removing exposed photoresist after patterning and for cleaning of contacts prior to bonding. Ion milling (reverse sputtering) is being investigated as an alternative to wet cleans.

2.3.7.1 Wet Cleaning

The traditional cleaning process used in silicon semiconductor fabrication was developed by Radio Corporation of America (RCA) in 1965[18]. The RCA clean has become the standard clean for most silicon fabrication processes because it is a batch process that is repeatable, easily performed, and provides a surface that is clear of organics, metallic particles, and oxides. However, the RCA clean does consume a vast quantity of de-ionized (DI) water and produces large amounts of chemical waste which must be treated.

Wet cleaning processes are not easily integrated with cluster tools, their cost-of-ownership is often high due to the escalating cost of used chemical disposal, and there are concerns that it will be difficult to get liquids in to and out of increasingly fine geometries[19]. In addition, environmental restrictions on water use and the cost of

waste treatment are forcing the semiconductor industry to seek alternative cleaning methods[20,21].

2.3.7.2 Plasma Cleaning

Plasma cleaning is a dry process in which a plasma is used to clean the wafer surface. The cleaning can occur through either a physical process as the plasma ions impinge on the wafer surface with sufficient energy to knock off surface atoms and molecules or through a chemical process where the plasma ions react at the wafer surface to form gaseous products. Plasma cleaning occurs at low temperatures and the plasma cleaning process is readily controllable through environment pressure, RF energy, gas used to form the plasma, and time. One of the most common applications for plasma cleaning is to remove used photoresist from the surface of the wafer after patterning using atomic oxygen plasma. The plasma cleaning process is also used to clean the interior of CVD reactor chambers, sputter chambers, and other pieces of equipment.

2.3.7.3 Sputter Cleaning

Sputter cleaning is commonly used at the start of a sputter deposition process to remove any surface contamination on the wafer prior to sputter depositing a thin film. This dry process can be extended as a cleaning process in general, in which case it is referred to as ion milling. The advantage of sputter cleaning is that it is a low temperature process that occurs in a moderate vacuum. It removes all surface contamination uniformly through impingement of ions at the surface of the wafer. It is a physical process with little waste. However, sputter cleaning is not a batch process and is much slower than the wet cleaning processes commonly employed.

2.3.8 Testing/Inspection

High yields in semiconductor fabrication depend upon monitoring the individual processes and rapidly correcting variations[22]. Such monitoring occurs by monitoring process parameters, production wafers, and test wafers.

Process parameters are monitored in real-time through sensors connected to a the diagnostic/monitoring equipment. Production wafers are inspected at several stages in the fabrication process to ensure that only good wafers proceed to subsequent processing steps. In some cases, such as DRAM memory, defects are detected and corrected during such inspections. Test wafers are wafers that are run through a process to assess process variability. Such wafers may contain test structures that are used to determine geometry variances and electrical characteristics.

Inspection of wafers often involves the use of scanning electron microscopes and other test equipment. Interprocess testing of wafers adds additional transportation and cleaning steps to the basic process flow.

After fabrication, the finished wafers are cut using a diamond saw (diced) into "chips". The finished integrated circuit is then functionally tested, and the working chips are packaged.

2.3.9 Typical Process Flow Description

As described above, a semiconductor device is fabricated through the repeated use of separate process steps. Each device type uses a different sequence of process steps, referred to as the process flow.

Table 2.1 shows a description of the major steps used to fabricate a simple complementary metal oxide semiconductor (CMOS) device[23,24]. This device has eight levels and requires eight masks.

Table 2.1 - Steps in Fabricating Typical CMOS Device

Step	Process	Step	Process
1	Clean wafer.	28	Develop photoresist.
2	Grow think oxide.	29	P+ Implant.
3	Apply photoresist.	30	Strip photoresist.
4	Pattern P-Well. (Mask #1)	31	Apply photoresist.
5	Develop photoresist.	32	Pattern N-channel drains and sources and
6	Deposit and diffuse p-type impurities.		N+ guard rings (top ohmic contact to
7	Strip photoresist.		substrate). (Mask #5)
8	Strip thin oxide.	33	Develop photoresist.
9	Grow thin oxide.	34	N+ Implant.
10	Apply layer of silicon nitride.	35	Strip photoresist.
11	Apply photoresist.	36	Strip thin oxide.
12	Pattern silicon nitride (active area	37	Grow oxide.
	definition). (Mask #2)	38	Apply photoresist.
13	Develop photoresist.	39	Pattern contact openings. (Mask #6)
14	Etch silicon nitride.	40	Develop photoresist.
15	Strip photoresist.	41	Etch oxide.
16	Grow field oxide.	42	Strip photoresist.
17	strip silicon oxide.	43	Apply metal.
18	strip thin oxide.	44	Apply photoresist.
19	Grow gate oxide.	45	Pattern metal. (Mask #7)
20	Polysilicon deposition.	46	Develop photoresist.
21	Apply photoresist.	47	Etch metal.
22	Pattern polysilicon. (Mask #3)	48	Strip photoresist.
23	Develop photoresist.	49	Apply passivation.
24	Etch polysilicon.	50	Apply photoresist.
25	Strip photoresist.	51	Pattern pad openings. (Mask #8)
26	Apply photoresist.	52	Develop photoresist.
27	Pattern P-channel drains and sources	53	Etch passivation.
	and P+ guard rings (p well ohmic	54	Strip photoresist.
	contacts). (Mask #4)	55	Assemble, package and test.

2.4 Processing Methodologies

The eight processes described in Section 2.3 *Processes* may be applied to either batches of wafers or to individual wafers. Batch processing is used in the majority of semiconductor fabrication facilities. It has been the standard method used for wafer processing from the start of the semiconductor industry. However, the use of larger wafers (200 and 300 mm) and more stringent cleanliness requirements, have produced difficulties in extending batch processing concepts to meet future semiconductor industry needs. Single wafer processing equipment has now been

developed to provide rapid processing of single wafers under extremely controlled conditions. The increased availability of single wafer processing equipment has led to a revolution in the configuration of semiconductor fabrication facilities where many such single wafer processing modules are now co-located. Such cluster tools simplify wafer transport and may even be used to provide mini environments with tighter control over particles than the general clean room environment.

2.4.1.1 Batch Processing

Batch processing is used to process a number of wafers in parallel in a single piece of equipment. Such batches are contained within a wafer carrier that is loaded onto the process equipment. In some equipment, such as furnaces, the wafers are kept in the carrier throughout the process. In other equipment, such as a photoresist processing system which pre-bakes, applies resist, and bakes wafers, the wafers are automatically unloaded from the wafer carrier for sequential processing through the machine and then automatically reloaded in the carrier.

The use of batch processing greatly speeds the process time per wafer and provides a uniform method of tracking wafers through processes. However, it does not allow fine control over individual wafers and is not well suited to many new processes such as rapid thermal annealing.

2.4.2 Single Wafer Processing

The current trend is towards single wafer processing, and it is expected that future semiconductor fabrication facilities will be largely composed of highly reliable cluster tools processing one wafer at a time[25,26].

Single wafer processing is used to process individual wafers. Increased process time per wafer is offset by the improved control and repeatability of the process. Single wafer process modules are significantly smaller than comparable

batch processing equipment as they need only accommodate one wafer at a time. This allows for more rapid pumpdown cycles when vacuum environments are desired. It also reduces the amount of reactant needed for CVD applications. Finally, thermal processing is greatly speeded up by the small chamber size.

2.4.3 Cluster Tools

Co-location of several single wafer process modules is used to create a cluster tool which is capable of performing a variety of processes. In such a cluster tool, an automated interprocess wafer transfer system is used to move the wafer from module to module[27]. The programmability of the cluster tool allows it to vary the sequence of processes to which the wafer is subjected. Thus, a single cluster tool may be used to perform a variety of process flows[28]. Optimization of the cluster design and wafer visitation schedule can dramatically improve throughput, increasing the performance-cost ratio of cluster tools in comparison to other types of tools[29].

2.4.4 Mini Environments

The development of cluster tools allows the creation of mini environments. Such a mini environment is a clean room within a clean room[30] and is intended to minimize the introduction of contaminants to the wafer. The standard clean room within which the equipment is located must accommodate people (dressed in cleanroom garb) as well as equipment. The cost of providing increasingly stringent requirements for particle size and count to such a large space is very expensive. By creating smaller sub clean rooms with mini environments, very clean environments can be obtained in the cluster tool for wafer processing, where it is required, while allow relaxed tolerances for the outer clean room in general. Such mini environments can include operation at desired vacuum levels so that process module pumpdown

times are eliminated of reduced. Mini environments can speed overall process times and improve process cleanliness.

2.5 Devices

There are many types of electronic devices that can be fabricated on silicon wafers. Three of the most common high end devices are microprocessor units (MPU), dynamic random access memory (DRAM), and application specific integrated circuits (ASIC). These three device types define the envelope for semiconductor fabrication. Microprocessors require many levels of wiring interconnect and many process steps to fabricate. DRAM's are the most densely populated devices, comprised of many repeated patterns. ASIC's are designed for particular applications and require rapid production turnaround times for their customers. All three device types can be fabricated by the same types of processes.

Table 2.2 – Device Characteristics

Characteristic	Value
Chip size (mm^2) [31]	340 – 800
Maximum number of wiring levels[32]	7
Maximum number of Masks Levels[33]	24
Minimum feature size (nm) [31]	140 – 230
Minimum turnaround time (weeks)	6
Process	CMOS
Value per finished wafer (200 mm)[34]	$800 – $40,000

High end devices are often fabricated on the largest size silicon wafer available in order to maximize yield and reduce costs. As device size increases, so does wafer size. The 100 mm diameter wafers used for many years have now almost universally been replaced by 200 mm diameter wafers, and larger wafers are beginning to appear in use. Table 2.2 shows typical characteristics for these device types.

2.5.1 MPU

Microprocessors are found in a wide range of electronic equipment from personal computers to automobiles to toasters. The versatility of the microprocessor unit has led to it being embedded in many appliances, replacing discrete digital logic or mechanical systems for control. The microprocessor is essentially a logic device that is characterized by a large number of internally interconnected wiring levels. The complexity of an MPU is determined by number of transistors and the speed at which it operates. Present commercially available MPU's have 28 million transistors and operate at speeds up to 933 MHz[35].

2.5.2 DRAM

Dynamic random access memory is a semiconductor device that is fabricated in very high volumes, primarily for consumer applications. Device standardization and price competition have resulted in DRAM's being considered a commodity in the global semiconductor market. This has driven a need for low cost, high yield production. DRAM fabrication is critically dependent upon high density packing of memory cells and production line defect correction with lasers. The complexity of a DRAM is determined by the number of memory storage bits per chip. Current DRAM's have up to 1.07 gigabits per chip[31].

DRAM chip sizes are comparable to MPU chip sizes, although they have far fewer interconnect levels.

2.5.3 ASIC

Application specific integrated circuits are utilized in many electronic devices to provide the logic interface between system components, reducing the number of discrete components required. They are also used to provide custom functions and a

high degree of integration between system components. As such, they are designed for specific applications, generally for specific equipment by the customer. In contrast with mass produced MPU and DRAM devices where the customer develops the electronic system around the device specifications, ASIC customers design the ASIC device to fit their electronic system requirements. This customer driven design approach places a high premium upon rapid device production once the design is defined. Typical production turnaround times for ASIC's are 6 weeks[36].

ASIC's can have chip sizes that exceed MPU's or DRAM's by a factor of two. The customer specific nature of ASIC devices leads to the highest value per finished wafer of all device types.

2.5.4 Wafer Size

The number of devices that can be fabricated on a single wafer is dependent upon the chip size of the device and the size of the wafer. The size of wafer used in most semiconductor fabrication facilities at present is 200 mm in diameter. Some new production facilities are built to accommodate 300 mm diameter wafers, and it is expected that 450 mm diameter wafers will be introduced around 2011[37].

Unfortunately, process equipment suited for one size of wafer is not suited to any other size. Thus, a new process line is required when a fabrication facility moves to a new, larger wafer size. Common practice is to use older process equipment to fabricate less profitable devices on smaller wafers, and to utilize new equipment to fabricate high end devices such as MPU's, DRAM's, and ASIC's on larger wafers. The typical lifetime of the tools used in a facility is 7 to 10 years[38], roughly corresponding to the period between changes in wafer size.

2.6 Facilities and Equipment

The size and cost of the semiconductor fabrication facility is dependent upon the processes used, the size of the wafers, and the production volume. The largest fabrication facilities are now costing about $2 billion to construct and are capable of producing 30,000 200 mm diameter wafers per month[39] or 25,000 300 mm diameter wafers per month.

Table 2.3 presents the characteristics of an advanced semiconductor fabrication facility located in North America. The facility contains characteristics that are common to many fabrication facilities including a large, Class 1 cleanroom (less than one 0.5 micron diameter particle per cubic foot), extensive water and chemical treatment facilities, and high construction costs.

A semiconductor fabrication facility is comprised of a clean production area, administrative and office space, fabrication equipment, and support equipment. Current large fabrication facilities have approximately 10-20% of the total floor area as a clean room devoted to production[40]. The remainder of the area is devoted to administration, testing, and R&D (~72%), and heating, ventilation, and air conditioning (HVAC) equipment, water, and chemical treatment (~10%)[39].

Traditional production processes are carried out in a large clean room. The room is kept free of particulates by filtered air flowing vertically downward in a laminar sheet over the process equipment. This air is completely exchanged every 6 to 7 seconds on average[41] by large fans

The fabrication processes require supplies of extremely pure gases, chemicals, and de-ionized water[42]. A water treatment plant and central distribution center for consumables contribute to the plant costs. Increasingly stringent environment regulations are adding requirements for additional chemical and wastewater treatment equipment to semiconductor fabrication facilities.

Table 2.3 – Typical Commercial Fabrication Facility Characteristics[39]

Characteristic	Description
Product	• 64-Megabit DRAM chips on 200mm wafers
Initial geometry	• .35 micron
Fab capacity	• 1000 wafer starts per day at full production
Fabricator	• 600,000 square feet on three levels, with 154,000 square feet (two 75,000 square foot manufacturing lines, Mod 1 and Mod 2) under filter - Class 1
Additional site facilities	• Dedicated central utility plant • 80,000 square feet • Water treatment plant • Chemical distribution center • Building 130- 600,000 square feet total space, with approximately 150,000 square feet in use housing administrative offices, final test areas and a university lab
Projected total investment	• $1.7 billion (fabricator and utility plant construction, tools and modification of existing building and facilities)
Chronology	• Joint venture announced in August 1995 • Ground broken, November 1995 • Facility ready for tool installation, January 1997 • Initial tool installation in Mod 1 completed, July 1997 • First integrated wafer lots, July 1997 • Initial commercial wafer lots, Fourth Quarter 1997

The cost of constructing fabrication facilities is rising rapidly. Much of the expense comes from building a isolated manufacturing space inside of a large clean room area[43]. Inside this manufacturing space can be hundreds of pieces of equipment, each costing up to $4 million. It is estimated that 65-75% of the facility costs are for equipment[43].

2.7 Conclusions

This chapter has presented an overview of the fabrication of semiconductor devices on silicon wafers in commercial facilities.

Semiconductor fabrication is the manufacture of electronic devices, and several types of devices were described together with their primary production characteristics. It was shown that the same types of processes could be used to fabricate most common devices including MPU's, DRAM's, and ASIC's.

Key processes and equipment used for patterning, deposition, etching, and doping were described. It was shown that fabrication occurred inside a cleanroom which contained all processing equipment. The other functions of a semiconductor fabrication plant were explained and the high cost of new semiconductor fabrication facilities was highlighted.

This chapter has covered how current semiconductor fabrication is carried out on Earth. The next chapter will start the investigation of how the microfabrication process is changed for the space environment.

Chapter 3
Space-Based Processing

3.1 Introduction

This chapter will describe the advantages and disadvantages associated with performing semiconductor fabrication in a space-based, near-Earth environment such as low Earth orbit (LEO).

It will be shown that many of the characteristics of the space environment surrounding Earth provide advantages for typical semiconductor processes in commercial use on Earth. However, implementing all the current standard microfabrication processes in such an environment is shown to be difficult. Three main problems are identified and potential solutions presented.

Manufacturing, whether on Earth or in space, has certain logistic requirements. These requirements will be presented for space-based facilities. It will be shown that transportation, accommodation, disposition, and energy must be taken into account when comparing space-based to Earth-based semiconductor fabrication.

Finally, the chapter will conclude by defining the scope of processing that is best suited for space-based semiconductor fabrication. This scope will then be used as the basis for comparison between Earth-based and space-based processing in the remainder of this thesis.

3.2 Background

Manufacturing semiconductor devices in orbit around the Earth offers advantages that may reduce the capital and operational costs of semiconductor fabrication:

- a good native vacuum level
- a clean environment with few particles
- availability of atomic oxygen

The clean, vacuum environment eliminates much of the facility equipment required to maintain the clean room environment on Earth and also reduces the need for inert gases and other consumables. Fast moving atomic oxygen, which comprises much of the near Earth environment, has been shown during a series of space flight experiments to be very effective at removing organics and capable of growing thick oxides on silicon[44].

Table 3.1 shows some of the key characteristics of the environment around a satellite in near Earth orbit (see Section 3.3 for details).

Table 3.1 - Properties of Near-Earth Satellite Environment

Property	LEO (~300 km)
Native Vacuum Level	10^{-7} to 10^{-8} torr[45]
Possible Wake Vacuum Level	10^{-12} to 10^{-14} torr[45]
Ambient Population O	~10^{9} particles/cm^3 [46]
Ambient Population H	~10^{5} particles/cm^3 [46]
Ambient Population He	~10^{7} particles/cm^3 [46]
Energy of Atomic Oxygen on Ram Edge	5 eV[45]
Atomic Oxygen Flux on Ram Edge	10^{14} particles/cm^2 [47]
Solar radiation	1371 W/m^2 [48]
Gravity Level	Microgravity

3.3 Advantages of Orbital Manufacturing

Low Earth orbit (LEO) offers a unique environment for manufacturing. The near lack of gravity, high vacuum, and fast moving particles can be used to advantage by an orbiting space fabrication facility[49].

The prospect of space industrialization based upon processes utilizing the unique environment of space have been extensively debated. However, in almost all instances, it was found that processes in which microgravity was required could be duplicated on Earth for much less expenditure[50,51]. Thus, crystal growth and other initially attractive processes have not been commercialized in space. However, semiconductor fabrication in orbit would make use of several native environmental factors in addition to microgravity which, together, could contribute to an attractive economic scenario for space manufacturing.

3.3.1 Free Vacuum

The native vacuum in low Earth orbit (~300 km) is 10^{-7} to 10^{-8} torr. This vacuum level exceeds process requirements for many semiconductor fabrication processes. The large available volume of such vacuum offers a semi-infinite pumping speed for non-vacuum processes, limited only by the piping system.

The vacuum level can readily be improved to 10^{-12} - 10^{-14} torr in the wake behind a properly designed orbiting satellite moving at high velocity. Such a wake shield has been demonstrated on several space shuttle missions and has achieved vacuum levels of 10^{-12} torr during molecular epitaxial growth processes[52,45,53,54].

Table 3.2 - Process Vacuum Requirements

Process	Process Type	Process Vacuum Level Req'd (torr)	LEO Vacuum Sufficient
LPCVD	Deposition	1×10^{1}	✓
PECVD	Deposition	6×10^{-3}	✓
Plasma Etch	Removal	6×10^{-3}	✓
Ion Implantation	Doping	1×10^{-6}	✓
Ion Milling	Removal	1×10^{-3}	✓
Sputter Deposition	Deposition	1×10^{-1}	✓
Evaporation	Deposition	1×10^{-3}	✓

It can be seen from Table 3.2 that the vacuum available in LEO is sufficient for all common semiconductor fabrication processes. Prior to processing, equipment is typically pumped to a base vacuum level of 10^{-7} to 10^{-8} torr in order to reduce contamination[55]. LEO vacuum is sufficient for this application also.

3.3.2 Clean Environment

The particle count in orbit is much lower than in the best filtered air clean room. In fact, it has been shown that because of the high airflow rates in contemporary clean rooms, air handling systems are actually very efficient transporters of chemical contamination[56].

If the entire semiconductor fabrication process could be conducted in the native vacuum, then less particle contamination would occur and there is the possibility for reducing the number of cleaning steps between processes.

Additionally, it has been shown that particle size is linked to minimum feature size, indicating that the cleaner environment of space could aid in achieving small device geometries. The log-log plot of particle size versus particle quantity in Figure 3.1 shows that the near-Earth space environment exceeds the cleanliness of existing Class 1 cleanrooms by a factor of 1000.

In the most advanced fabrication facilities currently in use, wafers are stored in a hermetically sealed container between processes in order to reduce particle contamination[57]. Storage in the same vacuum environment as used for processing would eliminate the hermetic container.

A common cleaning step prior to processing is to remove silicon oxide that spontaneously forms on the surface of silicon when exposed to air. Such a cleaning step is not required when the wafer is stored and processed in a vacuum.

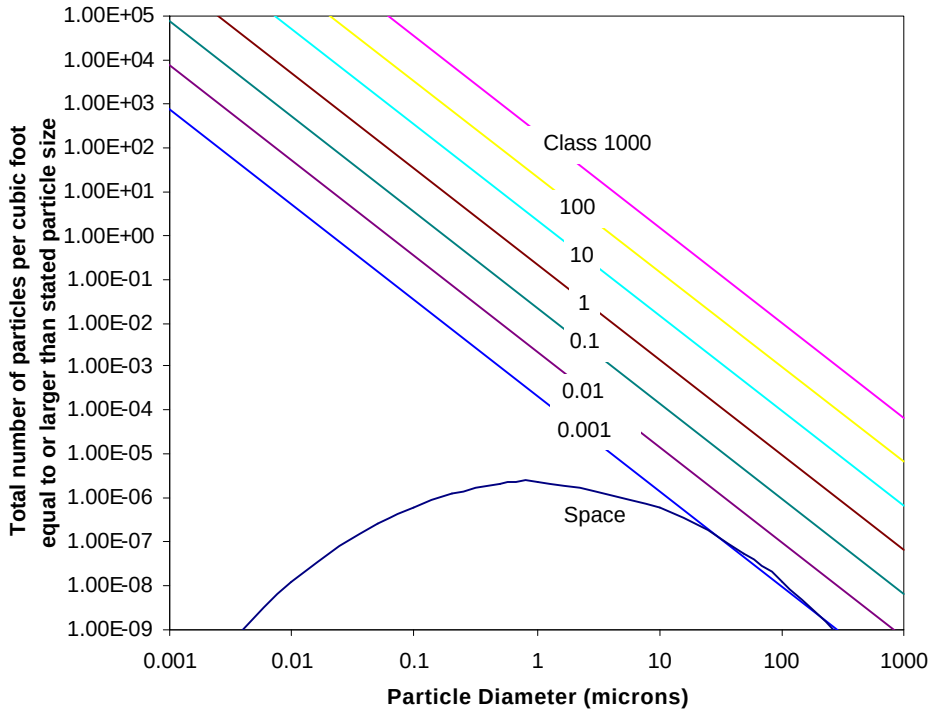

Figure 3.1 – Cleanliness of Space and Cleanroom Environments

3.3.3 Atomic Oxygen

The absorption of ultraviolet light from the Sun results in the dissociation of oxygen in the upper atmosphere[46]. In LEO, there is sufficient atomic oxygen to use as a consumable.

Atomic oxygen is often used for plasma cleaning of the wafer and can be used to remove organics from the surface of the wafer. The high velocity of a satellite in orbit results in each collision with an oxygen atom yielding 5 eV of impact energy. This energy is near the bonding energy of many molecules and allows chemical reactions to occur with a wide range of materials at low ambient temperatures[58]. Experiments in space beginning in the early 1980's have demonstrated that fast

atomic oxygen in orbit reacts with a wide range of solids at rates that exceed by an order of magnitude that of molecular oxygen or thermal atomic oxygen[58].

3.3.4 Microgravity

Applications such as space-based crystal growth rely upon the absence of gravity-driven convection currents to grow more perfect crystals. In contrast, the case for space-based semiconductor fabrication is primarily based upon the availability of free vacuum and the inherent cleanliness of vacuum. However, microgravity can provide advantages for space-based semiconductor fabrication.

Earth-based fabrication facilities are inherently horizontal, with each piece of equipment occupying a fixed amount of floor area. Without gravity, an orbital fabrication facility would not have this constraint and the process equipment could be arranged in unique, three dimensional configurations to minimize volume and mass. In addition, the strength of the structure of space-based processing equipment can be reduced, determined primarily by the ability to survive launch stresses.

3.4 Difficulties for Orbital Manufacturing of Semiconductors

All semiconductor fabrication (with the exception of research done during the Wake Shield Project) has been done on Earth using the available resources. These resources include abundant power, water, and heat as well as an atmosphere of air at 101.3 kPa (mean sea level pressure) and a gravity of 1 g. As a result, the processes developed for commercial semiconductor fabrication have been optimized to take advantage of this environment.

In a high vacuum, microgravity environment, the optimum processes are likely to be different from those currently in use on Earth. Three identified difficulties with existing processes are the use of liquid organic polymer resists for

photolithography, the high use of de-ionized water and liquid chemicals for cleaning, etching, and polishing, and the use of mechanical grips, vacuum pickups, and conveyer systems for wafer transport and fixturing.

3.4.1 Lithography

Conventional lithography uses a photosensitive liquid polymer to form a thin film on the wafer surface. The film is most commonly applied as a liquid to the center of a spinning wafer such that centripetal forces cause the liquid to flow outwards and evenly coat the entire wafer. Problems with such an approach in a microgravity, vacuum environment include clamping of the wafer to the spinning fixture and vaporization of the volatile organic liquid.

On Earth, clamping is accomplished using a vacuum hold in which vacuum is applied to the backside of the wafer and atmospheric pressure is applied to the front side of the wafer. This pressure difference creates a strong clamping force. In a vacuum environment, there is no pressure difference between front and back sides of the wafer and alternative clamping methods are required.

The liquids used as photoresist are not compatible with a vacuum environment. Upon exposure to vacuum, the volatile constituents such as solvents will vaporize from the resist, leaving unevenly cured polymer that can not be applied to the wafer.

The spin coating process partially relies upon gravity acting perpendicular to the spinning wafer to level the film coating. Spin coating in a microgravity environment may not produce films with uniform thickness.

A new, thermal lithographic process has been developed for the printing industry[59]. Research on the application of this process to semiconductor fabrication is currently underway[60,61]. The thermal resist enhanced optical lithography (TREOL)

method utilizes a thermally sensitive resist that allows higher resolution to be achieved than with photosensitive resists using the same mask.

In conventional photoresist processes, the reaction of the photoresist follows the law of reciprocity where the total exposure is integrated over time. This means that two separate exposures for half the time has the same effect as one exposure for the full time. In the TREOL process, the thermal resist does not follow the law of reciprocity, rather the resist only reacts when the temperature of the resist is raised above a certain threshold. If the resist is heated to just below this threshold and allowed to cool, the resist will remain completely unreacted.

The TREOL process exploits the non-linear reaction of the thermal photoresist by exposing the resist through both a mask and a submask. Only the resist that is exposed through both the mask and submask reacts. The submask is moved in such a manner as to expose adjacent sections of the resist separately. In a microfabrication DSW exposure system, the resist is exposed to pulses of UV light that are a few tens of nanometers in duration and are spaced hundreds of microseconds apart. This allows the resist material to cool before the next exposure. The result is a higher resolution image in the resist than can be achieved by photolithographic methods. Computer modeling has shown that the TREOL process can double the achievable resolution of current optical systems. It has been simulated that a 248 nm DSW system with the TREOL process can produce minimum feature sizes of 0.09 microns, similar to that achieved with the more expensive 195 nm DSW's[60].

The TREOL process can be made vacuum compatible. The thermal resist is not an organic liquid, but can be a variety of inorganic materials such as aluminum oxide (AlOx) or a bismuth and indium compound (BiIn) that may be applied to the wafer by a sputter deposition system. Research work is being conducted at Simon Fraser University (SFU) on adapting the TREOL process to semiconductor

fabrication. The system being examined is a bi-layer resist wherein the bottom layer is a protective layer and the top layer is the thermal resist layer[13].

In this system, a bottom layer of amorphous carbon or other similar material is sputter deposited on the wafer, followed by a top layer of a thermal sensitive material such as AlOx that is also sputter deposited. The top layer is developed using the TREOL process, leaving the bottom layer unaffected. The bottom layer is then patterned in oxygen plasma, duplicating the pattern of the top layer. The substrate is unaffected by the above processes. This yields a bi-layer resist pattern that can be used for subsequent processing such as deposition, etching of the substrate, ion implantation, etc. Once all processing for that wafer level has been complete, the bi-layer resist is removed by a combination of plasma etching and ion milling.

This process is compatible with existing DSW equipment, can be performed in a vacuum environment, and is not dependant upon gravity. The one disadvantage of the AlOx resist process is that it is much less sensitive than current organic resists, requiring exposures of 40 mJ/cm^2 compared to 10 mJ/cm^2 with regular resists. This makes it difficult to use in current exposure systems. However, new classes of inorganic thermal resists, such as BiIn, overcome these problems and offer advantages such as exposure wavelength independence. Should such resists achieve commercial acceptance, it would increase the vacuum requirement for lithographic processing. Chapter 6 explores the use of the AlOx thermal resist process in detail and develops candidate process flows for vacuum-based thermal lithography.

Conventional photolithographic processes pose problems for space-based semiconductor fabrication, but processes, such as the AlOx process and those being developed by SFU, indicate that vacuum-compatible lithographic processes are readily possible and may even provide advantages over conventional lithography.

3.4.2 Wet Processes

Abundant, available water has shaped the processes used in semiconductor fabrication. Early work in the field centered upon developing a cleaning process that yielded repeatable results. The RCA process has become the industry standard and modified versions of the process continue to be used today. The process requires large amounts of de-ionized water which has been so finely filtered that only very low concentrations (less than parts per million) of other contaminants (dissolved ions) exist in it.

It is estimated that wafer cleaning processes account for 2,500 to 5,600 liters of water per wafer[62].

Wet processes are also used for material removal. Etching of the wafer substrate or thin film in liquid chemicals such as hydrofluoric acid (HF) are common. Micromachining, a growing industry based upon semiconductor fabrication processes, also relies upon pure liquid chemicals for bulk anisotropic etching of silicon.

Planarization, or smoothing of the top surface of the wafer, is critical to achieving uniform metal traces in complex devices. Chemical mechanical polishing (CMP) is used to accomplish this step and requires liquid chemicals and DI water.

All of the processes involving liquids are incompatible with a vacuum environment. Upon exposure to a vacuum, the liquids would immediately boil, rendering the process useless. Fortunately, there are alternative dry processes for cleaning and etching. Indeed, there is a growing effort in existing semiconductor fabrication processes to reduce or remove wet process steps due to the high cost of supplying DI water and treating waste chemical process streams[20].

A dry cleaning process that is commonly in use today is that of plasma cleaning. In this process, the wafer is subjected to a plasma induced by either DC or

RF means. The energy of the plasma ions is sufficient to break the bonds holding the particles to the substrate and, given sufficient exposure, the wafer is cleaned.

In LEO there is an abundance of fast moving, atomic oxygen. The impact energy of an oxygen atom against a satellite is on the order of 5 keV, sufficient to break the bonds of many molecules. Exposure of the wafer to atomic oxygen could result in a low cost cleaning process that efficiently utilizes the available resources of LEO.

Plasma etching, another dry process, is similar to plasma cleaning. In a plasma etching system, the plasma selectively removes certain materials depending on the chemistry of the plasma. A plasma etching system may operate at higher pressures and lower energies than a plasma cleaning system with mean free paths that are less than the chamber dimensions, thus ensuring that the etching process is primarily dependent upon the etch chemistry[63].

Ion milling accelerates particles using an electric field to knock molecules from the surface of the wafer. This cleaning process is not material selective and produces a uniformly clean surface. It also produces little waste and occurs in moderate vacuum, but is slower than wet cleaning processes and is primarily suited for single wafer processing.

Wet processes cannot be readily accomplished in a vacuum, but alternative dry processes are already in widespread use. Such dry processes can be readily adapted to space-based semiconductor fabrication and offer the advantage of greatly reduced requirement for consumables.

3.4.3 Wafer Handling

In a semiconductor fabrication facility, the wafers must be transported from process to process and must be held in place within process equipment. Most new semiconductor fabrication facilities use an overhead monorail system to form a

material flow loop serving equipment bays within the facility[64,17]. As semiconductor fabrication is a highly reentrant process, this results in substantial material flow between bays.

Wafer cassettes are commonly used to group many wafers (typically 25 per cassette) in a secure, often hermetically sealed, environment for transport within the semiconductor fabrication facility. The use of wafer cassettes reduces the risk of breakage, simplifies transport by automated systems, and reduces particle contamination. Wafers must be loaded and unloaded from cassettes at each piece of process equipment. Such loading/unloading is often performed automatically by the process equipment itself.

Fixturing of the wafer to the process equipment is accomplished by means of vacuum holds or mechanical clamps. Transport of the wafers between processes is accomplished by manual transfer of wafer cassettes, overhead transport systems, magnetically levitated transport systems, or other automated transport systems. Loading and unloading of the wafers from wafer cassettes is performed by manual means using vacuum tweezers (pickups) or automated means using robotic or mechanical manipulators. Cluster tools, groups of single wafer processing equipment, utilize robotic manipulators for transfer of individual wafers from station to station within the cluster.

Wafer handling methods based upon vacuum holds and vacuum tweezers are not suitable for a vacuum environment. The holding forces developed by the difference between ambient atmospheric pressure and vacuum on the wafer's top and bottom surface are absent when vacuum is present on both sides. This poses problems for fixturing of wafers to process equipment and manually unloading wafers from wafer cassettes.

Similarly, wafer handling methods that utilize gravity to hold the wafer in place during transport are not possible in a microgravity environment. Robotic

manipulators that mechanically grip the wafer are possible in a vacuum, microgravity environment, although they can induce damage to the wafer itself and scatter particles, decreasing the cleanliness of the environment.

A system that can transport and fixture wafers in a microgravity, vacuum environment without resorting to mechanical grips does not presently exist and has been identified as a critical link in realizing the full potential of space-based semiconductor fabrication. As such, much of the work in this thesis centers around the development, characterization, and modeling of a wafer transport and fixturing system suitable for use in a space-based environment. Chapter 4 describes a scheme for the transport and fixturing of silicon wafers using magnetic levitation.

3.5 Logistics of Space-Based Manufacturing

All space-based manufacturing facilities share a common set of logistic requirements: materiel must be transported to and from the facility, raw materials and components must be processed to produce finished goods, the facility must be assembled and maintained, consumables must be supplied and waste materials removed, and processing energy is required and processing heat must be removed. These requirements can be grouped into the logistic categories of transportation, accommodation, disposition, and energy.

3.5.1 Transportation

Transportation requirements include one time transportation activities as well as operational transportation activities.

One-time transportation activities include transporting the manufacturing equipment and facility from Earth to its orbital location, transporting the construction crew to the facility (if on-site fabrication is required), and transporting the power

supply to orbit. These one time transportation activities may be accomplished with a single launch, or, as in the case of the International Space Station currently under construction, through several launches[65].

Operational transportation activities are concerned with the scheduled delivery of raw materials from Earth to orbit and finished product from orbit to Earth. In addition, transportation of maintenance crews and production workers, if required, must be provided. The mode of operational transport may be one to one where each launch provides raw materials to the facility and returns finished goods to Earth, or may be one to many where each launch provides raw materials to the facility, but finished goods are returned to Earth asynchronously, in small return capsules.

Table 3.3 shows the transport logistic functions that must be fulfilled.

Table 3.3 – Transport Logistic Functions[66]

Item	Earth to Orbit	Orbit to Earth
Manufacturing equipment/facility	One time	
Power supply	One time	
Millwright/construction crew	One time	One time
Raw materials	Recurring	
Support expendables/consumables/wastes	Recurring	Recurring
Finished goods		Recurring
Maintenance crew	Recurring	Recurring
Production workers	Recurring	Recurring

3.5.2 Accommodation

The facility must accommodate production equipment, raw materials, work in process (WIP), finished goods, spare parts/tool, waste products, and optionally, personnel.

The purpose of the facility is to convert raw materials to finished goods and therefore must support the complete manufacturing process. The equipment that must be accommodated includes not only the processing equipment, but also intra-facility

transportation systems and control/monitoring/inspection equipment. Storage of readily accessible raw materials must be provided along with intermediate storage of partially processed goods. Separate storage for packaged, finished goods is required.

Maintenance of the facility and production equipment must be intermittently performed. Unless accommodation for maintenance crews is provided externally (i.e. aboard the space shuttle or a central housing module), some form of accommodation must be provided for extended visits.

Fully automated production facilities do not have to accommodate production workers. However, facilities which do employ production workers must either provide living quarters for the workers or provide a housing space that is shared between several co-located orbital production facilities.

Table 3.4 shows the accommodation logistic functions that must be fulfilled.

Table 3.4 – Accommodation Logistic Functions[66]

Item	Use
Manufacturing equipment	Continuous
Millwright/construction crew	One time
Raw materials	Recurring
Finished goods	Recurring
Maintenance crew	Intermittent
Waste products	Recurring
Spare parts/tools	Recurring

3.5.3 Disposition

In addition to producing finished goods, all manufacturing facilities produce byproducts which must be disposed of. Process wastes are produced by the individual processes and include waste chemicals, gases, and material. Support wastes are produced by the equipment, the facility, and maintenance, and include

used parts, damaged tools, and packaging. Heat waste is produced by the processes themselves.

All orbital manufacturing facilities must have some means of disposing of process and support waste products. The traditional method of jettisoning such wastes will not function in the ever more crowded space of near Earth orbit. Already, there is an effort to reduce and eliminate foreign particles jettisoned from spacecraft in order to minimize impact hazards for orbiting bodies. In addition, there are preliminary proposals to eliminate deliberate outgassing from such spacecraft[66]. It appears that the space environment is fragile and that environmental protection efforts for Earth orbit satellites will increase.

Heat waste can be dissipated by heat rejection (radiation) into space without affecting the orbital environment or other satellites.

As the cost of injecting material waste into high or escape orbits is large, it is likely that the disposition of process and support wastes from orbit to Earth will become a transportation logistic requirement for all orbital manufacturing facilities.

Table 3.5 shows the disposition logistic functions that must be fulfilled.

Table 3.5 – Disposition Logistic Functions[66]

Item	Onsite Storage	Orbit to Earth Transportation
Process wastes	Recurring	Recurring
Support wastes	Recurring	Recurring
Heat Waste	N/A	N/A

3.5.4 Energy

Energy is required for all production processes. Some processes require heat, others require electromagnetic or electrical stimulation. All process equipment requires electrical power as does control, monitoring, and data management

equipment. The facility itself requires power for housekeeping and environmental control as well as attitude and altitude stabilization.

Table 3.6 – Energy Logistic Functions[66]

Item	Electricity	Chemical	Solar
Process heat	✓	✓	✓
Process electromagnetics, potentials, emissions	✓		
Process equipment	✓		
Process control and data management	✓		
Housekeeping	✓		
Attitude/Altitude control	✓	✓	

Process heat can be provided by either solar collectors, chemical or nuclear, or by electrically powered heaters. Waste process heat from one process may be able to be used for other processes, thereby minimizing the heat power requirement.

Electricity, used for process heating, electromagnetic processes, process equipment operation, and facility operation can be produced by chemical, nuclear, or solar means. As the requirement for electricity is ongoing, it is likely that it will be generated by onsite solar cells in order to minimize ongoing launch costs required to supply chemicals or batteries.

All orbiting satellites require a means of maintaining position and attitude. The common method of reaction wheels and thrusters imposes additional requirements for energy. Depending on the facility orbit and expected lifetime, additional fuel for the thrusters must be provided through resupply flights. It is expected that reaction wheels would operate on electrical power.

Table 3.6 shows the energy logistic functions that must be fulfilled.

3.6 Definition of Space-Based Fabrication Facility

It is useful to define the scope of a space-based facility for semiconductor fabrication. Obviously, such a facility must be capable of performing all of the

processes needed to fabricate a well defined portion of the finished electronic device. As the manufacture of the wafer itself is very energy intensive and requires large amounts of material, it is not a good candidate for space-based fabrication at this time. Similarly, the final inspection and packaging of the completed device does not benefit from space-based fabrication as the packaging is a material intensive, low value process. However, the wafer fabrication process, consisting of repeated steps of material deposition, patterning, material removal, doping, and heating, is a high value, low mass process that has high cleanliness and vacuum requirements. Values for completed wafers range from $20,000/kg for logic devices up to $1,000,000/kg for fast-turnaround ASIC devices[34]. An orbital facility capable of producing 10,000 200 mm diameter wafers per month would require only 500 to 600 kg of raw materials per month, depending on device type[34].

The threshold voltage of MOS transistors in CMOS devices is affected by trapped charges in the gate oxide. While it might be thought that the radiation in orbit would induce sufficient damage to greatly increase the quantity of trapped charges in the gate oxide, it can be shown that, in the absence of an applied electric field, a wafer that spends up to one month in LEO would receive less than 10 rads of effective radiation damage. This amount of damage in electronics can safely be ignored and is reduced even further by a low temperature (450°C) anneal on Earth prior to packaging, similar to that done for current Earth-based production[67].

The cost of providing the appropriate environment on Earth for wafer fabrication is high, leading to large capital and operational costs. This implies that the space-based semiconductor fabrication facility should be limited to processing pre-manufactured wafers shipped from Earth and that the completed wafers should be shipped back to Earth for final inspection and packaging.

Depending on the delivery schedule for raw materials and the required device turnaround time, the onboard fabrication of masks from blanks may also be a desirable process to include in a space-based semiconductor fabrication facility.

Figure 3.2 shows a summarized process flow for a semiconductor device produced in a space-based fabrication facility.

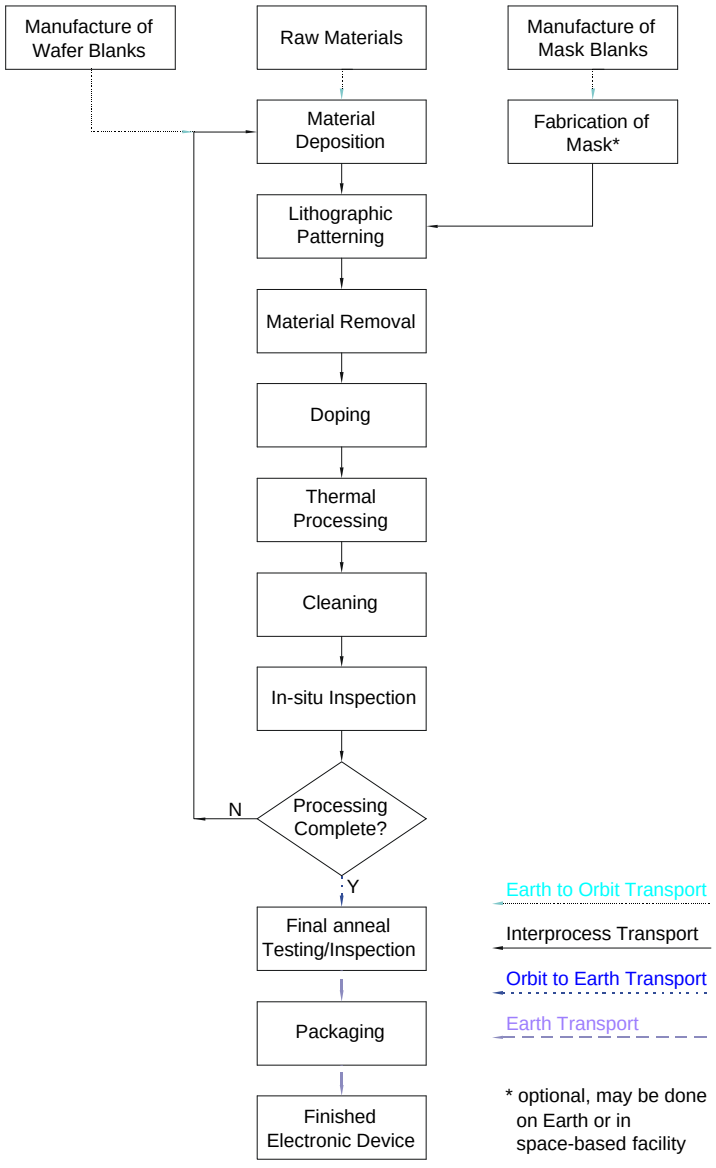

Figure 3.2 – Process Flow for Space-Based Microfabrication Facility

3.7 Conclusions

This chapter has described advantages of manufacturing in orbit, as well as the difficulties in adapting semiconductor processing to such an environment. The logistics of an orbital manufacturing facility were examined and the functions of a space-based semiconductor fabrication facility defined.

Manufacture of semiconductor devices in low Earth or higher orbit was shown to offer many advantages including a clean, native vacuum environment with atomic oxygen. The near absence of gravity was shown to provide opportunities for reducing processing equipment mass and volume.

However, present microfabrication processes were shown to be difficult to duplicate in the near-Earth space environment. Lithography, processes using liquids, and wafer handling were identified as potential problem areas.

The logistics of a space-based manufacturing facility were examined and it was found that transportation, accommodation, disposition, and energy were important factors that must be included in any study of the feasibility of space-based fabrication.

Finally, the scope of a space-based semiconductor fabrication facility was reviewed. It was determined that the most effective use of space resources (clean, vacuum environment) lay in limiting the microfabrication steps to wafer processing (patterning, deposition, etching, doping) and performing wafer growth, final testing, and packaging in a conventional Earth-based facility.

Chapter 4

Wafer Handling Using Electromagnetic Levitation

4.1 Introduction

This chapter describes a scheme for the transport and fixturing of silicon wafers using electromagnetic levitation. The basic theory is reviewed and a numerical model is developed. The results of that model are examined for two cases: fixturing of the wafer to an end effector, and non-contact wafer transport and fixturing using a two-dimensional linear motor.

It is found that an array of solenoids is able to exert controllable forces on a wafer with embedded eddy current conductor loops. The magnitude of the forces are found to be suitable for wafer transport in a low or microgravity environment using moderate power levels. In one scenario, accelerations of 1.91 m/s^2 perpendicular to the wafer and 0.16 m/s^2 parallel to the wafer are produced for a 200 mm diameter wafer using 24 watts of power.

4.2 Background

In Section 3.4 *Difficulties for Orbital Manufacturing of Semiconductors*, three items were identified as barriers to manufacturing semiconductor devices in a microgravity, vacuum environment: lithography, wet processes, and wafer handling. There appear to be viable alternatives for lithography and wet processes in such an environment, but no alternatives for wafer handling that do not utilize mechanical grips. While semiconductor fabrication is feasible with wafer handling systems using

mechanical grips, the potential cleanliness of the vacuum environment is not fully realized due to particulate scatter and mechanical wafer damage caused by the grips. Therefore, much of the research in this thesis focuses on the development and modeling of a wafer handling system suitable for use in an orbital semiconductor fabrication facility.

As described earlier in Section 3.4.3, wafers must be transported between processes and secured during processing. Traditional means of handling wafers, such as vacuum holds, mechanical clamps, and gravity-assisted robotic manipulators, are not well suited for the microgravity, vacuum environment of an orbital semiconductor fabrication facility. Vacuum holds are ineffective in a native vacuum environment. Mechanical grips can cause wafer damage and scatter particulates. Gravity assist is not available for a non-spinning orbital fabrication facility.

A system has been developed by the author to accomplish wafer transport and fixturing in a microgravity, vacuum environment[68]. This system is based upon the induction of electric currents in predefined conductors embedded in each wafer. The magnetic field produced by those currents reacts with external magnetic fields to produce forces on the wafer. Control of both the induced wafer currents and the external magnetic fields allows directed forces to be generated at the wafer. Because the wafers will exist in a microgravity environment, only very small forces are required to maintain position control[69]. Similarly, quasi-static displacements can be accomplished by imposing small forces.

Similar systems are used in other applications: a magnetically levitated automated contact analytical probe tool[70], mag-lev stage for a lithography DSW stepper[71], and a magnetically levitated wafer carrier[72]. This system is thought to be the first application of directly manipulating a wafer (instead of a wafer carrier) by electromagnetic means.

Figure 4.1 shows a single wafer with four embedded eddy current conductor loops (anticipated to be constructed from refractory metals or silicides) and four external solenoid coil assemblies. Forces are generated at each eddy current conductor loop and transferred to the wafer.

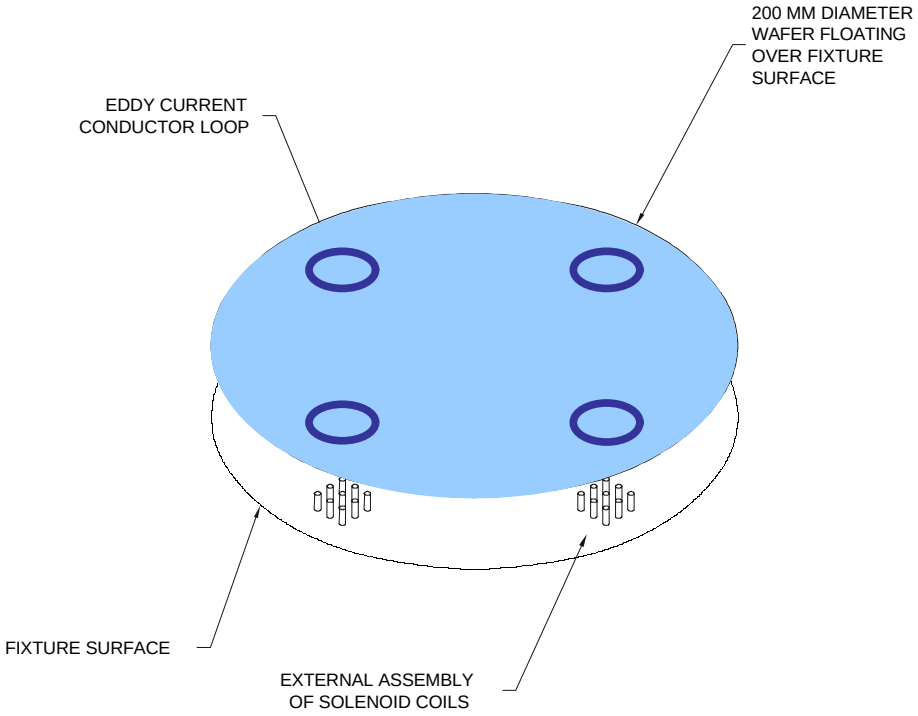

Figure 4.1 – Wafer and Electromagnetic Handling Solenoids

The electromagnetic wafer handling (EMWH) system is best suited to fixturing and transport of individual wafers, rather than wafer batches. The proposed orbital processing facility, described later in this thesis, is developed on the basis that only single wafer processes are utilized. The advantages of single wafer processing[73], coupled with the inherently clean vacuum environment, allow batch wafer storage means such as cassettes to be eliminated and processing equipment requirements to be reduced.

4.3 Wafer Handling Design Goals

The design goal of an EMWH system is to allow the transport and fixturing of single wafers within a microgravity, vacuum environment. To meet that goal, such a system should be able to provide one or more modes of operation required to transport or fixture wafers and should be compatible with all wafer processing requirements.

4.3.1 Modes of Operation

There are three distinct modes of operation for such a system: wafer holddown mode, vertical positioning mode, and horizontal positioning mode.

4.3.1.1 Wafer Holddown Mode

In the simplest mode, the EMWH system must be capable of supplying a holddown force to the wafer similar in nature to that available from a vacuum clamp. In this mode of operation, the EMWH system maintains the wafer in continuous contact with a fixture surface using an attractive force. Uses of this mode of operation, shown in Figure 4.2, are to hold the wafer to a robotic end effector during movement of the robot, to clamp the wafer in position during processing, and for heat sinking of the wafer during ion implantation.

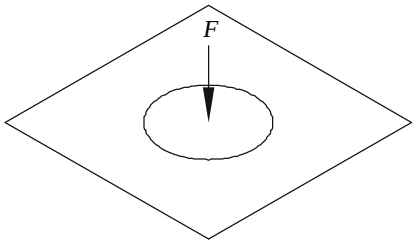

Figure 4.2 – Wafer Holddown Mode

4.3.1.2 Vertical Positioning Mode

The vertical positioning mode, shown in Figure 4.3, is similar to the wafer holddown mode in that it is used for holding the wafer in position during processing. However, in this mode the wafer is not in contact with the fixture surface, but is held at a controlled distance from the surface. Attractive and repulsive forces generated perpendicular to the plane of the wafer are considered as vertical forces and are used to control the height of the wafer from the fixture. Centering forces parallel to plane of the wafer are considered as horizontal forces and are required to maintain the position of the wafer within the fixture. Uses of this mode of operation include loading/unloading of the wafer from a robotic end effector and fixturing of the wafer in position during processing when contact with the fixture surface is not desired.

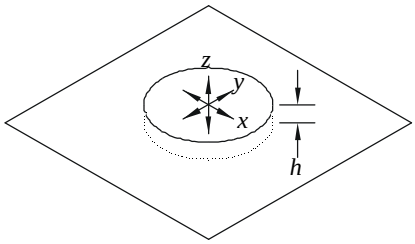

Figure 4.3 – Vertical Positioning Mode

4.3.1.3 Horizontal Positioning Mode

The most complex mode of operation is the horizontal positioning mode shown in Figure 4.4. In this mode, the EMWH system produces continuous vertical and horizontal forces at the wafer as the wafer moves over a surface with controlled position, velocity and height. The primary use of this mode is to transport wafers from process to process without the use of an external carrier such as a wafer cassette.

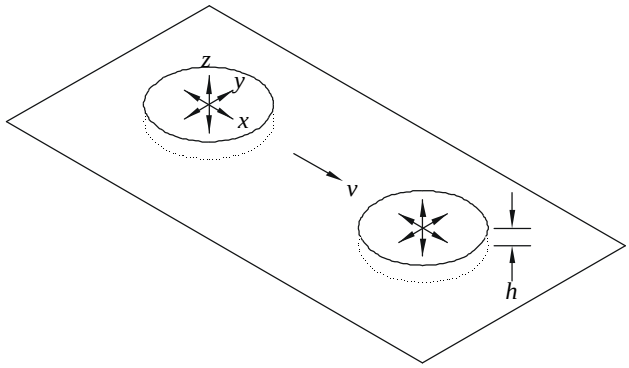

Figure 4.4 – Horizontal Positioning Mode

4.3.2 Wafer Processing Requirements

In order for the EMWH system to be viable, it must be easily applied to the wafer and must not hinder downstream wafer processing. It is noted that processes that may be affected by the magnetic fields required will need to be studied in order to confirm the viability of the EMWH system in those cases.

Preprocessing of the wafer to enable control by the EMWH system must be possible without impairing the base properties of the silicon wafer.

All processes required to fabricate semiconductor devices must be compatible with the wafer after preprocessing and transport by the EMWH system. The EMWH preprocessing must not be affected by deposition of new material, patterning of layers, removal of material, doping, cleaning, and heating of the wafer.

Research is being conducted at Simon Fraser University on a direct-write method of forming thick, silicide conductors on the back side of wafers using laser-induced chemical vapor deposition. It is hypothesized that successful application of this technique will lead to a preprocessing method of forming eddy current conductors that meets the above wafer processing requirements. The deposition of

these silicide rings is beyond the scope of this thesis and will be done in future research.

4.4 Simulation Models

The following sections detail the development of basic models to determine the feasibility of EMWH for orbital semiconductor fabrication.

The goal of modeling the EMWH system in this thesis is to determine whether such a system is possible, and if so, can it be applied to wafer handling in a microgravity, vacuum environment. Many of the fine details of such a system have been neglected in this "first pass" system modeling as they are not necessary to meet the goal. However, implementation of such a system would require that a more sophisticated model be developed.

Table 4.1 – Key Modeling Assumptions

Item	Assumption
Wafer	
Wafer Diameter	200 or 300 mm
Wafer Thickness	0.0005 m (0.5 mm)
Wafer Mass	36 g or 88 g
Wafer Holddown Mode	
Maximum Vertical Acceleration	1 m/s^2
Vertical Positioning Mode	
Nominal Positioning Height	0.001 m (1 mm)
Maximum Vertical Acceleration at Nominal Height	0.1 m/s^2
Horizontal Positioning Mode	
Nominal Positioning Height for Wafer Transport	0.001 m (1 mm)
Maximum Vertical Acceleration at Nominal Height	0.1 m/s^2
Maximum Horizontal Acceleration at Nominal Height	0.1 m/s^2

Although all of the models described below assume a feedback EMWH system, only the actuation of the wafer (the generation of forces at the wafer) is modeled. The incorporation of control and position sensing, not an insignificant problem, is only briefly described.

All modeling has been done using a combination of custom programming and spreadsheets. The program listing is available in Appendix A. The key assumptions used in developing the models are listed in Table 4.1.

4.4.1 Basic Magnetic Equations

The system models build upon basic magnetic equations. Equations common to all models are described briefly below.

The magnetic field **B** in a material with permeability μ due to magnetic field **H** is defined (in MKS units) by[74]

$$\mathbf{B} = \mu\mathbf{H} = \mu_0(1+\chi)\mathbf{H} \tag{4.1}$$

The magnetization **M** in a linear isotropic media with magnetic susceptibility χ in a magnetic field **H** is defined by[74]

$$\mathbf{M} = \chi\mathbf{H} \tag{4.2}$$

The force **F** exerted on a particle with charge *q* moving in direction **v** in a magnetic field of strength **B** is described by[75]

$$\mathbf{F} = q\mathbf{v} \times \mathbf{B} \tag{4.3}$$

For a conductor with current *i* flowing along length **l** in a magnetic field of strength **B,** the force **F** exerted on the conductor is described by

$$\mathbf{F} = i\mathbf{l} \times \mathbf{B} \tag{4.4}$$

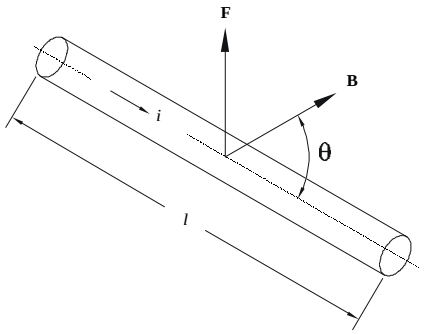

Figure 4.5 – Force on a Conductor

When the magnetic field **B** is perpendicular to the conductor, the magnitude of the force **F** can be calculated by

$$F = ilB \tag{4.5}$$

In all cases, the direction of **F** is perpendicular to both the conductor and the magnetic field **B**.

The magnetic flux Φ_B measures the number of magnetic lines that pass through a surface **S** enclosed by a conductor and is defined by[76]

$$\Phi_B = \int \mathbf{B} \bullet d\mathbf{S} \tag{4.6}$$

A conductor experiences an induced emf $\mathcal{E}$ in the presence of a changing magnetic flux according to Faraday's law of induction[76]

$$\mathcal{E} = -\frac{d\Phi_B}{dt} \tag{4.7}$$

In a closed loop conductor, the induced emf $\mathcal{E}$ gives rise to a current i based on the resistance R and inductance L of the conductor as defined by

$$\mathcal{E} = iR + L\frac{di}{dt} \tag{4.8}$$

Each point $\mathbf{P_0}$ in a conductor carrying current i contributes d$\mathbf{B}$ to the magnetic field at a point $\mathbf{P_1}$. Letting $\mathbf{r}$ define a distance vector from $\mathbf{P_0}$ to $\mathbf{P_1}$, d$\mathbf{B}$ is calculated by the Biot Savart law[77]

$$d\mathbf{B} = \left(\frac{\mu_0}{4\pi}\right)\frac{id\mathbf{l}\times\mathbf{r}}{|\mathbf{r}|^3} \tag{4.9}$$

For a circular current loop of radius a, shown in Figure 4.6, the magnitude of the radial and axial components of the magnetic field, B_r and B_z, can be calculated by integrating (4.9) around the current loop.

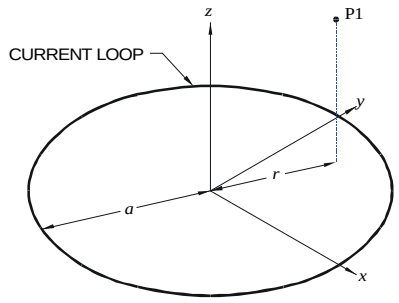

Figure 4.6 – Current Loop Coordinate System

For points (r, z) that lie along the z axis, the result is[78]

$$B_r(z) = 0 \tag{4.10}$$

and

$$B_z(z) = \frac{\mu_0 i a^2}{2\left(a^2 + z^2\right)^{3/2}} \tag{4.11}$$

However, for points not on the *z* axis, the calculation of radial and axial components of the magnetic field **B** is more complex[79]

$$B_r(r,z) = \frac{\mu_0 i z a^2}{4U^5} \sum_{k=0}^{\infty} \frac{(4k+3)!!}{(k!)^2 (k+1)} \left[\frac{r^2 a^2}{4U^4}\right]^k \tag{4.12}$$

and

$$B_z(r,z) = \frac{\mu_0 i}{4} \sum_{k=0}^{\infty} \left[\frac{2a^2}{U^3} \frac{(4k+1)!!}{(k!)^2} - \frac{r^2 a^2}{U^5} \frac{(4k+3)!!}{(k!)^2 (k+1)}\right] \left[\frac{r^2 a^2}{4U^4}\right]^k \tag{4.13}$$

U in equations (4.8) and (4.9) is defined by[79]

$$U = \left(r^2 + z^2 + a^2\right)^{1/2} \tag{4.14}$$

Equations (4.12) and (4.13) for the magnetic field components are utilized in place of other available equation forms which commonly involve elliptic integrals[80] due to the ease with which they can be calculated numerically.

4.5 Single Solenoid Model

The first model examined for the EMWH system is composed of four circular current loops embedded in the wafer and four external solenoids attached to a fixture.

Four circular current loops were chosen so that the forces exerted on the wafer due to the EMWH system could be evenly distributed and because the size of the current loops was such that they could be included, if needed, in lieu of devices on the wafer. These loops may be located in the outer, unused sections of the wafer or on the backside of the wafer.

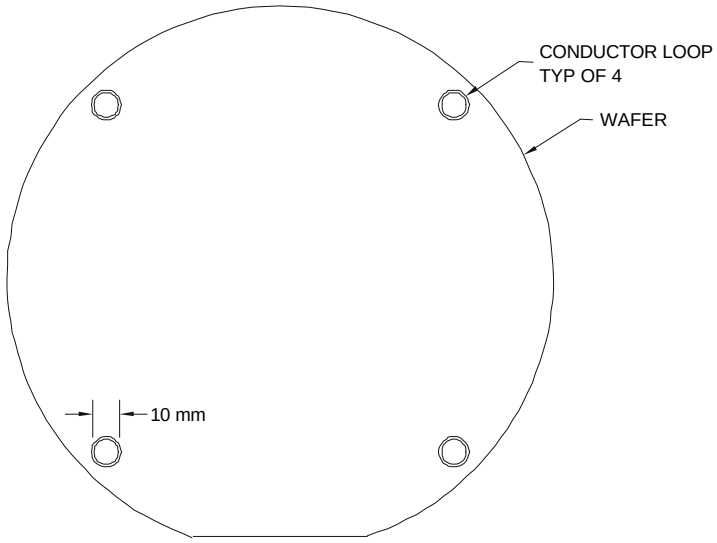

Figure 4.7 – Wafer with Embedded Conductor Loops

Each of the identical circular current loops forms a 0.005 m (5 mm) radius circle that is concentric with the external solenoids. The conductors are composed of deposited refractory metals (i.e. tungsten) or silicides, so as to be compatible with downstream thermal processes.

As all four conductor/solenoid assemblies are identical, only a single assembly is modeled. Figure 4.8 shows a detail view of a single current loop and solenoid assembly.

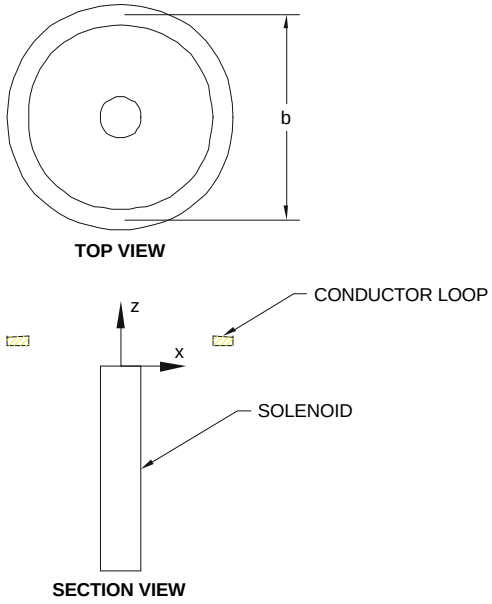

Figure 4.8 – Single Conductor Loop and Solenoid Assembly

Key assumptions and limiting criteria for this model are shown in Table 4.2.

Table 4.2 – Single Solenoid Model Key Assumptions and Limiting Criteria

Symbol	Description	Value
b	circuit diameter of conductor loop on wafer	0.005 m (5 mm)
R_e	circuit resistance of conductor loop on wafer	1 ohm
e_{max}	maximum induced EMF in wafer	1 volt
f	maximum solenoid current waveform frequency	10 kHz
μ_0	permeability of vacuum environment	$4\pi \times 10^{-7}$ H/m

The maximum EMF is limited to 1 volt in order to avoid inducing voltages in semiconductor devices during wafer transport that exceed device ratings. The frequency of alternating current in the external solenoid is limited to restrict the di/dt slope to achievable values.

It is predicted that attractive and repulsive forces can be generated on the circular conductor loop embedded in the wafer by the varying magnetic field of the

external solenoid. A lagging phase shift in the eddy current induced in the conductor loop due to conductor loop inductance is expected to cause a time averaged force perpendicular to the conductor loop to be generated for the appropriate solenoid current waveform.

4.5.1 Model Development

The multiturn solenoid, shown in Figure 4.9, is modeled as a series of circular current loops each separated by distance *d* using equations (4.12) and (4.13). The solenoid is comprised of *N* turns of conductor wire of diameter *d* that are wound around a ferromagnetic core of susceptibility χ.

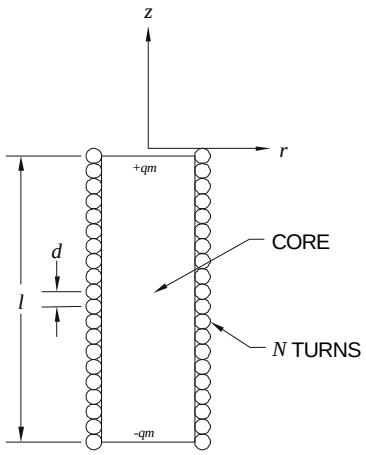

Figure 4.9 – Multiturn Solenoid with Core

The external magnetic field $\mathbf{B_s}$ is the sum of the magnetic field $\mathbf{B_0}$ due to the current loops alone and the magnetic field $\mathbf{B_m}$ due to the magnetization of the ferromagnetic core

$$\mathbf{B_s} = \mathbf{B_0} + \mathbf{B_m} = \mu_0(\mathbf{H_0} + \mathbf{H_m}) \tag{4.15}$$

The radial and axial components of the magnetic field $\mathbf{B_0}$ due to the solenoid without the ferromagnetic core are calculated by

$$B_{0r}(r,z) = \sum_{n=0}^{N-1} B_r(r, z+nd) \tag{4.16}$$

$$B_{0z}(r,z) = \sum_{n=0}^{N-1} B_z(r, z+nd) \tag{4.17}$$

To simplify the calculation of the external magnetic field $\mathbf{B_m}$ of the solenoid with the ferromagnetic core, it is possible to replace it with a distributed, fictitious magnetic charge of $\pm q_m$ that is assumed to lie at each end of the solenoid on the z axis.

The magnetic charge over a closed surface is zero and the magnetic charge q_m for a surface **S** is calculated by[81]

$$q_m = \int_{\mathbf{S}} \mathbf{M} \bullet d\mathbf{S} \tag{4.18}$$

For a long solenoid, the normal component M_n of magnetization **M** only occurs at the ends of the solenoid and the magnetic charge dq_m for each piece of surface area dA on the end is calculated by[81]

$$dq_m = -M_n dA \tag{4.19}$$

The normal component M_n of **M** at the ends of the long solenoid is approximated as

$$M_n = \frac{\mathrm{c}}{\mu_0} B_{0z} \tag{4.20}$$

using equations (4.1), (4.2) and (4.17) and the total magnetic charge q_m at each end is calculated by

$$q_m = -\int M_n dA \tag{4.21}$$

A single, fictitious magnetic charge dq_m in space at point $\mathbf{P_0}$ gives rise to a magnetic field $d\mathbf{B_m}$ at a point $\mathbf{P_1}$. Letting $\mathbf{r}$ define a distance vector from $\mathbf{P_0}$ to $\mathbf{P_1}$, the magnetic field for each solenoid end $\mathbf{B_{mend}}$ is calculated by[82]

$$\mathbf{B}_{\mathbf{mend}} = \frac{\mu_0}{4\pi}\int \frac{\mathbf{r}}{|\mathbf{r}|^3} dq_m = \frac{-c}{4\pi}\int \frac{\mathbf{r}}{|\mathbf{r}|^3} B_{0z} dA \tag{4.22}$$

and the magnetic field $\mathbf{B_m}$ due to the magnetization of the ferromagnetic core is the sum of the magnetic field $\mathbf{B_{mend}}$ for each end of the solenoid

$$\mathbf{B_m} = \mathbf{B}_{\mathbf{m}_{z=0}} + \mathbf{B}_{\mathbf{m}_{z=l}} \tag{4.23}$$

The final magnetic field due to the solenoid is the sum of $\mathbf{B_0}$ and $\mathbf{B_m}$.

$$\mathbf{B_s} = \mathbf{B_0} + \mathbf{B_m} = \mathbf{B_0} + \mathbf{B}_{\mathbf{m}_{z=0}} + \mathbf{B}_{\mathbf{m}_{z=l}} \tag{4.24}$$

Appendix A contains a program listing of the functions BrMultiLongCore and BzMultiLongCore defined using equations (4.15) to (4.24) to model the radial and axial components of the external $\mathbf{B_s}$ field of a long solenoid with a ferromagnetic core.

4.5.2 Simulation Parameters

The reference solenoid used has the characteristics shown in Table 4.3.

Table 4.3 – Reference Solenoid Characteristics

Symbol	Description	Value
N	number of turns	25
d	conductor diameter	0.0004 m (0.4 mm)
l	length	0.01 m (10 mm)
a	radius	0.001 m (1 mm)
R_s	resistance	0.0196 ohms
c	magnetic susceptibility	2000

A magnetic susceptibility of 2000 was chosen so as to be readily achievable with a low cost core. For comparison, the magnetic susceptibility of ferrite is 1000, and of transformer iron is 4000[83].

The radial component B_{sr} and axial component B_{sz} of the solenoid magnetic field $\mathbf{B}_s$ at heights z = 0.0005 m to 0.003 m for a current i_s of 16 amps is shown in Figure 4.10 to Figure 4.13 for the solenoid with a ferromagnetic core (c » 2000) and without a ferromagnetic core (c = 0).

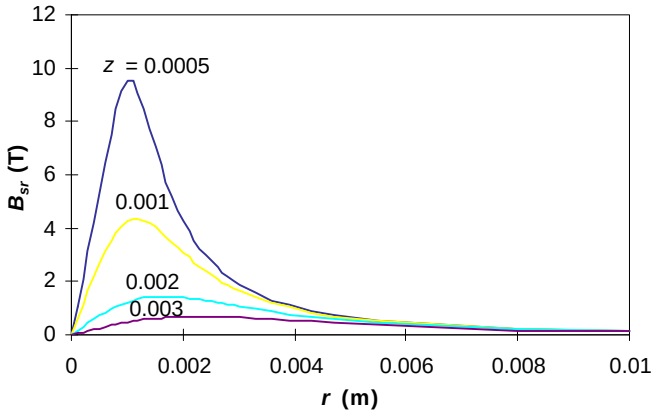

Figure 4.10 – Radial B Field for Reference Solenoid with c=2000

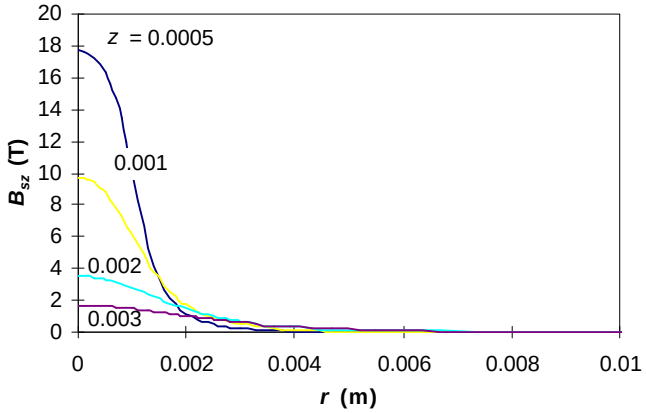

Figure 4.11 – Axial B Field for Reference Solenoid with C=2000

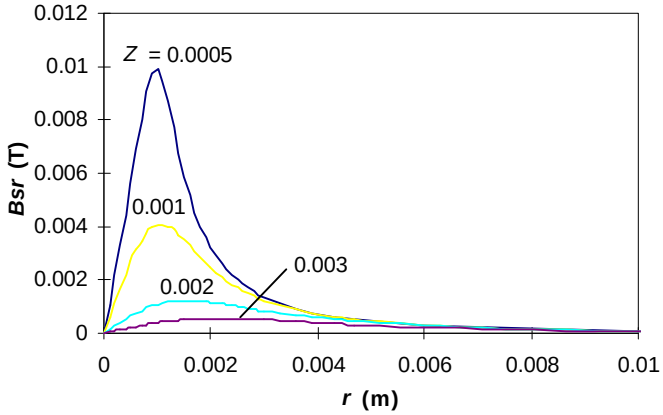

Figure 4.12 – Radial B Field for Reference Solenoid with C=0

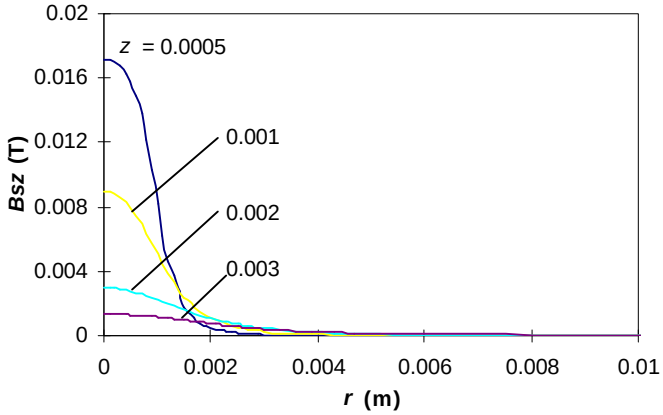

Figure 4.13 – Axial B Field for Reference Solenoid with C=0

To determine the force **F** produced by induced current i_e in the conductor loop due to the external magnetic field $\mathbf{B_s}$, a complete cycle with period p is modeled. The solenoid current i_s is varied with time according to a predefined waveform. The induced current at each point in time is calculated from equation (4.8) and the instantaneous axial force F_z is calculated from equation (4.5). The average axial force $\overline{F_z}$ is calculated by

$$\overline{F_z} = \frac{1}{p}\int_{t=0}^{p} F_z dt \tag{4.25}$$

The instantaneous solenoid power P_s required to produce current i_s is calculated by

$$P_s = {i_s}^2 R_s + L_s \frac{di_s}{dt} \tag{4.26}$$

Assuming that the inductive power requirement is balanced by external capacitors, the average power consumption $\overline{P_s}$ over a complete cycle is calculated by

$$\overline{P_s} = \frac{R_s}{p}\int_{t=0}^{p} {i_s}^2 dt \tag{4.27}$$

The reference cycle used has the characteristics shown in Table 4.4.

Table 4.4 – Reference Cycle Characteristics

Symbol	Description	Value
f	cycle frequency	10 kHz
p	cycle period	1×10^{-4} s
i_{smax}	maximum solenoid current	16 amps
$(di_s/dt)_{max}$	maximum rate of change of current	320000 amps/s

4.5.3 Simulation Results

For a wafer ring centered on the coil with an axial displacement z = 0.001 m, using the modeling process described above with the reference cycle shown, Figure 4.14 to Figure 4.17 shows the applied solenoid current i_s, the induced eddy current i_e, the instantaneous axial force F_z, and the instantaneous power requirement P_s.

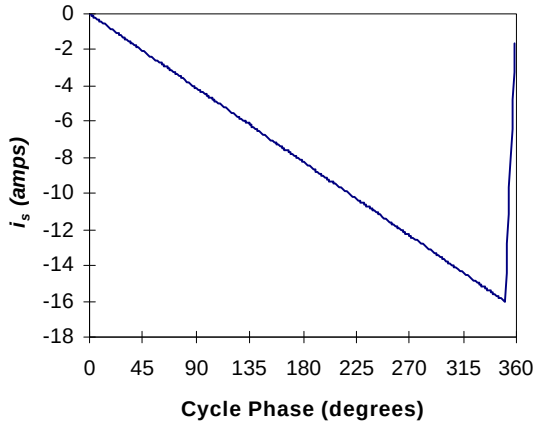

Figure 4.14 – Solenoid Current for Single Solenoid Model

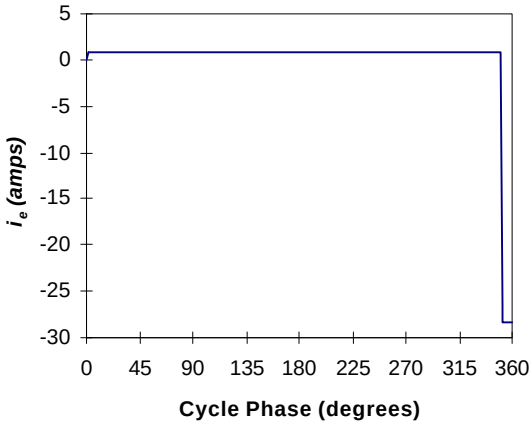

Figure 4.15 – Eddy Current for Single Solenoid Model

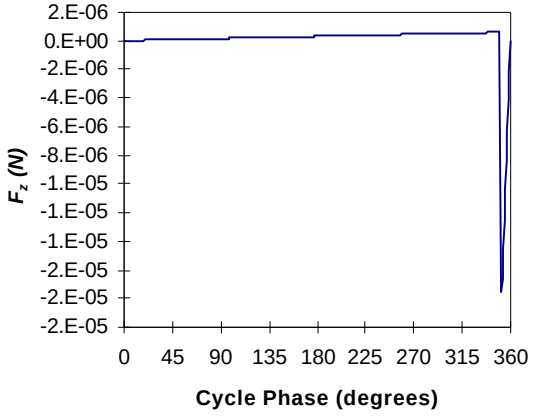

Figure 4.16 – Axial Force for Single Solenoid Model

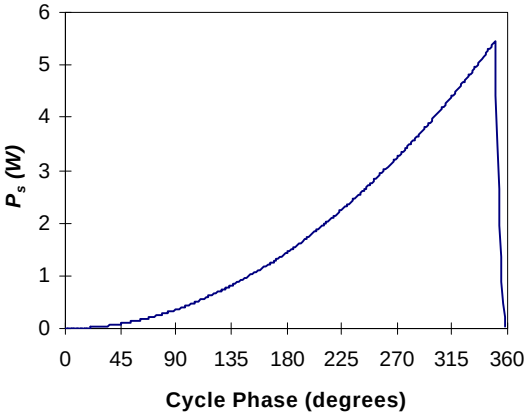

Figure 4.17 – Solenoid Power for Single Solenoid Model

The results of this simulation for a single solenoid are shown in Table 4.5.

Table 4.5 – Single Solenoid Simulation Results

Symbol	Description	Value
$\overline{F}_z$	average axial force	3.33 x 10^{-08} N
$\overline{P}_s$	average power consumed	1.81 watts

The low average axial force is due to the very small phase shift developed between the external magnetic field $\mathbf{B_s}$ and the induced eddy current i_e. The time constant of the wafer conductor loop is only 1.82 x 10^{-8} seconds, well below that of the applied current waveform. The application of a much higher frequency waveform would create a larger phase difference, and hence a larger force, but would result in *di*/*dt* slopes for the solenoid that are impractical to achieve.

4.6 Circular Solenoid Array Model

The next model examined for the EMWH system is again composed of four circular conductor loops embedded in the wafer and four external solenoid assemblies attached to a fixture. The circular conductor loops are identical to those described in Section 4.5 *Single Solenoid Model*. The external solenoid assemblies are different. As all four conductor/solenoid assemblies are identical, only a single assembly, shown in Figure 4.18, is modeled.

The key assumptions and limiting criteria for this model are the same as those for the Single Solenoid Model and are shown in Table 4.2.

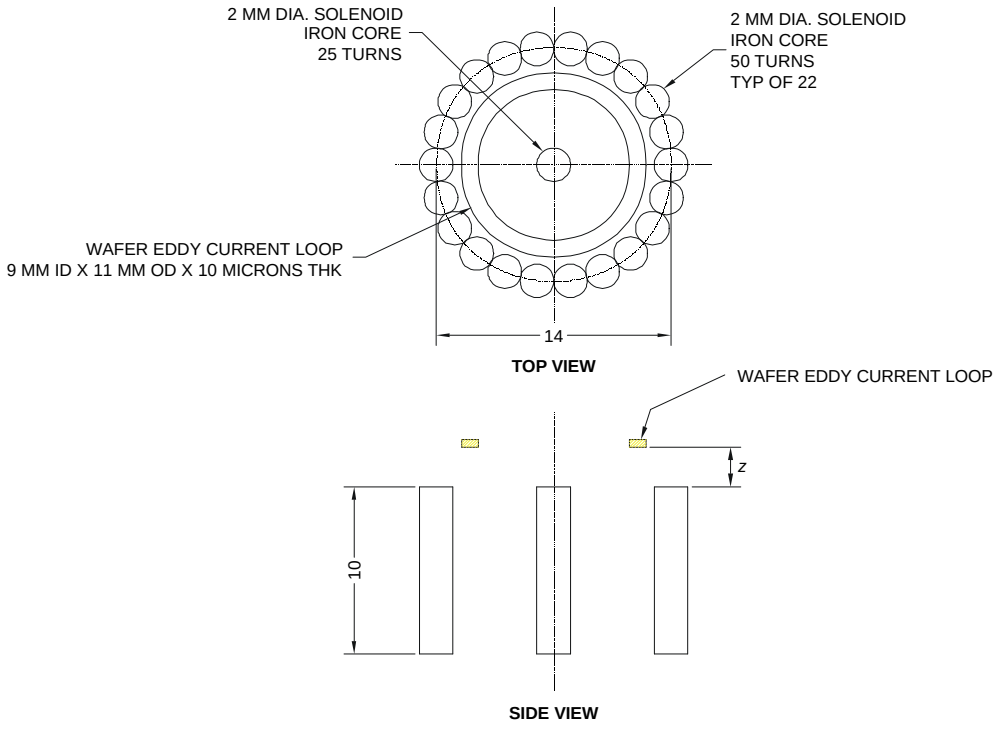

Figure 4.18 – Circular Solenoid Array Assembly

It was not possible to generate large axial forces using the Single Solenoid Model due to the small phase difference between the applied and induced currents. As the force is a function of the induced current and the external magnetic field, it is reasoned that a solenoid assembly comprised of two or more separately controllable solenoids can be used to induce an eddy current while providing a strong magnetic field at the wafer conductor loop. One such configuration is comprised of a central solenoid and a circular array of solenoids surrounding the central solenoid, and is shown in Figure 4.18.

In this model, the current in the central solenoid is independently controlled from the current in the outer circle of solenoids. In the base case, the same current waveform is applied to all outer solenoids.

It is predicted that attractive and repulsive forces can be generated on the circular conductor loop embedded in the wafer by independently varying the magnetic field of the central and outer external solenoids.

4.6.1 Model Development

Each multiturn solenoid in the circular solenoid array is modeled as a series of circular current loops each separated by distance *d*. The solenoid is comprised of *N* turns of conductor wire of diameter *d* that are wound around a ferromagnetic core of susceptibility χ.

The magnetic field $\mathbf{B_c}$ for the solenoid circle is the sum of the magnetic fields $\mathbf{B_s}$ for each individual solenoid

$$\mathbf{B_c} = \sum \mathbf{B_s} \tag{4.28}$$

The external magnetic field $\mathbf{B_s}$ of each solenoid can be calculated by equation (4.24). However, use of equation (4.24) for each solenoid is computationally intensive. A less complex model, based on a magnetic dipole, has been developed.

The dipole model of the solenoid is based upon the fictitious magnetic charge q_m that was described in Section 4.5.1.

From equation (4.15) it is shown that the external magnetic field $\mathbf{B_s}$ is comprised of the magnetic field $\mathbf{B_0}$ that is due to the solenoid alone without a core, and the magnetic field $\mathbf{B_m}$ that is due to magnetization of the core.

With a lumped magnetic charge q_{mend} replacing the distributed magnetic charge in equation (4.22), the magnetic field $\mathbf{B_{mend}}$ due to the magnetic charge is calculated by

$$\mathbf{B_{mend}} = \frac{\mu_0 q_{mend}}{4\pi} \frac{\mathbf{r}}{|\mathbf{r}|^3} \tag{4.29}$$

The magnetic field $\mathbf{B_0}$ can be approximated by a lumped magnetic charge q_{m0end} on each end of the solenoid. This approximation is exact for the far field, but has errors near the end of the solenoid. The magnetic field $\mathbf{B_{0end}}$ due to the magnetic charge on a single solenoid end is calculated by

$$\mathbf{B_{0end}} = \frac{\mu_0 q_{m0end}}{4\pi} \frac{\mathbf{r}}{|\mathbf{r}|^3} \tag{4.30}$$

The magnetic charge q_{m0end} is assumed to arise from a uniform axial magnetic field B_{0z} across the end of the solenoid

$$q_{0mend} = \frac{-B_{0z} A}{\mu_0} \tag{4.31}$$

The approximation of the magnetic field $\mathbf{B_s}$ is the sum of the magnetic fields produced by the lumped magnetic charges on each end of the solenoid

$$\mathbf{B}_s \approx \mathbf{B}_{\mathbf{0}_{z=0}} + \mathbf{B}_{\mathbf{0}_{z=1}} + \mathbf{B}_{\mathbf{m}_{z=0}} + \mathbf{B}_{\mathbf{m}_{z=1}} \tag{4.32}$$

The accuracy of the magnetic field $\mathbf{B_s}$ calculated using the dipole model versus that calculated using the solenoid model can be determined by the error fraction ε_s of the axial and radial components of the magnetic field. Equations (4.33) and (4.34) show how the error fraction ε_s is calculated.

$$e_{sr} = \frac{B_{sr_{dipole}} - B_{sr_{solenoid}}}{B_{sr_{solenoid}}} \tag{4.33}$$

$$e_{sz} = \frac{B_{sz_{dipole}} - B_{sz_{solenoid}}}{B_{sz_{solenoid}}} \tag{4.34}$$

Figure 4.19 shows the error fraction of the radial and axial components of $\mathbf{B_s}$ calculated with the dipole model for the reference solenoid at z = 0.001 m. It is seen that the error asymptotically approaches zero at large radial distances from the solenoid. At typical radial distances used in the model (0.002 m), the error in the calculated magnetic field is approximately 10%, leading to similar size errors in the final calculated forces. This level of error is considered to be acceptable in this "first pass" model of the EMWH system in order to show the feasibility of the concept. Later models will require more accurate magnetic field calculations.

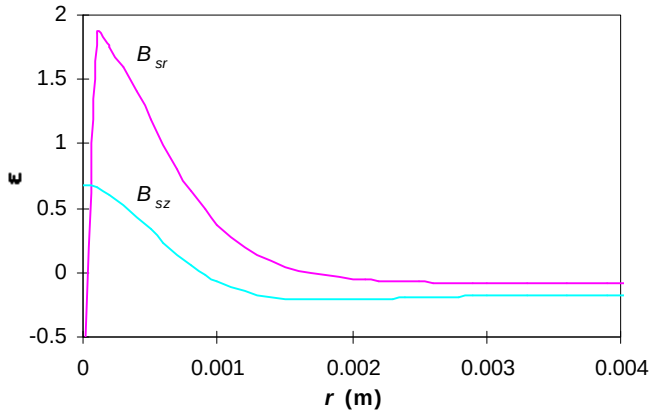

Figure 4.19 – Error Fraction of Magnetic Field Strength Calculated by Dipole Model

Appendix A contains a program listing of the functions BrDipoleCircle and BzDipoleCircle defined using equations (4.28) to (4.32) to model the radial and axial components of the external $\mathbf{B_c}$ field of a circular solenoid array.

4.6.2 Simulation Parameters

Table 4.6 shows the characteristics of the center solenoid in the circular solenoid array.

Table 4.6 – Center Solenoid Characteristics

Symbol	Description	Value
N	number of turns	25
d	conductor diameter	0.0004 m (0.4 mm)
l	length	0.01 m (10 mm)
a	radius	0.001 m (1 mm)
R_s	resistance	0.0196 ohms
c	magnetic susceptibility	2000

Each solenoid in the outer solenoid circle has the characteristics shown in Table 4.7.

Table 4.7 – Outer Solenoid Characteristics

Symbol	Description	Value
N	number of turns	50
d	conductor diameter	0.0002 m (0.2 mm)
l	length	0.01 m (10 mm)
a	radius	0.001 m (1 mm)
R_s	resistance	0.163 ohms
c	magnetic susceptibility	2000

The characteristics of the reference circular solenoid array are shown in Table 4.8.

Table 4.8 – Reference Circular Solenoid Array Characteristics

Symbol	Description	Value
j	number of outer solenoids	22
c	radius of solenoid circle	0.007 m (7 mm)

The radial component B_{cr} and axial component B_{cz} of the reference circular solenoid array magnetic field $\mathbf{B_c}$ for an inner solenoid current i_{si} of 0 amps and an outer solenoid current i_{so} of 4 amps for each solenoid in the circle is shown in Figure 4.20 and Figure 4.21.

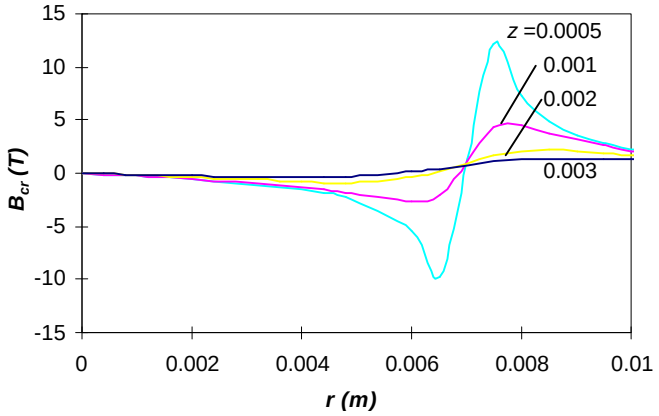

Figure 4.20 – Radial B_c Field for Reference Circular Solenoid Array

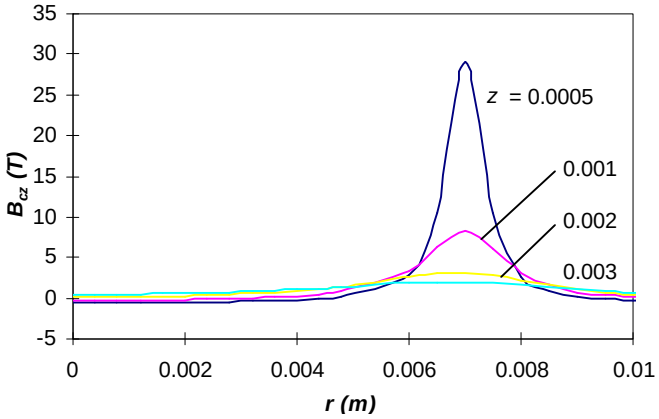

Figure 4.21 – Axial B_c Field for Reference Circular Solenoid Array

4.6.3 Simulation Results

The solenoids are driven with 10 kHz waveforms. The center solenoid current is out of phase with the outer solenoid current. For a centered wafer with an axial

displacement z = 0.001 m, using process described above, Figure 4.22 to Figure 4.25 shows the applied inner solenoid current i_{si}, applied outer solenoid current i_{so}, the induced eddy current i_e, the instantaneous axial force F_z, and the instantaneous total power requirement P_c.

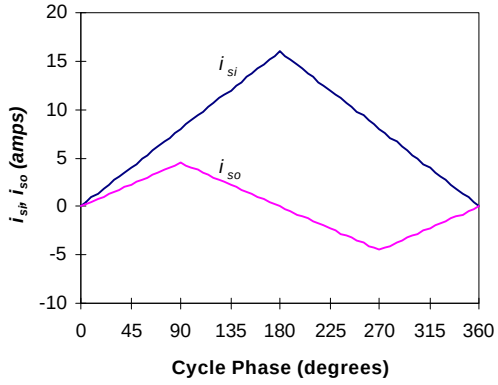

Figure 4.22 – Solenoid Current for Circular Solenoid Array

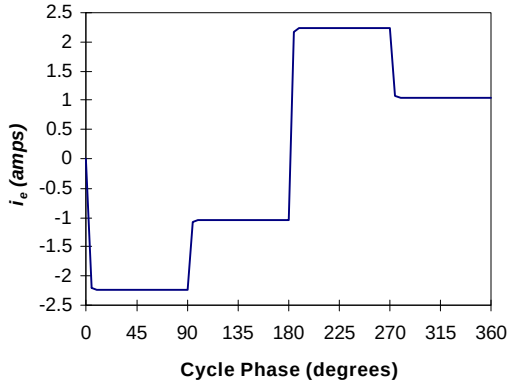

Figure 4.23 – Eddy Current for Circular Solenoid Array

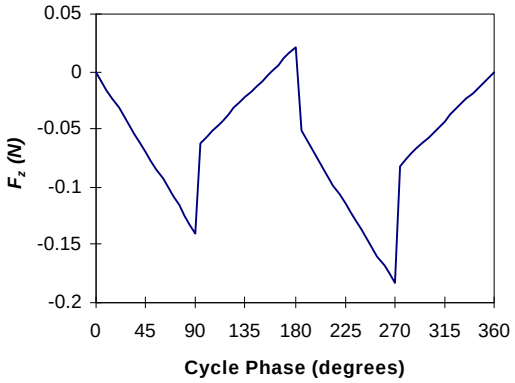

Figure 4.24 – Axial Force for Circular Solenoid Array

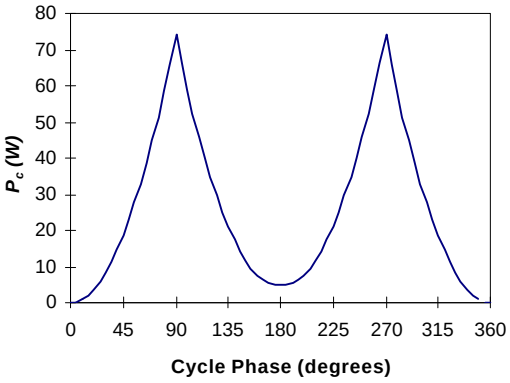

Figure 4.25 – Power for Circular Solenoid Array

The results of this simulation for a single circular solenoid array are shown in Table 4.9 and indicate that the circular solenoid array is capable of providing a significant axial force to the conductor loop in the wafer.

Table 4.9 – Circular Solenoid Array Simulation Results

Symbol	Description	Value
$\overline{F}_z$	average axial force	-0.055 N
$\overline{P}_c$	average power consumed	25.9 watts

For a centered wafer (r = 0 m), Figure 4.26 and Figure 4.27 show calculated variations in average axial forces $\overline{F}_z$ and power consumption $\overline{P}_c$.

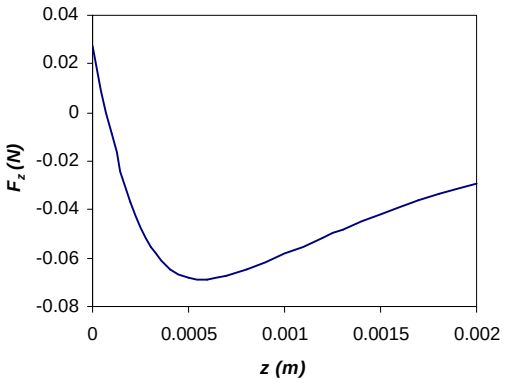

Figure 4.26 – Axial Force Variation with Axial Distance

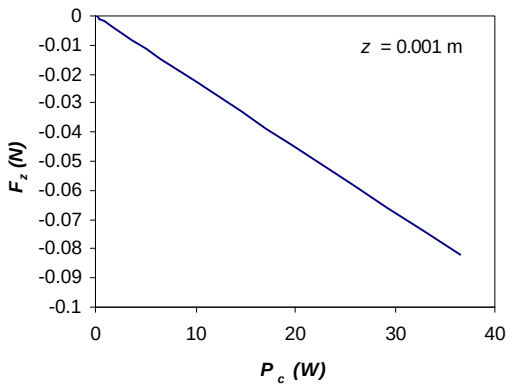

Figure 4.27 – Axial Force Variation with Power Consumption

It is seen that the direction of axial force reverses as the conducting loop is brought very close to the solenoid and that the maximum force occurs at approximately z = 0.0005 m.

Figure 4.27 shows the linear relationship between applied solenoid power and axial force for a specific position of the conducting loop. For the specific conditions shown (z = 0.001 m), the force developed per unit power is –0.00225 N/W. As the axial distance between the conducting loop and the circular solenoid array is decreased, the force developed per unit power is increased.

Figure 4.28 and Figure 4.29 show the average axial force $\overline{F}_z$ and the average radial force $\overline{F}_r$ exerted on the conductor loop in the wafer for a range of displacements *r* and *z*.

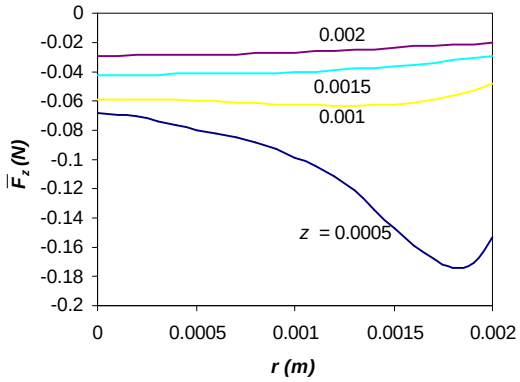

Figure 4.28 – Axial Force due to Circular Solenoid Array

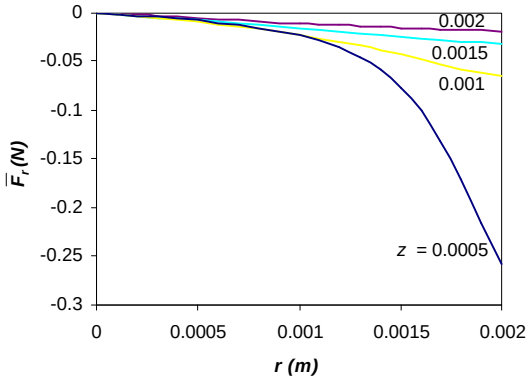

Figure 4.29 – Radial Force due to Circular Solenoid Array

It is seen that for the current waveform shown in Figure 4.22, the average axial force $\overline{F}_z$ is negative, indicating that the wafer is attracted to the solenoid assembly. With this same waveform, the average radial force $\overline{F}_r$, for positive displacements of *r*, is negative. The negative radial force provides a centering action on the wafer.

However, in order to maintain the wafer at constant distance z from the solenoid assembly in the presence of external axial disturbances, both positive and negative axial forces $\overline{F}_z$ are required. Positive axial forces are generated by shifting the phase of the outer solenoid current i_{so} by 180°.

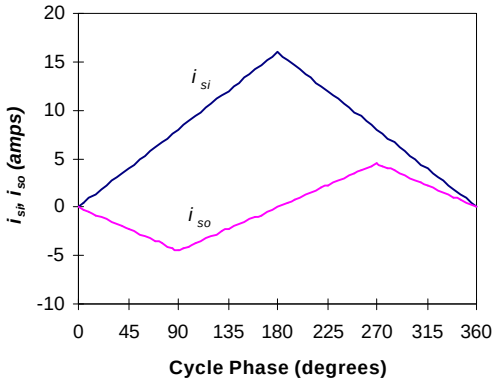

Figure 4.30 – Phase Shifted Solenoid Current for Circular Solenoid Array

For a conductor loop that is at a distance of z = 0.001 m from the solenoid assembly and offset from the center of the solenoid assembly by r = 0.001 m, the simulation results produced by the reference waveform in Figure 4.22 and the 180° phase shifted waveform of Figure 4.30 are shown in Table 4.10.

Table 4.10 – Circular Solenoid Array Simulation Results for z = 0.001, r = 0.001

Symbol	Description	Ref. Waveform	Phase Shifted Waveform
$\overline{F}_z$	average axial force	-0.062 N	0.062 N
$\overline{F}_r$	average radial force	-0.022 N	0.022 N
$\overline{P}_c$	average power consumed	25.9 W	25.9 W

It is seen that the magnitude of the forces remains the same for the reference waveform and the phase shifted waveform, but the direction of the forces is reversed. It is also seen that waveforms that produce positive axial forces also generate positive radial forces and that waveforms that create negative axial forces also cause negative radial forces. Thus, assuming that the external axial disturbance on the wafer requires equal applications of positive and negative axial forces to maintain a specified axial distance, the net radial force applied to the wafer is zero.

4.7 Recto-linear Solenoid Array Model

The final model examined for the EMWH system is again composed of four circular conductor loops embedded in the wafer and four external solenoid assemblies attached to a fixture. The circular conductor loops are identical to those described in Section 4.5 *Single Solenoid Model*. The external solenoid assemblies are rectangular solenoid arrays. As all four conductor/solenoid assemblies are identical, only a single assembly is modeled.

The key assumptions and limiting criteria for this model are the same as those for the Single Solenoid Model and are shown in Table 4.2.

While significant axial forces could be generated using the Circular Solenoid Array Model, it was not possible to generate net radial forces. The radial forces produced in the model were a result of wafer radial offset only, and alternated between positive and negative radial forces depending on the applied current waveforms.

It is theorized that individual control of the current waveform in each outer solenoid could be used to achieve net radial forces on the wafer conductor loop, independent of wafer offset. It is also reasoned that with individual solenoid control, the solenoid array, previously circular, can be generalized to a recto-linear array

without loss of force control. One such configuration is comprised of an array of 25 identical solenoids and is shown in Figure 4.31.

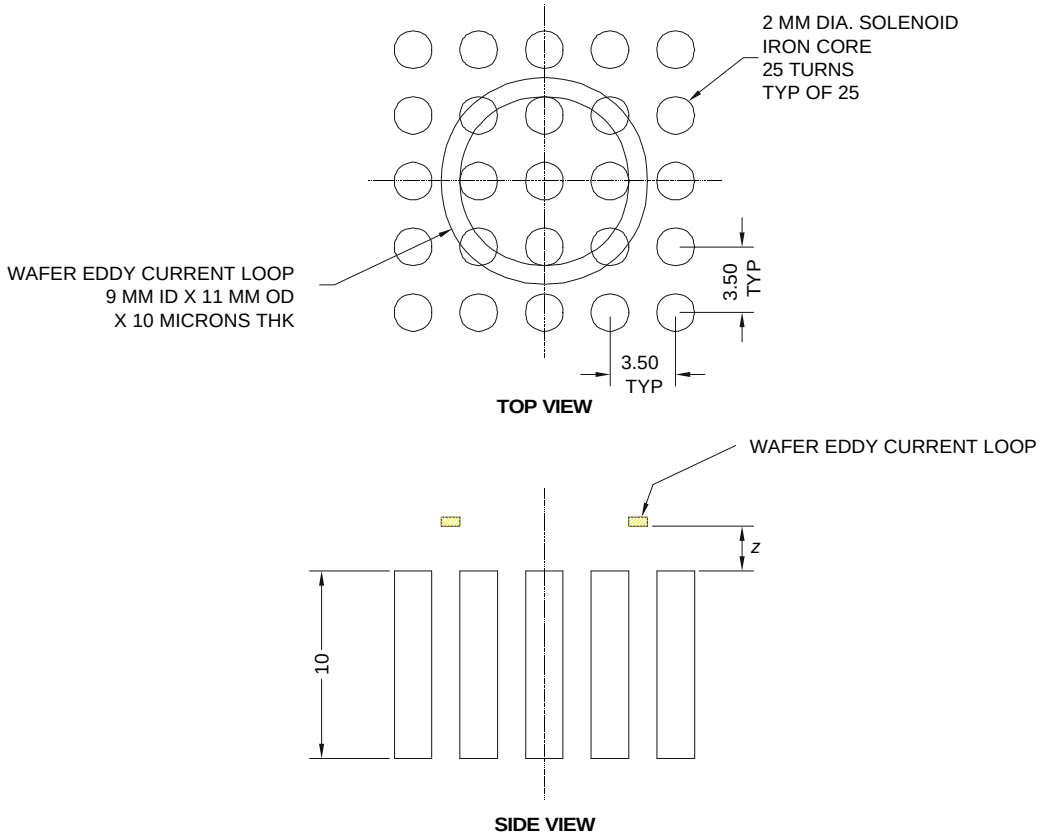

Figure 4.31 – Recto-Linear Solenoid Array Assembly

4.7.1 Model Development

As with the circular solenoid array model, each multiturn solenoid in the recto-linear solenoid array is modeled as a series of circular current loops each separated by distance *d*. The solenoid is comprised of *N* turns of conductor wire of diameter *d* that are wound around a ferromagnetic core of susceptibility χ.

The magnetic field $\mathbf{B_l}$ for the linear solenoid array is the sum of the magnetic fields $\mathbf{B_s}$ for each individual solenoid

$$\mathbf{B_l} = \sum \mathbf{B_s} \tag{4.35}$$

The external magnetic field $\mathbf{B_s}$ of each solenoid can be calculated by equation (4.32) using the magnetic dipole model developed in Section 4.6.1.

Appendix A contains a program listing of the function BSolenoid defined using equations (4.28) to (4.32) and (4.35) to model the radial and axial components of the external $\mathbf{B_l}$ field of a recto-linear solenoid array.

The external magnetic field generates forces on the wafer eddy current loop that can be resolved into forces acting through the center of the eddy current loop and torques that cause a moment about the center of the eddy current loop.

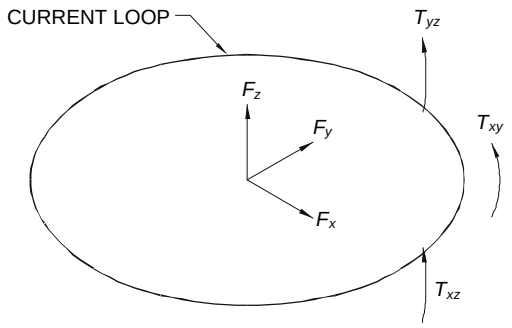

Figure 4.32 – Forces and Torques on Current Loop

Letting $\mathbf{F_p}$ designate the instantaneous force at a point on the eddy current loop due to the external magnetic field $\mathbf{B_l}$ and the current i_e, the total instantaneous force **F** (with components F_x, F_y, and F_z) acting through the center of the eddy current loop is calculated by integrating $\mathbf{F_p}$ around the loop

$$\mathbf{F} = \frac{1}{2\pi}\oint_{\theta} \mathbf{F_p}\, d\theta \tag{4.36}$$

However, the action of a force $\mathbf{F_p}$ acting through a point that is not at the center of the eddy current loop causes a torque **T**.

Designating F_{xp}, F_{yp}, and F_{zp} as the components of $\mathbf{F_p}$ acting through a point (x, y, z) from the origin of the eddy current loop, the components of the instantaneous torque **T** are determined by[84]

$$T_{xy} = \sum xF_{yp} - \sum yF_{xp} \tag{4.37}$$

$$T_{xz} = \sum xF_{zp} - \sum zF_{xp} \tag{4.38}$$

$$T_{yz} = \sum yF_{zp} - \sum zF_{yp} \tag{4.39}$$

Restating equations (4.37) to (4.39) in terms of eddy current loop radius b, replacing the summation with integration, and assuming that the eddy current loop lies in the x-y plane yields

$$T_{xy} = \frac{b}{2\pi}\oint_{\theta} \left(F_{yp}\cos\theta - F_{xp}\sin\theta\right) d\theta \tag{4.40}$$

$$T_{xz} = \frac{b}{2\pi}\oint_{\theta} \left(F_{zp}\cos\theta\right) d\theta \tag{4.41}$$

$$T_{yz} = \frac{b}{2\pi}\oint_{\theta} \left(F_{zp}\sin\theta\right) d\theta \tag{4.42}$$

The average forces and torques are calculated by integrating over the period p of a complete current waveform cycle

$$\overline{F_x} = \frac{1}{p}\int_{t=0}^{p} F_x dt \tag{4.43}$$

$$\overline{F_y} = \frac{1}{p}\int_{t=0}^{p} F_y dt \tag{4.44}$$

$$\overline{F_z} = \frac{1}{p}\int_{t=0}^{p} F_z dt \tag{4.45}$$

$$\overline{T_{xy}} = \frac{1}{p}\int_{t=0}^{p} T_{xy} dt \tag{4.46}$$

$$\overline{T_{xz}} = \frac{1}{p}\int_{t=0}^{p} T_{xz} dt \tag{4.47}$$

$$\overline{T_{yz}} = \frac{1}{p}\int_{t=0}^{p} T_{yz} dt \tag{4.48}$$

4.7.2 Simulation Parameters

All solenoids in the reference recto-linear solenoid array have the characteristics shown in Table 4.11.

Table 4.11 –Recto-linear Solenoid Characteristics

Symbol	Description	Value
N	number of turns	25
d	conductor diameter	0.0004 m (0.4 mm)
l	length	0.01 m (10 mm)
a	radius	0.001 m (1 mm)
R_s	resistance	0.0196 ohms
c	magnetic susceptibility	2000

The solenoids were grouped into three categories: Internal, External, and Unused. Current waveforms i_{si} and i_{so} were applied to the Internal and External (outer) solenoids respectively. No current waveform was applied to the Unused solenoids.

Figure 4.33 below shows the solenoid array with the Internal and External solenoids marked.

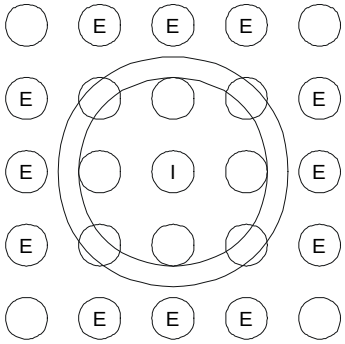

Figure 4.33 – Internal and External Solenoids

4.7.3 Simulation Results

The solenoids are driven with 10 kHz waveforms. The internal solenoid current is out of phase with the external solenoid current. For a centered wafer with an axial displacement z = 0.001 m, Figure 4.34 to Figure 4.37 show the applied inner

solenoid current i_{si}, applied outer solenoid current i_{so}, the induced eddy current i_e, the instantaneous axial force F_z, and the instantaneous total power requirement P_l for the reference recto-linear solenoid array.

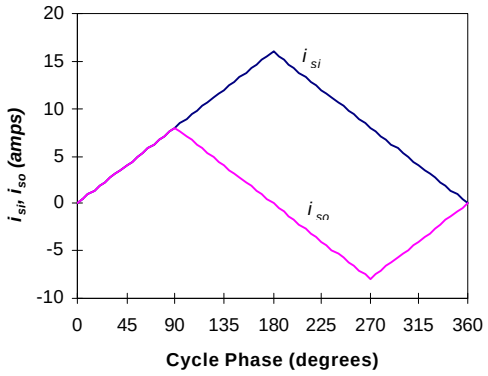

Figure 4.34 – Solenoid Current for Recto-linear Solenoid Array

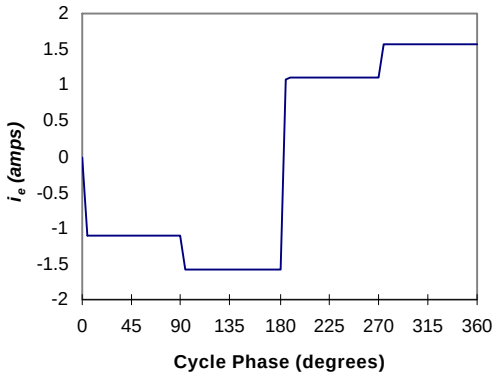

Figure 4.35 – Eddy Current for Recto-linear Solenoid Array

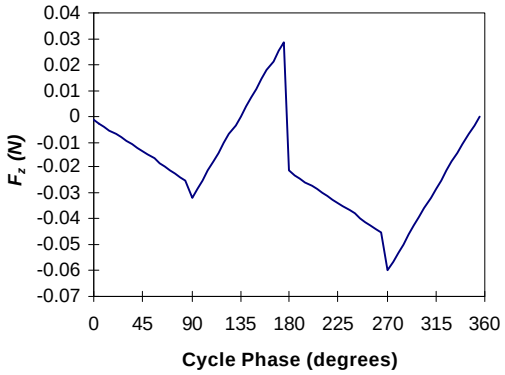

Figure 4.36 – Axial Force for Recto-linear Solenoid Array

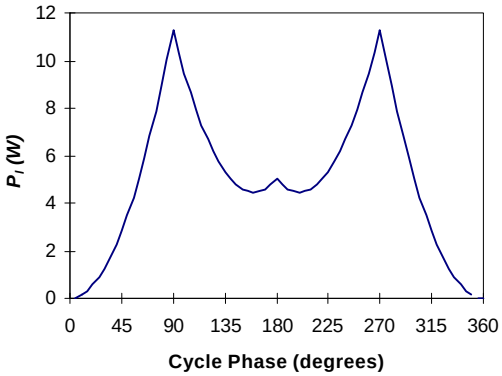

Figure 4.37 – Power for Recto-linear Solenoid Array

The results of this simulation for a single solenoid array are shown in Table 4.12.

Table 4.12 – Recto-linear Solenoid Array Simulation Results

Symbol	Description	Value
$\overline{F}_x$	average force in x direction	0.00 N
$\overline{F}_y$	average force in y direction	0.00 N
$\overline{F}_z$	average axial force in z direction	-0.0205 N
$\overline{T}_{xy}$	average torque in x-y plane	0.00 N
$\overline{T}_{xz}$	average torque in x-z plane	0.00 N
$\overline{T}_{yz}$	average torque in y-z plane	0.00 N
$\overline{P}_l$	average power consumed	6.7 watts

The results indicate that the recto-linear solenoid array is capable of providing a significant axial force to the conductor loop in the wafer.

For a centered wafer ($x = y = 0$), Figure 4.38 and Figure 4.39 show calculated variations in average axial forces $\overline{F}_z$ and power consumption $\overline{P}_l$.

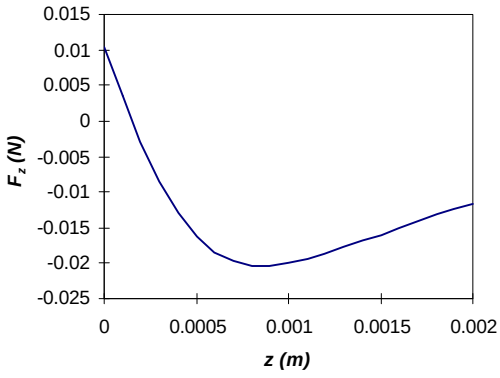

Figure 4.38 – Axial Force as a Function of Distance

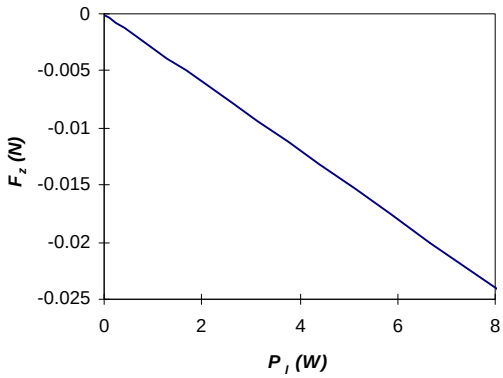

Figure 4.39 – Axial Force as a Function of Power Consumption

Figure 4.39 shows the linear relationship between applied solenoid power and axial force for $z = 0.001$ m. For the specific conditions shown, the force developed per unit power is –0.00299 N/W. As the axial distance z between the conducting loop

and the circular solenoid array is decreased, the force developed per unit power is increased.

Figure 4.40 and Figure 4.41 show the average forces $\overline{F}_x$, $\overline{F}_y$, $\overline{F}_z$ and the average torques $\overline{T}_{xy}$, $\overline{T}_{xz}$, $\overline{T}_{yz}$ exerted on the conductor loop in the wafer for a range of displacements x for z = 0.001 m.

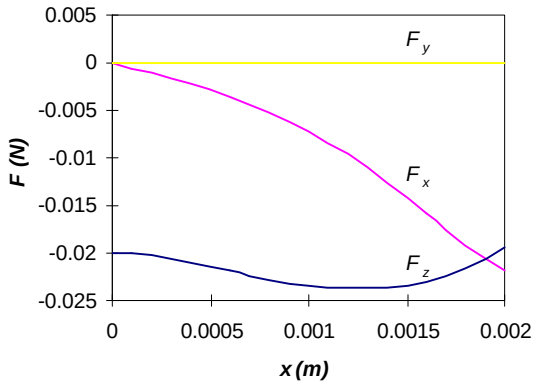

Figure 4.40 –Force on Wafer Conductor Loop

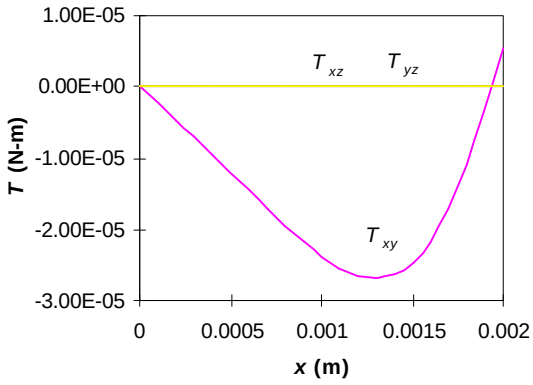

Figure 4.41 – Torque on Wafer Conductor Loop

It is seen that for the current waveform shown in Figure 4.34, the average axial force $\overline{F}_z$ is negative and varies between –0.020 and –0.026 N for the range of x displacements shown. The negative axial force indicates that the wafer is attracted to the solenoid assembly. With this same current waveform, the average radial force $\overline{F}_x$, for positive displacements of x, is negative. This negative radial force provides a centering action on the wafer.

While torques T_{xy} and T_{yz} remain zero with increasing displacement x, torque T_{xz} is seen to reach a maximum at x = 0.0012 m.

As with the circular solenoid array, in order to maintain the wafer at constant distance z from the solenoid assembly in the presence of external axial disturbances,

both positive and negative axial forces $\overline{F}_z$ are required. Positive axial forces are generated by shifting the phase of the outer solenoid current i_{so} by 180°.

For a conductor loop that is at a distance of z = 0.001 m from the solenoid assembly and offset from the center of the solenoid assembly by x = 0.001 m, y = 0.000 m, Table 4.13 summarizes the simulation results produced by the reference waveform in Figure 4.34 and the 180° phase shifted waveform.

Table 4.13 – Recto-Linear Solenoid Array Simulation Results for z = 0.001 m, x = 0.001 m

Symbol	Description	Reference Waveform	Phase Shifted Waveform
$\overline{F}_x$	average force in x direction	-0.0072 N	0.0072 N
$\overline{F}_y$	average force in y direction	0.00 N	0.00 N
$\overline{F}_z$	average axial force in z direction	-0.023 N	0.023 N
$\overline{T}_{xy}$	average torque in x-y plane	0.00 N-m	0.00 N-m
$\overline{T}_{xz}$	average torque in x-z plane	-2.4×10^{-5} N-m	2.4×10^{-5} N-m
$\overline{T}_{yz}$	average torque in y-z plane	0.00 N-m	0.00 N-m
$\overline{P}_l$	average power consumed	6.7 W	6.7 W

It is seen that the magnitude of the forces and torques remains the same for the reference waveform and the phase shifted waveform, but the direction of the forces and torques is reversed. It is also seen that waveforms that produce positive axial forces also generate positive horizontal forces and that waveforms that create negative axial forces also cause negative horizontal forces. Thus, assuming that the external axial disturbance on the wafer requires equal applications of positive and negative axial forces to maintain a specified axial distance, the net horizontal force applied to the wafer is zero.

It is possible to generate net horizontal forces using the recto-linear solenoid array by turning off the current waveform in selected external solenoids or by otherwise causing an imbalance in the external magnetic field.

The simplest method to cause such an imbalance is by disabling an External solenoid, thereby converting it to an Unused solenoid, as shown in Figure 4.42.

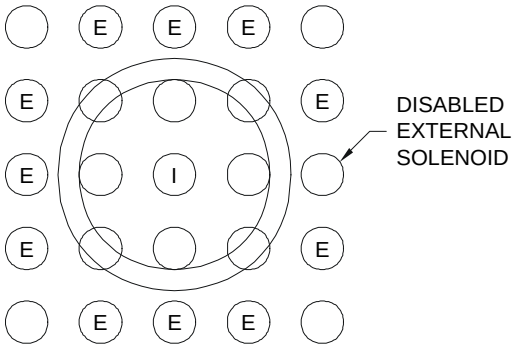

Figure 4.42 – Disabled External Solenoid

Figure 4.43 and Figure 4.44 show the average forces $\overline{F}_x$, $\overline{F}_y$, $\overline{F}_z$ and the average torques $\overline{T}_{xy}$, $\overline{T}_{xz}$, $\overline{T}_{yz}$ exerted on the conductor loop in the wafer for a range of displacements x for z = 0.001 m using the imbalanced solenoid array shown in Figure 4.42.

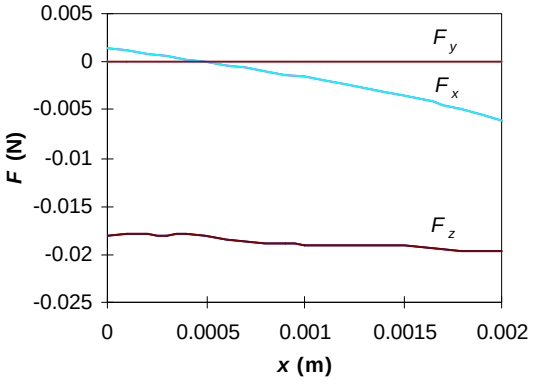

Figure 4.43 – Force on Wafer Conductor Loop

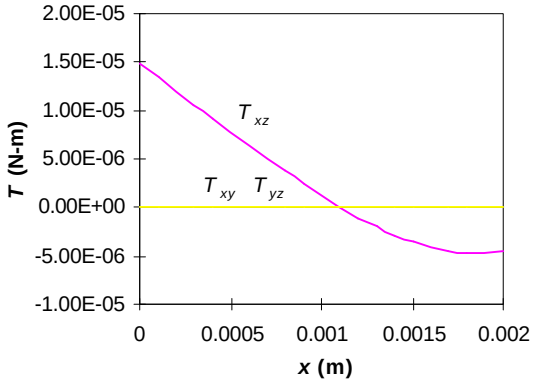

Figure 4.44 – Torque on Wafer Conductor Loop

It is seen that, for a centered wafer at z = 0.001 m, disabling of a single external solenoid produces a horizontal force of 0.0015 N in the x direction while only reducing the axial force by 10%. Disabling additional external solenoids can increase the horizontal force produced.

4.8 Discussion of Magnetic Levitation Model Results

Of the three models examined, the Circular Solenoid Array Model and the Recto-Linear Solenoid Array Model appear suitable for use in a space-based wafer handling system. As described in Section 4.5, each wafer has four identical conducting loops situated over solenoid array assemblies.

Two sizes of silicon wafers are in common use in commercial semiconductor fabrication facilities: 200 and 300 mm. A 200 mm diameter wafer is 0.5 mm thick and has a mass of 36 to 37 grams while a 300 mm diameter wafer is also approximately 0.5 mm thick with a mass of 88 grams.

The acceleration **a** on a wafer with mass m created by an applied force **F** is calculated by Newton's Second Law[85]

$$\mathbf{a} = \frac{\mathbf{F}}{m} \tag{4.49}$$

For a power consumption of 24 watts, the magnitude of the average forces and accelerations attainable on a centered wafer (x = 0.000 m, y = 0.000 m) with the two solenoid array models using the appropriate reference waveforms are summarized in Table 4.14 and Table 4.15.

Table 4.14 – Summary for Circular Solenoid Array Model

Symbol	Description	200 mm Wafer	300 mm Wafer
$\overline{F}_z$	clamping force (z = 0.0005 m)	0.063 N	0.063 N
$\overline{a}_z$	clamping acceleration (z = 0.0005 m)	1.74 m/s^2	0.72 m/s^2
$\overline{F}_z$	axial force (z = 0.001 m)	0.054 N	0.054 N
$\overline{a}_z$	axial acceleration (z = 0.001 m)	1.50 m/s^2	0.62 m/s^2
$\overline{F}_r$	radial force (z = 0.001 m)	0.000 N	0.000 N
$\overline{a}_r$	radial acceleration (z = 0.001 m)	0.00 m/s^2	0.00 m/s^2

Table 4.15 – Summary for Recto-Linear Solenoid Array Model

Symbol	Description	200 mm Wafer	300 mm Wafer
$\overline{F}_z$	clamping force (z = 0.0005 m)	0.058 N	0.058 N
$\overline{a}_z$	clamping acceleration (z = 0.0005 m)	1.61 m/s^2	0.72 m/s^2
$\overline{F}_z$	axial force (z = 0.001 m)	0.069 N	0.069 N
$\overline{a}_z$	axial acceleration (z = 0.001 m)	1.91 m/s^2	0.85 m/s^2
$\overline{F}_r$	radial force (z = 0.001 m)	0.0056 N	0.0056 N
$\overline{a}_r$	radial acceleration (z = 0.001 m)	0.16 m/s^2	0.069 m/s^2

In Section 4.2 *Design Goals*, three modes of operation were described: the wafer holddown mode requires a clamping force only; the vertical positioning mode requires axial and centering forces; and the horizontal positioning mode requires axial and horizontal forces. Table 4.16 lists the applicability of the three simulation models to the desired modes of operation.

Table 4.16 – Applicability of Simulation Models to Modes of Operation

Model	Wafer Holddown Mode	Vertical Positioning Mode	Horizontal Positioning Mode
Single Solenoid	×	×	×
Circular Solenoid Array	✓	×	×
Recto-linear Solenoid Array	✓	✓	✓

Two means of transporting wafers using electromagnetic levitation have been described. Both means meet the stated design goals. While the recto-linear solenoid

array model provides the widest range of choices for modes of operation, it is also the most difficult to control, requiring individualized current waveforms for the solenoids in the array. The circular solenoid array, with two fixed current waveforms, provides a simple means of clamping wafers to end effectors and fixtures. Such a clamped wafer can then be transported between process equipment or secured for individual processing.

4.9 Use of a 2D Linear Motor for Wafer Transport

The recto-linear solenoid array examined in Section 4.7 can be used to generate axial and horizontal forces on a wafer eddy current loop. Such a solenoid array can be extended into a larger, two dimensional array of equally spaced solenoids.

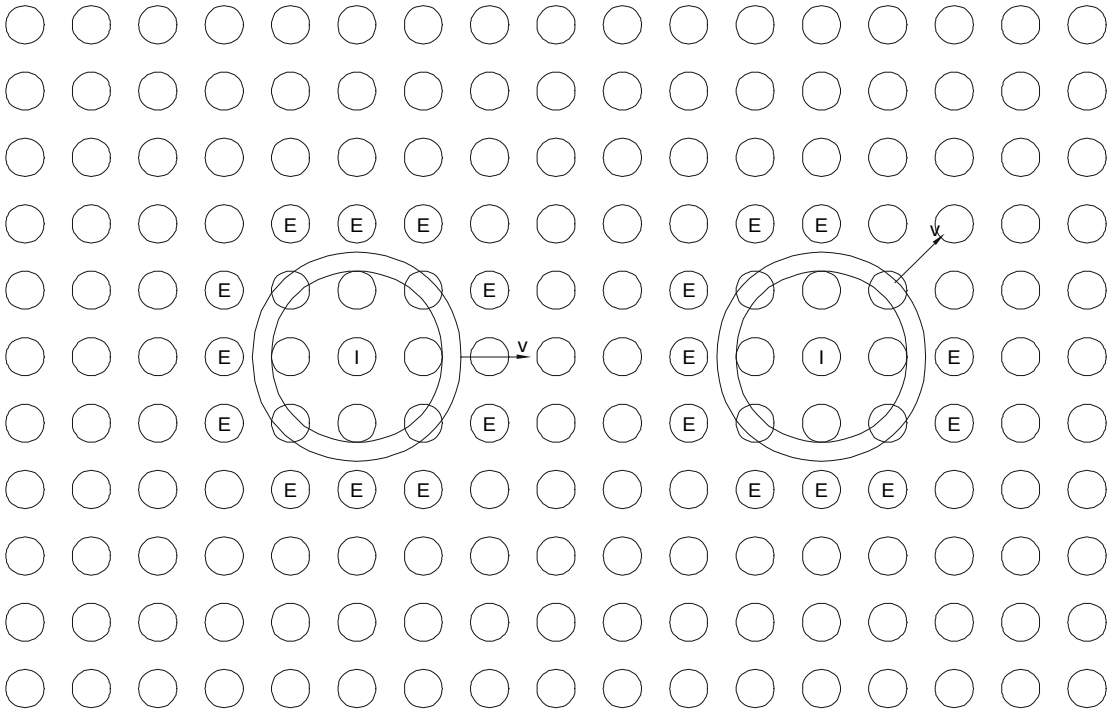

Figure 4.45 – Two Dimensional Linear Motor

In this larger array, only the solenoids near the wafer conducting loop would be utilized to generate forces. By selectively disabling external solenoids, as described in Section 4.7.3, horizontal forces can be generated to move the wafer in the x-y plane. The wafer will move in the x-y plane until a new point of equilibrium of *x* and *y* forces $\overline{F}_x$ and $\overline{F}_y$ is achieved or until the wafer is decelerated by opposing horizontal forces. With position sensing and feedback, a two dimensional linear motor can be created which is capable of precisely positioning wafers in the horizontal *x-y* plane. Figure 4.45 shows a single wafer current loop on such a two dimensional solenoid array.

4.9.1 Applications

A two dimensional linear motor could be used for several different applications in a space-based semiconductor fabrication facility: intraprocess, interprocess, and storage.

Intraprocess applications include holddown and fixturing of the wafer, in place spinning of the wafer by the simultaneous control of horizontal forces on the four conducting loops embedded in the wafer, loading/unloading of the wafer from process equipment, and precise horizontal stepping of the wafer for lithographic and ion implantation applications.

Interprocess applications include all wafer transport between processes. The use of the 2D linear motor operating in a vacuum would eliminate the need for intermediate cassette containers for transport of wafer batches as all wafers would be individually transported and routed.

Storage applications include intermediate storage for work in progress (WIP) and final storage/parking for wafers awaiting packaging for shipment.

Figure 4.46 shows the author's concept of an integrated electromagnetic wafer transport system based upon the 2D linear motor.

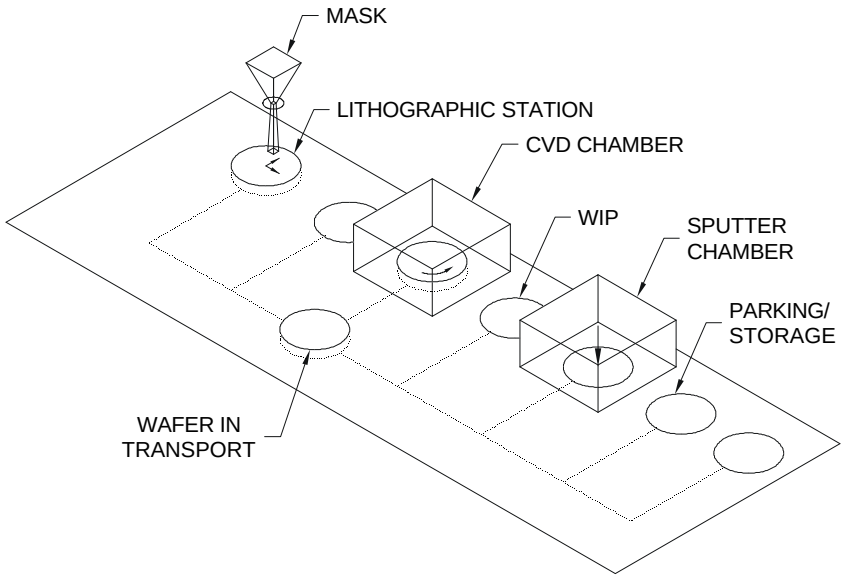

Figure 4.46 – Integrated Electromagnetic Wafer Transport System

4.9.2 Control

Wafer position and velocity feedback is required to enable the 2D linear motor concept to be applied to wafer handling as envisioned above. While the detailed investigation of the control of the 2D linear motor is beyond the scope of this thesis, a brief summary of the topic is described below.

A feedback control system has three components: the actuators, the sensors, and the controller.

The actuator for the 2D linear motor is the recto-linear solenoid array that is used to exert forces on the wafer. The magnitude and direction of those forces can be varied by applying the appropriate current waveforms to the individual solenoids.

Each solenoid must have the frequency, ramp rate, and magnitude of current controlled.

The sensors used in the 2D linear motor include position and velocity sensors. One method of position sensing may be to use non-active solenoids embedded in the transport surface to sense the magnetic field produced by the eddy currents in the wafer conducting loops. The phase shift between the applied magnetic field of the solenoid and the induced magnetic field of the conductor loop may enable a solenoid sensor to discriminate between the two. Alternatively, Hall-effect sensors can be used to sense flux density[86] or more conventional optical position and velocity sensors may be distributed across the transport surface.

The controller in such a wafer transport system must track the actual position and velocity of each wafer as it is transported across the transport surface and compare it to the desired position and velocity. Any deviations from the desired track is corrected by adjusting the current waveforms in the appropriate solenoids in accordance with an internal control model that takes into account the wafer and actuator characteristics. The complexity of the control problem is illustrated by the fact that a single transport surface may be 2 m x 10 m and contain 1.6 million individual solenoids on a 3.5 mm square spacing. Several wafers may simultaneously be in transport or be fixtured. It is envisioned that the control problem may be broken down into smaller portions by subdividing the transport surface into regions, each with its own local microcontroller[87] responsible for local wafers. Coordination would be provided by a central controller. Alternatively, neural network techniques employed for control of unstable magnetic levitation systems[88] may be applied.

4.9.3 Fabrication

The construction of a transport surface containing 1.6 million individual solenoids is a challenge. It is theorized that some of the automated fabrication

techniques currently utilized for the production of LCD pixel arrays may be employed to produce the transport surface. Fabrication of the solenoids from layers of deposited conductors may be feasible. Such active substrate techniques may offer the ability to co-deposit the power driver and control circuits needed for each solenoid as the solenoids themselves are produced.

4.10 Conclusions

This chapter has described a scheme for the transport and fixturing of silicon wafers using electromagnetic levitation. Two detailed numerical models have been developed and evaluated for use in an orbital semiconductor fabrication facility. The circular solenoid array model was shown to be suited for clamping applications. The more complex recto-linear solenoid array model was shown be suited for clamping, vertical positioning, and horizontal transport applications. Both models were shown to be able to provide sufficient forces at reasonable power consumption levels for use with both 200 mm and 300 mm diameter silicon wafers in space. One configuration was able to provide accelerations of -1.91 m/s^2 perpendicular to the wafer and 0.16 m/s^2 parallel to the wafer for a 200 mm diameter wafer using 24 watts of power.

The chapter concluded with a brief description of the issues surrounding the control system required for a two dimensional linear motor based upon the recto-linear solenoid array. Further work in this area is required in order to prove the concept of an electromagnetic wafer handling system. In particular, a more detailed numerical model of the solenoid assembly is required to develop the appropriate control laws for the control system.

Chapter 5

Semiconductor Fabrication Process Modeling

5.1 Introduction

This chapter describes the modeling of semiconductor fabrication processes on Earth and in space with emphasis on the equipment, consumable, and power requirements. The basic processes are identified and a numerical model of each is developed. A detailed process flow for a typical 12 level bi-metal CMOS semiconductor device is specified and used as the basis for simulation of the fabrication process.

A numerical model of the entire fabrication process is developed based on the submodeled individual processes and the specified process flow. The output of this model is a detailed listing of the process time, consumable, energy, and equipment requirements for each process step. The purpose of this process model is to enable the impact of changes in the process flow on these variables to be readily observed.

Using the reference process flow CMOS12_STD, the production parameters per mask level of process time, consumable mass, and energy are found to be: 1.09 days, 65 kg, and 4.7 kW-h. These results compare favourably with industry averages and indicate the overall viability of the model.

5.2 Background

In Section 2.3 *Processes*, eight types of processes used to fabricate semiconductors were identified: material deposition, patterning, material removal,

doping, heating, interprocess transportation, cleaning, testing/inspection. All of the processes, except testing/inspection, are modeled by this simulation.

Semiconductor fabrication is the repeated, sequential application of individual processes to a wafer to build and define the structures of the finished electronic device. Each process may occur in a single piece of equipment or in several pieces of equipment. Each process may be applied to a single wafer or to several wafers in a batch.

A process may be a single step or a series of smaller steps. In order to provide a fine-grained model, all processes have been broken down into single steps which can be represented by simple processes: deposition, patterning, etching, doping, heating, transportation, or cleaning.

The sequence and timing of processes form a recipe called the process flow. Different process flows are used to create different types of devices and the exact process flow used for a given production lot is a function of both the capabilities (equipment and personnel) of the fabrication facility and the type of device.

In order to simulate the entire semiconductor fabrication process, several levels of modeling are required. At the base level are process definitions which specify the types of process (deposition, etching, cleaning), the consumables needed for each process, the process' parameters (temperature, pressure, batch size), and the effects of the processes (deposition rate for thin films, etch rate for material removal). As individual processes may be performed in different types of equipment, equipment definitions are also specified. Each equipment definition describes the mass, volume, cost, and power requirements as well as the type of wafer for which it is suited. Process parameters, including temperatures, pressures, times, batch sizes, process types, and equipment types are specified at an intermediate level of modeling. The process definitions, equipment definitions, and process input parameters are combined through software functions to create a single process model.

In order to allow rapid changes and simplify development, all process modeling is implemented using spreadsheets. Each process and each piece of equipment is defined as a separate worksheet. Process input parameters are specified on a single line of the process flow spreadsheet and are used as arguments to purpose-written software which calculates the process simulation. The resulting process outputs for a single process, such as time, consumables, and energy, are displayed on the same line of the process flow spreadsheet as the input parameters. Appendix B contains the program listing for the process flow modeling software.

The fabrication of an entire wafer is simulated by multiple process lines on the process flow spreadsheet. Post-processing of the spreadsheet allows extraction of key process parameters such as equipment requirements, total processing time, consumable requirements by individual type, and power requirements,

The goal of the simulation is to compare the effects of semiconductor fabrication in space with fabrication on Earth. A key advantage of space-based semiconductor fabrication is the presence of a native vacuum suitable for the majority of fabrication processes. In order to provide an accurate comparison, detailed models of vacuum pumps and the vacuum systems employed in semiconductor fabrication equipment have been developed. These models allow the cost, volume, mass, and power requirements of Earth-based equipment employing vacuum to be accurately estimated.

5.3 Process Definitions

As described above, each process model starts with the definition of the process. A typical process definition, for the thermal oxidation of silicon dioxide, is shown in Table 5.1.

Table 5.1 - Typical Process Definition

Field Tag	Field Value	Field Units
ProcessName	GROW_SIO2	
ProcessType	DEPOSIT	
DepositMatlName	SiO2	
Temperature	1373	deg K
Pressure	1.01E+05	Pa
BasePressure	1.01E+05	Pa
DepositionRate	3.47222E-11	m/s
Power	0	W
BatchSize	120	
WaferSize	200	mm
Matl1Name	N2	
Matl1Type	GAS	
Matl1MassFlow	3.7269E-05	kg/s
Matl1VolumeRatio		
Matl2Name	O2	
Matl2Type	GAS	
Matl2Massflow	5.32414E-06	kg/s
Matl2VolumeRatio		
Matl3Name		
Matl3Type		
Matl3Massflow		kg/s
Matl3VolumeRatio		
Matl4Name		
Matl4Type		
Matl4Massflow		kg/s
Matl4VolumeRatio		

The process definition includes the process name and process type as well as consumable material requirements. Each process also defines process specific parameters such as temperature, pressure, base pressure (the pressure to which the processing chamber must be pumped down to prior to being raised to the process pressure), deposition or etch rate, and process power required.

Table 5.2 shows the eight types of processes that are defined for the parameter ProcessType.

Table 5.2 – Types of Processes

Process Type	Description
DEPOSIT	thin film deposition
ETCH	material removal
PATTERNTRANSFER	exposure for lithographic pattern transfer
DOPE	application of dopants
THERMAL	heating
CLEAN	cleaning
TRANSPORT	transportation of wafer between processes
PRESSURECHANGE	pumpdown or venting of process chamber

The PRESSURECHANGE process was added to the seven previously described process types so that the effects of pressure changes due to pumping down vacuum chambers could be accurately modeled.

A single process definition only describes one step of a multi-step process. The complete process may require many different process definitions. For example, Table 5.3 shows that the complete process flow for the thermal oxidation of silicon to form silicon dioxide can be described by four separate steps: three transport steps and one deposition step.

Table 5.3 – Process Flow for Thermal Oxidation

Process Step	Process Name	Process Equipment	Process Type
Transport to furnace	INTERPROCESSTRANSPORT_CASSETTE	INTERPROCESSCONVEYOR	TRANSPORT
Load into furnace	INTRAPROCESSTRANSPORT_BATCH	FURNACE_BATCH	TRANSPORT
Grow thermal oxide	GROW_SIO2	FURNACE_BATCH	DEPOSIT
Unload from furnace	INTRAPROCESSTRANSPORT_BATCH	FURNACE_BATCH	TRANSPORT

Process definitions for 65 different processes are shown in Appendix C. These processes are shown in Table 5.4 to Table 5.11.

Table 5.4 - Deposition Processes

Process Name	Description
APCVD_PSG	atmospheric pressure chemical vapor deposition of phosphosilicate glass (dielectric)
DEPOSIT_RESIST	deposition of photoresist
GROW_SIO2	thermal (dry) oxidation of silicon to form silicon dioxide
GROW_SIO2_SPACE	thermal (dry) oxidation of silicon to form silicon dioxide in space
GROW_SIO2_WET	thermal (wet) oxidation of silicon to form silicon dioxide
GROW_SIO2_WET_SPACE	thermal (wet) oxidation of silicon to form silicon dioxide in space
PECVD_CARBON	plasma enhanced chemical vapor deposition of amorphous carbon
PECVD_CARBON_SPACE	plasma enhanced chemical vapor deposition of amorphous carbon in space
PECVD_POLYSI	plasma enhanced chemical vapor deposition of polysilicon
PECVD_POLYSI_SPACE	plasma enhanced chemical vapor deposition of polysilicon in space
PECVD_SI3N4	plasma enhanced chemical vapor deposition of silicon nitride
PECVD_SI3N4_SPACE	plasma enhanced chemical vapor deposition of silicon nitride in space
PECVD_SIO2	plasma enhanced chemical vapor deposition of silicon dioxide
PECVD_SIO2_SPACE	plasma enhanced chemical vapor deposition of silicon dioxide in space
SPUTTER_AL	sputter deposition of aluminum
SPUTTER_AL_SPACE	sputter deposition of aluminum in space
SPUTTER_ALOX	sputter deposition of aluminum oxide
SPUTTER_ALOX_SPACE	sputter deposition of aluminum oxide in space

Table 5.5 - Etch Processes

Process Name	Description
DEVELOP_RESIST	develop photoresist
HF_DIP	dip wafer in hydrofluoric acid
ION_MILL	ion milling
PLASMAETCH_AL	plasma etching of aluminum
PLASMAETCH_AL_SPACE	plasma etching of aluminum in space
PLASMAETCH_ORGANICS	plasma etching of organic films
PLASMAETCH_ORGANICS_SPACE	plasma etching of organic films in space
PLASMAETCH_POLYSI	plasma etching of polysilicon
PLASMAETCH_POLYSI_SPACE	plasma etching of polysilicon in space
PLASMAETCH_RESIST	plasma etching of photoresist
PLASMAETCH_SI3N4	plasma etching of photoresist in space
PLASMAETCH_SIO2	plasma etching of silicon dioxide
PLASMAETCH_SIO2_SPACE	plasma etching of silicon dioxide in space
STRIP_RESIST	total removal (stripping) of photoresist
STRIP_SIO2	total removal (stripping) of silicon dioxide

Table 5.6 - Pattern Transfer (Lithographic) Processes

Process Name	Description
PATTERN_LITHO	lithographic pattern transfer
PATTERN_LITHO_DSW	lithographic pattern transfer in direct step and write exposure system
PATTERN_LITHO_DSW_193	lithographic pattern transfer in direct step and write exposure system using 193 nm UV

Table 5.7 - Doping Processes

Process Name	Description
ION_IMPLANT_N_100keV	implant N type dopant using 100 kEv
ION_IMPLANT_N_100keV_SPACE	implant N type dopant using 100 kEv in space
ION_IMPLANT_N_150keV	implant N type dopant using 150 kEv
ION_IMPLANT_N_150keV_SPACE	implant N type dopant using 100 kEv in space
ION_IMPLANT_P_16keV	implant P type dopant using 16 kEv
ION_IMPLANT_P_16keV_SPACE	implant P type dopant using 16 kEv in space
ION_IMPLANT_P_180keV	implant P type dopant using 180 kEv
ION_IMPLANT_P_180keV_SPACE	implant P type dopant using 180 kEv in space
ION_IMPLANT_P_30keV	implant P type dopant using 30 kEv
ION_IMPLANT_P_30keV_SPACE	implant P type dopant using 30 kEv in space
ION_IMPLANT_P_45keV	implant P type dopant using 45 kEv
ION_IMPLANT_P_45keV_SPACE	implant P type dopant using 45 kEv in space

Table 5.8 – Thermal Processes

Process Name	Description
ANNEAL_AL	anneal aluminum
ANNEAL_AL_SPACE	anneal aluminum in space
ANNEAL_IMPLANT	anneal implant damage
ANNEAL_IMPLANT_SPACE	anneal implant damage in space
DIFFUSE_IMPLANT	diffuse implanted dopant
DIFFUSE_IMPLANT_SPACE	diffuse implanted dopant in space
HARDBAKE	hardbake organic photoresist
REFLOW_OXIDE	reflow deposited oxide
REFLOW_OXIDE_SPACE	reflow deposited oxide in space
SOFTBAKE	softbake organic photoresist

Table 5.9 – Cleaning Processes

Process Name	Description
RCA_SC1	RCA Standard Clean 1
RCA_SC2	RCA Standard Clean 2

Table 5.10 – Transport Processes

Process Name	Description
INTERPROCESSTRANSPORT_CASSETTE	transport cassette of wafers between separate process equipment
INTRAPROCESSTRANSPORT_BATCH	transport batch of wafers within single piece of process equipment
INTRAPROCESSTRANSPORT_WAFER	transport single wafer within single piece of process equipment

Table 5.11 – Pressure Change Processes

Process Name	Description
VACUUMPUMPDOWN	pumpdown vacuum chamber
VACUUMPUMPUP	pump up vacuum chamber

5.4 Equipment Definitions

A process step does not occur in isolation, but in concert with a specific piece of equipment. All of the salient characteristics of each piece of equipment are specified in an equipment definition. A typical equipment definition, for a batch furnace used for the thermal oxidation of silicon, is shown in Table 5.12.

Table 5.12 – Typical Equipment Definition

Field Tag	Field Value	Field Units	Field Description
EquipmentName	FURNACE_BATCH		
EquipmentType	THERMAL		
Mass	500	kg	mass of equipment
Volume	2.88	m^3	total volume of equipment
ChamberVolume	2	m^3	volume of chamber that is pumped down
Cost	500000	$USD	cost of equipment
RatedPower	5000	W	rated power of equipment
WaferSize	200	mm	size of wafer for which equipment is designed

The equipment definition includes the equipment name and equipment type as well as physical dimensions, cost and power. The seven types of equipment defined for the parameter EquipmentType use the same names as the types of processes

shown in Table 5.2 with the exception of PRESSURECHANGE which is not a separate equipment type.

Equipment definitions have been made for 13 different pieces of equipment. These definitions are shown in Table 5.13 and are for equipment used in existing commercial semiconductor fabrication facilities on Earth. Characteristics of space-based equipment and advanced Earth-based equipment are derived from the above equipment definitions through a method of functional decomposition whereby the mass, volume, power, and cost of each function of the equipment is assigned and a weighted composite is created. This method is described in detail in Section 6.6.

Table 5.13 – Equipment Definitions

Equipment Name	Equipment Type	Description
PHOTORESIST_SYSTEM	DEPOSIT	system for depositing organic photoresist
PLASMA_CVD_SYSTEM	DEPOSIT	system for plasma enhanced chemical vapor deposition
SPUTTER_SYSTEM	DEPOSIT	system for sputter deposition
LITHO_DSW	PATTERNTRANSFER	direct step on wafer lithographic system
LITHO_DSW_193	PATTERNTRANSFER	direct step on wafer lithographic system using 193 nm exposure
ASHER	ETCH	system for plasma stripping of organic photoresist
DEVELOP_SYSTEM	ETCH	system for developing organic photoresist
PLASMA_ETCHER	ETCH	system for plasma etching
ION_IMPLANTER	DOPE	system for implanting P and N type ions
FURNACE_BATCH	THERMAL	horizontal furnace for batch thermal processes
RTP_SYSTEM	THERMAL	system rapid thermal processing for single wafers
INTERPROCESSCONVEYOR	TRANSPORT	conveyor for wafer cassette transport between separate equipment
WETBENCH	CLEAN	system for batch wet cleaning

It should be noted that while Chapter 4 focused on developing a vacuum-compatible, wafer handling system based upon electromagnetic levitation, such a wafer transport system is not assumed in the following models. Rather, conventional robotic transfer systems, relying upon vacuum and mechanical grips, are assumed for

interprocess conveyor and intraprocess wafer transfer equipment. While there are potential benefits in using an electromagnetic wafer handling system, such as reduced particulate scatter and decreased wafer mechanical damage, it is difficult to quantify the cost and performance of such a system at this time. Therefore, a conservative approach based upon current technology has been adopted for modeling of the wafer transport equipment, both on Earth and in space.

5.5 Process Input Parameters

A single process step is defined by the process definition, the equipment definition, and the process input parameters. These input parameters are shown in Table 5.14.

Table 5.14 – Process Input Parameters

Parameter Name	Units	Description
Wafer Size	mm	size of the wafer used in the process
Starting Pressure	Pa	the absolute pressure at the start of the process
Starting Temperature	deg. K	the absolute temperature at the start of the process
Deposit/Etch Thickness	m	the desired thickness of material to be deposited or removed
Desired Process Pressure	Pa	the desired process pressure
Implant Dose	atoms/cm^2	the implant dose
Desired Process Time	sec	the desired time for the process to last

Not all input parameters are used with each process. For example, only doping processes utilize the Implant Dose parameter and only deposit and etch processes utilize the Deposit/Etch Thickness parameter.

The starting pressure parameter is used to determine the starting pressure during pumpdown cycles and the starting temperature parameter is used to determine the energy required to alter the temperature of wafers and consumables.

The desired process time is used to override default process times specified in process definitions.

The process definition, the equipment definition, and the process input parameters are used by the process model functions described in 5.7 *Process Model Functions* to calculate the process output values.

5.6 Process Output Values

The output values for each process step form the building blocks of the simulation. The values are calculated by purpose-written software based on the input parameter values. Typical process output values are shown in Table 5.15.

Table 5.15 – Process Output Values

Value Name	Units	Description
Process Type		type of process as defined in Table 5.2
Batch Size		number of wafers being processed simultaneously
Process Time	sec	total process time
Incremental Process Time	sec	total process time divided by the number of wafers in batch
Process Temperature	deg. K	process temperature
Process Pressure	Pa	process pressure
Process Base Pressure	Pa	base pressure that process chamber is pumped down to prior to processing
Incremental Pump Energy	J	energy used to pumpdown chamber divided by the number of wafers in batch
Incremental Wafer Mass Energy	J	energy used to heat up single wafer
Incremental Material Mass Energy	J	energy used to heat up consumables divided by the number of wafers in batch
Incremental Doping Energy	J	energy used to dope single wafer
Incremental Process Energy	J	energy used for processing (i.e. RF plasma) divided by the number of wafers in batch
Matl1Name		name of first consumable material
Malt1Type		type (GAS, LIQUID, SOLID) of first consumable material
Incremental Matl1Mass	kg	mass of first consumable material used for single wafer
Matl2Name		name of second consumable material
Malt2Type		type (GAS, LIQUID, SOLID) of second consumable material
Incremental Matl2Mass	kg	mass of second consumable material used for single wafer
Matl3Name		name of third consumable material
Malt3Type		type (GAS, LIQUID, SOLID) of third consumable material
Incremental Matl3Mass	kg	mass of third consumable material used for single wafer
Matl4Name		name of fourth consumable material
Malt4Type		type (GAS, LIQUID, SOLID) of fourth consumable material
Incremental Matl4Mass	kg	mass of fourth consumable material used for single wafer

Many of the output values are shown as incremental values to aid in determining the cost in time, energy and mass of processing a single wafer. The incremental process time is of particular use in calculating equipment requirements; this time may be thought of as the amount of additional equipment time needed to process one more wafer.

The energy is divided into several categories based on the method by which it is used. Energy to operate the vacuum pumps is separated from energy used to heat up the wafer or consumables and energy used for doping and general processing.

The name, phase and mass of up to four separate consumables are tracked for each process step.

5.7 Process Model Functions

Modeling of each process entails determining the time used to achieve the desired process environment, the time needed to conduct the process, the energy required to achieve the desired process environment, the energy required for processing, and the mass and type of consumable materials required.

The process environment is often a vacuum environment and the time $t_{pumpdown}$ to achieve it is dependent upon the starting pressure of the process chamber, the base pressure to which the process chamber is pumped down, and the nature of the vacuum system utilized. Modeling of vacuum pumps and vacuum systems can provide both the time and energy required to achieve a desired process pressure.

The total time $t_{processstep}$ for a single process step is the sum of the time to pumpdown the process chamber $t_{pumpdown}$ and the time for processing $t_{processing}$.

$$t_{processstep} = t_{pumpdown} + t_{processing} \tag{5.1}$$

It is advantageous to calculate the incremental process time $\Delta t_{processstep}$ for each process step as this directly indicates the amount of time required to process a single wafer. The incremental process time $\Delta t_{processstep}$ is the total process time $t_{processstep}$ divided by the number of wafers $n_{processstep}$ in the process batch.

$$\Delta t_{processstep} = \frac{t_{processstep}}{n_{processstep}} \tag{5.2}$$

In many processes, such as thermal oxidation, wet cleaning, diffusing, and annealing, chemical vapor deposition, an elevated temperature T is used. Energy E is required to raise the temperature of both the wafer and process consumables to the process temperature $T_{process}$.

The total energy $E_{processstep}$ for a single process step is the sum of the energy required to pumpdown the chamber $E_{pumpdown}$, the energy required to conduct the processing $E_{processing}$, the energy required to raise the wafers to the process temperature E_{wafer}, the energy required to raise the consumable materials to the process temperature $E_{material}$, and the energy required in that process step to dope the wafer using ion implantation E_{doping}.

$$E_{processstep} = E_{pumpdown} + E_{processing} + E_{wafer} + E_{material} + E_{doping} \tag{5.3}$$

The incremental energy components indicate the amount of energy required to process a single wafer and are calculated by dividing the process energy component by the batch size $n_{processstep}$.

$$\Delta E_{pumpdown} = \frac{E_{pumpdown}}{n_{processstep}} \tag{5.4}$$

$$\Delta E_{processing} = \frac{E_{processing}}{n_{processstep}} \tag{5.5}$$

$$\Delta E_{wafer} = \frac{E_{wafer}}{n_{processstep}} \tag{5.6}$$

$$\Delta E_{material} = \frac{E_{material}}{n_{processstep}} \tag{5.7}$$

$$\Delta E_{doping} = \frac{E_{doping}}{n_{processstep}} \tag{5.8}$$

Process consumables range from DI water for RCA type wet cleans, to aluminum used to form metal interconnects. The type, phase, and mass m of consumables for each step is a function of the process type, film thickness and batch size. As no process step in the model utilizes more than four different consumables, only four consumables are tracked.

The total mass of consumables $m_{processstep}$ for a single process step is the sum of mass m_i for each consumable i used.

$$m_{processstep} = \sum_i m_i \tag{5.9}$$

The incremental mass Δm_i of each consumable is the mass required to process a single wafer and is calculated by dividing the consumable mass m_i by the batch size $n_{processstep}$.

$$\Delta m_i = \frac{m_i}{n_{processstep}} \tag{5.10}$$

The process modeling software functions are available in Appendix B.

5.7.1 Vacuum System Modeling

As shown in Table 3.2, many processes require a vacuum. Achieving this vacuum is the purpose of the vacuum system comprised of one or more vacuum pumps, load lock, piping, valves, and accessories.

It is estimated that approximately 90% of wafer transfers in a contemporary semiconductor fabrication facility occur between process chambers with different ambient conditions (75% are between a vacuum and atmosphere and 14% are between a low and a high vacuum ambient)[89]. Each time the wafer is transferred to a chamber with a different environment, a vacuum pump is used to equalize pressures. In many systems, a small chamber (load lock) is used to minimize the vacuum pumping requirements.

The goal of the vacuum system modeling is to provide the pump speed, pump energy, and pump time needed to achieve a desired process pressure as well as to provide the mass, volume, and cost of the required pump. However, vacuum systems are prone to contamination from many sources, including the seals and components within the system itself[90]. Issues surrounding the periodic preventive maintenance required to deal with hydrocarbons, water vapor, and other contaminants are not included in the following vacuum system model. Nevertheless, this analysis provides a more complete model for estimating those pump parameters than is available in the literature today. They permit the model to answer the important question: what does it cost in terms of those parameters to perform a particular vacuum cycle in a given volume?

5.7.1.1 Types of Vacuum Pumps

The degree of vacuum required is a function of the process. This vacuum degree is arbitrarily divided into four levels with pressure ranges shown in Table 5.16.

Table 5.16 - Vacuum Levels

Vacuum Level	Absolute Pressure Range (torr)
Rough Vacuum	1 - 760 torr
Medium Vacuum	10^{-3} - 1 torr
High Vacuum	10^{-7} to 10^{-3} torr
Ultrahigh Vacuum	< 10^{-7} torr

Different vacuum levels require different types of vacuum pumps. Mechanical pumps are used to achieve rough and medium vacuum levels and form 90% of the number of vacuum pumps used in a typical terrestrial semiconductor fabrication facility[91]. The remaining 10% of the vacuum pumps are used to achieve high and ultrahigh vacuum levels. In a 50,000 sq. ft. fabrication facility, there may be 250 to 300 different vacuum pumps.

There are many types of mechanical pumps. Those used to create a rough vacuum are: piston pump, diaphragm pump, liquid ring pump, rotary pump, rotary piston pump, turbine pump, gaseous ring pump, and liquid jet pump. Other mechanical pumps are used for creating both a rough vacuum and a medium vacuum: sliding vane rotary pump, rotary plunger pump, and Roots pump.

Higher vacuum levels require both a mechanical pump for creating a rough to medium vacuum and a high or ultrahigh vacuum pump. The high and ultrahigh vacuum pumps are extremely sensitive to outlet pressure and require a mechanical "roughing" pump downstream. Typical pumps used to create a high and ultrahigh vacuum are: diffusion pump, sublimation pump, sputter ion pump, cryopump, and turbomolecular pump. The high vacuum pumps most commonly used in today's

processes are the turbopump and the cryopump[91,92], although the diffusion pump is still widely used in many facilities. Turbopumps are increasingly used due to their high reliability and low maintenance requirements, lack of oil vapor backstreaming, simple push-button on-off operation, and tolerance to exposure to atmospheric pressure[93,94,95].

5.7.1.2 Vacuum Pump Performance

Vacuum pump performance is governed by the pumping speed of the pump, the vacuum chamber volume, the vacuum level desired, the type of gas present, and the outgassing rate of the vacuum chamber.

The pumping speed of a vacuum pump is the volume flow rate, commonly expressed as liters per second. The outgassing rate is the volume flow rate that the material in the chamber and the chamber itself produces as the pressure is decreased. Outgassing is caused by gas evolution at low pressures. Both pumping speed and outgassing rate are pressure dependent for a given system.

For a roughing or mechanical pump, the required pump speed S needed to pumpdown a chamber is determined by the chamber volume V, the starting pressure P_0, the ending pressure P_1, and the desired pumpdown time t[96].

$$S = \frac{V}{t} \ln\left(\frac{P_0}{P_1}\right) \tag{5.11}$$

For a high or ultrahigh vacuum pump, the required pump speed for the application is based on the outgassing rate Q and the desired pressure P[97].

$$S = \frac{Q}{P} \tag{5.12}$$

Within the vacuum industry, pressures P_0, P_1, and P in (5.11) and (5.12) are often specified in torr, millibar, or Pascals. Modeling for the simulation has generally been done with all pressures expressed in Pascals except where industry conventions for pump ratings in torr and mbar are used. The conversion between these units is:

$$1\ torr = 133.289\ Pa \tag{5.13}$$

and

$$1\ mbar = 100\ Pa \tag{5.14}$$

5.7.1.3 Manufacturers' Data

Prior to creating a model of the vacuum pumps, a database of characteristics of existing, commercially available vacuum pumps was created. Appendix D contains the entire database, which includes data from 200 combination pumps, cryogenic pumps, diffusion pumps, Roots pumps, roughing pumps, and turbomolecular pumps.

Vacuum pumps are manufactured by a variety of companies for semiconductor fabrication. Representative characteristics, based on manufacturers' data, of different vacuum pumps and different rated pump speeds, are shown in Figure 5.1 to Figure 5.5.

It can be seen that the characteristics are clearly grouped by pump type. Based on the assumption that mechanical roughing pumps and turbomolecular pumps form the bulk of new vacuum systems[93], only these two types of vacuum pumps are modeled. Using this data, empirical models have been fitted for important pump characteristics (mass, volume, and cost) to aid in scaling the process model between various systems. It is noted that outlying data exist in all of these curves. However,

the aim is to develop engineering estimates that are valuable for preliminary system design analyses and for the process flow model.

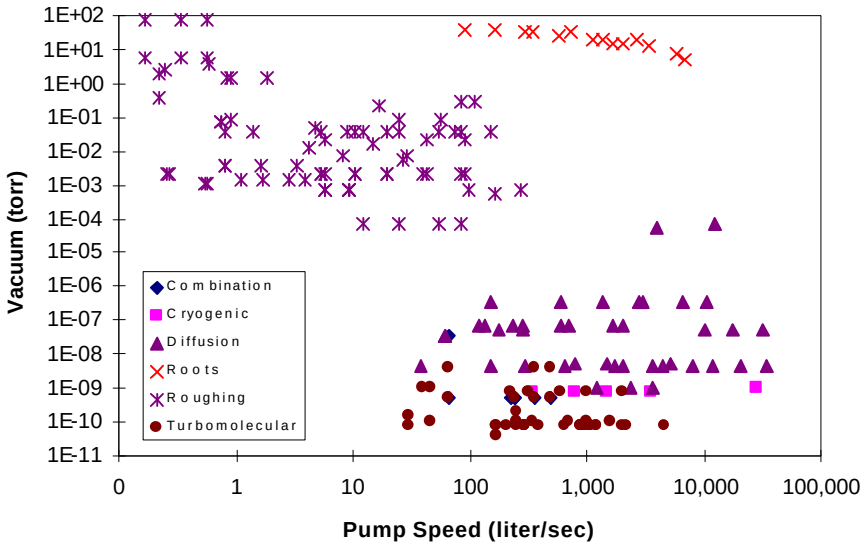

Figure 5.1 – Manufacturers' Data of Vacuum Level

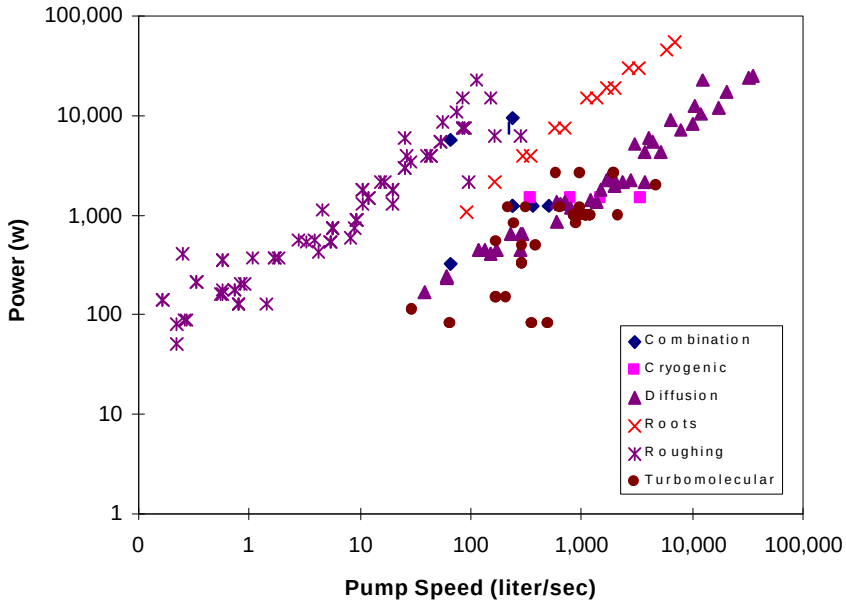

Figure 5.2 – Manufacturers' Data of Vacuum Pump Power

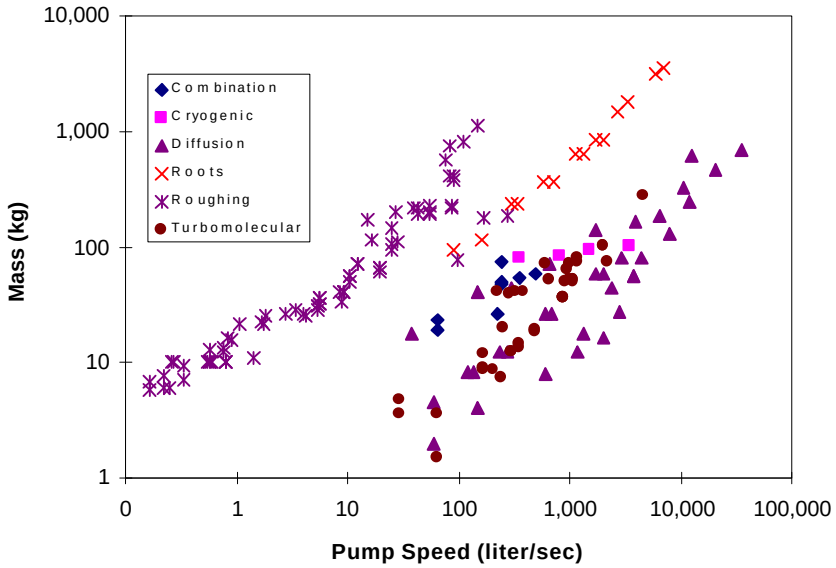

Figure 5.3 – Manufacturers' Data of Vacuum Pump Mass

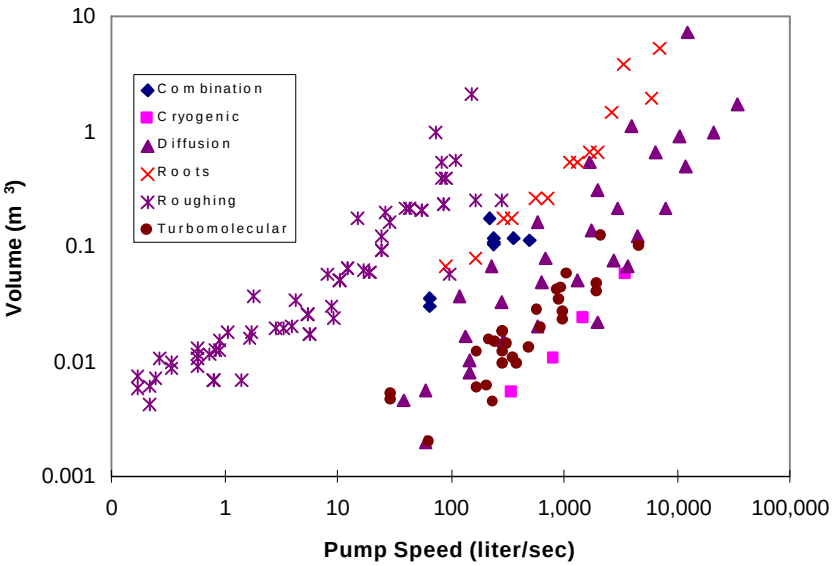

Figure 5.4 – Manufacturer Data of Vacuum Pump Volume

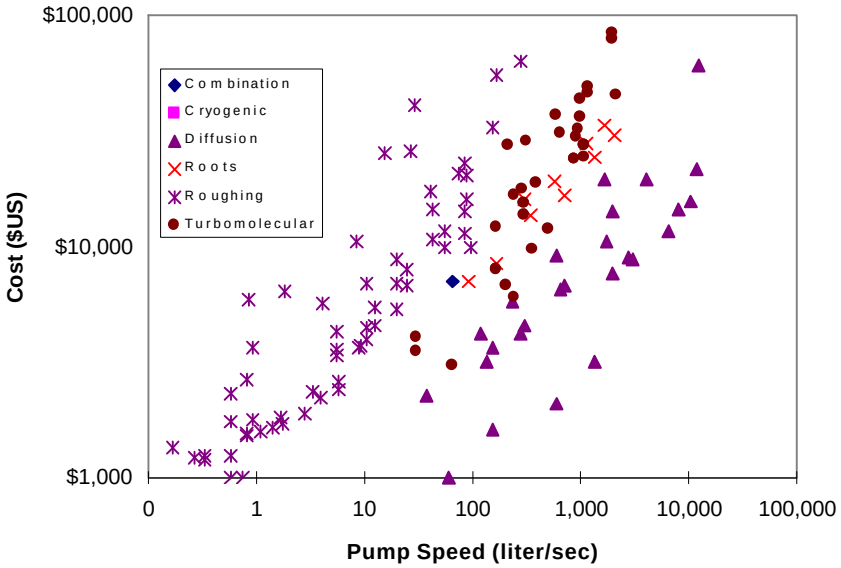

Figure 5.5 – Manufacturers' Data of Vacuum Pump Cost

5.7.1.4 Pump Mass, Volume, and Cost Models

The data shown in Figure 5.3 to Figure 5.5 was used to develop models of pump mass, volume, and cost for roughing pumps and turbomolecular pumps.

The mass of the roughing pump (without accessories) $m_{roughpump}$ was modeled using a least squares fit of pump speed S to the data.

$$m_{roughpump} = -4.8366725 + 5.5432651 * S \tag{5.15}$$

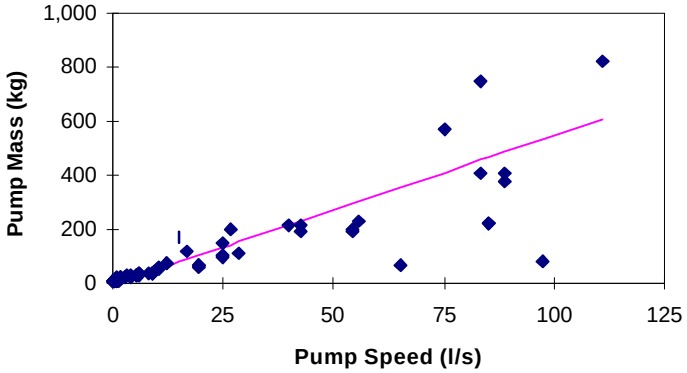

Figure 5.6 – Least Squares Fit of Rough Pump Mass

The mass of the turbomolecular pump (without accessories) $m_{turbopump}$ was modeled using a least squares fit of pump speed S to the data.

$$m_{turbopump} = 8.319785 - 0.039579 * S + 3.63\text{x}10^{-6} * S^2 \tag{5.16}$$

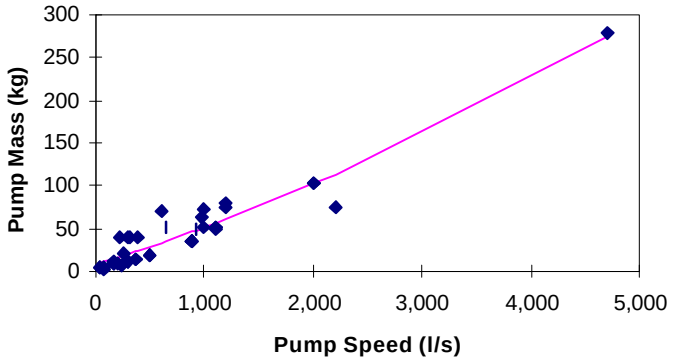

Figure 5.7 – Least Squares Fit of Turbomolecular Pump Mass

The volume of the roughing pump (without accessories) $V_{roughpump}$ was modeled using a least squares fit of pump speed S to the data.

$$V_{roughpump} = 0.049031 - 0.00322 * S + 9.43\text{x}10^{-5} * S^2 \tag{5.17}$$

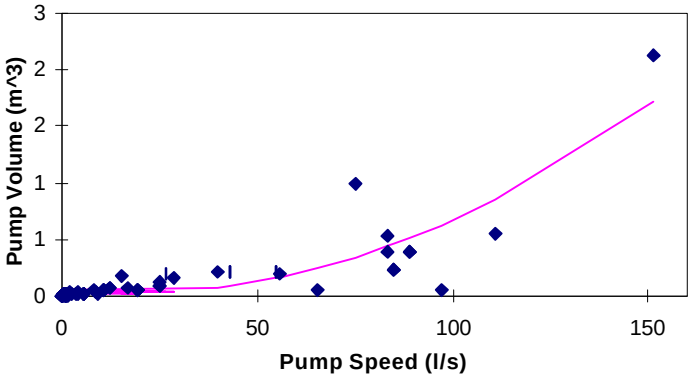

Figure 5.8 – Least Squares Fit of Rough Pump Volume

The volume of the turbomolecular pump (without accessories) $V_{turbopump}$ was modeled using a least squares fit of pump speed S to the data.

$$V_{turbopump} = 0.000041 * S - 4\text{x}10^{-9} * S^2 \tag{5.18}$$

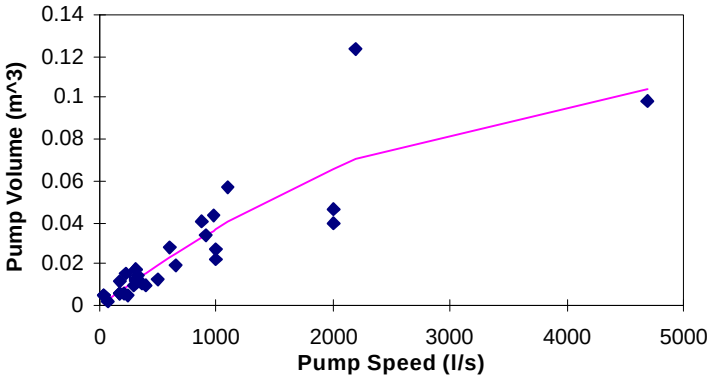

Figure 5.9 – Least Squares Fit of Turbomolecular Pump Volume

The cost of the roughing pump (without accessories) $C_{roughpump}$ was modeled using a least squares fit of pump speed S to the data.

$$C_{roughpump} = 3706.858 + 193.2625 * S - 0.09444 * S^2 \tag{5.19}$$

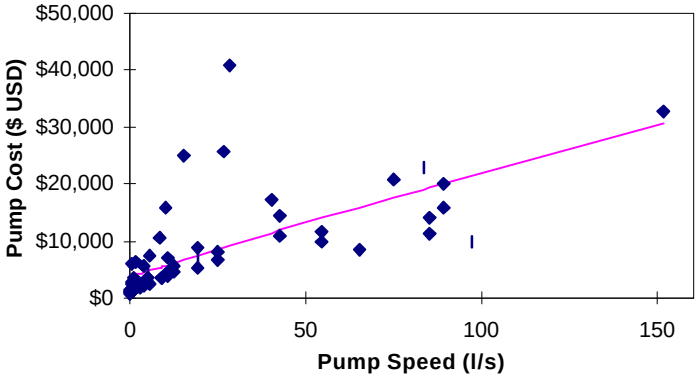

Figure 5.10 – Least Squares Fit of Roughing Pump Cost

The cost of the turbomolecular pump (without accessories) $C_{turbopump}$ was modeled using a least squares fit of pump speed S to the data.

$$C_{turbopump} = 6604.2511 + 27.81521 * S + 0.000307 * S^2 \quad (5.20)$$

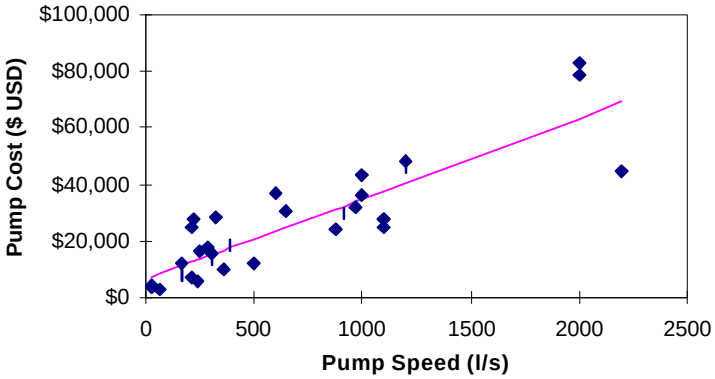

Figure 5.11 – Least Squares Fit of Turbomolecular Pump Cost

5.7.1.5 Pump Speed Models

It is a characteristic of roughing pumps that the pump speed decreases as the pressure at the pump inlet decreases (i.e. with increasing vacuum levels). Turbomolecular pumps, however, have the opposite characteristic that the pump speed increases as the pump inlet pressure decreases, provided that the pump outlet is maintained below a critical pressure.

In order to model pumping speed for a wide range of roughing and turbomolecular pumps, a normalized model has been developed. The normalized pump speed S_{norm} at a given pump inlet pressure P is related to the pumping speed S by the manufacturer's rated speed for the pump S_{rated}.

$$S = S_{norm} * S_{rated} \quad (5.21)$$

Manufacturers' data for four different two-stage, rotary, roughing pumps was used to develop a normalized pump speed curve for mechanical pumps.

$$S_{norm} = 0.004826 + 0.591344 * 0.935114^{\left(\frac{0.952672}{P}\right)} + 0.410706 * 0.76086^{\left(\frac{8.63 \times 10^{-5}}{P^2}\right)} \quad (5.22)$$

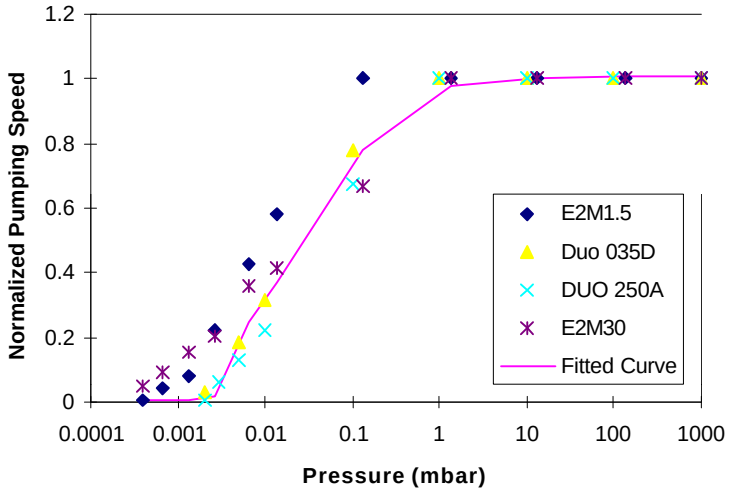

Figure 5.12 – Least Squares Fit of Normalized Pump Speed for Two-Stage Rotary Roughing Pump

Manufacturers' data for four different turbomolecular pumps was used to develop a normalized pump speed curve for turbomolecular pumps.

$$S_{norm} = 1.002665 - 24.2936 * P + 225.6546 * P^2 - 651.085 * P^3 + 448.7343 * P^4 \quad (5.23)$$

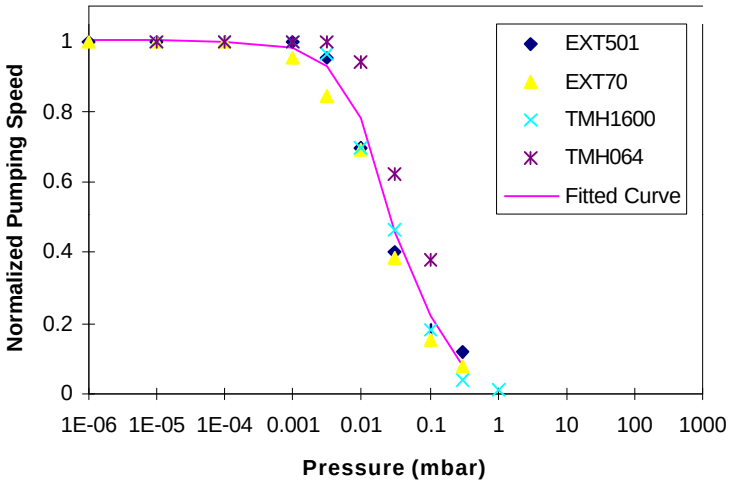

Figure 5.13 – Least Squares Fit of Normalized Pump Speed for Turbomolecular Pump

5.7.1.6 Pump Power Models

The instantaneous input power to the pump motor depends on the pump load and the motor efficiency. The pump load is dependent on the inlet pressure, the pump speed, and the type of pump. For mechanical roughing pumps, the pump power requirement is highest near atmospheric inlet pressure and decreases as the inlet pressure nears the pump's rated vacuum level. The power required for turbomolecular pumps is more uniform and is largely independent of the inlet pressure.

The electrical power required $\dot{W}_{roughpump}$ for mechanical roughing pumps is the sum of the power required for compression $\dot{W}_{compression}$ and the power required to overcome mechanical losses $\dot{W}_{mechloss}$ divided by the motor efficiency η_{motor}.

$$\dot{W}_{roughpump} = \frac{\dot{W}_{compression} + \dot{W}_{mechloss}}{\eta_{motor}} \tag{5.24}$$

The power required for compression arises from the fact that energy is needed to compress a gas. Due to an exhaust orifice restriction in the pump, the highest pressure occurs internally, and the power required is that needed to compress the gas from the inlet pressure P_2 to the internal pressure P_3. Internal pressure P_3 is dependent on the volume flow rate S, the gas density ρ through the orifice, the pump exit pressure P_0, and the loss coefficient K_1 for the pump orifice. A loss coefficient K_1 of 8 x 10^9 was determined from a least squares fit of experimentally measured data from a 4.65 liter/second CD 700 rough mechanical vacuum pump attached to the sputter deposition chamber located at the Simon Fraser University cleanroom.

$$P_3 = P_0 + \rho * S^2 * K_1 \tag{5.25}$$

$$\dot{W}_{compression} = S * (P_3 - P_2) \tag{5.26}$$

The power required to overcome mechanical losses is assumed to increase linearly with the pump speed S. A power loss factor K_2 of 2 Wh/m^3, double that of Roots-type vacuum pumps, is assumed for a two-stage rotary mechanical pump.

$$\dot{W}_{mechloss} = K_2 * S \tag{5.27}$$

Figure 5.14 shows the agreement between measured and calculated power with time for the CD 700 mechanical vacuum pump at the Simon Fraser University cleanroom during a pumpdown of the sputter deposition chamber from atmospheric pressure.

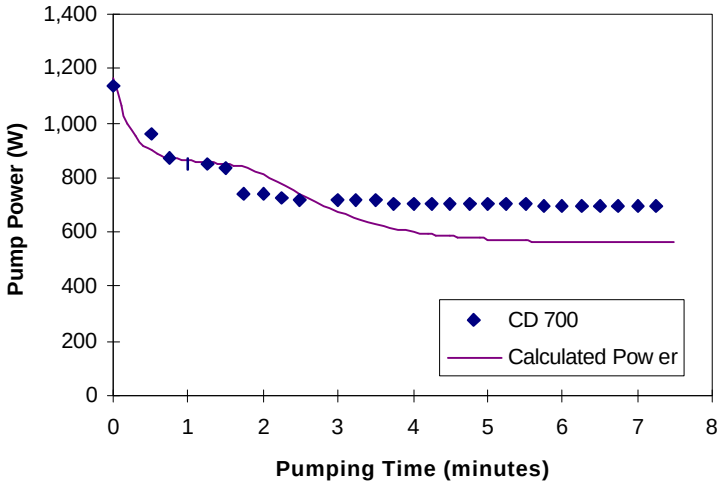

Figure 5.14 – Comparison of Measured and Calculated Rough Pump Power

The electrical power required $\dot{W}_{turbopump}$ for turbomolecular pumps is modeled using a least squares fit of pump speed S to the manufacturers' rated pump power requirements.

$$\dot{W}_{turbopump} = 64.5763 + 1.056991 * S \tag{5.28}$$

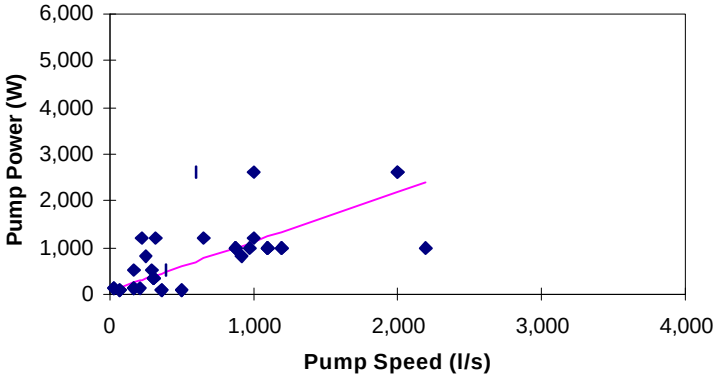

Figure 5.15 – Least Squares Fit of Turbomolecular Pump Power

5.7.1.7 Vacuum Systems Models

The vacuum pump(s) are only one component in the entire vacuum system. The entire system is comprised of the process chamber, the loadlock, the piping between the vacuum chamber and the pumps, the piping from the pumps to the exhaust, and any valves and fittings installed in the piping.

All pipes in the vacuum system restrict the flow of gases and have a conductance value. The conductance C is a measure of the ease with which gas flows from the chamber to the pump and is based on the pipe diameter d, pipe length l, and average pressure in the pipe $\overline{P}$. The conductance C in liters/sec can be determined for a wide range of pressures using (5.29) with pipe diameter d and length l in cm, and average pressure $\overline{P}$ in mbar[98].

$$C = \frac{135 * d^4}{l} * \overline{P} + \frac{12.1 * d^3}{l} * \frac{l + 192 * d * \overline{P}}{l + 237 * d * \overline{P}} \tag{5.29}$$

The effective pump speed S_{eff} at the end of the pipe is less than the pump speed S at the pump inlet due to the resistance to flow in the pipe[98]. Large diameter pipes reduce the losses and enable S_{eff} to be closer to S.

$$Se_{ff} = \frac{C * S}{C + S} \tag{5.30}$$

A single pump, rough or medium vacuum system is modeled as a chamber of volume V connected by a pipe of diameter d and length l to the pump inlet as shown in Figure 5.16.

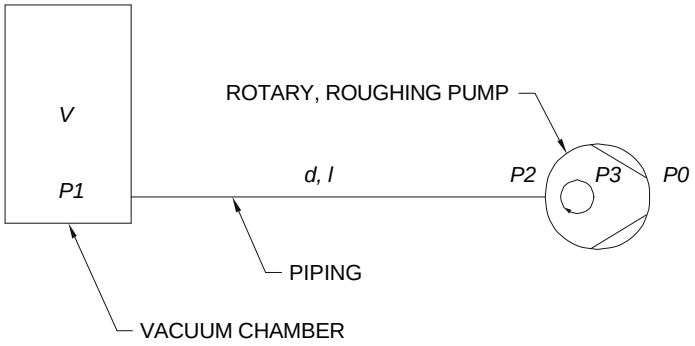

Figure 5.16 – Single Pump Vacuum System

The time and energy required to pumpdown the chamber from the starting pressure of P_{start} to the ending pressure P_{end} with a specified pump size is calculated in an iterative manner using a series of small time steps *dt*. In each time step, the conductance *C* is calculated based on the current chamber pressure and pump inlet pressure. The normalized pump speed is calculated for the inlet pressure and multiplied by the rated pump speed to determine the actual pump speed for the time step. The pump power at the current pump speed and pump pressure is calculated from (5.24) to (5.27). The total energy $E_{pumpdown}$ required during the pumpdown cycle is the integration of the power required for each time step.

$$E_{pumpdown} = \int \dot{W}_{roughpump} * dt \tag{5.31}$$

In each time step, a volume of gas *dV* is removed from the vacuum chamber.

$$dV = S_{eff} * dt \tag{5.32}$$

The quantity of gas added to the chamber through outgassing is subtracted from the quantity of gas removed from the chamber by the vacuum system to determine the net quantity of gas removed from the vacuum chamber. Using the equation of state for an ideal gas[99]

$$P*V = n*R*T \tag{5.33}$$

the new chamber pressure P_0 at the end of the timestep dt can be calculated from the knowledge of the number of moles n of gas remaining in the chamber, the chamber temperature T, and chamber volume V.

The timesteps dt are repeated until the chamber pressure is less than or equal to the desired chamber pressure P_{end}.

Figure 5.17 shows a comparison of the measured and calculated pressure during a pumpdown of the sputter deposition chamber at the Simon Fraser University cleanroom. Note that the initial slope of the pumpdown curve is very close to that predicted by (5.11).

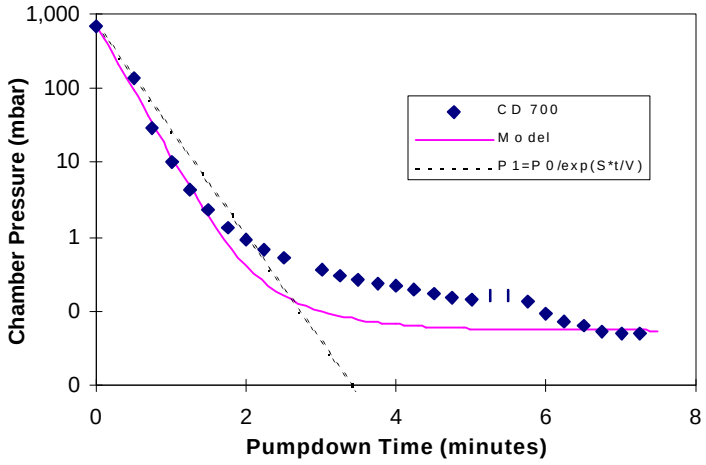

Figure 5.17 – Comparison of Measured and Calculated Chamber Pressure

A two pump, high vacuum system, with the turbomolecular pump installed upstream of the roughing pump, is shown in Figure 5.18. This system is modeled in a manner similar to that of the one pump vacuum system described above, with the addition of another pipe of conductance C_2 between the outlet of the turbo molecular pump and the inlet of the roughing pump. The energy and time required for a pumpdown cycle with two pumps is calculated by the same type of iterative procedure described for the single pump system.

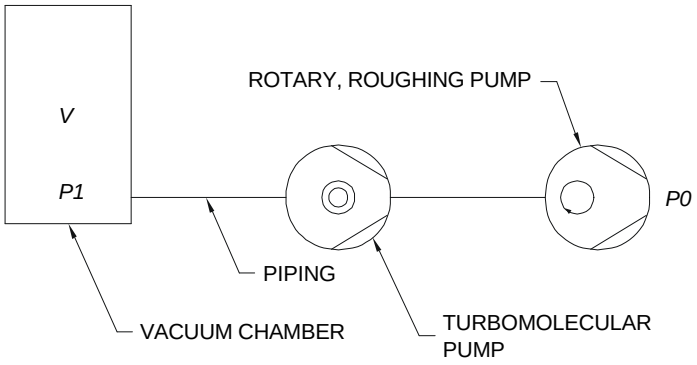

Figure 5.18 – Two Pump Vacuum System

5.7.2 Energy Use Modeling

The total energy used in a process is calculated according to (5.3). The energy used to create a vacuum $E_{pumpdown}$ is calculated by (5.31). The energy used for processing $E_{processing}$ is determined by the power field value $\dot{W}_{processing}$ in the Process Definition record and the processing time $t_{processing}$.

$$E_{process\,ing} = \dot{W}_{processing} * t_{processing} \tag{5.34}$$

The energy E_{wafer} used to heat a wafer from starting temperature T_{start} to process temperature $T_{process}$ is modeled based on the wafer mass m_{wafer} and specific heat C_{wafer}.

$$E_{wafer} = m_{wafer} * C_{wafer} * \left(T_{process} - T_{start}\right) \tag{5.35}$$

Energy lost to the environment due to cooling of the wafer is assumed to be lost from the model and is not recaptured for subsequent processing.

Energy $E_{material}$ is used to heat consumables such as gases during CVD processes or DI water during wet clean processes. This energy is determined by the mass m_i and specific heat C_i of each consumable i used.

$$E_{material} = \sum_i m_i * C_i * \left(T_{process} - T_{start}\right) \tag{5.36}$$

Energy E_{doping} is used to accelerate doping ions during ion implantation processes. E_{doping} is based on the area to be doped A, the implant dose per unit area $Dose$, the energy of a single ion E_{ion}, and the unit charge of one electron q.

$$E_{doping} = A * Dose * E_{ion} * q \tag{5.37}$$

5.7.3 Consumable Use Modeling

The mass m_i of consumable i is calculated by two different methods depending on whether the process uses a continuous flow or a batch quantity of the consumable during processing.

The Process Definition record (Table 5.1) for a process indicates whether the mass flow or volume ratio is used to calculate the quantity of consumable *i* used in processing.

5.7.3.1 Continuous Flow

For continuous flow processes, the MassFlow field value $\dot{m}_i$ is specified and the mass m_i of consumable *i* used in the process is determined by the time for processing $t_{processing}$.

$$m_i = \dot{m}_i * t_{processing} \tag{5.38}$$

5.7.3.2 Batch Flow

For a process that uses a single batch of consumables, the number of moles of all consumables Δn required to raise the chamber pressure from the base pressure P_{base} attained during pumpdown to the process pressure $P_{process}$ is calculated through rearranging (5.33).

$$\Delta n = \frac{\left(P_{process} - P_{base}\right) * V}{R} \tag{5.39}$$

The number of moles Δn_i of consumable *i* is determined by the VolumeRatio field value vf_i using an ideal gas assumption for all consumables.

$$\Delta n_i = vf_i * \Delta n \tag{5.40}$$

The mass m_i of consumable *i* is calculated from the molecular weight MW_i and the number of moles Δn_i.

$$m_i = MW_i * \Delta n_i \tag{5.41}$$

5.7.4 Summary of Process Modeling

The preceding section described the basic methods by which time, energy, and mass flows are determined by the semiconductor fabrication process model. The functions to calculate the desired variables are implemented in purpose-written software listed in Appendix B.

Each process step in a complete process flow is modeled using these methods. Combining such steps leads to a multi-process model, post-processing of which allows key parameters such as cumulative time, energy, and mass to be extracted.

5.8 Process Flow

A multi-process model is a sequential series of individual process steps, each of which is modeled using the methods described in Section 5.7. The sequence of process steps, referred to as the process flow, forms the recipe by which the semiconductor device is fabricated. The process flow determines the sequence of layers and the methods used to fabricate each layer.

The process flow used to create the reference model is for a 12 level bi-metal CMOS device. This process flow had previously been used for modeling semiconductor fabrication optimization[100] and was adopted on the basis that it provides a readily verifiable model. A condensed version of the process flow is shown in Table 5.17. The reference process flow CMOS12_STD has 386 individual process steps and is fully listed in Appendix E.

Each process listed in the condensed process flow above is composed of many individual process steps, each of which is included in the model.

Table 5.17 – Reference Process Flow CMOS12_STD (12 Level Bi-metal CMOS)

Major Step	Process	Major Step	Process
1	**Form N-tub**	**8**	**Form Spacer**
	Lithography (Mask #1 - NW)		Oxide
	N-Tub Etch		Anisotropic Etch
	Strip Resist		Screening Oxide
	Screening Oxide		Lithography (Mask #5 - SN)
	N-Tub Implant		N Source/Drain Implant
	N-Tub Diffusion		Strip Resist
	Strip Oxide	**9**	**Form P-S/D**
2	**Form Nitride**		Lithography (Mask #6 - SP)
	Oxide		P Source/Drain Implant
	Nitride Deposition	**10**	**Form Contacts**
	Lithography (Mask #2 - OD)		Oxide
	Nitride Etch		Reflow
	Strip Resist		Lithography (Mask #7 - CO)
3	**Form Channel Stop**		Oxide Etch
	Lithography (Mask #3 - NWI)		Strip Resist
	Oxide Etch	**11**	**Form Metal 1**
	Channel Stop Implant		Al Deposition
4	**Form Anti-Punch-Through**		Lithography (Mask #8 - IN)
	Anti-Punch-Through Implant		Al Etch
	Strip Resist	**12**	**Planarize**
5	**Form Field Oxide**		Plasma Oxide
	Field Oxidation		Resist Spin-On
	Etchback		Etchback
6	**Form Gate**	**13**	**Form Vias**
	Gate Oxidation		Lithography (Mask #9 - COS)
	Screening Poly		Oxide Etch
	Threshold Adjust Implant		Strip Resist
	Gate Poly	**14**	**Form Metal 2**
	Lithography (Mask #4 - PS)		Al Deposition
	Poly Etch		Lithography (Mask #10 - INS)
	Strip Resist		Al Etch
7	**Form N-S/D**		Strip Resist
	Lithography (Mask #5 - SN)	**15**	**Package**
	N-LDD Implant		

Table 5.18 –Example of Expanded Process Flow to Form N Tub

Process Step	Sub Process Step	Sub Sub Process Step
	Clean Wafer	Transport to RCA Clean
		RCA Clean 1
		Transport to RCA Clean 2
		RCA Clean 2
	Grow thin oxide	Transport to furnace
		Load into furnace
		Thermal oxide growth
		Unload from furnace
	Apply photoresist	Transport to photoresist system
		Prebake wafers
		Transport to deposit resist
		Deposit resist
		Transport to softbake
		Softbake wafers
Lithography (Mask #1 - NW)	Pattern N-Well. (Mask #1)	Transport to aligner
		Expose wafer
	Develop photoresist	Transport to developer
		Develop resist
		Transport to hardbake
		Hardbake wafers
N-Tub Etch	Etch oxide	Transport to etcher
		Etch oxide
Strip Resist	Strip photoresist	Transport to asher
		Strip photoresist
	Clean Wafer	Transport to RCA Clean
		RCA Clean 1
		Transport to RCA Clean 2
		RCA Clean 2
Screening Oxide	Grow thin oxide	Transport to furnace
		Load into furnace
		Thermal oxide growth
		Unload from furnace
N-Tub Implant	Deposit N type impurities	Transport cassette to implanter
		Transport to loadlock
		Pumpdown loadlock
		Transport to implant chamber
		Implant n type
		Transport to loadlock
		Pumpup loadlock
		Transport to cassette

Table 5.18 –Example of Expanded Process Flow to Form N Tub continued

Process Step	Sub Process Step	Sub Sub Process Step
N-Tub Diffusion	Diffuse N type impurities	Transport to furnace
		Load into furnace
		Diffuse impurities
		Unload from furnace
Strip Oxide	Strip Oxide	Transport to oxide strip
		Strip oxide

Table 5.18 shows the expanded process flow to form the N tub from Table 5.17. Appendix F contains time, energy, and mass results for the process flow of Table 5.18.

5.9 Material Properties

Calculation of energies, pressures and consumable masses is dependent upon the properties of the materials used. A database of properties for the materials shown in Table 5.19 is used by the model and is available in Appendix G.

Table 5.19 – Materials in Properties Database

No.	Material	No.	Material	No.	Material
1	Al	9	DIWATER	17	NH4OH
2	Ar	10	H2O2	18	O2
3	BCl3	11	HCl	19	PH3
4	BF3	12	He	20	PhotoResist
5	C4H8	13	HF	21	PhotoResistDeveloper
6	CARBON	14	N2	22	SF6
7	CF4	15	N2O	23	SiH4
8	Cl2	16	NH3		

5.10 Fabrication Simulation Modeling

Implementation of the multi-process model described in Section 5.8 provides a model suitable for simulation of the entire fabrication process. Post-processing of

the results of individual process steps provides the information needed to determine energy, consumable, and equipment requirements for a particular process flow.

The output of post-processing the fabrication simulation results are three summaries: equipment use, material use, and energy use.

The equipment use summary lists for each piece of equipment: process time, incremental process time, number of uses of that piece of equipment for a single wafer. This information is used in Section 7.2.1 as the basis for determining equipment requirements to meet a given production goal.

The mass use of materials is categorized by both phase and wafer level.

The energy use during fabrication is categorized by both energy category and wafer level. The energy categories are: Pump Energy, Wafer Mass Energy, Material Mass Energy, Doping Energy and Process Energy as described in Section 5.7 and equation (5.3).

5.11 Fabrication Simulation Results

The fabrication simulation model described in the preceding sections was run with the reference process flow (12 level bi-metal CMOS) to reflect conventional semiconductor fabrication processes in an Earth-based facility. Detailed results are available in Chapter 7. Summarized results are shown in Table 5.20 to Table 5.22.

The total process time of 227,206 seconds provides a per layer average of 1.09 days assuming that the wafers spend five times as much waiting for equipment as they do processing[73]. This is at the lower end of the results of the University of California at Berkeley's Competitive Semiconductor Manufacturing Survey, which showed that actual cycle times in modern semiconductor fabrication facilities varied from 1.2 to 3.3 days per masking level[101].

The amount of liquid consumed during the fabrication of a single wafer can be attributed primarily to the RCA-type cleans extensively utilized. Each RCA clean

requires approximately 38 liters of DI water. The 779 kg of liquid used equates to a per layer average of 65 kg. For comparison, the Semiconductor Industry Association estimates that up to 650 to 1,500 gallons of DI water are required to process a 200 mm wafer from start to finish[62], leading to a minimum per layer average of approximately 82 kg. The underestimation of DI water consumption by the model is thought to be due to the use of a simple CMOS process flow (12 level bi-metal) which does not utilize CMP processes, a large consumer of DI water.

The energy use of 201,351,743 J per wafer provides a per layer average of 4.7 kW-h. The Semiconductor Industry Association estimates that 3.2 to 4.5 kW-h per square inch are required to process a 200-mm wafer[102], leading to a minimum per layer average of approximately 5.4 kW-h. Again, the underestimation of energy by the model is due to the use of a simple CMOS process flow (12 level bi-metal) which does not utilize CMP processes, a large consumer of DI water. Of the energy used, the model shows that 97% is used to heat consumable material, primarily liquids for RCA cleans.

Table 5.20 – Equipment Use for Reference Process Flow

	Process Time		**Incremental Process Time**		
Equipment	**(sec)**	**(%)**	**(sec)**	**(%)**	**Uses**
INTERPROCESSCONVEYOR	33,251	15%	1,385	5%	108
WETBENCH	66,778	29%	1,341	5%	52
FURNACE_BATCH	39,624	17%	840	3%	27
PHOTORESIST_SYSTEM	45,630	20%	2,275	8%	65
LITHO_DSW	864	0%	864	3%	12
DEVELOP_SYSTEM	20,244	9%	1,016	4%	36
PLASMA_ETCHER	5,276	2%	5,276	18%	15
ASHER	2,086	1%	2,086	7%	12
ION_IMPLANTER	1,653	1%	1,653	6%	49
PLASMA_CVD_SYSTEM	7,457	3%	7,457	26%	7
SPUTTER_SYSTEM	4,313	2%	4,313	15%	2
RTP_SYSTEM	30	0%	30	0%	1
Total	**227,206**	**100%**	**28,537**	**100%**	**386**

Table 5.21 – Consumable Material Use (kg) for Reference Process Flow

	Level 1 N-well	Level 2 Nitride	Level 3 Channel Stop	Level 4 Gate	Level 5 N-LDD	Level 6 N source /drain
GAS	0.0072	0.0130	0.0056	0.0082	0.0012	0.0051
LIQUID	89.5017	47.2517	90.3975	89.5017	47.2517	47.2517
SOLID	0.0000	0.0000	0.0000	0.0000	0.0000	0.0000
All Phases	**89.5089**	**47.2647**	**90.4032**	**89.5099**	**47.2529**	**47.2568**

	Level 7 P source /drain	Level 8 Contacts	Level 9 Metal 1	Level 10 Vias	Level 11 Metal 2	Level 12 Cover Glass
GAS	0.0013	0.0053	0.0016	0.0166	0.0021	0.0165
LIQUID	47.2517	47.2517	47.2517	89.5034	47.2517	89.5017
SOLID	0.0000	0.0000	0.0002	0.0000	0.0002	0.0000
All Phases	**47.2530**	**47.2570**	**47.2534**	**89.5200**	**47.2540**	**89.5182**

	Total
GAS	0.0838
LIQUID	779.1679
SOLID	0.0003
All Phases	**779.2521**

Table 5.22 – Energy Use (J) for Reference Process Flow

Energy Category	Level 1 N-well	Level 2 Nitride	Level 3 Channel Stop	Level 4 Gate	Level 5 N-LDD	Level 6 N source /drain
Pump	130,220	97,665	227,886	162,775	32,555	130,220
Wafer	267,726	103,632	97,099	128,355	10,376	103,632
Material	22,985,794	11,492,052	22,982,851	22,984,371	11,490,391	11,491,945
Doping	37,699	0	41	2	101	25,133
Process	78,857	179,357	108,857	675,857	36,000	144,857
All	**23,500,296**	**11,872,706**	**23,416,733**	**23,951,360**	**11,569,422**	**11,895,787**

Energy Category	Level 7 P source /drain	Level 8 Contacts	Level 9 Metal 1	Level 10 Vias	Level 11 Metal 2	Level 12 Cover Glass
Pump	65,110	97,665	97,665	162,775	97,665	97,665
Wafer	35,611	88,260	10,376	27,925	43,810	23,570
Material	11,490,400	11,492,118	11,490,391	22,985,631	11,490,644	22,985,631
Doping	4,524	0	0	0	0	0
Process	66,857	144,857	678,857	409,714	678,857	378,857
All	**11,662,503**	**11,822,901**	**12,277,289**	**23,586,046**	**12,310,976**	**23,485,724**

	Total
Pump	1,399,869
Wafer	940,371
Material	195,362,219
Doping	67,499
Process	3,581,786
All	**201,351,743**

5.12 Conclusions

This chapter has described a model for the simulation of the semiconductor fabrication process. A detailed numerical model was developed and evaluated using a reference semiconductor process flow. The results indicated that the model underestimated material use and energy compared with more sophisticated process flows used in industry, and it was found that such results were consistent with the simple process flow used.

The model does provide a means to examine changes to the process flow, process parameters, and equipment in order to evaluate the feasibility of space-based semiconductor fabrication.

In Chapter 6 the model will be used to compare modified process flows for both Earth and space-based environments.

Chapter 6
Optimization of Process Flows

6.1 Introduction

This chapter will describe the manner in which process flows are optimized for space-based semiconductor fabrication. Related processes and equipment will be examined, and new models that are suited for a high vacuum, microgravity environment will be developed.

It will be shown that the removal of liquids from the entire process flow is a requirement to allow semiconductor processing in a vacuum environment. Alternative, dry cleaning and lithographic processes will be introduced, and issues surrounding the use of these new processes will be examined.

6.2 Background

In Section 3.4 *Difficulties for Orbital Manufacturing of Semiconductors*, wet processes and lithography were identified as barriers to manufacturing semiconductor devices in a microgravity, vacuum environment. Alternatives to both of these processes must be developed in order to allow space-based semiconductor fabrication to be feasible.

Wet processes pose two problems for a space-based fabrication system: high transport mass and material handling. The high mass adds significantly to the transport cost to orbit, shown later in Table 9.4 to dominate the economic feasibility of space-based semiconductor fabrication. The difficulty in handling and applying a liquid material in a high vacuum environment is due to the fact that the vapor pressure of liquids (such as DI water) is very high compared to the desired ambient

vacuum environment ($<10^{-7}$ torr), resulting in immediate vaporization of the liquid upon exposure to the vacuum environment.

It is seen in Table 5.21 that the amount of liquid material used in wafer fabrication with the reference process flow constitutes 779 kg or almost 100% of the consumable material use on a mass basis. Based on this, it is theorized that the elimination of all liquid consumables would greatly reduce the consumable mass requirements.

Table 6.1 shows the processes in the reference process flow that use liquid as a consumable.

Table 6.1 – Wet Processes in Reference Process Flow

Process Name	Description	Liquids Used
RCA_SC1	remove organics, particles	DIWATER, HF, H2O2, NH4OH
RCA_SC2	remove metals	DIWATER, HCl, H2O2
DEPOSIT_RESIST	deposit organic photoresist	PHOTORESIST
DEVELOP_RESIST	develop organic photoresist	PHOTORESISTDEVELOPER, DIWATER
HF_DIP	remove native silicon dioxide	DIWATER, HF

A breakdown of the quantities of liquids used with the reference process flow is shown in Table 6.2.

Table 6.2 – Liquids Used in Reference Process Flow

Liquid Name	Mass Used (kg)	% of Consumable Mass
DIWATER	702.6	90.16%
HF	12.81	1.64%
H2O2	31.88	4.09%
NH4OH	17.00	2.18%
HCl	14.88	1.91%
PhotoResist	0.022	0.00%
PhotoResistDeveloper	7.540E-07	0.00%

These tables shown that the wet cleaning processes (RCA_SC1, RCA_SC2, HF_DIP) are responsible for almost all of the liquid consumption. Based on this

information, it is seen that dry, alternative cleaning processes must be developed that provide the same functionality as the wet cleaning processes in the reference process flow. Table 6.3 shows the process flow for the wet cleaning step employed in the reference process flow.

Table 6.3 –Conventional, Wet Cleaning Process Flow

Process Step	ProcessName	ProcessEquipment
Transport to RCA Clean	INTERPROCESSTRANSPORT_CASSETTE	INTERPROCESSCONVEYOR
RCA Clean 1	RCA_SC1	WETBENCH
Transport to RCA Clean 2	INTRAPROCESSTRANSPORT_BATCH	WETBENCH
RCA Clean 2	RCA_SC2	WETBENCH

Table 6.2 also shows that alternatives to liquid photoresist and photoresist developer must be developed if the goal of a completely dry process is to be achieved. While the mass of liquid photoresist and developer is small compared with that of the cleaning fluids, the difficulty in applying and utilizing the photoresist in a high vacuum, microgravity environment remains.

Section 2.3.2.1 *Optical Lithography with Conventional Photoresist* described the current lithographic process employed for commercial semiconductor fabrication. This process utilizes a photosensitive liquid polymer as a resist. Droplets of the resist are applied to a spinning wafer to form a uniform, thin (1 micron) film. The resist is exposed to a UV source through a mask to define a pattern, and the unneeded resist is removed by a liquid photoresist developer. The wafer is then washed in DI water before proceeding to the next processing step (deposition, etching, doping). Once the patterned resist is no longer required, it is removed by a combination of plasma etching and wet chemical cleaning. Any dry, alternative lithographic process developed for a high vacuum, microgravity environment must provide the same

functionality as the lithographic process described above with respect to resist application, exposure, development, and removal.

6.3 Alternative Cleaning Processes

Alternatives to wet cleaning processes already exist and semiconductor fabrication facilities are adopting them in a move to conserve water[103,20]. The Semiconductor Industry Association predicts that water consumption will need to be reduced by 40% over the next decade[62]. With the construction of the pure DI water production and chemical waste handling facility estimated to be 15% of the construction costs for a semiconductor plant[104], operators of semiconductor fabrication facilities are seeking means to reduce the amount of liquids utilized in the production process. In addition, wet processes are not easily integrated with cluster tools and their cost-of-ownership is increasing due to the cost of used chemical disposal[103].

The Microelectronics Manufacturing Science and Technology (MMST) program, a study to lower the capital cost of fabrication facilities and decrease the cycle time, determined that 100% single wafer processing and a minimum of 95% dry processing was required to achieve that goal[105]. Determining replacements for wet cleaning processes was a part of that project.

Methods to reduce the amount of liquids used in processing include the re-use of DI water, changing from liquid cleaning baths to sprays, and the use of plasma processes. In general, these processes readily remove native oxides and organics, but do little to remove particles on the surface of the wafer.

The need to replicate the functionality of the RCA or similar type wet cleans currently employed has resulted in the development of a cleaning process flow that includes the following steps: plasma etch in oxygen to remove organics, plasma etch

in CF_4 to remove silicon dioxide, and ion milling to remove particles. The process flow for this alternative, dry cleaning process is shown in Table 6.4

Table 6.4 –Alternative, Dry Cleaning Process Flow

Process Step	ProcessName	ProcessEquipment
Transport to dry clean process	INTERPROCESSTRANSPORT_CASSETTE	INTERPROCESSCONVEYOR
Remove organics	PLASMAETCH_ORGANICS_SPACE	PLASMA_ETCHER
Remove oxide	PLASMAETCH_SIO2_SPACE	PLASMA_ETCHER
Transport to ion mill process	INTERPROCESSTRANSPORT_CASSETTE	INTERPROCESSCONVEYOR
Remove metals & particles	ION_MILL	SPUTTER_SYSTEM

Compared to the RCA cleaning process flow shown in Table 6.3, the alternative clean is conducted in two separate pieces of equipment: a plasma etcher capable of supplying both O_2 and CF_4, and an ion milling system. Both plasma processes and the ion milling process are conducted in a partial vacuum and are suitable for use in both a gravity and a microgravity environment.

Plasma etching is currently used in production facilities for the removal of organics such as photoresist (asher) and oxides, but is not used for particle removal due to the time required for ion milling.

Ion milling requires a high base vacuum and is itself a slow process. The combination results in large pumpdown and processing times. It is proposed that the presence of a native vacuum in a space-based facility will eliminate the pumpdown time and make ion milling a feasible option for particle removal.

6.4 Alternative Lithographic Processes

Alternatives to conventional photolithography do exist. Section 2.3.2 *Patterning* describes three alternatives: electron beam direct write, x-ray lithography, and thermal lithography with dry resist.

Near term approaches include the use of shorter wavelength lasers such as the 157 nm fluorine excimer laser to pattern 70 nm feature sizes. However, problems with resist technology suitable for the shorter wavelengths have yet to be resolved and there is no indication that such resists would be suitable for a vacuum environment.

Longer term approaches center around Next Generation Lithography (NGL) efforts. There are several NGL proposals: extreme-ultraviolet, two types of electron-beam projection lithography, ion-beam projection lithography, x-ray lithography, and a new approach to electron-beam direct write that uses multiple columns[106]. The aim of this effort is to be able to pattern 50 nm line widths.

A thermal lithographic process has been developed which uses a two layer resist. Section 2.3.2.4 *Thermal Lithography with Dry Resist* described this process briefly. An expanded description is repeated here, with application to a space-based semiconductor fabrication.

Many inorganic materials do not exhibit a photoresponse to short duration pulses at the wavelengths of excimer lasers (193 nm). This is in contrast to the response of organic photoresists which react to cumulative exposure. This difference enables smaller features to be patterned than possible with traditional resists using the same exposure source[107]. The benefit to space-based applications is that the inorganic materials can be applied by thin film deposition techniques (CVD) and contain no volatile liquids. However, the inorganic materials are not suitable protection for downstream processes such as etching and doping.

A two layer resist has been developed to utilize the advantages of an inorganic thermal resist[108]. An organic bottom layer such as amorphous carbon (*a*-C:H) provides protection for etching and doping processes, while an inorganic top layer such as AlOx is patterned using thermal lithography. Exposure converts the deposited AlOx (primarily aluminum) to AlO_2. Developing of the top layer is

performed by etching of the unexposed aluminum material, leaving the converted AlO_2. The pattern is transferred to the bottom layer by etching the bottom layer material through the previously etched opening in the top layer. The top layer of resist is then removed through an ion milling or similar process, leaving only the patterned bottom resist layer of amorphous carbon. Downstream processing is then performed normally. The amorphous carbon resist is finally stripped using a cleaning process that removes organics.

Figure 6.1 to Figure 6.8 show a typical patterning sequence for the dry, inorganic thermal resist process. For comparison, Figure 6.9 to Figure 6.13 show the standard photoresist process. It can be seen that the primary differences between the two processes are the addition and subsequent removal of the top resist layer.

The AlOx resist process described above, developed in 1989, has not yet seen commercial use. However, improvements to the basic process, using other inorganic materials such as BiIn, have reduced the exposure energy requirements and improved the resolution. These changes improve the feasibility of a completely dry lithographic process for space-based semiconductor fabrication. These alternative processes, such as the SFU bi-metallic resists of Section 2.3.2.4, tend to follow similar deposition, development and stripping requirements.

The TREOL process, described in Section 2.3.2.4, is not used in the following space-based lithography model. While the characteristics of thermal resists allow for improved resolution with the TREOL process, it is not yet in commercial use for semiconductor lithography applications and is not required to evaluate the feasibility of thermal resists for vacuum-based lithography. Use of the TREOL process would require additional exposure steps and require additional masks.

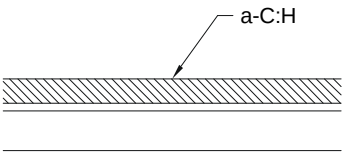

Figure 6.1 – Deposit Amorphous Carbon

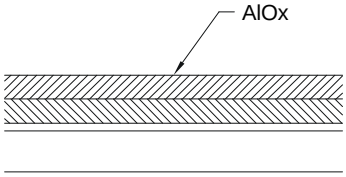

Figure 6.2 – Deposit Aluminum Oxide

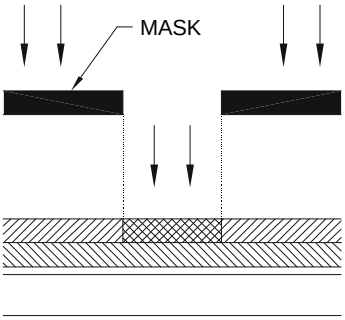

Figure 6.3 – Expose Top Resist

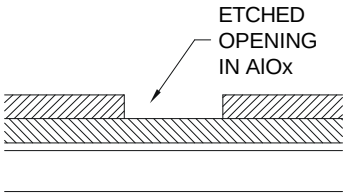

Figure 6.4 – Develop Top Resist

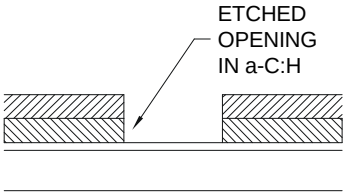

Figure 6.5 – Transfer Pattern to Bottom Resist

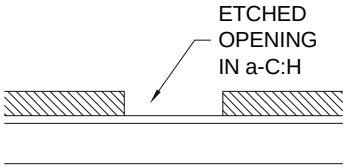

Figure 6.6 – Remove Top Resist

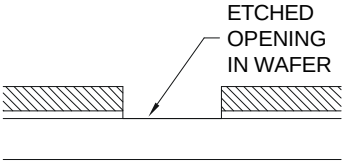

Figure 6.7 – Transfer Pattern to Wafer

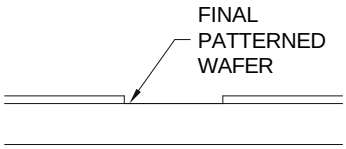

Figure 6.8 – Patterned Wafer

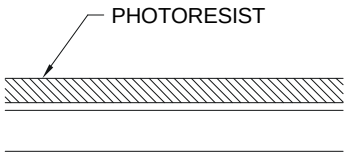

Figure 6.9 – Deposit Organic Photoresist

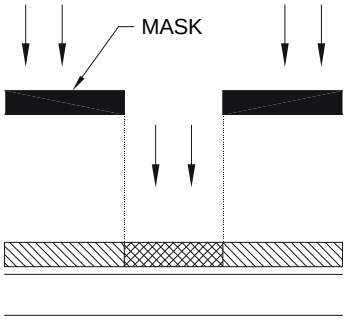

Figure 6.10 – Expose Photoresist

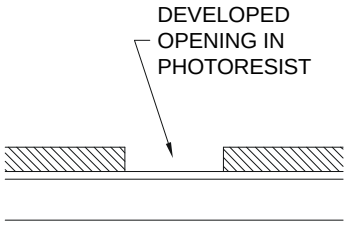

Figure 6.11 – Develop Photoresist

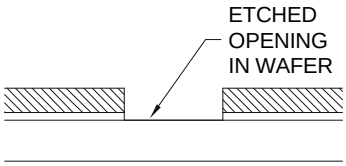

Figure 6.12 – Transfer Pattern to Wafer

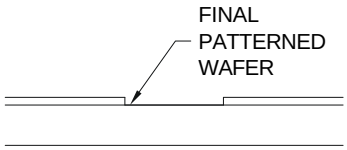

Figure 6.13 – Patterned Wafer

The process flow used by the simulation model for a space-based, dry, lithographic process is shown in Table 6.5 to Table 6.8.

Table 6.5 –Process Flow to Apply Dry, Inorganic Resist

Process Step	ProcessName	ProcessEquipment
Transport to resist system	INTERPROCESSTRANSPORT_CASSETTE	INTERPROCESSCONVEYOR
Deposit bottom layer (amorphous carbon) resist	PECVD_CARBON_SPACE	PLASMA_CVD_SYSTEM
Transport to top resist layer deposit system	INTERPROCESSTRANSPORT_CASSETTE	INTERPROCESSCONVEYOR
Deposit top layer (AlOx) resist	SPUTTER_ALOX_SPACE	SPUTTER_SYSTEM

Table 6.6 –Process Flow to Expose Dry, Inorganic Resist

Process Step	ProcessName	ProcessEquipment
Transport to aligner	INTERPROCESSTRANSPORT_CASSETTE	INTERPROCESSCONVEYOR
Expose wafer	PATTERN_LITHO_DSW_193	LITHO_DSW_193

Table 6.7 –Process Flow to Develop Dry, Inorganic Resist

Process Step	ProcessName	ProcessEquipment
Transport to plasma etch system	INTERPROCESSTRANSPORT_CASSETTE	INTERPROCESSCONVEYOR
Plasma etch unexposed Al	PLASMAETCH_AL_SPACE	PLASMA_ETCHER
Plasma etch exposed amorphous carbon	PLASMAETCH_ORGANICS_SPACE	PLASMA_ETCHER
Transport to ion mill process	INTERPROCESSTRANSPORT_CASSETTE	INTERPROCESSCONVEYOR
Remove top resist layer AlOx	ION_MILL	SPUTTER_SYSTEM

Table 6.8 –Process Flow to Remove Dry, Inorganic Resist

Process Step	ProcessName	ProcessEquipment
Transport to dry clean process	INTERPROCESSTRANSPORT_CASSETTE	INTERPROCESSCONVEYOR
Remove organics	PLASMAETCH_ORGANICS_SPACE	PLASMA_ETCHER

6.5 Other Alternative Processes

Although not included in the reference process flow model, chemical mechanical polishing (CMP) and copper electroplating are both important processes used to produce many types of semiconductor devices. CMP is the planarization method of choice when more than two metal layers are deposited. Copper electroplating is used for the deposition of copper for the topmost metal layers in high frequency applications such as high-end microprocessors.

6.5.1 Alternatives for CMP

CMP is a process used to level or "planarize" the surface of the wafer. As multiple levels of thin films are deposited and patterned on the surface of the wafer, the lines and vias comprising the surface structures form a non-planar surface and considerable topology can be created. Without a leveling process such as CMP, the distance between the high and low points on the wafer's surface can grow to several microns. This large difference in height can cause problems with downstream processes: step coverage of depositions, uniform resist thickness, and exposure depth of focus.

CMP is the latest of many planarization processes and is used primarily for devices with more than two metal layers. Its advantage is that it produces a very uniform surface level, but its disadvantage is that it is a wet process that contaminates wafers and requires large amounts of process time. In a typical CMP process, a layer such as glass or nitride is deposited through CVD until the topology on the wafer surface is fully covered. For example, a topology of 1 micron might be covered by a CVD glass layer that is 1.5 microns thick. Following CVD, the wafer is covered by a liquid slurry consisting of water and an abrasive polishing compound, and a polishing disk is applied to the surface. The polishing disk is rotated mechanically in such a

manner that it removes high points, eventually leaving the wafer with a very uniform, flat surface. This polishing process can be likened to lens grinding.

As discussed previously, wet processes pose problems for a high vacuum, microgravity environment. Therefore, an alternative to the CMP process is required in order to produce semiconductor devices with more than two metal layers in space. The inherently dirty nature of CMP has lead many researchers to study dry alternatives. The following paragraphs present a preliminary concept developed at SFU for a dry process that is compatible with the space environment and achieves planarization equal to that obtained with CMP.

The dry process is based upon the concept of photoablation. Using an intense source of short wavelength light, such as a laser, it is possible to remove material from an object without heating. The process, called photoablation, works by directing high energy photons at the surface of an object. If the photon energy is higher than the binding energy of the material's molecules, then the material disintegrates when hit by the photon. In the case of plastics (comprised of hydrogen and carbon), photoablation in air results in the release of hydrogen and carbon dioxide gases, which are easily removed from the object's surface. A key point to note is that photoablation only occurs above a well-defined intensity threshold.

While the development of a detailed planarization process based upon photoablation is beyond the scope of this thesis, one concept of such a process is presented. As with CMP, the first step is to CVD deposit a glass layer that completely covers the topology. The second step is to expose the wafer to an intense source of UV light through a lens with a very small depth of focus. A simplified description of the depth of focus of a lens is the distance from the lens over which the image is clear (the beam power is at the maximum). While lenses for lithography are optimized for a large depth of focus (to ensure a clear image across the wafer surface), lenses for the photoablative process described would be optimized for a very

small depth of focus. This would allow the intensity necessary for photoablation to only occur over a very small distance (of say 0.1 microns). To photoablate the silicon dioxide glass covering the topology, the photons would need to break the silicon oxygen bond. The intensity of light required to achieve photoablation of the glass would only occur at the focal point of the lens within the depth of focus distance. If the top layer of the glass coincides with the focal point distance, then portions of the top layer that lie within the depth of focus will be removed through photoablation. This would be done in a gas environment which would react with the disassociated products, and carry them away to prevent their redeposition on the surface.

For layers that lie outside of the depth of focus, photoablation will not occur. Also, as photoablation requires a threshold intensity to occur, it is not a cumulative effect and lower layers will only be removed by photoablation when they are moved to lie within the depth of focus and exposed to the light source. Thus, the dry planarization process is the repeated exposure of the wafer to the UV light source while the wafer is moved slightly closer to the lens with each step. It is estimated that each step could remove 0.1 microns, resulting in a planarized wafer after five to ten steps. The end product, a wafer with a surface uniform to within 0.1 microns, could be achieved by this vacuum compatible process in much less time than current CMP processes require.

6.5.2 Alternatives for Copper Electroplating

Copper electroplating is a process used to deposit thick copper conductors on the topmost layers of the most advanced current devices. Such conductors have advantages over aluminum and other metals with regards to high frequency operation. However, copper is a highly mobile ion and can easily, unless precautions are taken, contaminate the silicon in the device.

The present method of depositing copper for this application is to use a liquid electrochemical plating process. In this process, positive Cu^{++} copper ions suspended in a liquid solution (such as copper sulfate) are attracted to the negatively charged wafer by the electrical potential difference. Copper deposited in this manner is stress free and can form thick (1.5 microns or more) films. The slow motion of the copper ions in the liquid solution allows them to be attracted to the ends of high aspect ratio structures, such as vias, so that they may be filled.

An equivalent dry process is required for fabrication of high end MPU's and other similar devices in space. Due to stress concentrations, standard deposition methods such as CVD and sputtering are unable to form the thick copper films required. However, by replicating the main parameters of the liquid-based electroplating process, a dry electroplating process has been devised.

While it is beyond the scope of this thesis to develop a detailed dry, replacement process for copper electroplating, one such concept is presented. The key factors in the success of the liquid electroplating process over that of CVD, evaporation, and sputter deposition processes are the slow speed of the copper ions and the use of an electromotive force to attract the ions to the wafer's surface. In CVD, the copper ions are in a vapor and diffuse through the vapor to the surface, leading to low deposition rates. In evaporation and sputter deposition, the ions impinge upon the surface with speed and direction, leading to poor step coverage. The dry electroplating process replaces the liquid solution of copper ions with a charged metal vapor. In this vapor, copper ions and argon gas co-exist. Collisions between charged copper ions and argon molecules result in the exchange of ion velocity for a temperature increase, leading to copper ions with a low mean velocity. If the copper ions are kept charged through an external means, such as a copper laser that affects only the copper ions and not the argon molecules, then the copper ions will maintain a charge even after undergoing multiple collisions with argon

molecules. This situation has now replicated the situation found in the liquid solution, namely charged copper ions with low mean velocity existing at low temperatures.

Use of an argon gas with a few millitorr of pressure will provide a mean free path that is small enough that multiple collisions between copper ions and argon molecules will readily occur. In this situation the copper ions would rapidly thermalize to the temperature of the argon gas. In this vapor, the positively charged copper ions would tend to repel each other and not coalesce. Placing the negatively charged wafer in the chamber to act as a cathode would attract the copper ions to the wafer. As the velocity of the copper ions is low, the electric field forces will be able to attract the ions into deep, high aspect ratio structures such as vias. This dry process is compatible with a vacuum, microgravity environment and duplicates the key factors found in the liquid electro-chemical plating process.

6.6 Alternative Equipment Requirements

Semiconductor fabrication equipment has reached a level of maturity and standardization over the past thirty years that has allowed operators of existing semiconductor fabrication facilities to consider most types of equipment to be a commodity item. Such will not be the case for a space-based semiconductor fabrication facility.

Semiconductor fabrication equipment comprises the equipment used for the processing and transport of wafers, and Table 5.13 shows the list of equipment used in the simulation model. Such equipment is designed to provide functionality in an Earth environment and is unsuited to space use without design changes. Such changes would reduce the mass of the equipment, eliminate unneeded systems, and optimize the equipment for the high vacuum, microgravity environment of a space-based semiconductor fabrication facility.

Functional decomposition is one method by which the changes needed for space-based equipment can be evaluated. Using this method, each piece of equipment is divided into functions and each function is evaluated for use in space. Typical functions provided by semiconductor fabrication equipment are shown in Table 6.9.

Table 6.9 –Functions Provided by Equipment

Function
Consumable Delivery
Power Supply
Process Chamber
Processing Components
Support Structure
Vacuum Pump & System
Wafer Transport

Consumable delivery will change for a space-based application: less material will be required per wafer, the material may not be delivered continuously but rather in batches.

The power supply needed is a function of the input power source and the power requirements. It is shown later in Section 7.2.4 that the power requirements for most types of equipment is dramatically reduced by dry processing in a native vacuum environment.

While the process chamber size will be unaffected by a space environment, the thickness of the walls can be reduced as there will be very little pressure differential between the inside of the process chamber and the ambient, vacuum environment. This is in contrast to Earth-based processing in a one atmosphere environment where the pressure differential can approach 101.3 kPa.

The processing components such as ion sources, plasma generators, etc. are the least likely components to require changes for the space environment. However, electronic controls may need to be modified to take into account radiation induced

errors (soft errors) in the systems. Also, any components that have mechanical movement (valves, robots, actuators) will need to be redesigned for the space environment to cope with lubrication, outgassing, and other specific requirements.

The support structure for space-based equipment need only be strong enough to support the forces encountered during transportation, including launch. Unless vibration concerns are paramount, this will result in structures that are substantially thinner and less massive than those used in Earth-based equipment.

For all processes that operate at vacuum levels below that obtainable in orbit ($\sim 10^{-8}$ torr), the vacuum pump and related system is no longer required. In its place will be a means to exhaust process gases. Vacuum pumpdown will be a matter of opening the exhaust port to expose the interior of the process chamber to the ambient orbital vacuum.

Wafer transport inside of equipment will be used to move wafers from load locks to process chambers (lock locks will no longer be required for an ambient vacuum environment), and between process chambers (as found in cluster tools).

In addition to redesigning equipment to provide the appropriate functions, it must also be designed for reliability. Maintenance of Earth-based cleanroom equipment may, at the worst case, require shutting down production. Maintenance of space-based equipment will require expensive travel to orbit to correct and may be difficult to arrange in a timely manner. Section 10.4.6 explores the impact of equipment reliability on fabrication in more detail.

Table 6.10 shows the functional breakdown of mass, volume, and cost used for space-based equipment in the simulation model. The entire vacuum system has been eliminated and the mass and volume reduced appropriately for the other functional categories. The cost for functional categories other than vacuum has not been reduced as it is assumed that cost savings attained through the reduction of systems and components would be matched by the increased complexity of designing

for the vacuum environment. Non-recoverable engineering costs due to new product development are not considered in this model.

Table 6.10 – Normalized Functional Values for Space-Based Equipment

Item	Vacuum Pump	Vacuum System	Wafer Transport	Process Chamber	Support Structure	Consumable Delivery	Processing Components	Power Supply
Mass	0%	0%	75%	10%	10%	75%	75%	75%
Volume	0%	0%	75%	100%	10%	75%	75%	75%
Cost	0%	0%	100%	100%	100%	100%	100%	100%

Table 6.11 shows the effect of the normalized functional decomposition values on equipment mass, volume, and cost for space-based equipment, and Table 6.12 shows a comparison of the mass, volume, and cost of both Earth-based and space-based semiconductor fabrication equipment. The values shown in Table 6.12 are used by the simulation model.

While the mass and volume reductions seem reasonable, they are only engineering estimates. However, this model assumes a conservative approach regarding equipment costs - the only cost reductions used are those that occur where the vacuum pumps and controls are removed. No allowance is made for reduced costs due to reductions in mass and volume of other equipment components.

Details on parameters such as mass, volume, and cost for Earth-based equipment used by the simulation model can be found in Appendix H. The parameters for space-based equipment are determined by the method of functional decomposition of Earth-based equipment described above.

Table 6.11 – Normalized Mass, Volume, and Cost for Space-Based Equipment

Equipment	Mass (%)	Volume (%)	Cost (%)
INTERPROCESSCONVEYOR	75%	75%	100%
WETBENCH	56%	65%	100%
FURNACE_BATCH	49%	67%	100%
PHOTORESIST_SYSTEM	49%	58%	100%
LITHO_DSW_193	52%	57%	100%
DEVELOP_SYSTEM	46%	64%	100%
PLASMA_ETCHER	28%	51%	68%
ASHER	32%	41%	68%
ION_IMPLANTER	33%	42%	65%
PLASMA_CVD_SYSTEM	28%	51%	68%
SPUTTER_SYSTEM	28%	51%	68%
RTP_SYSTEM	46%	68%	100%

Table 6.12 – Mass, Volume, and Cost for Earth and Space-Based Equipment

	Earth-Based Equipment			Space-Based Equipment		
Equipment	Mass (kg)	Volume (m^3)	Cost (USD)	Mass (kg)	Volume (m^3)	Cost (USD)
INTERPROCESSCONVEYOR	50	0.1	$100,000	38	0.075	$100,000
WETBENCH	500	4	$1,800,000	278	2.58	$1,800,000
FURNACE_BATCH	500	2.88	$500,000	245	1.9296	$500,000
PHOTORESIST_SYSTEM	300	0.8	$750,000	147	0.464	$750,000
LITHO_DSW_193	500	5	$2,800,000	261	2.8375	$2,800,000
DEVELOP_SYSTEM	300	0.8	$785,714	137	0.51	$785,714
PLASMA_ETCHER	300	0.64	$900,000	85	0.3248	$612,000
ASHER	500	1.92	$200,000	158	0.7776	$136,000
ION_IMPLANTER	1000	20	$2,600,000	325	8.3	$1,690,000
PLASMA_CVD_SYSTEM	300	0.64	$800,000	85	0.3248	$544,000
SPUTTER_SYSTEM	500	4	$1,000,000	141	2.03	$680,000
RTP_SYSTEM	500	4	$800,000	229	2.73	$800,000

6.7 Conclusions

This chapter has shown that the elimination of wet (liquid) processes is a requirement for space-based microfabrication. Two new processes, a dry cleaning process and a dry lithographic process, have been introduced and have been shown to

be effective alternatives for conventional wet-based processes. Detailed numerical models of the alternative processes were developed.

To allow comparison between standard Earth-based and space-based microfabrication, the reference simulation model was extended to include the alternative dry processes in place of wet processes in a vacuum environment. In order to compare the improvements attainable by use of the dry processes on Earth, a third model was developed which included dry processes, but assumed a standard Earth (non-vacuum) environment. The results of these simulations will be discussed in Chapter 7.

Chapter 7
Process Simulation Results

7.1 Introduction

This chapter will present the results of process flow simulations incorporating the dry processes developed in Chapter 6.

The results of process simulation runs for a completely dry, Earth-based process flow and a completely dry, space-based process flow will be presented and compared to the reference process flow (Table 5.17) results It will be shown that space-based semiconductor fabrication is feasible with respect to time, mass, and energy requirements and that there are significant improvements in process time, consumable use, and energy use compared to the equivalent Earth-based process.

7.2 Results

Based on the equipment and process optimizations described in Sections 6.3 to 6.5, a simulation run was performed for a dry, space-based process flow. The reference space process flow CMOS12_DRY_SPACE, fully shown in Appendix I, is based on the reference process flow CMOS12_STD with changes to accommodate a dry cleaning process and a dry lithographic process.

An additional simulation run was performed for a dry, Earth-based process flow in order to provide a comparison of the improvements attainable on Earth using a completely dry process flow. The reference dry Earth-based process flow CMOS12_DRY_EARTH, shown in Appendix J, was developed from the reference space process flow CMOS12_DRY_SPACE by maintaining the vacuum pumpdown

processes found in the Earth-based reference process flow and using continuous flow consumable flows.

7.2.1 Equipment Use

For comparison, the equipment usage for the three reference process flows is shown in Table 7.1 to Table 7.3 (Table 7.1 repeats Table 5.20 for clarity). It should be noted that the process time shown in these tables is the actual time that a single wafer spends in processing equipment. This process time does not include time spent waiting in work-in-progress queues. This wait time is estimated to be 5 times as long as the total process time for a typical Earth-based microfabrication facility[73].

Table 7.1 – Equipment Use for Reference Process Flow CMOS12_STD

Equipment	Process Time (sec)	Process Time (%)	Incremental Process Time (sec)	Incremental Process Time (%)	Uses
INTERPROCESSCONVEYOR	33251	15%	1385	5%	108
WETBENCH	66778	29%	1341	5%	52
FURNACE_BATCH	39624	17%	840	3%	27
PHOTORESIST_SYSTEM	45630	20%	2275	8%	65
LITHO_DSW	864	0%	864	3%	12
DEVELOP_SYSTEM	20244	9%	1016	4%	36
PLASMA_ETCHER	5276	2%	5276	18%	15
ASHER	2086	1%	2086	7%	12
ION_IMPLANTER	1653	1%	1653	6%	49
PLASMA_CVD_SYSTEM	7457	3%	7457	26%	7
SPUTTER_SYSTEM	4313	2%	4313	15%	2
RTP_SYSTEM	30	0%	30	0%	1
Total	**227206**	**100%**	**28537**	**100%**	**386**

Table 7.2 – Equipment Use for Reference Process Flow CMOS12_DRY_EARTH

Equipment	Process Time (sec)	Process Time (%)	Incremental Process Time (sec)	Incremental Process Time (%)	Uses
INTERPROCESSCONVEYOR	42179	30%	1757	3%	137
WETBENCH	0	0%	0	0%	0
FURNACE_BATCH	39624	28%	840	1%	27
PHOTORESIST_SYSTEM	0	0%	0	0%	0
LITHO_DSW	864	1%	864	1%	12
DEVELOP_SYSTEM	0	0%	0	0%	0
PLASMA_ETCHER	19692	14%	19692	33%	75
ASHER	0	0%	0	0%	0
ION_IMPLANTER	1653	1%	1653	3%	49
PLASMA_CVD_SYSTEM	21494	15%	21494	36%	20
SPUTTER_SYSTEM	14096	10%	14096	23%	42
RTP_SYSTEM	30	0%	30	0%	1
Total	**139632**	**100%**	**60427**	**100%**	**363**

Table 7.3 – Equipment Use for Reference Process Flow CMOS12_DRY_SPACE

Equipment	Process Time (sec)	Process Time (%)	Incremental Process Time (sec)	Incremental Process Time (%)	Uses
INTERPROCESSCONVEYOR	42179	41%	1757	5%	137
WETBENCH	0	0%	0	0%	0
FURNACE_BATCH	25854	25%	266	1%	27
PHOTORESIST_SYSTEM	0	0%	0	0%	0
LITHO_DSW	864	1%	864	2%	12
DEVELOP_SYSTEM	0	0%	0	0%	0
PLASMA_ETCHER	7939	8%	7939	22%	75
ASHER	0	0%	0	0%	0
ION_IMPLANTER	171	0%	171	0%	7
PLASMA_CVD_SYSTEM	18360	18%	18360	50%	20
SPUTTER_SYSTEM	7246	7%	7246	20%	42
RTP_SYSTEM	30	0%	30	0%	1
Total	**102643**	**100%**	**36633**	**100%**	**321**

7.2.2 Process Time

It is seen that dry processing results in reduced process times, but increased incremental process times. The reduced process times indicate that a batch of wafers completes the entire fabrication cycle more quickly using dry process flow. This results from the increased use of single chamber equipment such as plasma etch and CVD systems which allows batches of wafers to proceed in parallel. However, the dry cleaning and lithography processes last longer than the equivalent processes used in reference process flow CMOS12_STD, resulting in increased incremental time (i.e. each wafer spends more time in the processing equipment). It will be shown in Section 8.5 that the increased incremental process time for the dry Earth-based process flow CMOS12_DRY_EARTH leads to a requirement for more equipment compared with the reference process flow CMOS12_STD.

Table 7.4 – Process Time (sec) for Reference Process Flows

Process Type	CMOS12_STD	CMOS12_DRY_EARTH	CMOS12_DRY_SPACE
TRANSPORT	49,726	57,829	43,709
CLEAN	66,463	0	0
DEPOSIT	29,734	42,561	36,964
THERMAL	66,030	12,630	12,630
PATTERNTRANSFER	864	864	864
`ETCH	13,086	24,445	8,305
PRESSURECHANGE	1,132	1,132	0
DOPE	171	171	171
All process types	**227,206**	**139,632**	**102,643**

Table 7.4 summarizes the reduction in process time attainable with the dry cleaning and lithographic processes. The reduction in process time per wafer from 227,206 seconds for the standard Earth process flow to 102,643 seconds for the dry space process flow represents a 55% reduction and is attributable to the replacement of wet cleaning processes with dry cleaning processes (plasma etching and ion milling) and the reduction of lithographic thermal processes (prebake, softbake,

hardbake). A comparison of process times for dry processing on Earth and in space shows that a savings of 36,989 seconds or 26% per wafer relative to the dry Earth process flow is attainable, due solely to the elimination of vacuum pumpdown cycles.

Figure 7.1 to Figure 7.3 show the breakdown of process time by process type and level for the three reference process flows. It is seen that cleaning and thermal processes dominate all mask levels for the standard Earth-based reference process flow. In both the dry Earth-based and dry space-based reference process flows, it is seen that transport and deposition processes consume a significant portion of the time for all mask levels.

7.2.3 Consumable Use

Table 7.5 shows the reduction in consumables attainable with the dry cleaning and lithographic processes.

Table 7.5 – Consumable Material Use (kg) for Reference Process Flows

Phase	CMOS12_STD	CMOS12_DRY_EARTH	CMOS12_DRY_SPACE
GAS	0.0838	0.0876	0.0037
LIQUID	779.1679	0.0000	0.0000
SOLID	0.0003	0.0004	0.0004
All Phases	**779.2521**	**0.0880**	**0.0041**

Going from the CMOS12_STD process flow to any of the dry process flows results in a tremendous reduction in consumables from 779 kg to 88 grams or less. This comes primarily from the removal of the wet cleaning processes. The reduction of consumables from 88 grams to 4.1 grams when going from the CMOS12_DRY_EARTH process flow to the CMOS12_DRY_SPACE process flow is attributable to the change from continuous flows of gases in Earth-based processes to single, batch flows of gases in space-based processes. Thus, the dry space process

flow reduces consumable mass to only 0.00053% that of the standard Earth process flow. This reduction is very important in making the mass requirements for space-based processing reasonable.

Figure 7.4 to Figure 7.6 show the breakdown of consumable materials by phase and level for the three reference process flows. It is seen that liquid use (from the wet cleaning processes) dominates all mask levels for the standard Earth-based reference process flow. In the dry Earth-based reference process flow, it is seen that gas use dominates all mask levels. In the dry space-based reference process flows, it is seen that gases also form the largest portion of consumables, with small quantities of solids (aluminum) used for resist layers. The use of metal solids is clearly seen in the dry space-based process for the two metal deposition steps.

7.2.4 Energy Use

Table 7.6 shows the reduction in energy use attainable with the dry cleaning and lithographic processes.

Table 7.6 – Energy Use (J) for Reference Process Flows

Energy Category	CMOS12_STD	CMOS12_DRY_EARTH	CMOS12_DRY_SPACE
Pump	1,399,869	4,694,596	0
Wafer	940,371	923,077	923,077
Material	195,362,219	25,576	2,892
Doping	67,499	67,499	67,499
Process	3,581,786	6,583,860	6,583,860
Total	**201,351,743**	**12,294,609**	**7,577,328**

Going from the CMOS12_STD process flow to any of the dry process flows results in a significant reduction in power used per wafer from 201,351,743 J (4.7 KW-h per layer) to 0.28 KW-h or less. Again, most of the energy saved comes from the removal of the wet cleaning processes. The reduction of energy use per wafer from 12,294,609 J (0.28 kW-h per layer) to 7,577,328 J (0.18 kW-h per layer) when

going from the CMOS12_DRY_EARTH process flow to the CMOS12_DRY_SPACE process flow is attributable to the elimination of vacuum pumps and the reduction in consumable materials for the space-based process flow. Thus, the dry space process flow reduces energy usage to only 3.8% that of the standard Earth process flow. This reduction is a very important requirement for space-based processing because, currently, the creation of energy generation systems in space is very expensive (see Chapter 8).

Figure 7.7 to Figure 7.9 show the breakdown of energy use by phase and level for the three reference process flows. It is seen that energy used to heat material (for liquids in wet cleaning processes) dominates all mask levels for the standard Earth-based reference process flow. In the dry Earth-based reference process flow, it is seen that vacuum pumps consume a significant portion of the energy for all mask levels. The use of dry processes increases the use of vacuum pumps over that of the standard Earth process flow. In the dry space-based reference process flows, it is seen that energy used to operate the processes and energy used to heat up the wafer are the two most significant uses of energy for all mask levels.

7.3 Conclusions

The results of the three simulation models showed that when comparing space-based microfabrication to standard Earth-based microfabrication, process time was reduced by 55%, consumable mass requirements were reduced by 99.99947%, and energy requirements were reduced by 96.24%.

The production parameters per mask level of process time, consumable mass, and energy for a single 200 mm wafer fabricated in orbit using a 12 level bi-metal CMOS dry process flow were found to be: 0.49 days, 0.004 kg, and 0.18 kW-h. These results are significantly below those found using the reference Earth-based process flow.

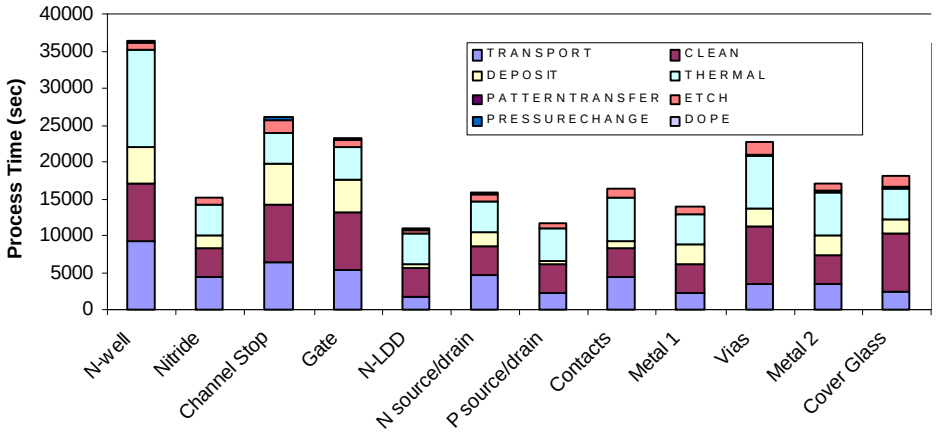

Figure 7.1 – Process Time by for Reference Flow CMOS12_STD

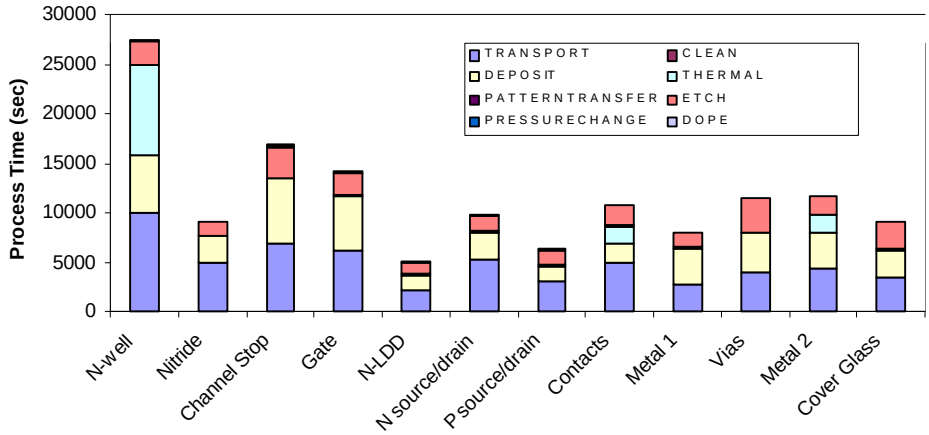

Figure 7.2 – Process Time for Reference Flow CMOS12_DRY_EARTH

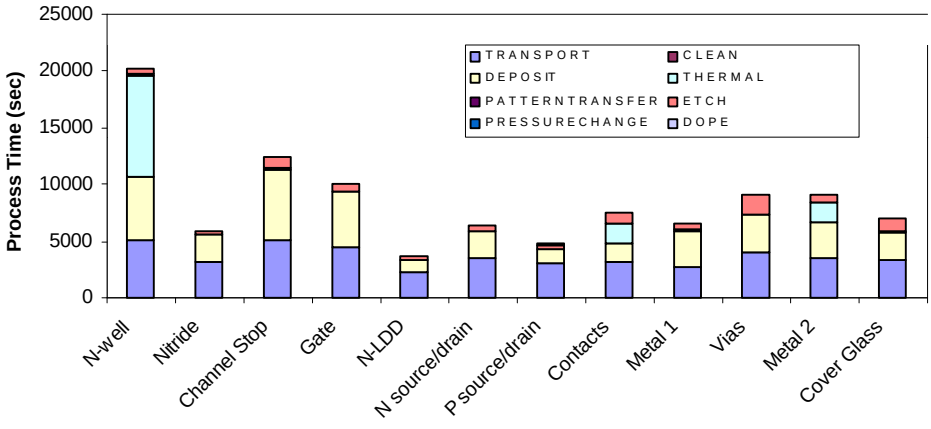

Figure 7.3 – Process Time for Reference Flow CMOS12_DRY_SPACE

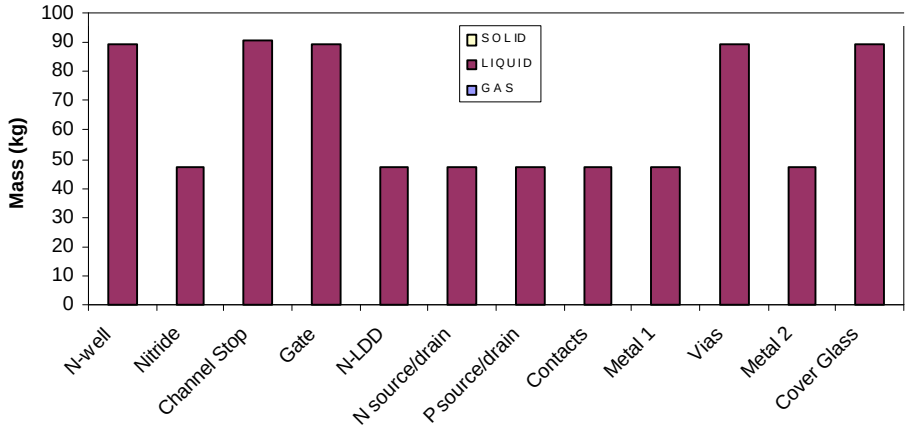

Figure 7.4 – Consumable Use for Reference Flow CMOS12_STD

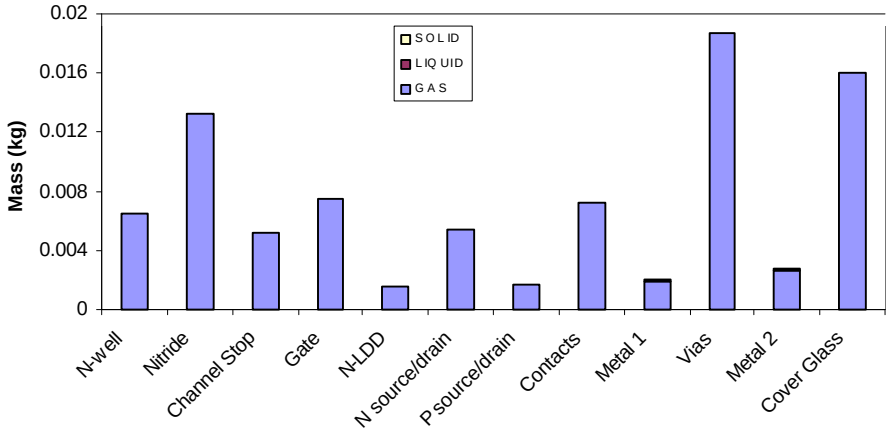

Figure 7.5 – Consumable Use for Reference Flow CMOS12_DRY_EARTH

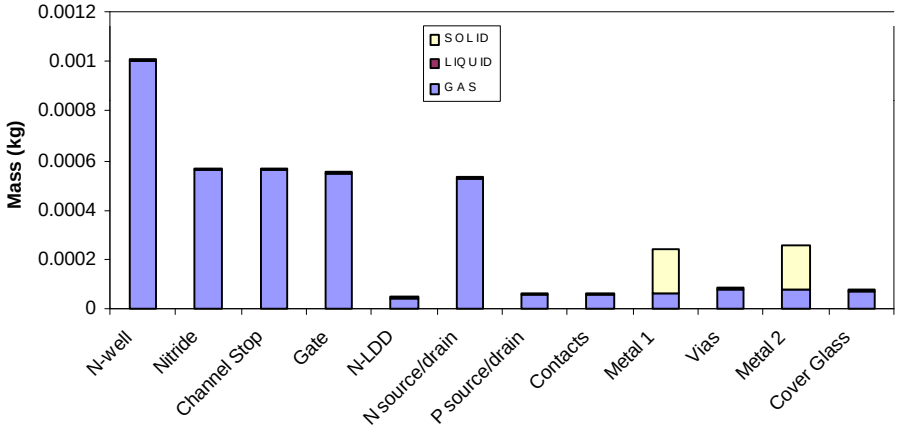

Figure 7.6 – Consumable Use for Reference Flow CMOS12_DRY_SPACE

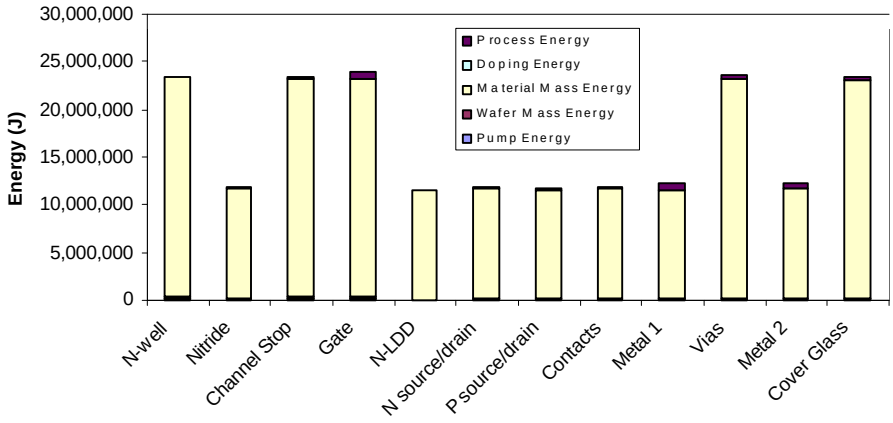

Figure 7.7 – Energy Use for Reference Flow CMOS12_STD

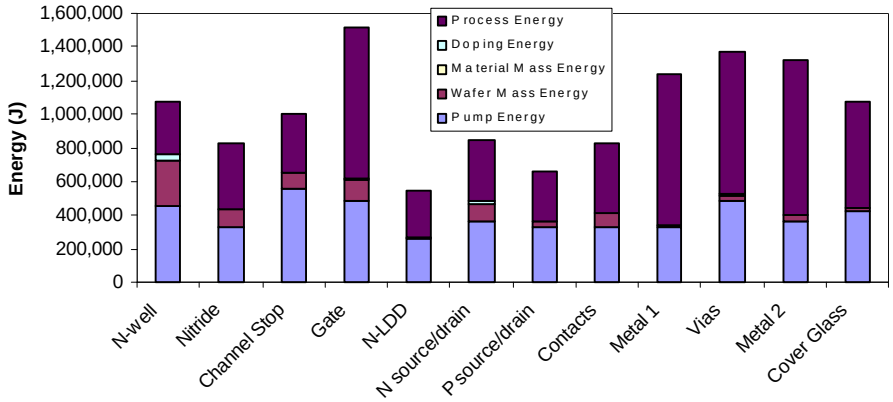

Figure 7.8 – Energy Use for Reference Flow CMOS12_DRY_EARTH

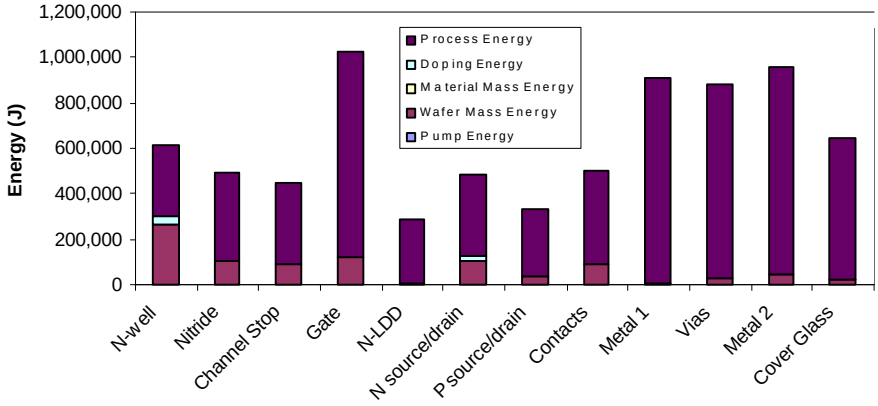

Figure 7.9 – Energy Use for Reference Flow CMOS12_DRY_SPACE

Chapter 8
Operating Cost Modeling

8.1 Introduction

This chapter will develop a model to determine operating cost for space and Earth-based semiconductor fabrication based upon the process flow results presented in Chapter 7.

Operating cost per wafer is the cost to fabricate a single wafer taking into account depreciation, energy and material consumption, and transportation. This chapter will detail the main factors that affect operating cost.

The method by which Earth and space-based equipment requirements are calculated is described and summary examples will be presented. In addition to the process equipment, the facility, power generation, and heat transfer requirements will be determined for a range of production cases.

One of the factors affecting operating cost will be shown to be the transportation cost of raw materials and finished goods to/from the production facility. A detailed model proposing an asynchronous delivery mechanism to/from orbit will be described.

Note that all of the costs given in this chapter will use 1999 values for equipment and operating costs. The effects of changes in equipment and facility capital costs will be discussed later in Chapter 9.

8.2 Background

It was shown in Chapter 5 that microfabrication processes could be modeled in such a manner as to determine the processing time required, the consumables

required, and the energy required to produce a single finished wafer. Chapter 7 extended that model to account for dry processes used in space in order to allow comparisons to be made between the results for Earth-based and space-based processes. Based on those results, space-based microfabrication is technically feasible.

However, in order for space-based semiconductor fabrication to be commercially feasible, it must offer economic advantages over terrestrial production methods. One measure of economic feasibility is the operating cost per unit wafer. The operating cost C_o is the cost to operate the production facility and includes allowances for the cost of depreciation of capital items C_d, utilities such as power and heat rejection C_u, maintenance costs C_m, ongoing costs such as consumable materials C_c, shipping costs for raw materials and finished goods C_s, as well as any other costs required to produce the wafers. For simplicity, costs related to personnel and administration are neglected in the following model.

$$C_o = C_d + C_u + C_m + C_c + C_s \tag{8.1}$$

The operating cost per unit wafer $_o$ is simply the operating cost within a certain period divided by the number of wafers n_w produced by the facility during that period.

$$\hat{C}_o = \frac{C_o}{n_w} \tag{8.2}$$

SEMATECH, an industry consortium, provides a similar measure of economic feasibility, cost-of-ownership[109,110]. The cost-of-ownership $C_{ownership}$ model relates the fixed cost of equipment and facilities C_{fixed}, the variable cost to operate the

facility $C_{variable}$, the cost due to yield loss $C_{yieldloss}$, the production rate or throughput $R_{throughput}$, the yield due to mechanical losses during production $Y_{mechloss}$, and the utilization of the equipment U.

$$C_{ownership} = \frac{C_{fixed} + C_{variable} + C_{yieldloss}}{R_{throughput} * Y_{mechloss} * U} \tag{8.3}$$

Since yield is very dependent on chip design as well as operation of the fabrication facility, it is difficult to estimate in advance. Thus, die yield is often ignored and assumed to be equal for competing tool sets in a cost-of-ownership comparison[111]. A common method used by commercial silicon foundries (semiconductor fabrication facilities that process customer designs) is to sell a set number of wafer starts, as the foundry's costs are not set by yield. This is the same as assuming a 100% yield factor for the customers' wafers.

Therefore, for an orbital semiconductor facility operating as a silicon foundry (as is the case for the base production case of ASIC wafer production), the production yield can be assumed to be 100%. With this assumption and the assumption that the equipment is available to be utilized 100% of the time (no downtime), the SEMATECH model becomes

$$C_{ownership} = \frac{C_{fixed} + C_{variable}}{R_{throughput}} \tag{8.4}$$

Over the life of the facility and equipment, the depreciation is equal to the fixed cost and the rate of throughput is the total number of wafers produced. The variable cost is the sum of the cost of consumables, power, heat rejection, and shipping. Therefore, the SEMATECH cost of ownership model reduces to

$$C_{ownership} = \frac{C_d + \left(C_c + C_p + C_r + C_s\right)}{n_w} = \hat{C}_o \tag{8.5}$$

The following sections detail how the unit cost per wafer is determined for the three reference process flows.

8.3 Base Case

The operating cost models, and the equipment, facility, and transportation requirements that drive them, are all based upon specific production parameters. The three main productions parameters utilized are:

- Wafers per Month
- Number of Layers
- Wafers per Mask Set

The number of wafers per month indicates the production rate, the number of layers indicates the level of complexity of the fabrication process, and the number of wafers per mask set indicates the size of the production run for that type of wafer design.

The three main types of devices described in Section 2.5 are MPU, DRAM, and ASIC. Table 8.1 shows the typical production parameters associated with these devices.

Table 8.1 – Production Parameters of Devices

Device Type	Number of Layers	Wafers per Mask Set[112]
MPU	30	1,500
DRAM	25	10,000
ASIC	20	250

While the following operating cost models are generalized for a wide variety of production scenarios, a base case has been established in order to provide simplified comparisons between reference process flow models. Based upon preliminary market research, it has been determined that a space-based microfabrication satellite capable of producing 5,000 ASIC wafers per month with a three week turnaround would fill a needed market niche in the current demand for ASIC devices. This has produced a base production case for the Earth and space-based models of:

Table 8.2 – Base Case Production Parameters

Symbol	Description	Value
r_w	Wafers per Month	5,000
l	Number of Layers	20
$n_{maskset}$	Wafers per Mask Set	250

8.4 Extension of Process Flow Models to Multi-Layer Devices

The reference process flow model developed in Chapter 5 was for a 12 layer CMOS device with two metal layers and 0.50 μm features. Chapter 6 and Chapter 7 extended the reference process flow model to incorporate dry Earth and dry space processing.

In order to extend the models to generic multi-layer devices, it is necessary to introduce the concept of layer averages. The output of the reference process flow model was equipment use, consumable use, and energy use for 12 layer CMOS devices, with the equipment use calculated from the incremental process time. The layer average of each of these values is calculated by dividing the sum of all individual layer values by the number of layers in the reference device (twelve in this

case). Table 8.3 shows the layer averages for total incremental time, consumable use, and energy use for the reference process flows.

Table 8.3 – 12 Level CMOS Layer Averages

Item	CMOS Standard Earth-Based	CMOS Dry Earth-Based	CMOS Dry Space-Based
Incremental Time (sec)	2,378	5,036	3,053
Consumable Use (kg)	65	0.0073	0.00034
Energy Use (kW-h)	4.67	0.28	0.18

The total incremental time, consumable use, or energy use for a device with l layers is the layer average shown in Table 8.3 multiplied by the number of layers l.

In order to compare the results of extending the 12 level CMOS averages to other devices, process flow models of a simple, three level device, representative of a sensor, were constructed. The three levels in this device were comprised of thermal growth of an 850 nm silicon dioxide film, sputter deposition of a 1 μm aluminum conductor layer, and CVD deposition of a 1.2 μm cover glass of silicon dioxide. The layer averages for this three level device, shown in Table 8.4, are in close agreement with those of the 12 level device, lending credibility to the use of layer averages as a means of modeling multi-layer devices.

Table 8.4 – 3 Level CMOS Layer Averages

Item	CMOS Standard Earth-Based	CMOS Dry Earth-Based	CMOS Dry Space-Based
Incremental Time (sec)	2,576	4,584	3,181
Consumable Use (kg)	60	0.0098	0.00028
Energy Use (kW-h)	4.40	0.26	0.18

8.5 Process Equipment

Section 6.6 *Alternative Equipment Requirements* described the method of functional decomposition used to determine the mass and cost of each piece of equipment for the space-based microfabrication model. Use of this method resulted in reductions in equipment mass ranging from 25% to 72% and reductions in equipment cost ranging from 0% to 32% compared with standard Earth-based processing equipment.

In order to determine the total mass and cost of all processing equipment, it is necessary to determine the quantity of each piece of equipment required to meet the production goals.

The quantity n_i of equipment of type i is determined by the rate at which wafers are produced r_w, the number of layers used to fabricate the wafer l, the average yield of the entire process Y, the utilization of equipment U, and the incremental process time for a single wafer in that type of equipment, normalized for a single layer, $\Delta\bar{t}_i$.

$$n_i = \frac{r_w * l * \Delta\bar{t}_i}{Y * U} \tag{8.6}$$

If the yield Y and the utilization U are assumed at 100%, the rate at which wafers are produced is specified in wafers per month, and the normalized process time per wafer is specified in seconds, then the above equation can be expressed as

$$n_i = \frac{r_w * l * \Delta\bar{t}_i}{2592000\text{sec/month}} \tag{8.7}$$

The normalized process time $\Delta\bar{t}_i$ is determined by the sum of incremental process time $\Delta t_{processstep,i}$ for type of equipment i and the number of layers l. The incremental process time $\Delta t_{processstep}$ for each process step is defined in (5.2).

$$\Delta\bar{t}_i = \frac{\sum \Delta t_{processstep,i}}{l} \tag{8.8}$$

Based on the three reference process flows, the normalized incremental time (amount of equipment time required per wafer per layer) for all equipment types is shown in Table 8.5.

Table 8.5 - Normalized Incremental Process Times (secs) for Equipment Types

Equipment Type	CMOS Standard Earth-Based	CMOS Dry Earth-Based	CMOS Dry Space-Based
INTERPROCESSCONVEYOR	115	146	146
WETBENCH	112	0	0
FURNACE_BATCH	70	70	22
PHOTORESIST_SYSTEM	190	0	0
LITHO_DSW_193	72	72	72
DEVELOP_SYSTEM	85	0	0
PLASMA_ETCHER	440	1641	662
ASHER	174	0	0
ION_IMPLANTER	138	138	14
PLASMA_CVD_SYSTEM	621	1791	1530
SPUTTER_SYSTEM	359	1175	604
RTP_SYSTEM	3	3	3

These layer averages, determined from the 12 level CMOS model, will be multiplied by the number of layers l in a device to determine the amount of equipment time each wafer requires. This equipment time requirement and the production rate r_w establishes the minimum required quantity of each piece of equipment.

Using (8.7) with the base case production parameters of $l = 20$ and $r_w = 5{,}000$, the quantity of each piece of equipment can be calculated and is shown in Table 8.6

It can be seen that the quantity of equipment is lowest for the standard Earth-based process and highest for the dry Earth-based process. This is due to the increased incremental process time required for plasma clean and etch processes used for the dry cleaning and lithography methods. The dry plasma processes are performed one wafer at a time while the wet cleaning processes are performed on a batch of 50 wafers at a time.

The decrease in equipment quantities from the dry Earth-based process to the dry space-based process is due to the fact that less time is required to perform most processes in a vacuum environment (no pumpdown required) so that each piece of equipment is able to accommodate more wafers in a given period of time.

Table 8.6 – Quantity of Equipment Required for Base Case $l = 20$, $r_w = 5{,}000$

Equipment Type	CMOS Standard Earth-Based	CMOS Dry Earth-Based	CMOS Dry Space-Based
INTERPROCESSCONVEYOR	5	6	6
WETBENCH	5	0	0
FURNACE_BATCH	3	3	1
PHOTORESIST_SYSTEM	8	0	0
LITHO_DSW_193	3	3	3
DEVELOP_SYSTEM	4	0	0
PLASMA_ETCHER	17	64	26
ASHER	7	0	0
ION_IMPLANTER	6	6	1
PLASMA_CVD_SYSTEM	24	70	60
SPUTTER_SYSTEM	14	46	24
RTP_SYSTEM	1	1	1
Total	**97**	**199**	**122**

Using the quantities determined in Table 8.6 and the equipment characteristics shown in Table 6.12, it is possible to determine the total mass, volume and cost of all

equipment. Table 8.7 shows this mass, volume, and cost of all equipment for the base case.

Note that the equipment costs shown in Table 8.7 are for the base case of 5,000 wafers per month. If extrapolated to standard commercial fabrication facilities (25,000 wafers per month), the equipment costs scale to those expected for a current microfabrication facility as shown in Table 8.8.

Table 8.7 – Mass, Volume, Cost of Equipment Required for Base Case

	CMOS Std. Earth-Based			CMOS Dry Earth-Based			CMOS Dry Space-Based		
Equipment Type	**Mass (kg)**	**Vol (m^3)**	**Cost (USD)**	**Mass (kg)**	**Vol (m^3)**	**Cost (USD)**	**Mass (kg)**	**Vol (m^3)**	**Cost (USD)**
INTERPROCESS CONVEYOR	250	0.5	$500,000	300	0.6	$600,000	225	0.45	$600,000
WETBENCH	2,500	20	$9,000,000	0	0	$0	0	0	$0
FURNACE _BATCH	1,500	8.64	$1,500,000	1,500	8.64	$1,500,000	245	1.93	$500,000
PHOTORESIST _SYSTEM	2,400	6.4	$6,000,000	0	0	$0	0	0	$0
LITHO_DSW _193	1,500	15	$8,400,000	1,500	15	$8,400,000	784	8.51	$8,400,000
DEVELOP _SYSTEM	1,200	3.2	$3,142,857	0	0	$0	0	0	$0
PLASMA _ETCHER	5,100	10.88	$15,300,000	19,200	40.96	$57,600,000	2,204	8.44	$15,912,000
ASHER	3,500	13.44	$1,400,000	0	0	$0	0	0	$0
ION _IMPLANTER	6,000	120	$15,600,000	6,000	120	$15,600,000	325	8.3	$1,690,000
PLASMA_CVD _SYSTEM	7,200	15.36	$19,200,000	21,000	44.8	$56,000,000	5,085	19.5	$32,640,000
SPUTTER _SYSTEM	7,000	56	$14,000,000	23,000	184	$46,000,000	3,390	48.7	$16,320,000
RTP_SYSTEM	500	4	$800,000	500	4	$800,000	229	2.73	$800,000
Total	**38,650**	**273**	**$94,842,857**	**73,000**	**418**	**$186,500,000**	**12,486**	**99**	**$76,862,000**

Table 8.8 to Table 8.10 show the process equipment requirements, including total average power consumption, for a range of production scenarios for Earth and space-based facilities. It can be seen that the process power requirement for a space-based microfabrication facility is well within the capabilities of existing space power supplies (25 to 75 kW).

Table 8.8 – Process Equipment Requirements for CMOS Standard Earth-Based Process Flow

Wafers per Month	Layers	Qty	Mass (kg)	Volume (m^3)	Cost (USD)	Avg. Power (kW)
50	10	11	4,750	41	$12,235,714	3.2
100	10	11	4,750	41	$12,235,714	6.5
250	10	12	5,250	45	$13,035,714	16.2
500	10	13	5,550	45	$13,835,714	32.4
750	10	15	6,350	50	$15,735,714	48.6
1,000	10	16	6,650	51	$16,535,714	64.7
2,500	10	29	11,800	89	$29,085,714	161.8
5,000	10	52	20,750	146	$50,971,429	323.7
10,000	10	97	38,650	273	$94,842,857	647.3
25,000	10	235	92,900	645	$227,721,429	1,618.4
50	20	11	4,750	41	$12,235,714	6.5
100	20	12	5,250	45	$13,035,714	12.9
250	20	13	5,550	45	$13,835,714	32.4
500	20	16	6,650	51	$16,535,714	64.7
750	20	21	8,550	59	$20,185,714	97.1
1,000	20	24	10,150	80	$24,485,714	129.5
2,500	20	52	20,750	146	$50,971,429	323.7
5,000	20	97	38,650	273	$94,842,857	647.3
10,000	20	188	74,650	517	$182,850,000	1,294.7
25,000	20	464	183,350	1,264	$449,507,143	3,236.7
50	30	12	5,250	45	$13,035,714	9.7
100	30	12	5,250	45	$13,035,714	19.4
250	30	15	6,350	50	$15,735,714	48.6
500	30	21	8,550	59	$20,185,714	97.1
750	30	27	11,000	85	$26,385,714	145.7
1,000	30	35	14,000	98	$33,535,714	194.2
2,500	30	76	30,200	207	$73,857,143	485.5
5,000	30	143	56,750	390	$138,978,571	971.0
10,000	30	280	110,700	761	$270,957,143	1,942.0
25,000	30	694	274,100	1,884	$672,192,857	4,855.1

Table 8.9 – Process Equipment Requirements for CMOS Dry Earth-Based Process Flow

Wafers per Month	Layers	Qty	Mass (kg)	Volume (m^3)	Cost (USD)	Avg. Power (kW)
50	10	7	3,150	33	$8,700,000	0.2
100	10	7	3,150	33	$8,700,000	0.4
250	10	11	4,750	43	$12,200,000	1.0
500	10	16	6,450	49	$16,600,000	2.0
750	10	20	7,850	55	$20,100,000	3.0
1,000	10	24	9,250	61	$23,700,000	4.0
2,500	10	53	19,800	122	$50,300,000	9.9
5,000	10	101	37,250	215	$95,300,000	19.8
10,000	10	199	73,000	418	$186,500,000	39.5
25,000	10	490	178,850	1,009	$457,300,000	98.8
50	20	7	3,150	33	$8,700,000	0.4
100	20	10	4,250	39	$11,200,000	0.8
250	20	16	6,450	49	$16,600,000	2.0
500	20	24	9,250	61	$23,700,000	4.0
750	20	33	12,350	73	$31,600,000	5.9
1,000	20	44	16,700	109	$42,400,000	7.9
2,500	20	101	37,250	215	$95,300,000	19.8
5,000	20	199	73,000	418	$186,500,000	39.5
10,000	20	393	143,400	807	$366,900,000	79.1
25,000	20	975	355,350	1,990	$909,200,000	197.6
50	30	9	3,950	38	$10,300,000	0.6
100	30	12	5,050	43	$13,000,000	1.2
250	30	20	7,850	55	$20,100,000	3.0
500	30	33	12,350	73	$31,600,000	5.9
750	30	49	18,400	116	$46,800,000	8.9
1,000	30	61	22,600	134	$57,400,000	11.9
2,500	30	150	54,750	308	$140,400,000	29.6
5,000	30	295	107,650	604	$275,700,000	59.3
10,000	30	586	213,750	1,195	$547,200,000	118.6
25,000	30	1,460	531,850	2,970	$1,361,100,000	296.5

Table 8.10 – Process Equipment Requirements for CMOS Dry Space-Based Process Flow

Wafers per Month	Layers	Qty	Mass (kg)	Volume (m^3)	Cost (USD)	Avg. Power (kW)
50	10	7	1,180	16	$6,926,000	0.1
100	10	7	1,180	16	$6,926,000	0.2
250	10	9	1,493	19	$8,270,000	0.6
500	10	12	1,804	22	$10,106,000	1.2
750	10	14	1,973	22	$11,194,000	1.8
1,000	10	17	2,284	25	$13,030,000	2.4
2,500	10	34	3,847	35	$22,514,000	6.1
5,000	10	63	6,773	57	$41,326,000	12.2
10,000	10	122	12,486	99	$76,862,000	24.4
25,000	10	299	30,306	235	$186,580,000	60.9
50	20	7	1,180	16	$6,926,000	0.2
100	20	9	1,493	19	$8,270,000	0.5
250	20	12	1,804	22	$10,106,000	1.2
500	20	17	2,284	25	$13,030,000	2.4
750	20	22	2,764	28	$15,954,000	3.7
1,000	20	29	3,367	32	$19,590,000	4.9
2,500	20	63	6,773	57	$41,326,000	12.2
5,000	20	122	12,486	99	$76,862,000	24.4
10,000	20	241	24,517	192	$151,700,000	48.7
25,000	20	593	59,634	454	$369,390,000	121.8
50	30	8	1,408	19	$7,726,000	0.4
100	30	9	1,493	19	$8,270,000	0.7
250	30	14	1,973	22	$11,194,000	1.8
500	30	22	2,764	28	$15,954,000	3.7
750	30	32	3,678	35	$21,358,000	5.5
1,000	30	39	4,327	39	$25,438,000	7.3
2,500	30	94	9,821	79	$60,850,000	18.3
5,000	30	181	18,479	142	$114,474,000	36.5
10,000	30	357	36,101	277	$224,136,000	73.1
25,000	30	887	89,203	682	$553,346,000	182.7

8.6 Facility

A semiconductor fabrication facility has certain requirements, whether it be located on Earth or in space. As a first approximation, the facility can be divided into two distinct areas: the cleanroom within which all microfabrication occurs, and the remainder of the facility which comprises the building, the power generation and heat rejection equipment, the HVAC systems, the waste handling equipment, and other systems necessary for the functioning of the facility.

In order to properly determine the operating costs of a facility, it is necessary to determine all capital items including process equipment, the cleanroom and other facilities, and the power and heat rejection equipment so that depreciation can be properly accounted for.

The process equipment models described previously produced outputs of mass, volume, and cost. This section will describe a facility model that uses the volume of process equipment to calculate both cleanroom and non-cleanroom facility requirements based upon some key assumptions.

The key assumptions used in the model are shown Table 8.11.

Table 8.11 – Key Assumptions for Determining Facility Requirements

Item	CMOS Standard Earth-Based	CMOS Dry Earth-Based	CMOS Dry Space-Based
Cleanroom Volume Ratio	1050%	1050%	200%
Cleanroom Height (m)	3	3	
Cleanroom Area Cost[73] (USD/m^2)	$16,146	$16,146	
Cleanroom Volume Cost (USD/m^3)			$100,000
Cleanroom specific mass (kg/m^3)	130	130	10
Non-cleanroom facility mass ratio	1000%	620%	200%
Non-cleanroom facility volume ratio	1000%	620%	20%
Non-cleanroom facility cost ratio	137%	85%	200%

The cleanroom volume ratio is the ratio of internal volume of the cleanroom to the volume of the process equipment housed in the cleanroom and was determined by a review of existing facility cleanroom sizes[40]. The cleanroom area and volume cost are the cost in USD per unit internal area or volume of the cleanroom. The non-cleanroom facility ratios are used to calculate the non-cleanroom mass, volume, and cost as a percent of the cleanroom value.

The mass, volume, and cost of the Earth-based facility using a dry process flow is assumed to be 62% of the value for a similar facility using a standard (wet)

process flow. Table 8.12 shows a functional breakdown of the facility mass, volume, and cost used in the model.

Table 8.12 – Functional Breakdown of Facility Mass, Volume, and Cost

	CMOS Standard Earth-Based			CMOS Dry Earth-Based		
Functional Item	**Mass (%)**	**Volume (%)**	**Cost[104] (%)**	**Mass (%)**	**Volume (%)**	**Cost (%)**
Industrial water	1.00%	1.00%	1.00%	1.00%	1.00%	1.00%
Building	28.00%	28.00%	28.00%	28.00%	28.00%	28.00%
Air conditioning/exhaust	29.00%	29.00%	29.00%	29.00%	29.00%	29.00%
Pure water/waste water	15.00%	15.00%	15.00%	0.00%	0.00%	0.00%
Chemicals	2.00%	2.00%	2.00%	0.00%	0.00%	0.00%
Gas alarm	6.00%	6.00%	6.00%	0.00%	0.00%	0.00%
Electricity	16.00%	16.00%	16.00%	0.98%	0.98%	0.98%
Disaster prevention	3.00%	3.00%	3.00%	3.00%	3.00%	3.00%
Total	**100.00%**	**100.00%**	**100.00%**	**61.98%**	**61.98%**	**61.98%**

Based on the key assumptions shown in Table 8.11 and the equipment quantity calculations of Section 8.5, the facility requirements can be calculated. Table 8.13 to Table 8.15 show the facility requirements for a range of production scenarios for Earth and space-based facilities.

Table 8.13 – Facility Requirements for CMOS Std. Earth-Based Process Flow

Wafers per Month	Layers	Process Equipment Volume (m^3)	Cleanroom Mass (kg)	Cleanroom Volume (m^3)	Cleanroom Area (m^2)	Cleanroom Cost (USD)	Non-Cleanroom Mass (kg)	Non-Cleanroom Volume (m^3)	Non-Cleanroom Cost (USD)
50	10	41	55,665	428	143	$2,304,499	556,647	4,282	$3,157,164
100	10	41	55,665	428	143	$2,304,499	556,647	4,282	$3,157,164
250	10	45	61,125	470	157	$2,530,542	611,247	4,702	$3,466,842
500	10	45	61,998	477	159	$2,566,708	619,983	4,769	$3,516,390
750	10	50	68,332	526	175	$2,828,917	683,319	5,256	$3,875,616
1,000	10	51	69,206	532	177	$2,865,084	692,055	5,324	$3,925,165
2,500	10	89	121,976	938	313	$5,049,781	1,219,764	9,383	$6,918,200
5,000	10	146	199,263	1,533	511	$8,249,407	1,992,627	15,328	$11,301,688
10,000	10	273	373,218	2,870	957	$15,451,109	3,732,183	28,709	$21,168,019
25,000	10	645	880,861	6,775	2,259	$36,467,375	8,808,618	67,759	$49,960,304
50	20	41	55,665	428	143	$2,304,499	556,647	4,282	$3,157,164
100	20	45	61,125	470	157	$2,530,542	611,247	4,702	$3,466,842
250	20	45	61,998	477	159	$2,566,708	619,983	4,769	$3,516,390
500	20	51	69,206	532	177	$2,865,084	692,055	5,324	$3,925,165
750	20	59	80,126	616	205	$3,317,168	801,255	6,164	$4,544,520
1,000	20	80	109,173	840	280	$4,519,712	1,091,727	8,398	$6,192,006
2,500	20	146	199,263	1,533	511	$8,249,407	1,992,627	15,328	$11,301,688
5,000	20	273	373,218	2,871	957	$15,451,109	3,732,183	28,709	$21,168,019
10,000	20	517	705,896	5,430	1,810	$29,223,855	7,058,961	54,300	$40,036,682
25,000	20	1,264	1,725,770	13,275	4,425	$71,446,263	17,257,695	132752	$97,881,380
50	30	45	61,125	470	157	$2,530,542	611,247	4,702	$3,466,842
100	30	45	61,125	470	157	$2,530,542	611,247	4,702	$3,466,842
250	30	50	68,332	526	175	$2,828,917	683,319	5,256	$3,875,616
500	30	59	80,126	616	205	$3,317,168	801,255	6,164	$4,544,520
750	30	85	115,643	890	297	$4,787,572	1,156,428	8,896	$6,558,974
1,000	30	98	133,770	1,029	343	$5,538,032	1,337,700	10,290	$7,587,104
2,500	30	207	282,009	2,169	723	$11,675,075	2,820,090	21,693	$15,994,853
5,000	30	390	531,941	4,092	1,364	$22,022,153	5,319,405	40,919	$30,170,350
10,000	30	761	1,038,710	7,990	2,663	$43,002,253	10,387,104	79,901	$58,913,086
25,000	30	1,884	2,571,551	19,781	6,594	$106,461,317	25,715,508	197,812	$145,852,004

Table 8.14 – Facility Requirements for CMOS Dry Earth-Based Process Flow

Wafers per Month	Layers	Process Equipment Volume (m^3)	Cleanroom Mass (kg)	Cleanroom Volume (m^3)	Cleanroom Area (m^2)	Cleanroom Cost (USD)	Non-Cleanroom Mass (kg)	Non-Cleanroom Volume (m^3)	Non-Cleanroom Cost (USD)
50	10	33	45,400	349	116	$1,879,540	281,379	2,164	$1,595,912
100	10	33	45,400	349	116	$1,879,540	281,379	2,164	$1,595,912
250	10	43	58,067	447	149	$2,403,958	359,888	2,768	$2,041,193
500	10	49	67,022	516	172	$2,774,667	415,385	3,195	$2,355,961
750	10	55	75,102	578	193	$3,109,209	465,468	3,581	$2,640,020
1,000	10	61	83,183	640	213	$3,443,752	515,551	3,966	$2,924,079
2,500	10	122	166,312	1,279	426	$6,885,243	1,030,764	7,929	$5,846,238
5,000	10	215	293,393	2,257	752	$12,146,373	1,818,388	13,988	$10,313,447
10,000	10	418	570,570	4,389	1,463	$23,621,401	3,536,271	27,202	$20,056,856
25,000	10	1,009	1,377,476	10,596	3,532	$57,027,036	8,537,303	65,672	$48,421,474
50	20	33	45,400	349	116	$1,879,540	281,379	2,164	$1,595,912
100	20	39	52,607	405	135	$2,177,916	326,048	2,508	$1,849,261
250	20	49	67,022	516	172	$2,774,667	415,385	3,195	$2,355,961
500	20	61	83,183	640	213	$3,443,752	515,551	3,966	$2,924,079
750	20	73	100,218	771	257	$4,149,003	621,132	4,778	$3,522,905
1,000	20	109	149,276	1,148	383	$6,179,992	925,183	7,117	$5,247,411
2,500	20	215	293,393	2,257	752	$12,146,373	1,818,388	13,988	$10,313,447
5,000	20	418	570,570	4,389	1,463	$23,621,401	3,536,271	27,202	$20,056,856
10,000	20	807	1,101,173	8,471	2,824	$45,588,175	6,824,834	52,499	$38,708,773
25,000	20	1,990	2,715,722	20,890	6,963	$112,429,959	16,831,467	129,473	$95,463,919
50	30	38	51,734	398	133	$2,141,749	320,633	2,466	$1,818,552
100	30	43	58,941	453	151	$2,440,125	365,302	2,810	$2,071,902
250	30	55	75,102	578	193	$3,109,209	465,468	3,581	$2,640,020
500	30	73	100,218	771	257	$4,149,003	621,132	4,778	$3,522,905
750	30	116	158,231	1,217	406	$6,550,701	980,681	7,544	$5,562,179
1,000	30	134	182,473	1,404	468	$7,554,328	1,130,930	8,699	$6,414,355
2,500	30	308	420,611	3,235	1,078	$17,413,155	2,606,858	20,053	$14,785,454
5,000	30	604	823,996	6,338	2,113	$34,113,146	5,106,951	39,284	$28,965,364
10,000	30	1,195	1,631,639	12,551	4,184	$67,549,297	10,112,551	77,789	$57,355,892
25,000	30	2,970	4,053,968	31,184	10,395	$167,832,883	25,125,630	193,274	$142,506,364

Table 8.15 – Facility Requirements for CMOS Dry Space-Based Process Flow

Wafers per Month	Layers	Process Equipment Volume (m^3)	Cleanroom Mass (kg)	Cleanroom Volume (m^3)	Cleanroom Cost (USD)	Non-Cleanroom Mass (kg)	Non-Cleanroom Volume (m^3)	Non-Cleanroom Cost (USD)
50	10	16	316	32	$3,164,340	633	6	$6,328,680
100	10	16	316	32	$3,164,340	633	6	$6,328,680
250	10	19	378	38	$3,775,300	755	8	$7,550,600
500	10	22	431	43	$4,311,220	862	9	$8,622,440
750	10	22	444	44	$4,441,140	888	9	$8,882,280
1,000	10	25	498	50	$4,977,060	995	10	$9,954,120
2,500	10	35	705	71	$7,054,540	1,411	14	$14,109,080
5,000	10	57	1,144	114	$11,437,200	2,287	23	$22,874,400
10,000	10	99	1,971	197	$19,714,980	3,943	39	$39,429,960
25,000	10	235	4,695	469	$46,946,780	9,389	94	$93,893,560
50	20	16	316	32	$3,164,340	633	6	$6,328,680
100	20	19	378	38	$3,775,300	755	8	$7,550,600
250	20	22	431	43	$4,311,220	862	9	$8,622,440
500	20	25	498	50	$4,977,060	995	10	$9,954,120
750	20	28	564	56	$5,642,900	1,129	11	$11,285,800
1,000	20	32	639	64	$6,388,700	1,278	13	$12,777,400
2,500	20	57	1,144	114	$11,437,200	2,287	23	$22,874,400
5,000	20	99	1,971	197	$19,714,980	3,943	39	$39,429,960
10,000	20	192	3,841	384	$38,413,000	7,683	77	$76,826,000
25,000	20	454	9,088	909	$90,880,640	18,176	182	$181,761,280
50	30	19	371	37	$3,710,340	742	7	$7,420,680
100	30	19	378	38	$3,775,300	755	8	$7,550,600
250	30	22	444	44	$4,441,140	888	9	$8,882,280
500	30	28	564	56	$5,642,900	1,129	11	$11,285,800
750	30	35	692	69	$6,924,620	1,385	14	$13,849,240
1,000	30	39	772	77	$7,720,380	1,544	15	$15,440,760
2,500	30	79	1,590	159	$15,899,820	3,180	32	$31,799,640
5,000	30	142	2,848	285	$28,475,220	5,695	57	$56,950,440
10,000	30	277	5,537	554	$55,371,060	11,074	111	$110,742,120
25,000	30	682	13,641	1,364	$136,409,540	27,282	273	$272,819,080

8.7 Power and Heat Rejection

Two issues that become very important for any space-based facility are electrical power consumption and heat rejection. In Earth-based facilities the power is purchased from the local electrical utility (at wholesale rates) and heat is rejected

through heat exchangers to either the atmosphere (cooling towers) or to a local water source. In space, all electrical power must be generated on site and all heat must be rejected to space through radiation.

Electrical power can be generated in space by a number of methods: nuclear, fuel cells, and solar. Of these, only solar is suitable with present technology to meet the power requirements of a microfabrication facility.

Current solar power cells are arranged in long, flat sheets supported by an external framework. The efficiency of the solar cells in converting sunlight to electricity is dependent upon the type of semiconductor material used, the construction method, and the inclination of the face of cell to the sun. Current parameters for silicon solar cells (non thin film) are: 3.23 kg/kW and $58,823 USD/kW[113]. Other types of cells, notably GaAs/Ge, are capable of higher efficiencies, leading to lower unit mass but higher unit cost.

Solar cells absorb radiation and convert a portion of it to electricity. In contrast, solar radiators radiate waste heat to space. As radiation of heat is governed by radiator temperature and surface area, the ideal radiator is similar in appearance to a solar cell, and similar mass, volume, and cost characteristics have been assumed for the model.

On Earth, waste heat is transferred to the environment through some form of heat exchanger. One common method of transferring process heat is to use a liquid to liquid flat plate heat exchanger whereby heat is transferred from one fluid (such as a waste process stream) to another fluid (such as cooling water) across a non-permeable surface. Flat plate heat exchangers are compact and inexpensive.

The key assumptions concerning the characteristics of power generation and heat rejection equipment on Earth and in space are shown in Table 8.16. It can be seen that specific cost of Earth-based power generating equipment is zero, reflecting the fact that electrical power is purchased from the local utility on Earth. For the

purposes of this model, the effect of emergency power generation equipment, such as diesel generators, is neglected and the cost ignored. It should be noted that the cost of electricity transmission and transforming equipment is included within the overall facilities costs shown in Table 8.12.

In order to be conservative, the specific mass and specific cost of space-based power generating equipment is assumed to be higher than that available with current silicon solar cell technology[113]. The specific cost and mass of space-based heat rejection equipment is assumed to be the same as that of the power generating equipment.

Table 8.16 – Key Assumptions for Determining Power Generating and Heat Rejection Equipment

	Earth-Based			Space-Based		
Item	**Mass (kg/kW)**	**Volume (m^3/kW)**	**Cost (USD/kW)**	**Mass (kg/kW)**	**Volume (m^3/kW)**	**Cost (USD/kW)**
Power Generation Equipment	0	0	$0	10	0.04	$100,000
Heat Rejection Equipment	3.59	0.00134	$233	10	0.04	$100,000

Additional assumptions, shown in Table 8.17, are required for the model in order to determine the amount of power required for supporting (non-process equipment) and the amount of heat which must be rejected. The support power ratio is the amount of power required by non-process equipment (such as HVAC) as a percent of the process power requirement. The heat rejection ratio is the amount of heat that must be rejected from the facility as a percent of the process power requirement, and it can be seen that a conservative value of 100% (all of the heat generated) is used. The safety factors are used to ensure that the power generating and heat rejection capacity is sufficient for peak loads.

Table 8.17 – Additional Assumptions for Determining Power Generating and Heat Rejection Equipment

Item	Earth-Based	Space-Based
Support Power Ratio	104%	20%
Power Generation Safety Factor	120%	120%
Heat Rejection Ratio	100%	100%
Heat Rejection Safety Factor	120%	120%

It should be noted that alternatives are available to reduce the electrical energy requirements for a space-based facility. The use of solar heating for furnaces and thermal processes would greatly reduce the need for solar cells and would utilize the available solar energy more efficiently. However, such a solar heating system is unproven and the conservative approach using solar cells has been taken in modeling this equipment.

For the Base Case of l = 20 layers and r_w = 5,000 wafers per month, the above assumptions produce the mass, volume, and costs shown in Table 8.18.

Table 8.18 – Power Generating and Heat Rejection Equipment Mass, Volume and Cost for Base Case

Item	CMOS Standard Earth-Based	CMOS Dry Earth-Based	CMOS Dry Space-Based
Process Equipment Average Power (kW)	647	40	24
Required Power Generating Capacity (kW)	1583	97	35
Power Generating Equipment Mass (kg)	0	0	351
Power Generating Equipment Volume (m^3)	0.00	0.00	1.40
Power Generating Equipment Cost (USD)	$0	$0	$3,508,022
Required Heat Rejection Equipment Capacity	1583	97	35
Heat Rejection Equipment Mass (kg)	5689	347	351
Heat Rejection Equipment Volume (m^3)	2.12	0.13	1.40
Heat Rejection Equipment Cost (USD)	$368,217	$22,483	$3,508,022

8.8 Summary of Equipment and Facility Requirements

Section 8.2 to Section 8.7 have described the modeling of capital equipment and facility requirements. A summary of the total mass and cost of the capital items required for a microfabrication facility is shown in Table 8.19 for a range of production scenarios.

Table 8.19 – Summary Total Mass and Cost of Capital Items

Wafers/ Month	Layers	CMOS Std Mass (kg)	Earth-Based Cost (USD)	CMOS Dry Earth-Based Mass (kg)	Earth-Based Cost (USD)	CMOS Dry Space-Based Mass (kg)	Space-Based Cost (USD)
50	10	617,000	$17,600,000	329,000	$12,100,000	2,100	$16,400,000
100	10	617,000	$17,700,000	329,000	$12,100,000	2,100	$16,400,000
250	10	677,000	$19,000,000	422,000	$16,600,000	2,600	$19,700,000
500	10	687,000	$19,900,000	488,000	$21,700,000	3,100	$23,300,000
750	10	758,000	$22,400,000	548,000	$25,800,000	3,300	$25,000,000
1,000	10	768,000	$23,300,000	608,000	$30,000,000	3,800	$28,600,000
2,500	10	1,354,000	$41,100,000	1,216,000	$63,000,000	6,100	$45,400,000
5,000	10	2,215,000	$70,700,000	2,149,000	$117,700,000	10,500	$79,100,000
10,000	10	4,149,000	$131,800,000	4,180,000	$230,200,000	19,100	$143,000,000
25,000	10	9,796,000	$315,000,000	10,094,000	$562,800,000	46,100	$344,900,000
50	20	617,000	$17,700,000	329,000	$12,100,000	2,100	$16,400,000
100	20	677,000	$19,000,000	382,000	$15,200,000	2,600	$19,700,000
250	20	687,000	$19,900,000	488,000	$21,700,000	3,100	$23,300,000
500	20	768,000	$23,300,000	608,000	$30,000,000	3,800	$28,600,000
750	20	890,000	$28,100,000	733,000	$39,200,000	4,500	$33,900,000
1,000	20	1,212,000	$35,200,000	1,091,000	$53,800,000	5,400	$40,100,000
2,500	20	2,215,000	$70,700,000	2,149,000	$117,700,000	10,500	$79,100,000
5,000	20	4,149,000	$131,800,000	4,180,000	$230,200,000	19,100	$143,000,000
10,000	20	7,850,000	$252,800,000	8,070,000	$451,200,000	37,400	$280,900,000
25,000	20	19,195,000	$620,600,000	19,904,000	$1,117,200,000	90,400	$677,100,000
50	30	677,000	$19,000,000	376,000	$14,200,000	2,500	$18,900,000
100	30	677,000	$19,000,000	429,000	$17,500,000	2,600	$19,800,000
250	30	758,000	$22,400,000	548,000	$25,800,000	3,300	$25,000,000
500	30	890,000	$28,100,000	733,000	$39,200,000	4,500	$33,900,000
750	30	1,284,000	$37,800,000	1,157,000	$58,900,000	5,900	$43,700,000
1,000	30	1,487,000	$46,700,000	1,336,000	$71,300,000	6,800	$50,700,000
2,500	30	3,136,000	$101,800,000	3,082,000	$172,600,000	15,100	$113,800,000
5,000	30	5,916,000	$191,700,000	6,039,000	$338,800,000	28,000	$210,400,000
10,000	30	11,553,000	$373,900,000	11,958,000	$672,100,000	54,800	$411,200,000
25,000	30	28,603,000	$927,200,000	29,714,000	$1,671,600,000	135,300	$1,015,100,000

The mass is an important factor in modeling transportation costs of equipment to orbit. The cost shown in Table 8.19 is the first cost of the equipment and does not include shipping or installation.

Equipment costs represent 65% to 75% of the cost of new semiconductor fabrication facilities[114], and it is seen from the process equipment, facility, and summary cost tables that the model also reflects this fact.

8.9 Transportation

Efficient transportation of equipment, raw material, and finished goods represents the single greatest challenge to an economically viable space-based microfabrication facility. Inexpensive, effective shipping is taken for granted on Earth, with next day service across the globe a common event. Use of trucks, ships, and aircraft to move large quantities of equipment and materiel great distances is a factor in the global economy, and the shipping infrastructure behind this movement is well established.

However, no such infrastructure currently exists for orbital goods transport. The single largest component of the space commercialization market is communication satellites[115,116] which need only be placed in orbit from a ground launch. Therefore, while the ability to place satellite-sized objects in low Earth and higher orbits exists, there is no capability to readily return material from orbiting facilities.

Estimates for the current cost of launching mass into low Earth orbit range from $10,000 to $22,000 per kg[117]. Compared with the estimated transportation cost of $4 per kg for transporting material from North America to Europe[118], the cost of space transporting is, and will remain, very high.

It is apparent from the differences in transportation costs that in order to compete on an economic basis with Earth-based manufacturing, the transportation

costs for space-based manufacturing must be carefully optimized. A review of the literature has indicated that little research into the optimization of two-way orbital transportation has been published, and yet, two-way transportation is a necessary precondition of any space-based manufacturing venture.

This section will describe a model developed by the author that attempts to address the main issues of two-way orbital transport. A key feature of this model will be the ability to return goods from orbit asynchronously.

Numerous factors affect the transportation costs to and from orbit for a space-based manufacturing facility. To simplify downstream economic analyses, this model will deliver the roundtrip total transportation cost as a function of the incremental launch cost ($/kg). The total transportation cost $c_{roundtriptotal}$ is the total cost of transportation (both raw materials and finished goods) per unit mass of finished goods delivered and is a function of the cost to launch goods up to orbit C_{up}, the cost to return goods down to Earth C_{down}, the mass of materials launched at a single time m_{up}, the mass of finished goods returned to Earth at a single time m_{down}, and the mass fraction of raw materials that are finished goods $f_{downmatl}$.

$$c_{roundtriptotal} = \frac{C_{up}}{m_{up} * f_{downmatl}} + \frac{C_{down}}{m_{down}} \tag{8.9}$$

If a synchronous mode of transport is assumed (each launch supplies the manufacturing facility with raw materials and returns finished goods), then optimization of the roundtrip cost is limited to determining how much mass will be launched in each trip and the most effective launch vehicle for that mass. The production goals of wafers per month (or other goods) automatically set the frequency of launches once the raw material launch mass is known.

However, it is important to understand that, for semiconductor processing in space, the mass of wafers and consumables required is very small. For 5,000 wafers per month, this is only 184 kg of wafers and 71 kg of consumables (ignoring packaging).

It is envisioned that for processes where the mass of finished goods is low and the delivery time of finished goods critical (such as semiconductor fabrication), it may be more efficient to launch large quantities of raw materials infrequently and retrieve finished goods from orbit frequently during the interval between launches. Such an asynchronous transport mode necessarily implies that the ability to return goods remotely from orbit exists and that such means, such as return capsules, are periodically included in the launches of supplies of raw materials.

For the purpose of this model, a return capsule is defined which has the capability to transport packaged, finished semiconductor wafers safely from Earth orbit to Earth. These return capsules would be small and light and would perhaps have a capacity of 1,000 finished wafers or 40 kg.

The key characteristics of such a capsule are:

- payload ability
- capsule mass
- capsule cost
- number of times that capsule can be reused

The return capsule payload ability $f_{payload}$ is expressed as the mass fraction of the total return mass that consists of payload (i.e. a $f_{payload}$ of 0.4 implies that 40% of the mass is payload and 60% is return capsule).

It is useful to develop a cost rate of the capsule per kg of payload mass returned expressed as a fraction of the incremental launch cost. The fractional

capsule cost rate $f_{capsule}$ is determined by the capsule cost $C_{capsule}$, the mass of the capsule payload $m_{payload}$, the number of times that the capsule can be reused n_{uses}, and the incremental launch cost per unit mass c_{up}. A fractional capsule cost of 0 indicates a completely reusable return capsule.

$$f_{capsule} = \frac{C_{capsule}}{m_{payload} * n_{uses} * c_{up}} \tag{8.10}$$

Given that launches are periodic events, it is useful to relate the period between launches p_{up} and the period between finished goods returns p_{down} by a non-dimensional launch fraction f_{launch}.

$$f_{launch} = \frac{p_{down}}{p_{up}} \tag{8.11}$$

It is obvious that the mass of finished goods returned per return capsule m_{down} is related to the rate at which finished goods are required r_{down} (assumed equal to the facility processing rate expressed in mass per unit time) and the period between finished goods returns p_{down}.

$$m_{down} = m_{payload} = r_{down} * p_{down} \tag{8.12}$$

Fixed costs play a large role in determining the overall transport cost. The non-dimensional fraction f_{fixed} is the ratio of fixed cost to retrieve a single return capsule $C_{fixeddown}$ to the fixed cost to perform a single launch $C_{fixedup}$.

$$f_{fixed} = \frac{C_{fixeddown}}{C_{fixedup}} \tag{8.13}$$

Having defined (8.10) through (8.13), the roundtrip total cost of (8.9) can be rewritten as

$$c_{roundtriptotal} = \left[\frac{1}{f_{downmatl}} + \frac{1}{f_{payload}} + f_{capsule} - 1 \right] * c_{up} + \left[\frac{f_{launch} + f_{fixed}}{r_{down} * p_{down}} \right] * C_{fixedup} \quad (8.14)$$

It can be seen in (8.14) that the first term relates to incremental launch costs and the second term relates to the fixed launch costs. Rewriting (8.14) to incorporate two new ratios R_1 and R_2 gives

$$c_{roundtriptotal} = (R_1 + R_2) * c_{up} \quad (8.15)$$

R_1 is a non-dimensional ratio that represents incremental costs.

$$R_1 = \frac{1}{f_{downmatl}} + \frac{1}{f_{payload}} + f_{capsule} - 1 \quad (8.16)$$

R_2 is a non-dimensional ratio that represents fixed costs. It is related by the launch fraction f_{launch}, the fixed cost fraction f_{fixed}, and a non-dimensional fraction of fixed launch costs f_{updown}.

$$f_{updown} = \frac{C_{fixedup}}{c_{up} * m_{down}} \quad (8.17)$$

$$R_2 = (f_{launch} + f_{fixed}) * f_{updown} \quad (8.18)$$

Note that both forms of the model given in (8.14) and (8.15) have two terms: the first determines the incremental costs and is governed by process considerations (ratio of finished goods to raw material mass) and return capsule capabilities; the second is governed by fixed costs, launch ratios, and mass flows.

Figure 8.1 shows a graph of R_1 versus $f_{downmatl}$ to demonstrate the relationship between capsule payload fraction $f_{payload}$ and mass fraction of raw materials that are finished goods for a $f_{capsule}$ of 0 (completely reusable return capsule). For typical semiconductor fabrication applications, $f_{downmatl}$ is 0.5 or greater and it is proposed that $f_{payload}$ of 0.5 is attainable, resulting in an R_1 value of approximately 3.

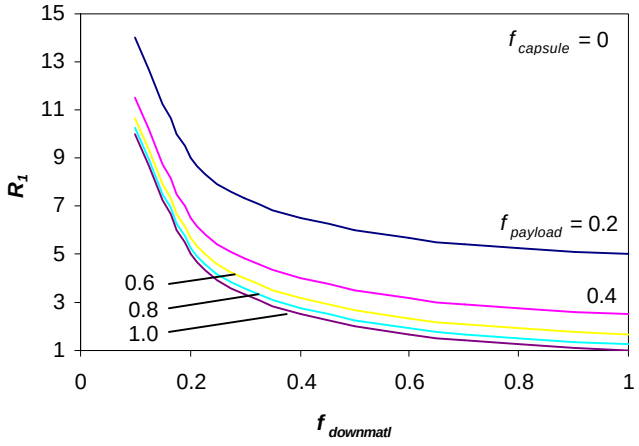

Figure 8.1 – Non-Dimensional Ratio of Incremental Orbital Transport Costs

Figure 8.2 shows the relationship of f_{updown} (non-dimensional fixed cost per kg of finished goods) and launch ratio f_{launch} (the launch ratio is the inverse of number of returns per launch). It is clear that amortizing the fixed costs over a large number of returns decreases R_2. More surprising is the scale of dependence of R_2 on f_{updown}. For typical semiconductor applications, it is envisioned that fixed launch cost C_{fixed} may be \$10,000,000 per launch, incremental launch cost c_{up} is \$1,000 to 5,000 per kg, and

m_{down} is 100 to 500 kg per return, resulting in an R_2 value of 7 to 100. Note that this is larger than the R_1 value of 3 calculated above, indicating that the roundtrip total transport cost $c_{roundtriptotal}$ is affected much more by fixed costs than by incremental costs.

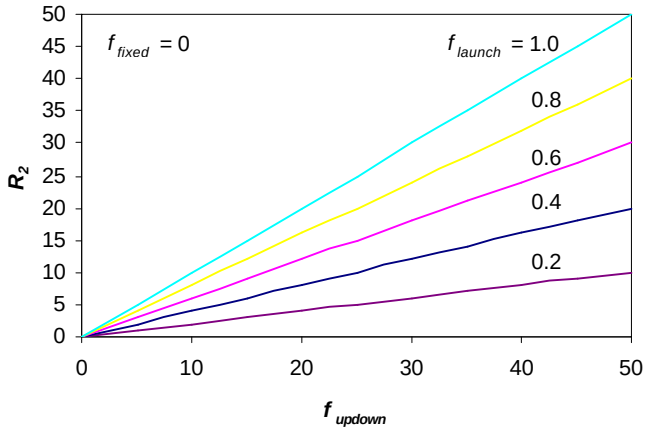

Figure 8.2 – Non-Dimensional Ratio of Fixed Orbital Transport Costs

This section has described an orbital transport cost model. The key benefit of this model is expressing the roundtrip total transport cost as a two term multiplier of the incremental launch cost. This allows the complexities of the transport model to be neglected in downstream economic analyses as all transport costs can be represented as either the incremental launch cost (for shipping equipment to the orbital facility) or the roundtrip total transport cost (for finished goods produced from raw materials shipped to the orbital facility).

8.10 Operating Cost

As described in Section 8.2, operating cost C_o is the cost to operate the production facility for a specific period. The operating cost accounts for the cost of

depreciation of capital items C_d, ongoing costs such as consumable materials C_c, power C_p and heat rejection C_h, shipping costs for raw materials and finished goods C_s, as well as any other costs required to produce the wafers.

8.10.1 Depreciation

Depreciation is the rate at which a capital item loses value. For the purposes of this model, straight-line depreciation is assumed whereby the capital items loses value at a steady rate over its useful lifetime such that it has full value at the start of its life and zero value at the end of its life. This lost value is shown as an expense and adds to the operating cost of the manufacturing facility. Depreciation can be simplistically viewed as the cost to rent the equipment.

The cost of capital items shown in Section 8.8 is the estimated cost to purchase the items, but does not include the cost of transporting the equipment to the facility location nor installation of the equipment. However, depreciation costs are based on the installed costs of the equipment, thus the cost of transportation and installation must also be depreciated. For a space-based facility with high transportation costs, the additional cost of shipping equipment can greatly increase the depreciation cost.

Table 8.20 shows the key assumptions used to arrive at the depreciation cost for the three reference models.

Table 8.20 – Key Assumptions for Determining Equipment Depreciation Costs

Symbol	Description	CMOS Standard Earth-Based	CMOS Dry Earth-Based	CMOS Dry Space-Based
c_{up}	Transportation Cost (USD/kg)	$4[118]	$4	$5,000
$f_{install}$	Installation Cost (% of first cost)	15%	15%	0%
f_{dep}	Depreciation Rate (% per year)	20%	20%	20%

While the installation cost for Earth-based facilities is shown as 15% of the purchase price of the equipment[73], the installation cost for space-based equipment is shown as zero. This is because it is assumed in this model that the equipment is installed in the facility on Earth and that its cost is included in the cost of the facility. Unlike Earth-based facilities where equipment is installed after the facility is built, the high integration requirement of a space-based facility dictates that the equipment and facility are constructed together.

A straight-line depreciation rate of 20% has been selected to reflect the five year useful life timeframe used by the semiconductor industry[73]. Use of a longer timeframe would result in a lower depreciation rate and lower depreciation costs.

The depreciation cost C_d is determined by the capital cost of the equipment and facility $C_{equipfacility}$, the mass of the equipment and facility $m_{equipfacility}$, the transportation cost per unit mass c_{up}, the installation rate $f_{install}$, and the depreciation rate f_{dep}.

$$C_d = f_{dep} * \left(C_{equipfacility} * (1 + f_{install}) + m_{equipfacility} * c_{up} \right) \tag{8.19}$$

The total installed capital cost of the equipment and facility $C_{totalequipfacility}$ is

$$C_{totalequipfacility} = C_{equipfacility} * (1 + f_{install}) + m_{equipfacility} * c_{up} \tag{8.20}$$

8.10.2 Utilities

On Earth, utility companies provide the power and water used for processing and heat rejection. In space, all such energy and mass must be provided locally or shipped to the facility. As this model treats water consumption as a consumable in a

later section, the cost of utilities is restricted to that required for power generation and heat rejection.

Table 8.21 shows the key assumptions used in the model to determine the power and heat rejection costs.

Table 8.21 – Key Assumptions for Determining Utility Costs

Symbol	Description	CMOS Standard Earth-Based	CMOS Dry Earth-Based	CMOS Dry Space-Based
c_p	Power Generation Operating Cost (USD/kW-h)	$0.05	$0.05	$0
c_h	Heat Rejection Operating Cost (USD/kW-h)	$0.05	$0.05	$0

The ongoing cost of providing power and heat rejection for a space-based facility is shown as zero as it is assumed that this capability is provided by onboard equipment such as solar cells and radiators and that the operating cost of such equipment is captured in the depreciation cost C_d .

Section 8.7 described the modeling of power and heat rejection requirements and the capital equipment needed to support them. The ongoing utility cost C_u of providing power and heat rejection are determined by the amount of power P and heat rejection H required and the cost rates c_p and c_h to provide that amount.

$$C_u = P * c_p + H * c_h \tag{8.21}$$

8.10.3 Maintenance

Equipment maintenance is the ongoing cost to ensure that the equipment is operational through regular maintenance and repairs and Table 8.22 shows the key assumptions used to determine this cost.

Table 8.22 – Key Assumptions for Determining Maintenance Costs

Symbol	Description	CMOS Standard Earth-Based	CMOS Dry Earth-Based	CMOS Dry Space-Based
f_{maint}	Annual Maintenance (% of total installed capital cost)	10%	10%	10%

While maintenance cost for Earth-based facilities is well established[73], it is hard to quantify for space-based enterprises. While the clean, vacuum environment could prolong equipment life, it could also lead to problems with lubrication. To account for the fact that the remoteness of space-based systems will add to the cost of transporting maintenance personnel to the facility, the maintenance cost has been assumed to be a fixed percent of the total installed cost, where this installed cost includes the higher transportation costs.

The maintenance cost C_m is determined by the maintenance rate f_{maint} and the total installed capital cost of the equipment and facility $C_{totalequipfacility}$.

$$C_m = f_{maint} * C_{totalequipfacility} \tag{8.22}$$

8.10.4 Consumables

The consumables used in microfabrication include the process consumables (gases, liquids, solids), the wafers, and the glass lithography masks for each level of the wafer fabrication process. Long runs devices, such as DRAM's, use the same mask set to produce many (up to 10,000) wafers. Short run items like ASIC's produce very few (250) wafers for a given mask set, leading to a requirement for more masks for a specified production volume.

Table 8.23 shows the key assumptions used to determine the cost of consumables. The consumable mass per level for each process flow has been taken from Table 7.5 and adjusted for the twelve level reference process.

Table 8.23 – Key Assumptions for Determining Consumable Costs

Symbol	Description	CMOS Standard Earth-Based	CMOS Dry Earth-Based	CMOS Dry Space-Based
c_{gas}	Gas Cost (USD/kg)	$3.713	$3.713	$3.713
c_{liquid}	Liquid Cost (USD/kg)	$0.000109[119]	$0.000109	$0.000109
c_{solid}	Solid Cost (USD/kg)	$14.74[120]	$14.74	$14.74
C_{wafer}	Wafer Cost (USD each)	$50	$50	$50
C_{mask}	Mask Cost (USD each)	$2000[121]	$2000	$2000
m_{gas}	Gas Mass (kg/level/wafer)	0.00698	0.00730	0.000304
m_{liquid}	Liquid Mass (kg/level/wafer)	64.93	0	0
m_{solid}	Solid Mass (kg/level/wafer)	2.827E-05	3.506E-05	3.506E-05
m_{wafer}	Wafer Mass (kg each)	0.0368	0.0368	0.0368
m_{mask}	Mask Mass (kg each)	0.0921	0.0921	0.0921

The cost of consumables C_c for a given period (such as a year) is determined the production rate r_w, the number of device levels l, the number of wafers per mask set $n_{maskset}$, and the appropriate consumable costs and masses, all in consistent units.

$$C_c = (m_{gas} * c_{gas} + m_{liquid} * cl_{iquid} + m_{solid} * c_{solid}) * l * r_w + m_{wafer} * r_w + \frac{m_{mask} * r_w * l}{n_{maskset}} \quad (8.23)$$

8.10.5 Shipping

Section 8.9 *Transportation* described the concept of roundtrip total transportation cost whereby the cost to ship raw materials to a facility and deliver finished goods from a facility is expressed in terms of the cost per unit mass of finished goods. The raw materials include the process consumables, the wafers, and

the masks as well as packaging and containers while the finished goods are the fully processed wafers.

The point of origin and return of the goods referred to above is assumed to lie within an Earth-based semiconductor fabrication facility where final packaging is performed. Thus, if the microfabrication process is conducted in this same facility, the shipping cost for consumables and finished goods (within the facility) would be zero. This is the case for Earth-based processes where it is assumed that all semiconductor fabrication occurs at a single facility. When fabrication, testing, and packaging are conducted in separate facilities (as is often the case with commercial semiconductor production), the previous assumption is incorrect. However, the scale of the transport costs on Earth ($4/kg) adds less than $0.50 to the wafer fabrication costs and is therefore neglected in this model. In contrast, space transportation costs are high ($1000's per kg) and must be considered. In space-based processing, the fabrication takes place in two separate facilities: the microfabrication occurs in orbit, and the final device packaging occurs on Earth. In this case, the shipping costs are the costs to ship material between the two facilities.

Table 8.24 shows the key assumptions used to determine the cost of shipping.

Table 8.24 – Key Assumptions for Determining Shipping Costs

Symbol	Description	CMOS Standard Earth-Based	CMOS Dry Earth-Based	CMOS Dry Space-Based
$c_{roundtriptotal}$	Total Transport Cost (USD/kg finished goods)	$0	$0	$15,000

In a space-based semiconductor fabrication facility, the mass of finished goods is a large fraction of the total mass of raw materials, leading to a roundtrip shipping cost that is approximately three times that of the incremental launch cost c_{up}.

The shipping cost is determined by the total roundtrip shipping cost $c_{roundtriptotal}$, the mass of a finished wafer m_{wafer} (assumed to be the same as the raw wafer with thin film masses neglected) and the production rate r_w.

$$C_s = c_{roundtriptotal} * m_{wafer} * r_w \tag{8.24}$$

8.10.6 Operating Cost

To finish, the operating cost C_o is determined by substituting (8.19) to (8.24) into (8.1). The operating cost per unit wafer $_o$ is determined from (8.2). These operating cost formulas will be applied to the process flow model results in Chapter 9 to provide a means of comparing the economics of space-based semiconductor fabrication with that of similar processing conducted on Earth.

8.11 Conclusions

This chapter has described a system for comparing the economics of space-based and Earth-based semiconductor fabrication. An operating cost model was constructed for use as the basis in determining the economic viability of space-based production. The primary metric produced by the model was the operating cost per wafer, comprised of the portion of depreciation, utilities, maintenance, consumables, and shipping attributable to fabricating a single 200 mm silicon wafer.

Transportation costs were shown to be a key factor in determining the operating cost. An asynchronous transportation scheme was proposed and modeled for the delivery of raw materials to orbit and the return of finished goods from orbit.

Chapter 9 will use these models to calculate the operating costs for each type of process flow.

Chapter 9
Operating Cost Results

9.1 Introduction

This chapter will show that space-based semiconductor fabrication can be economically competitive with Earth-based semiconductor fabrication under certain conditions.

This chapter will present the results of the operating cost model developed in Chapter 8. It will be shown that the operating cost for space-based fabrication is higher than Earth-based microfabrication for the base production case. However, a sensitivity analysis of the factors affecting operating cost will show that by optimizing the production parameters (such is already done on Earth), such as by reducing the wafer mass, the operating cost of processing in space can be lower than that for Earth-based semiconductor fabrication.

9.2 Results

Table 9.1 shows the breakdown of operating costs for the base production case of 5,000 wafers per month, 20 layer devices, and 250 wafers per mask set using 1999 equipment costs. While 5,000 wafers/month is small for an Earth-based fabrication facility, it is the expected size of an initial space-based facility.

It can be seen that the operating cost per unit wafer is least for traditional, Earth-based semiconductor fabrication and highest for space-based fabrication, with the all-dry Earth-based process somewhere in between. Table 9.1 also shows that the depreciation cost forms a large fraction of the total operating cost in all cases, reflecting the capital intensive nature and short timeframes of the semiconductor

fabrication industry. Shipping costs comprise 28% of the operating cost for space-based microfabrication, but none for Earth-based fabrication, one factor in the higher space-based costs. Despite the elimination of vacuum pumps and systems in the space-based equipment model, it was shown that the capital cost of the dry Earth process and the dry space process models are similar, leading to similar operating costs once space transportation costs are accounted for.

Table 9.1 – Operating Costs for Base Case

Symbol	Description	CMOS Standard Earth-Based	CMOS Dry Earth-Based	CMOS Dry Space-Based
C_d	Depreciation Cost (USD)	$29,257,844	$51,694,501	$47,706,695
C_u	Utilities Cost (USD)	$1,155,834	$70,576	$0
C_m	Maintenance Cost (USD)	$14,628,922	$25,847,250	$23,853,348
C_c	Consumables Cost (USD)	$12,640,074	$12,633,134	$12,601,977
C_s	Shipping Cost (USD)	$0	$0	$33,123,382
C_o	Operating Cost (USD)	$57,682,673	$90,245,461	$117,285,402
$_o$	Operating Cost per Unit Wafer (USD/wafer)	$961	$1,504	$1,955

It is useful to define an operating cost ratio. This ratio is the ratio of space-based to Earth-based unit operating cost. The lower the operating cost ratio below 100%, the more favourable semiconductor fabrication in space is compare with Earth-based fabrication. Operating cost ratios greater than 100% indicate that Earth-based fabrication is more economically favourable. Table 9.2 shows the calculated operating cost ratio for the base case.

Table 9.2 – Operating Cost Ratios for Base Case

Description	Dry Space/Standard Earth	Dry Space/Dry Earth
Operating Cost Ratio	203%	130%

To evaluate the feasibility of space based fabrication for a range of cases, it is useful to determine the operating cost and operating cost ratio for situations other

than the base production case. Table 9.3 shows the operating costs (per wafer) and the operating cost ratios for a range of production scenarios.

Table 9.3 – Operating Costs and Operating Cost Ratios

Wafers per Month	Layers	Wafers per Mask Set	Operating Cost CMOS Std. Earth-Based (USD/wafer)	Operating Cost CMOS Dry Earth-Based (USD/wafer)	Operating Cost CMOS Dry Space-Based (USD/wafer)	Operating Cost Ratio Dry Space/ Std. Earth (%)	Operating Cost Ratio Dry Space/ Dry Earth (%)
50	10	250	$9,917	$6,877	$14,240	144%	207%
100	10	250	$5,029	$3,504	$7,474	149%	213%
250	10	250	$2,242	$1,980	$3,981	178%	201%
500	10	250	$1,242	$1,343	$2,635	212%	196%
750	10	250	$969	$1,094	$2,077	214%	190%
1,000	10	250	$787	$972	$1,880	239%	193%
2,500	10	250	$596	$837	$1,443	242%	172%
5,000	10	250	$532	$792	$1,342	252%	169%
10,000	10	250	$506	$777	$1,278	253%	165%
25,000	10	250	$490	$763	$1,258	257%	165%
50	20	250	$10,008	$6,958	$14,346	143%	206%
100	20	250	$5,485	$4,443	$8,996	164%	202%
250	20	250	$2,434	$2,637	$4,667	192%	177%
500	20	250	$1,524	$1,895	$3,157	207%	167%
750	20	250	$1,269	$1,681	$2,654	209%	158%
1,000	20	250	$1,205	$1,718	$2,444	203%	142%
2,500	20	250	$1,015	$1,534	$2,081	205%	136%
5,000	20	250	$961	$1,504	$1,955	203%	130%
10,000	20	250	$932	$1,479	$1,933	207%	131%
25,000	20	250	$919	$1,467	$1,891	206%	129%
50	30	250	$10,828	$8,203	$16,653	154%	203%
100	30	250	$5,576	$5,163	$9,102	163%	176%
250	30	250	$2,806	$3,182	$5,026	179%	158%
500	30	250	$1,879	$2,496	$3,679	196%	147%
750	30	250	$1,714	$2,493	$3,285	192%	132%
1,000	30	250	$1,617	$2,295	$2,966	183%	129%
2,500	30	250	$1,451	$2,232	$2,736	189%	123%
5,000	30	250	$1,384	$2,196	$2,596	188%	118%
10,000	30	250	$1,358	$2,180	$2,556	188%	117%
25,000	30	250	$1,350	$2,171	$2,534	188%	117%
50	10	1,500	$9,850	$6,811	$14,173	144%	208%
100	10	1,500	$4,962	$3,438	$7,407	149%	215%
250	10	1,500	$2,175	$1,914	$3,914	180%	205%
500	10	1,500	$1,175	$1,277	$2,568	219%	201%
750	10	1,500	$902	$1,027	$2,010	223%	196%
1,000	10	1,500	$720	$906	$1,813	252%	200%
2,500	10	1,500	$529	$771	$1,377	260%	179%
5,000	10	1,500	$466	$725	$1,275	274%	176%
10,000	10	1,500	$439	$710	$1,212	276%	171%
25,000	10	1,500	$423	$696	$1,191	282%	171%

Table 9.3 – Operating Costs and Operating Cost Ratios continued

Wafers per Month	Layers	Wafers per Mask Set	Operating Cost CMOS Std. Earth-Based (USD/wafer)	Operating Cost CMOS Dry Earth-Based (USD/wafer)	Operating Cost CMOS Dry Space-Based (USD/wafer)	Operating Cost Ratio Dry Space/ Std. Earth (%)	Operating Cost Ratio Dry Space/ Dry Earth (%)
50	20	1,500	$9,875	$6,825	$14,213	144%	208%
100	20	1,500	$5,351	$4,310	$8,862	166%	206%
250	20	1,500	$2,300	$2,503	$4,534	197%	181%
500	20	1,500	$1,390	$1,762	$3,024	217%	172%
750	20	1,500	$1,136	$1,547	$2,520	222%	163%
1,000	20	1,500	$1,072	$1,585	$2,311	216%	146%
2,500	20	1,500	$881	$1,401	$1,948	221%	139%
5,000	20	1,500	$828	$1,371	$1,821	220%	133%
10,000	20	1,500	$798	$1,346	$1,799	225%	134%
25,000	20	1,500	$786	$1,333	$1,758	224%	132%
50	30	1,500	$10,628	$8,003	$16,453	155%	206%
100	30	1,500	$5,376	$4,963	$8,902	166%	179%
250	30	1,500	$2,606	$2,982	$4,826	185%	162%
500	30	1,500	$1,679	$2,296	$3,479	207%	152%
750	30	1,500	$1,514	$2,293	$3,085	204%	135%
1,000	30	1,500	$1,417	$2,095	$2,766	195%	132%
2,500	30	1,500	$1,251	$2,032	$2,536	203%	125%
5,000	30	1,500	$1,184	$1,996	$2,396	202%	120%
10,000	30	1,500	$1,158	$1,980	$2,356	203%	119%
25,000	30	1,500	$1,150	$1,971	$2,334	203%	118%
50	10	10,000	$9,839	$6,799	$14,162	144%	208%
100	10	10,000	$4,951	$3,426	$7,396	149%	216%
250	10	10,000	$2,164	$1,902	$3,903	180%	205%
500	10	10,000	$1,164	$1,265	$2,557	220%	202%
750	10	10,000	$891	$1,016	$1,999	224%	197%
1,000	10	10,000	$709	$894	$1,802	254%	201%
2,500	10	10,000	$518	$759	$1,365	264%	180%
5,000	10	10,000	$454	$714	$1,264	278%	177%
10,000	10	10,000	$428	$699	$1,200	281%	172%
25,000	10	10,000	$412	$685	$1,180	287%	172%
50	20	10,000	$9,852	$6,802	$14,190	144%	209%
100	20	10,000	$5,329	$4,287	$8,840	166%	206%
250	20	10,000	$2,278	$2,481	$4,511	198%	182%
500	20	10,000	$1,368	$1,739	$3,001	219%	173%
750	20	10,000	$1,113	$1,525	$2,498	224%	164%
1,000	20	10,000	$1,049	$1,562	$2,288	218%	146%
2,500	20	10,000	$859	$1,378	$1,925	224%	140%
5,000	20	10,000	$805	$1,348	$1,799	223%	133%
10,000	20	10,000	$776	$1,323	$1,777	229%	134%
25,000	20	10,000	$763	$1,311	$1,735	227%	132%
50	30	10,000	$10,594	$7,969	$16,419	155%	206%
100	30	10,000	$5,342	$4,929	$8,868	166%	180%
250	30	10,000	$2,572	$2,948	$4,792	186%	163%
500	30	10,000	$1,645	$2,262	$3,445	209%	152%
750	30	10,000	$1,480	$2,259	$3,051	206%	135%

Table 9.3 – Operating Costs and Operating Cost Ratios continued

Wafers per Month	Layers	Wafers per Mask Set	Operating Cost CMOS Std. Earth-Based (USD/wafer)	Operating Cost CMOS Dry Earth-Based (USD/wafer)	Operating Cost CMOS Dry Space-Based (USD/wafer)	Operating Cost Ratio Dry Space/ Std. Earth (%)	Operating Cost Ratio Dry Space/ Dry Earth (%)
1,000	30	10,000	$1,383	$2,061	$2,732	198%	133%
2,500	30	10,000	$1,217	$1,998	$2,502	206%	125%
5,000	30	10,000	$1,150	$1,962	$2,362	205%	120%
10,000	30	10,000	$1,124	$1,946	$2,322	207%	119%
25,000	30	10,000	$1,116	$1,937	$2,300	206%	119%

Figure 9.1 to Figure 9.3 graph the variation in operating cost per unit wafer for ASIC devices (l = 20, $n_{maskset}$ = 250) with increasing production rate. It can be seen that the per unit operating cost drops quickly as the production volume increases, eventually leveling at a constant value. The small kinks in the graphs at low production volumes are attributable to single increment changes in equipment requirements.

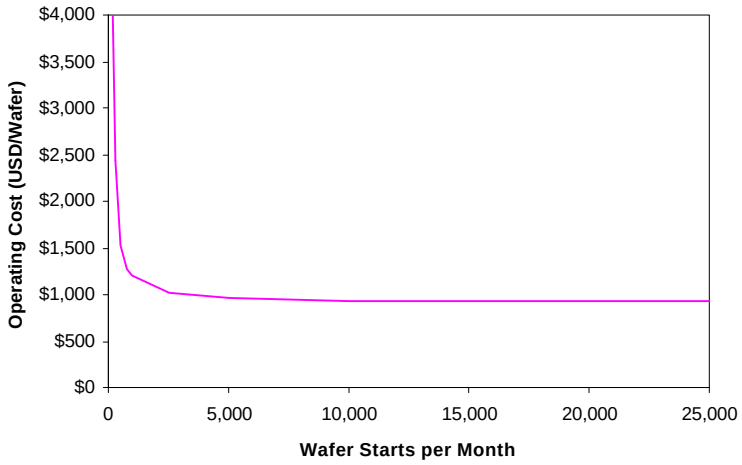

Figure 9.1 – Operating Cost of Standard Earth-Based Process for ASIC Devices (l = 20, $n_{maskset}$ = 250)

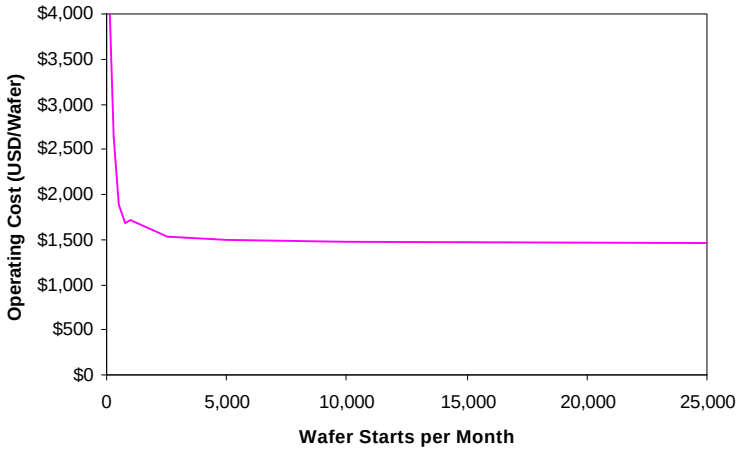

Figure 9.2 – Operating Cost of Dry Earth-Based Process for ASIC Devices (l = 20, $n_{maskset}$ = 250)

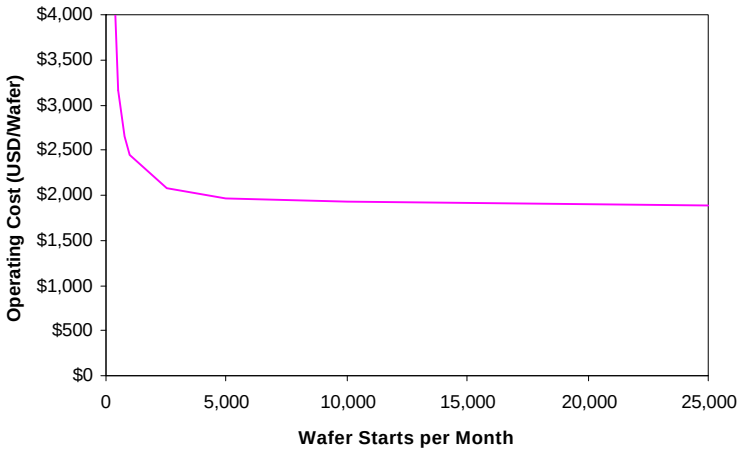

Figure 9.3 – Operating Cost of Dry Space-Based Process for ASIC Devices (l = 20, $n_{maskset}$ = 250)

Figure 9.4 and Figure 9.5 show the operating cost ratio of standard and dry Earth-based processing for the same ASIC devices. It can be seen from these figures that space-based processing most closely competes with standard Earth-based processing at low production levels. However, the model was developed with process equipment sized for larger production runs and may not accurately reflect optimized equipment quantities at very low production levels.

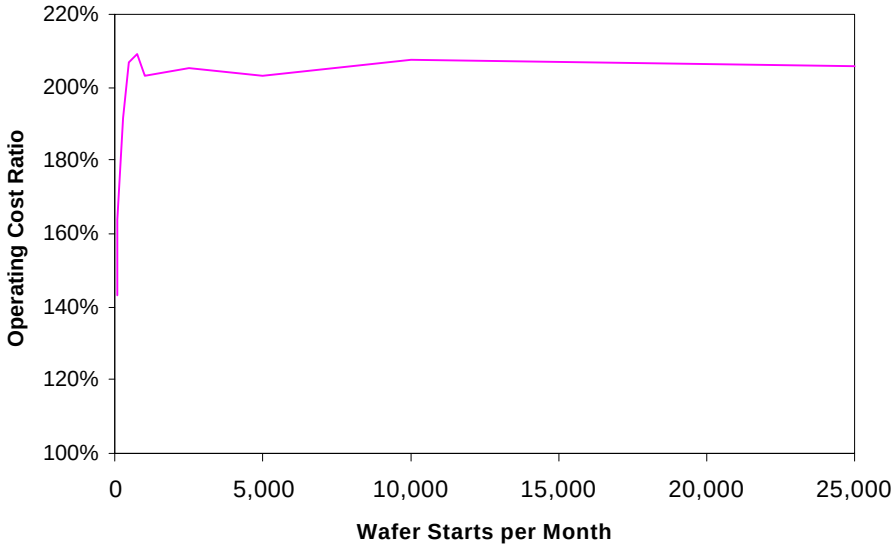

Figure 9.4 – Operating Cost Ratio Dry Space-Based versus Standard Earth-Based Process for ASIC Devices (l = 20, $n_{maskset}$ = 250)

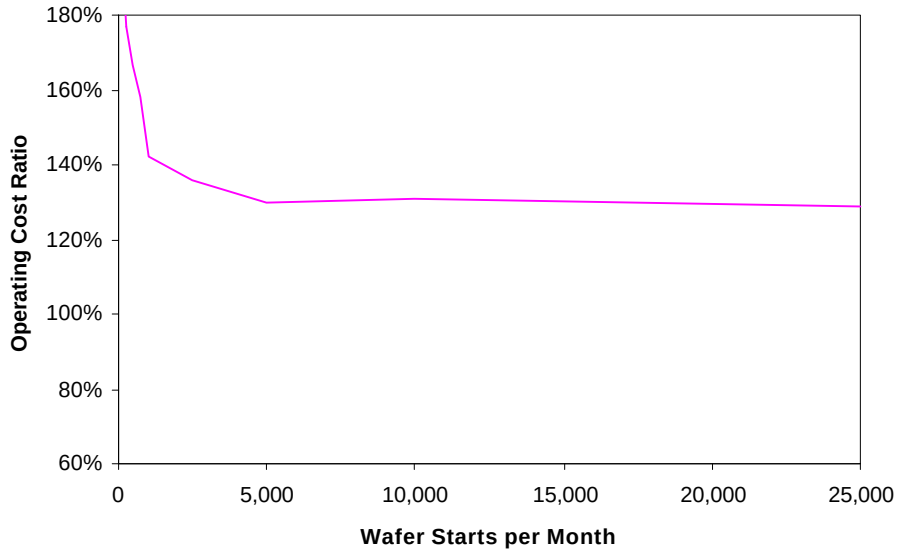

Figure 9.5 – Operating Cost Ratio Dry Space-Based versus Dry-Earth-Based Process for ASIC Devices (l = 20, $n_{maskset}$ = 250)

9.3 Sensitivity Analysis

The preceding section has shown that the space-based microfabrication process modeled is not able to economically compete directly against the two modeled Earth-based processes for the base production case. In order to be commercially viable, a space-based semiconductor fabrication facility must not only produce semiconductor devices, but it must do so in a cost effective manner that provides economic payback to the facility owner. It is important to note that the results are for fabrication facilities that are optimized for Earth-based resource usage, and year 1999 equipment costs. However, microfabrication is an industry that is constantly undergoing process changes. Various estimates place fabrication facility costs as rising by 10-30% per year. Similarly, for reasons discussed earlier, the dry Earth-based processing may become a standard in the future. Finally, it is clearly necessary to see what optimizations of the space microfabrication process will reduce its costs. Thus, as the space-based process model did not provide lower unit operating costs than equivalent Earth-based facilities, changes are required in order to produce an attractive economic incentive for space-based fabrication.

One method to determine which factors most affect the unit operating costs of space-based semiconductor fabrication is to perform a sensitivity analysis. A sensitivity analysis has been performed for the base production case in which each of the input parameters to the cost model has been varied by 1% of its value and new unit operating cost and operating cost ratios were calculated for each of the three processes: standard Earth, dry Earth, and dry space. The parameters were then ranked by operating cost ratio to determine which input parameters caused the largest change in operating cost ratio. Appendix K contains the details of the sensitivity analysis.

A total of 63 input parameters were selected from the following categories:

- capital items
- consumable items
- power/heat rejection items
- shipping/installation/maintenance items
- depreciation
- product related items

Table 9.4 shows the top ten most sensitive parameters that affect the dry space to standard Earth operating cost ratio. The % Change values shown are the change in operating cost ratio for a 1% increase in the input parameter, with negative values indicating that increasing the parameter value improves the economic viability of space-based fabrication.

Table 9.4 – Top Ten Sensitive Parameters Affecting Dry Space to Standard Earth Operating Cost Ratio

Input Parameter	Base Value	% Change
Process Equipment Cost Std. Earth (USD)	$94,843,000	-0.564%
Raw Wafer Mass (kg each)	0.0368	0.282%
Total Transport Cost Dry Space Earth (USD/kg finished goods)	$15,000	0.282%
Shipping Rate Dry Space (USD/kg)	$5,000	0.244%
Process Equipment Cost Dry Space (USD)	$76,862,000	0.197%
Wafer Starts per Month	5000	0.176%
Process Equipment Mass Dry Space (kg)	12486	0.160%
Support Facility Cost Std. Earth (USD)	$21,168,000	-0.110%
Support Facility Cost Std. Space (USD)	$39,430,000	0.101%
Depreciation Rate % per year)	20%	-0.100%

It can be seen that the cost of process equipment occupies the first and fifth slot, indicating that cost increases in Earth-based equipment, cost decreases in space-based equipment, or combinations of the two will greatly affect the operating cost ratio.

The high cost of transport to/from space is shown by the presence of four input parameters: raw wafer mass, total space transport cost, space shipping rate, and process equipment mass. Clearly, reducing the shipping rates or reducing the mass which must be transported (wafers, equipment) will improve the operating cost ratio.

Support facility costs and the depreciation rate are also shown to affect the operating cost ratio. As with process equipment, increases in Earth-based costs or decreases in space-based costs will improve the operating ratio. Increasing the depreciation rate (reducing equipment lifetimes) unexpectedly improves the operating cost ratio due to the larger fraction of operating cost that is comprised of depreciation in the standard Earth-based model. While Table 9.1 shows that the depreciation costs are higher for the space-based case, the presence of large shipping costs reduces the fraction of the operating cost that is due to depreciation to below that of the standard Earth-based case.

The dry Earth process was introduced in Section 7.2 in order to answer the question: What happens when an all dry process is done on Earth instead of in space? It has been shown that such a dry process is not economically competitive with the standard, wet Earth-based processing in current commercial semiconductor fabrication facilities. However, several factors make it plausible that such a dry process may yet be required in Earth-based facilities: the increasing cost of chemical waste treatment and the surrounding environmental issues, the increased resolution achievable with thermal lithographic techniques using inorganic resists, and the decrease in available water supplies. Given that such a dry process may still become dominant for Earth-based semiconductor fabrication, a sensitivity analysis has been performed to determine what factors would favour space-based fabrication over the dry Earth-based process.

Table 9.5 shows the top ten most sensitive parameters that affect the dry space to dry Earth operating cost ratio. As with Table 9.4, equipment costs, facility costs and transportation issues dominate.

Table 9.5 – Top Ten Sensitive Parameters Affecting Dry Space to Dry Earth Operating Cost Ratio

Input Parameter	Base Value	% Change
Process Equipment Cost Dry Earth (USD)	$186,500,000	-0.707925%
Raw Wafer Mass (kg each)	0.036804	0.282417%
Total Transport Cost Dry Space Earth (USD/kg finished goods)	$15,000	0.282417%
Wafer Starts per Month	5000	0.278035%
Shipping Rate Dry Space (USD/kg)	$5,000	0.244303%
Process Equipment Cost Dry Space (USD)	$76,862,000	0.196602%
Depreciation Rate (% per year)	20%	-0.165118%
Process Equipment Mass Dry Space (kg)	12486	0.159687%
Support Facility Cost Std. Space (USD)	$39,429,960	0.100856%
Installation Rate Dry Earth (% capital cost)	15%	-0.092921%

Figure 9.6 to Figure 9.11 show the effects of varying the most sensitive input parameters for the base production case. In each figure, a single input parameter or a combination of parameters is varied over a range of values to determine the standard Earth and dry Earth operating cost ratios.

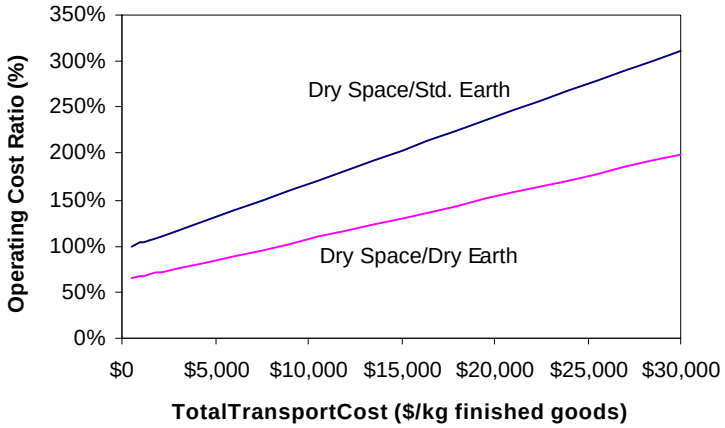

Figure 9.6 – Total Roundtrip Transport Cost to Space Varied

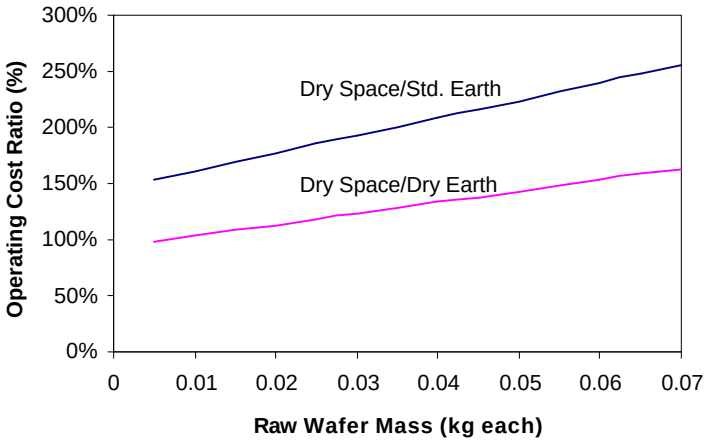

Figure 9.7 – Wafer Mass Varied

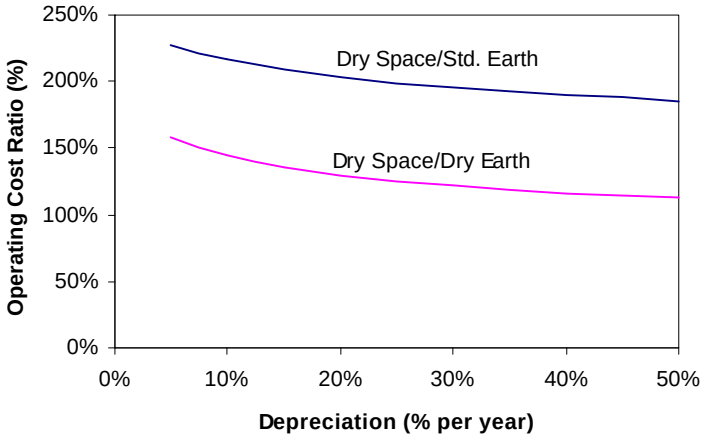

Figure 9.8 – Depreciation Varied

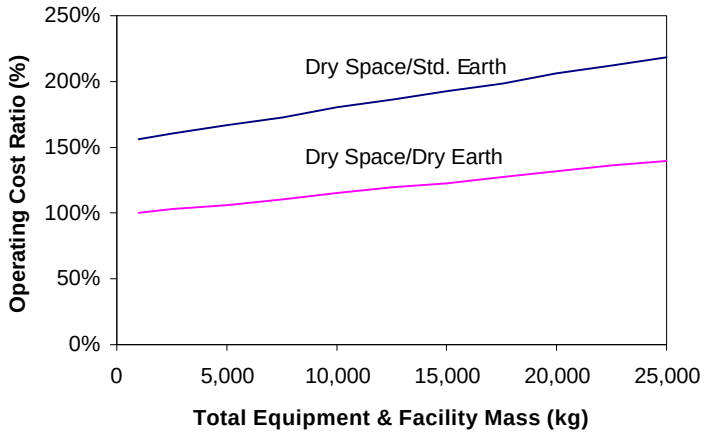

Figure 9.9 – Space Equipment & Facility Mass Varied

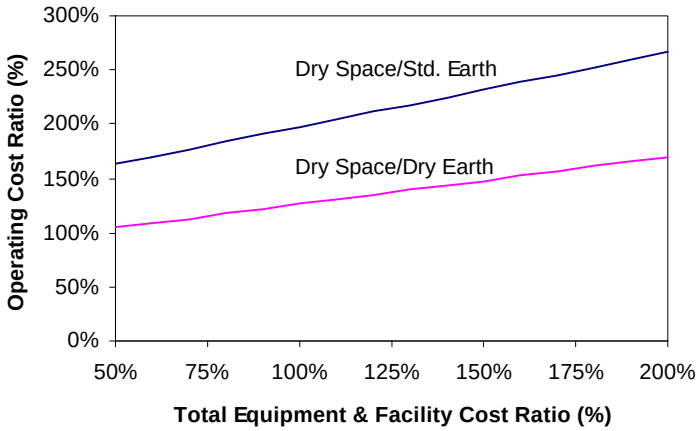

Figure 9.10 – Ratio of Space-Based to Standard Earth-Based Equipment & Facility Cost Varied

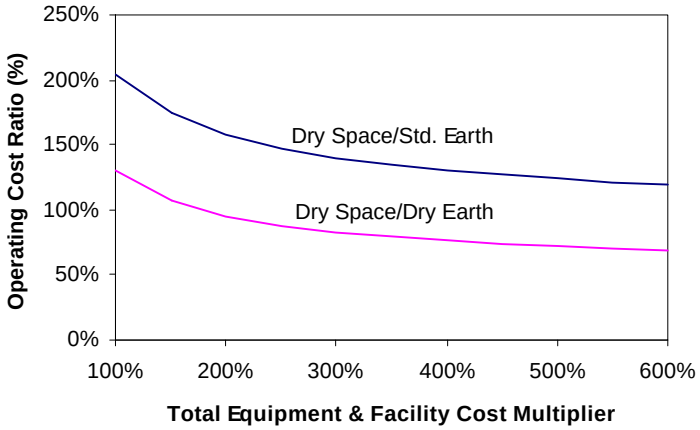

Figure 9.11 – Equipment & Facility Cost Increased

It can be seen from the above figures that the operating cost ratio can be reduced below 100% (indicating favourable economics for space-based fabrication) by several methods. Particularly interesting is Figure 9.11 which shows that as equipment and facilities become more expensive (both on Earth and in space), the relative cost of fabricating semiconductors in space becomes more favourable. At the current 18%[122] to 20%[123] per year rate of equipment and facility cost escalation, the space case becomes economically competitive with dry, Earth-based fabrication within four years. At the end of ten years at the 20% cost escalation from our base

cost date of 1999, approximately a 600% equipment cost multiplier would be expected and the standard Earth-based fabrication process would be 17% less expensive and the dry Earth-based fabrication process would be 44% more expensive than dry space-based semiconductor fabrication. Note that those Figure 9.11 curves show a saturation of the operating cost ratio reduction beginning at about 300% cost increase (6 years at 20% escalation). This is the long term scenario for full production.

Table 9.6 shows eight cases in which combinations of input parameters are varied to improve the economics of space-based semiconductor fabrication. It is apparent that the appropriate combination of input parameter variations is able to provide operating cost ratios that greatly favour space-based semiconductor fabrication. The largest improvements come from reducing the wafer mass and reducing space transportation costs, although the ever increasing cost of facilities and equipment continues to provide a cost benefit to space-based microfabrication.

As the space-based microfabrication process has been modeled using standard, commercially available wafers, no effort has been expended on developing specialized wafers for space. However, it appears readily feasible that thinner silicon wafers can be fabricated on Earth economically for use in space. Issues surrounding wafer thickness on Earth, such as thermal stability and handling may be mitigated by the microgravity, vacuum environment of a space-based semiconductor fabrication facility.

Should NASA reach its goal to "reduce the cost to low-Earth orbit by an order of magnitude in 10 years and another order of magnitude in 25 years"[124], then Table 9.6 shows that space-based microfabrication could be a very commercially viable venture. NASA has publicly committed to reduce launch costs below $2,200 per kg by the end of 2010[125].

Table 9.6 – Eight Cases to Improve Operating Cost Ratio

Case	Operating Cost Ratio Standard Earth	Operating Cost Ratio Dry Earth
Base Case	203%	130%
Case 1 As in Base Case but • wafer mass reduced to 50% • total transport cost to space reduced to $3000/kg • launch cost to space reduced to $1000/kg	112%	72%
Case 2 As in Case 1 but • Earth process equipment cost increased by 10% • space process equipment mass decreased by 10%	105%	71%
Case 3 As in Case 1 but • Earth process equipment cost increased by 20% • space process equipment mass decreased by 20%	99%	71%
Case 4 As in Case 3 but • total transport cost to space reduced to $2000/kg	98%	69%
Case 5 As in Case 4 but • wafer mass decreased to 25% of original mass • launch cost to space reduced to $500/kg	92%	65%
Case 6 As in Case 5 but • mask mass decreased to 50% of original mass • total transport cost to space reduced to $1250/kg	91%	65%
Case 7 As in Case 1 but • Earth and space equipment and facilities cost multiplied by 600%	101%	58%
Case 8 As in Case 7 but • Completely reusable supply ship • TotalTransportCost to space = $1000/kg • ShipRate to space=$1000/kg	100%	58%

9.4 Effect of Changing Wafer Size

Thus far, the process and economics models have been constructed assuming the use of 200 mm wafers. While it is expected that 200 mm wafers will continue in use for several more years[126], it is illustrative to examine the effect on operating cost ratio of a change in wafer size. Such a change is predicted to occur, on average, every nine years[126].

A simplified analysis was conducted to determine the operating cost ratios for the base production case of 5,000 ASIC wafers per month using 300 mm wafers in place of the 200 mm size. In this analysis, the mass, volume, cost, and power consumption of all process equipment was scaled in relation to the surface area between the two wafer sizes (225%). In addition, the wafer mass, mask mass, and consumable mass per level was also scaled by 225%. The result was a cost per wafer of $1,225, $1,767, and $2,907 respectively for the standard Earth, dry Earth, and dry space processes, leading to the results shown in Table 9.7.

Table 9.7 – Operating Cost Ratios for Base Case with 300 mm Wafers

Description	Dry Space/Standard Earth	Dry Space/Dry Earth
Operating Cost Ratio	237%	165%

Comparison with the operating cost ratios shown in Table 9.2 for the base case with 200 mm wafers, indicates that the economics become less favourable for space-based microfabrication as the wafer size increases in the base production case. An examination of the issues affecting the change in operating cost ratios shows that the increased wafer and mask mass are the primary factors in the change. It is expected that as space transportation costs decrease, the wafer and mask masses will have less effect on the overall economics, resulting in little or no change in operating cost ratios with increasing wafer size.

9.5 Conclusions

This chapter has described the results of the operating cost model developed in Chapter 8. It has been shown that the operating cost per wafer is a convenient metric for evaluating the economic feasibility of microfabrication[73]. Using a series of key assumptions, an operating cost model was constructed for the three reference process flows that indicated that the standard Earth-based process is the most economical for the base production case of 5,000 ASIC wafers per month. This model indicated that the operating per cost per wafer was $961, $1,504, and $1,955 respectively for standard Earth-based, dry Earth-based, and space-based microfabrication.

To allow comparisons over a range of changes in input parameters and key assumptions, the concept of operating cost ratio, the space-based cost per wafer divided by the Earth-based cost per wafer, was introduced. Operating cost ratios less than 100% designated favourable economics for space-based microfabrication.

Through the use of a sensitivity analysis, it was determined that the primary factors affecting the economics of space-based semiconductor fabrication were: process equipment cost, transport mass, and space transportation cost. It was found that by optimizing the wafer thickness for space-based fabrication, the wafer mass, forming the largest component of transport mass, could be significantly reduced. Forecasts by NASA and other companies indicate that launch and roundtrip transportation costs could significantly decrease in the future.

Modeling decreased wafer mass, decreased launch cost, and a relative decrease in the cost of process equipment showed that space-based semiconductor fabrication could economically compete in the base production case against both standard and dry Earth-based microfabrication with very few changes to the initial key assumptions. In the final two cases modeled, it was shown that the cost of

manufacturing semiconductors in space could be made equal to or less than that of using a standard process in an Earth-based facility and could be made significantly less than that of using an equivalent all dry process performed in an Earth-based facility. It should be noted that it has been assumed that the device yield of space-based processing would be the same as the device yield on Earth. However, any wafer yield advantage in space due to the superior cleanliness of the environment would provide a significant cost benefit to space-based processing.

With current trends, microfabrication equipment costs are rising with time in order to obtain finer geometries. At the same time, space transportation costs are declining. The results suggest that as time goes on, the trends will begin to generate a significant advantage for space-based microfabrication.

Chapter 10
Infrastructure

10.1 Introduction

This chapter will show that space-based semiconductor fabrication requires a support infrastructure that does not yet exist in order to compete on a commercial basis with Earth-based microfabrication facilities.

Transportation of raw materials and finished goods is an inherent requirement for any manufacturing facility. Yet, the existing space transportation system is designed only for one-way transport, with a primary mission of launching satellites into orbit. It will be shown that a space-based semiconductor fabrication facility will require frequent launches for supply of raw material and for servicing of equipment. It will also be shown that existing and proposed launch vehicles are not well suited for this application. Indeed this aspect of space transportation is not unique to orbital microfabrication, and would occur with any high value per mass and high volume product. Yet these are precisely the type of products which would drive initial space industrialization activities. Thus, this chapter will suggest another valuable aspect of this study: if any routine orbital manufacturing is to be accomplished, new space transportation products are required.

Other infrastructure systems will be briefly examined to determine the changes required to support a space-based fabrication facility. It will be shown that a new framework for launch and return capsule insurance will need to be developed to for the ongoing, two-way transport of raw materials and finished goods. It will also be shown that the risk in developing space-qualified, processing equipment can be reduced by stimulating early commercial acceptance of new, dry processes on Earth.

10.2 Background

It was shown in Chapter 8 that space-based microfabrication could be economically competitive with Earth-based processes under some circumstances. A key factor in the economic viability of the space-based case was the cost of transportation. However, in addition to the economic analysis of orbital transportation, it is necessary to examine the support infrastructure required for any space manufacturing venture in order to determine the practicality of the concept.

On Earth, the transportation infrastructure upon which global manufacturing is based is well established. A transportation infrastructure for space is also established, although it is based upon satellite deployment rather than manufacturing. The following two sections will examine the transportation requirements for an orbital semiconductor fabrication facility and compare them against the present space transportation infrastructure.

Insurance is a key component of space transportation, designed to minimize risk to the launch customer for the transport of payloads to orbit. The terrestrial equivalent, shipping insurance, is well known and plays an integral part of global commerce. However, two-way shipping to and from orbit involves two different modes of transport, and a comprehensive shipping insurance framework does not yet exist. The development of such an insurance infrastructure is required to allow the commercialization of the space-based semiconductor fabrication concept.

Finally, a large infrastructure exists to support the development of semiconductor process equipment. The continuing progress in semiconductor devices requires new generations of process equipment on a regular basis. Industry consortiums such as SEMATECH are often used to share the risk of new process and equipment development. Most manufacturers of process equipment use incremental improvements of existing designs to provide the increased functionality of each

successive generation. Only when such evolutionary approaches fail, are radically new paradigms used. However, a space-based facility will require space-qualified processing equipment and new, dry processes, such as inorganic resist for thermal lithography. Such equipment development is not well supported by the existing industry infrastructure which is focused on terrestrial, commercial fabrication facilities.

10.3 Existing Space Transportation Infrastructure

The space industry generates $75 billion annually[127]. This industry grew out of government funded space programs in the 1950's, 1960's, and 1970's, and is now equally divided between commercial and government expenditures. The global space industry is divided into the five broad categories shown in Table 10.1.

Table 10.1 – Space Industry Categories[128]

Sector	Percent of Space Industry
Ground Equipment	30%
Services Using Satellites	51%
Space-based Manufacturing	~0%
Satellite Manufacturing	12%
Space Transportation Services/Launch Vehicle Manufacturing	7%

10.3.1 Orbits and Satellites

The space transportation infrastructure has evolved from its space program roots to service the requirements of both commercial and military/government payloads. These payloads are comprised primarily of satellites for communications, navigation, research, remote sensing, and military/classified applications. The satellites are launched from Earth into one of several different orbits, with the most common orbits shown in Table 10.2.

Table 10.2 – Standard Earth Orbits[129]

Acronym	Description	Altitude
LEO	low Earth orbit, circular	450 to 1,000 km
MEO	medium Earth orbit, circular	15,000 km
GEO	geostationary Earth orbit, circular, satellite remains stationary over point on Earth's surface	35,800 km
ELI	elliptical orbit	varies

The bulk of the satellites launched (61%) are used for communications purposes as is shown by Table 10.3.

Table 10.3 – Total On-Orbit Operational Satellites[130]

Application	LEO	MEO	GEO	ELI	Other	Total
Communication	199	2	259	16	4	480
Navigation	21	54	0	0	0	75
Scientific & Research	43	2	2	18	19	84
Meteorological & Remote Sensing	39	1	10	1	0	51
Intelligence & Classified	37	1	13	14	22	87
Other	5	0	0	1	0	6
Total	**344**	**60**	**284**	**50**	**45**	**783**

The size of the satellites in orbit varies widely. Table 10.4 shows the mass distribution of all satellites launched between 1994 and 1998. It can be seen that satellites less than 910 kg comprise 48% of the satellites launched. These small satellites are most often used in telecommunications constellations, with up to 77 satellites being required for an LEO network to provide complete worldwide coverage[129]. Most often, several of these small satellites are placed into orbit in a single launch, in order to better utilize the payload capacity of the launch vehicles. Typical examples of such launches are the seven Iridium satellites (Iridium 62 to 67) placed into orbit by a Proton launch vehicle on April 6, 1998 and the eight ORBCOMM satellites (ORBCOMM FM13 to FM20) placed into orbit by a Pegasus XL launch vehicle on August 2, 1998[131]. However, Iridium has proved to be a commercial failure and has filed for bankruptcy. Iridium's satellite system is being sold off by the courts and, if a good operator is not found, it may even be de-orbited.

The whole LEO satcom market is uncertain as of 1999/2000 and that, in turn, is creating much uncertainty in the launch business market.

Table 10.4 – Mass Distribution of Satellite Launches[132]

Satellite Size	Satellite Mass (kg)	Percent of Total Launched from 1994 to 1998
Microsat	0 to 90	11%
Small	90 to 910	37%
Medium	910 to 2275	21%
Intermediate	2275 to 4545	22%
Large	4545 to 9090	8%
Heavy	greater than 9090 kg	1%

10.3.2 Launch Vehicles

Current space transportation is quite unique compared to Earth-based shipping. Almost all commercial space cargo flies on expendable launch vehicles. Thus, the shipping vehicle is destroyed in the process of delivering the cargo. Current satellites are placed into orbit exclusively through rocket launchers. Means do not yet exist to transport payloads from Earth to orbit by other methods, although many are proposed[133,134]. Table 10.5 shows the payload capacities of many available rocket launch vehicles.

Table 10.5 – Payload Capabilities of Existing Launch Vehicles[135,47]

Launch Vehicle Designation	Payload to LEO
Athena, Cosmos, Pegasus, Taurus	Small (<2,275 kg)
Ariane 40, Cyclone, Delta 2, Long March 2C, Long March 2D, Long March 3, Molniya, PSLV, Titan 2	Medium (2,275 to 5,454 kg)
Ariane 4, Atlas 2A, Atlas 2AS, Delta 3, H2, Long March 3A, Long March 2E, Soyuz	Intermediate (5,454 to 11,364 kg)
Ariane 5, Long March 3B, Proton, Space Shuttle, Titan 4B, Sea Launch, Zenit 2	Heavy (>11,364 kg)

Of the launch vehicles shown in Table 10.5, the Pegasus is most suited to small payload requirements with the ability to deliver from 220 to 454 kg to LEO[136]. The U.S. Space Shuttle, the only current reusable launch vehicle, is not well suited to low mass launch payload requirements and is most often employed for placing large satellites and structures in LEO.

The development of many new launch vehicles is in progress. The expected growth in commercial space transportation from $7.5 billion in 1997 to $15 billion in 2007[137] is driving a race to develop more cost effective launch vehicles with more rapid deployment times. Key to reducing costs is improving the reusability of launch vehicles and components. Table 10.6 shows a list of development efforts underway to develop reusable space transportation systems.

Table 10.6 – Payload Capabilities of Proposed Launch Vehicles[138]

Launch Vehicle Designation	First Planned Launch	Manufacturer	Payload to LEO (kg)
Advent heavy lift LV (USA)	TBA	Advent Launch Services	9,020
Astroliner E-100 (USA)	2001	Kelly Space and Technology	1,935
K-1 (USA)	1999	Kistler Aerospace Corporation	2,957
Pathfinder (USA)	TBA	Pioneer Rocketplane	2,506
Roton-C (USA)	1999	Rotary Rocket Company	3,182
SA-1 (USA)	TBA	Space Access LLC	5,011
Space Van (USA)	TBA	Third Millennium Aerospace Space	4,210
HOPE-X Spaceplane (Japan)	2001	NASDA	3,007
Sänger(Germany-ESA)	TBA	Daimler-Benz Aerospace AG	7,016
SSTO Spaceplane (Japan)	2010	National Aerospace Laboratory	10,023
Skylon (UK)	2005	Reaction Engines Ltd.	9,522
Spacecab/ Spacebus (UK)	TBA	Bristol Spaceplanes Limited	1,002

It can be seen from Table 10.6 that little effort is being devoted to developing reusable launch vehicles for small payloads.

The Kistler Aerospace K-1 is typical of the new generation of reusable launch vehicles, and is perhaps the most developed. The two stage K-1 is designed to significantly reduce the cost of reliably delivering payloads to LEO with an estimated cost of $17 million per launch (~$5700/kg)[139]. The K-1 is projected to provide rapid

launch response and schedule flexibility with the payload integration process estimated to be approximately 16 months from launch contract to payload deployment[140].

10.3.3 Launch Activity

The number of launches has remained relatively steady during the last decade. Following a flurry of activity in deploying LEO communications networks such as Iridium and ORBCOMM, the number of launches has declined in the last two years. Table 10.7 shows that the number of launches of commercial payloads has steadily increased until it is approximately equal to that of military/government payloads. It is forecast that commercial launches will exceed military/government launches in 2000.

Table 10.7 – Annual Launches[141,142,143,144]

Payload Type	1993	1994	1995	1996	1997	1998	1999	2000
Commercial	11	15	23	24	38	46	44	38
Military	72	78	57	53	51	41	34	40
Total	**83**	**93**	**80**	**77**	**89**	**87**	**78**	**78**

10.3.4 Summary

In summary, the existing space transportation infrastructure has satellite deployment as its primary mission with communications satellites receiving the greatest attention. While there are efforts underway to develop reusable launch vehicles in order to reduce launch costs, such vehicles are being designed around the concept of placing medium to intermediate size commercial payloads (or multiples of smaller payloads) in LEO or GEO. It is expected that commercial payloads and commercial launches will dominate the space transportation industry in the near future and that the number of annual launches will grow steadily.

10.4 Transportation Infrastructure Requirements for Space-Based Semiconductor Fabrication

The single biggest transportation requirement difference between semiconductor fabrication in LEO and a communications (or other satellite) in LEO is that the semiconductor facility has an ongoing requirement for mass to be uplifted from Earth to the facility and for mass to be returned from the facility to Earth on a delivery schedule. This flow of material is not required for the current and proposed satellites for which the space transportation infrastructure is adapted.

Note that while the following discussion is focused on semiconductor fabrication, it applies to many of the near-term space manufacturing concepts. All of those are concerned with high value/mass products, which in turn means modest masses of supplies being sent up and products returned to Earth. Perhaps the only important difference for semiconductor fabrication from many other products is the emphasis on a steady, high rate of return of the products to Earth (weekly or bi-weekly product returns). This may not be true for all other products.

One scheme for meeting the requirements of two-way material flow might be to have a launch vehicle place a supply capsule into orbit for rendezvous with the orbiting fabrication facility. The supply capsule would off-load raw materials such as wafers, masks, and consumables as well as return capsules. The supply capsule would take on used consumable containers and other items such as masks that are no longer needed at the facility and do not need to be recovered. The supply capsule would then de-orbit for a controlled burn in the atmosphere. The multiple return capsules would be used to periodically deliver finished wafers to Earth through a de-orbit maneuver coupled with a soft landing.

The launch payload for the semiconductor fabrication facility is determined by the raw material requirement, payload ability of the return capsule that delivers

finished goods, the production rate, and the frequency of launch. The return payload is determined by the mass of the finished wafer, the production rate, and the frequency of return deliveries.

10.4.1 Raw Material Requirement

The raw material requirement is the mass of material required to produce the finished goods (fabricated wafers) within the period between launches. Such materials includes the raw wafers, the lithography masks, the consumables (gases and solids), and consumable containers. For a semiconductor facility using the reference process flow to produce 5,000 finished, 200 mm diameter, standard thickness wafers per month, the raw material requirements are shown in Table 10.8 based on the modeling of Chapter 8 and Chapter 9. For the three device types, MPU, DRAM, and ASIC, with the production characteristics shown in Table 8.1, the raw material requirements per wafer $m_{wafermatl}$ are shown in Table 10.9.

Table 10.8 – Mass of Raw Materials

Item	Mass (kg)
Wafer Mass	0.0368
Gas Mass per Layer	0.000304444
Solid Mass per Layer	3.50602E-05
Mask Mass	0.092

Table 10.9 – Raw Material Requirements per Wafer

Device Type	Raw Material Mass per Wafer (kg)
MPU	0.053
DRAM	0.049
ASIC	0.054

10.4.2 Payload Ability of Return Capsule

In order to deliver finished goods from an orbiting semiconductor fabrication facility, it is necessary to have a means of transporting material from orbit to Earth. Section 8.9 *Transportation* described two possible cases: a synchronous mode in which the supply launch vehicle returns to Earth with the finished goods completed within the latest resupply interval, and an asynchronous mode in which the supply launch vehicle provides both raw materials and return capsules to the facility. Such return capsules would be capable of transporting a certain number of finished wafers from orbit back to Earth.

The return capsule payload ability can be described by the capsule payload fraction $f_{payload}$. This value, which expresses the mass fraction of the total return mass that consists of payload, can be used to describe both synchronous and asynchronous transport modes: an $f_{payload}$ value of 100%, indicating that all of the return mass is payload, would be used to describe the synchronous mode; an $f_{payload}$ value of less than 100% would be used to describe the asynchronous mode. The lower $f_{payload}$, the heavier the return capsule for a given payload mass.

10.4.3 Production Rate

The production rate r_w is the number of finished wafers produced in a given period. This rate determines the raw material mass which must be transported to orbit, as well as the mass of finished wafers that must be returned.

10.4.4 Frequency of Launch

The higher the launch frequency, the shorter the period between launches of material and return capsules to the semiconductor fabrication facility. For a given production rate, a shorter period means that less payload is required to be launched.

The ability to fabricate lithography masks at the orbital facility has an important effect on the frequency of launch. For masks that are generated on Earth, a new mask set must be launched for each new design. New wafer design turnarounds of three weeks, required by customers for ASIC devices (the base production case considered), would lead to launches of new mask sets at no more than three week intervals. However, for an orbital facility with the ability to fabricate masks on site (using electron beam direct write equipment for example), the launch frequency would not be not dictated by the customer design turnaround time. Except for the equipment needed to generate the masks, there is no difference in the mass of supplies required for such orbital mask productions. On-orbit mask production is not assumed in the base model in this work.

10.4.5 Frequency of Return Delivery

The higher the return delivery frequency, the shorter the period between use of return capsules. Devices such as ASIC's have short lead times and customer requirements are for delivery within two to six weeks[36] from order placement. DRAM's and MPU's are produced in larger production runs and have less stringent delivery requirements. For a given production rate, a shorter return period means that less payload ability is required for the return capsule.

10.4.6 Maintenance and Servicing

While it is envisioned that the processing equipment in a space-based semiconductor fabrication facility would be fully automated, it is recognized that periodic, manned visits are required for preventive maintenance[145] and servicing. Section 3.5 *Logistics of Space-Based Manufacturing* described the needs associated

with equipment maintenance, including transportation and accommodation of service personnel.

The frequency of equipment servicing is governed primarily by the reliability of the equipment. This system reliability is commonly expressed in failures per unit time or its inverse, mean time between failure (MTBF)[146]. For a system, such as a semiconductor fabrication facility, the failures of non-redundant, individual pieces of equipment are summed to calculate the number of failures per unit time. The MTBF of the facility is the inverse of the summed failures. In practice, different types of equipment have different failure rates and the failure of redundant pieces of equipment may only slow production rather than cause a complete halt.

To provide a comparison, some semiconductor processing equipment types and failure rates are shown in Table 10.10. It should be noted that some of these MTBF times include the requirements for regular, planned maintenance servicing, not the repair of failed equipment. For example, the advanced lithography systems must have gas added to the excimer laser light source roughly every 350 hours of operation. Such maintenance servicing is much more amenable to robotic operation than true repair of failed components in a systems. Thus, when using the MTBF's, the possibility of adding robotics to improve the MTBF's must be part of the overall fabrication satellite design.

Table 10.10 – MTBF of Some Processing Tools

Equipment	MTBF (hours)
dual-arm atmospheric robot capable of handling 200mm (eight-inch) and 300mm wafers	75,000[147]
SMIF tool for loading and unloading semiconductor wafer cassettes into the process equipment	6,000[148]
300-mm low-pressure CVD cluster tool	400[149]
advanced lithography tools, stepper plus track	325[150]

It is beyond the scope of this thesis to determine detailed reliability predictions for the space-based semiconductor fabrication facility. However, if it is assumed that all equipment has the same MTBF $p_{mtbfequip}$ and that the failures occur randomly, a simplified model of the reliability of the fabrication facility can be constructed. In this model, the predicted maintenance period p_{maint} is equal to the mean time between failure of the entire semiconductor fabrication facility, which in turn is dependent on the number of pieces of critical (non-redundant) equipment n_{equip} and the MTBF of the equipment $p_{mtbfequip}$.

$$p_{maint} = \frac{1}{\sum_{1}^{n_{equip}} \left(\frac{1}{p_{mtbfequip}} \right)} \tag{10.1}$$

Figure 10.1 shows the predicted service interval p_{maint} based upon the quantity of critical equipment and the equipment MTBF.

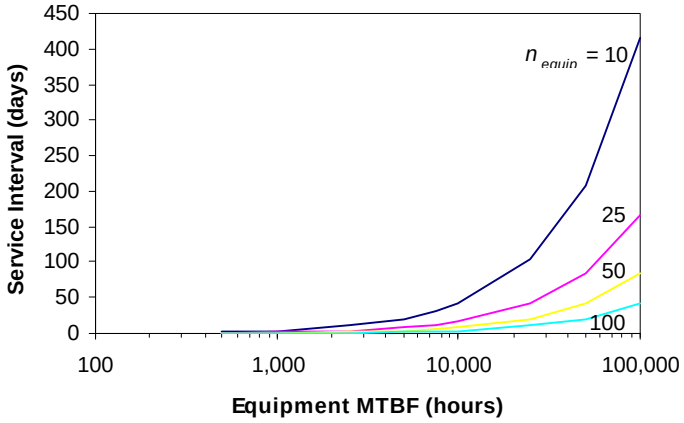

Figure 10.1 – Service Interval Requirements for Critical Equipment Numbers n_{equip}

It can be seen that the service interval is small for equipment with MTBF's less than 10,000 hours, resulting in frequent on-orbit servicing using either robotics or personnel.

The equipment requirements shown in Table 8.6 for the base production case of 5,000 ASIC's per month indicate that there are 12 critical items of equipment out of a total of 122 pieces leading to a service interval of 35 days for equipment with 10,000 hour MTBF and 87 days for equipment with 25,000 MTBF. The ratio of critical equipment to total equipment (10% in the example) is expected to remain constant with increasing production rates and for other devices types (MPU, DRAM) as the majority of the equipment is comprised of multiple, parallel tools for deposition (CVD, sputter) and etching (plasma).

While it is noted that the above model greatly simplifies the complexities associated with reliability prediction for a space-based fabrication facility, it does highlight the need for equipment with large MTBF's. Many of the present tools used for semiconductor fabrication do not have the high MTBF's required to allow unattended processing in a space-based facility, and the development of such tools is required to reduce the need for frequent manned launches for system maintenance purposes. It is clear from the reliability results that periodic maintenance of the facility (perhaps coincident with the delivery of raw materials) will be required.

10.4.7 Modeling Launch and Return Capsule Payload Requirements

Using equation (8.12), the mass of the return payload m_{down} can be determined from the rate at which finished goods are required r_{down} and the return period p_{down}. Substituting production rate r_w and the mass of the finished wafer m_{wafer} into (8.12) for r_{down} yields the number of wafers n_{down} produced in the return period and the mass of the return payload.

$$m_{down} = (r_w * p_{down}) * m_{wafer} = n_{down} * m_{wafer} \tag{10.2}$$

As the mass of the deposited thin films is negligible (totaling less than 1% of the wafer mass), the mass of the finished wafer can be assumed to be equal to the mass of the raw wafer. In such a case, Figure 10.2 shows the return payload m_{down} requirement for production rates r_w from 1,000 to 10,000 wafers per month and return periods p_{down} up to 100 days.

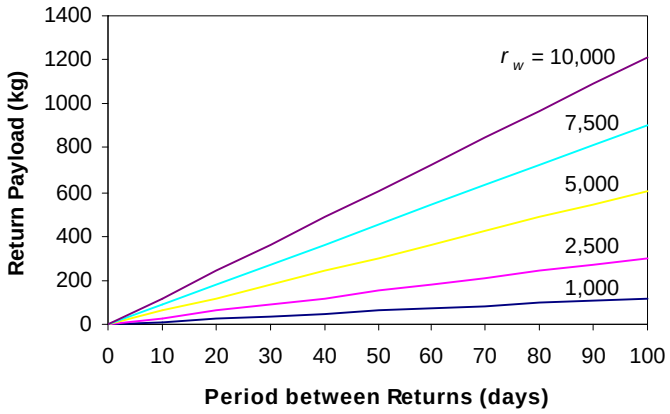

Figure 10.2 – Return Payload Requirements for the Production of r_w Wafers per Month

The return capsule mass is determined by the capsule payload fraction $f_{payload}$ and the return payload mass m_{down}

$$m_{capsule} = \frac{m_{down}}{\left(\frac{1}{f_{payload}} - 1\right)} \tag{10.3}$$

The launch payload mass m_{up} is determined by the period between launches p_{up}, the mass of the return capsule $m_{capsule}$, the number of wafers n_{down} produced in the

return period, the raw material mass per wafer $m_{wafermatl}$, and the period between returns p_{down}.

$$m_{up} = \frac{p_{up} * (m_{capsule} + n_{down} * m_{wafermatl})}{p_{down}} \tag{10.4}$$

For the base production case of 5,000 wafers per month, Figure 10.3 to Figure 10.5 show the launch payload requirements for ASIC, MPU, and DRAM devices for a range of capsule payload fractions. It is interesting to note that there is little overall difference in the payload mass requirements between device types, but that the return payload carrying ability per unit mass of return capsule has a very large effect on the launch payload mass.

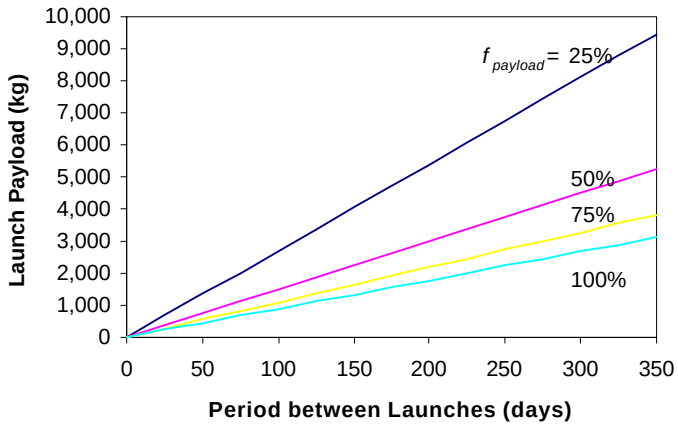

Figure 10.3 – Launch Payload Requirement for ASIC's (5,000 WPM) for Capsule Payload Fractions $f_{payload}$

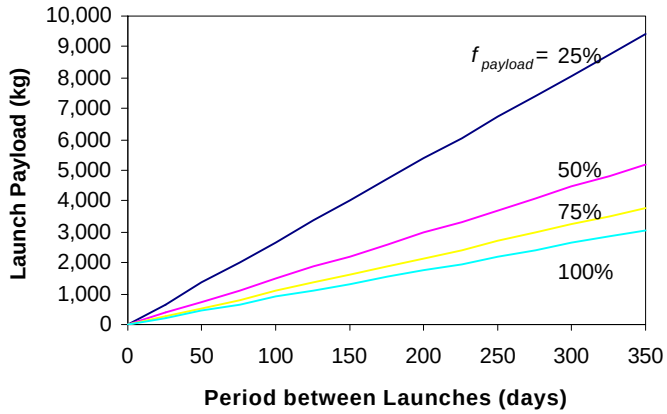

Figure 10.4 – Launch Payload Requirement for MPU's (5,000 WPM) for Capsule Payload Fractions $f_{payload}$

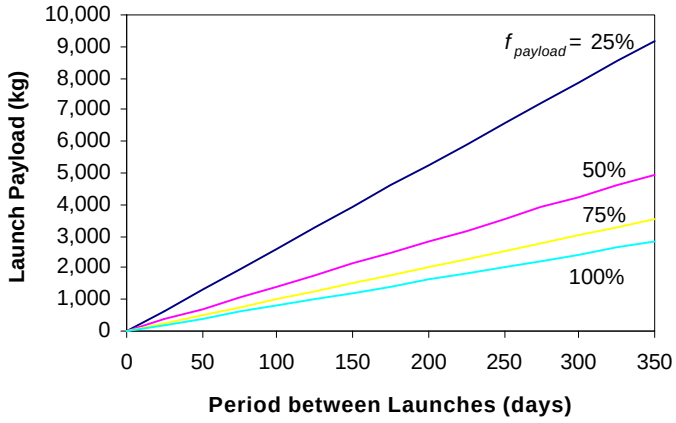

Figure 10.5 – Launch Payload Requirement for DRAM's (5,000 WPM)) for Capsule Payload Fractions $f_{payload}$

10.4.8 Launch Vehicle Requirements

It was shown in the above sections that launch vehicles are required for two purposes: to deliver replacement parts and service personnel, and to deliver raw materials and return capsules.

The launch vehicle for service personnel is manned and must necessarily return the maintenance crew to Earth. The launch vehicle for raw materials and return capsules is not required to return to Earth. While it is possible to combine the two functions into a single launch vehicle that delivers personnel and materiel to the station and returns personnel and finished goods, such a compromise limits the frequency with which finished goods can be returned.

For the base production case of 5,000 ASIC wafers per month, Figure 10.1 shows that equipment servicing is required every 30 to 90 days, depending on equipment reliability. If this servicing is performed by service personnel, then a manned launch is required. Alternatively, the use of tele-operated robotics on the fabrication facility may allow the servicing to be conducted remotely, reducing the manned launch requirement. The use of interchangeable equipment modules would facilitate remote, tele-operated servicing at the expense of lifting greater equipment mass to orbit.

For the base production case, finished goods are required every 2 to 6 weeks. If it is assumed that raw materials would be launched every 30 to 90 days and that between such flights finished goods are delivered by return capsule, then the launch payloads would be from 300 to 2,500 kg depending on the characteristics of the return capsule.

A review of the current and proposed launch vehicles in Table 10.5 and Table 10.6 shows that several launch vehicles capable of delivering small payloads of raw materials to LEO are available or under development.

10.4.9 Other Infrastructure Options

The transportation options examined thus far have been limited to transport to/from the Earth. While it is outside the scope of this thesis to speculate on the development of a manned presence in space, it is possible that such a presence may

change the assumptions used to determine launch and return payload and frequency requirements.

Specifically, if there is a manned presence in orbit, that periodic servicing of the semiconductor fabrication facility which cannot be conducted through tele-operated robotics, may best be accomplished by personnel already located in orbit. As equipment maintenance will be a requirement for all types of orbiting manufacturing facilities, it may be feasible to maintain a manned, central depot of spares in orbit to service all such facilities. Such a central depot would reduce the number of manned launches required by the above model to maintain the semiconductor fabrication equipment and would allow a more rapid response when repair/replacement of facility equipment becomes necessary.

10.4.10 Summary

It has been shown that the existing space transportation infrastructure has satellite placement as its primary goal and the space industry has not yet developed the means to deliver to and return mass from orbit on a routine basis. Examination of the transportation requirements for a semiconductor fabrication facility located in LEO indicate that frequent launches of material will be required to support the base production case of 5,000 ASIC wafers per month. The use of a lightweight, small return capsule is shown to reduce the number of ground-based launches required to meet customer delivery schedules.

10.5 Other Infrastructure Requirements for Space-Based Semiconductor Fabrication

The objective of this thesis is to perform a preliminary review of the feasibility of fabricating semiconductor devices in orbit. While it is outside the scope of this thesis to review all factors of the space and semiconductor industries for

suitability to supporting a space-based microfabrication facility, two areas do deserve mention: insurance and equipment development.

10.5.1 Insurance

Launch insurance is designed to protect the customer from loss of payload during transportation to orbit, and forms one of the primary components of transportation cost. For commercial satellites, the cost of launch insurance is estimated to be approximately 25% of the combined cost of constructing the satellite and transporting it to orbit[151]. Insurance costs are based upon the track record of the launch vehicle and support infrastructure, and the quality of design, manufacturing, inspection, and payload integration of the vehicle.

Statistical methods are used by insurance underwriters to determine risk. These statistical methods are based upon a sample of homogenous space events, such as identical launch vehicles and payloads at a given launch facility. The smaller the sample size and the wider the variation of launch parameters, the greater the statistical uncertainty.

The space insurance industry exists today to insure satellite payloads destined for orbit. Typically, such insurance does not come into effect until three to six months before launch, leading to a financing bottleneck during the construction of the satellite[152]. In addition, no insurance facility exists at present to cover the risk of transporting finished goods from orbit back to Earth. Such insurance would have to cover not only the loss of finished goods and the return capsule in the event of disaster, but also the cost of customer penalties, such as failure to deliver product according to an agreed upon schedule.

The requirement for new launch and return vehicles suitable for small payloads is expected to result in high transportation insurance costs initially. However, as the frequency of launches and retrievals for a space-based

semiconductor fabrication facility is expected to be high, and the payloads identical, it is likely that a statistical database will rapidly be developed, leading to high statistical confidence levels which will reduce the insurance costs.

Some important differences between the semiconductor supply missions and current satellites would affect the insurance costs. For satellites, the value of the systems themselves is very large ($50 million to more than $1 billion), their complexity is high, the time to order a replacement is long (measured in years), and their revenue stream is long lasting (a satellite may generate revenue for 5 to 10 years). This makes a single loss very costly. By comparison, the semiconductor fabrication supplies are of modest value (a week's worth of supplies is less than $1 million), they are of low complexity (the supplies themselves have few working parts although replacement equipment would have more complexity), it is easy to get replacements ready for launch, and their revenue stream is short term (at most a few months). This makes the cost of vehicle failure much closer to the price of the launch than with existing satellites. These factors are expected to reduce insurance risk and costs on resupply flights to the semiconductor facility.

10.5.2 Process Equipment Development

New process equipment will be required for space-based semiconductor fabrication. The development of this equipment poses two concerns for existing manufacturers of commercial fabrication equipment: is the market for the equipment large enough to warrant to cost of development, and can evolutionary techniques be used to migrate from existing equipment designs to space-based equipment designs?

If the market for space-based processing equipment is limited to a single orbital facility, the owner of that facility will likely bear the full cost of the equipment development as there is no market for other sales. In this case, it can be expected that the equipment will be purpose-built for the single client and will have high costs

when compared to the volume sales of Earth-based equipment . In contrast, if a viable space-based fabrication market is perceived by equipment manufacturers, then the cost of development will be recovered over multiple sales, reducing the cost of each piece of equipment.

New commercial processing equipment designs benefit from previous generations of product. The path of improvement in semiconductor processing equipment has been evolutionary rather than revolutionary. However, the all-dry process flows developed in Chapter 6 require equipment that does not currently exist and revolutionary equipment designs. Such design leaps involve increased risk leading to higher equipment cost.

One method to mitigate the risk inherent in the development of new equipment for a space-based processing facility is to have the equipment developed for commercial Earth-based processes. The challenges of next generation lithography (NGL) may favour the dry, inorganic resist process, and increased environmental pressures may lead to the use of dry cleaning processes to decrease water and energy use. The development of these processes and subsequent commercial use on Earth would greatly reduce the risk associated with developing space-qualified equipment for an orbital facility.

10.6 Conclusions

This chapter has described the infrastructure requirements for a space-based semiconductor fabrication facility with emphasis on transportation, insurance, and new equipment development. A launch and return capsule payload model was constructed for use as the basis in determining the suitability of existing and proposed space transportation vehicles for a microfabrication facility located in LEO.

It has been shown that while several existing or proposed launch vehicles are suitable for transporting raw materials to LEO, there is no existing means of meeting

the frequent, two-way mass transport requirements of an orbital microfabrication facility.

The base production case of 5,000 ASIC wafers per month was found to require servicing every 30 to 90 days, depending on MTBF of the equipment. If manned flights were used for servicing, then it was shown that launches would be more frequent than raw material requirements alone would dictate. However, the exact costs and frequency would depend on the service mode used (on-orbit personnel or tele-operated robotics against manned service flights).

A return capsule, capable of delivering finished wafers from orbit to Earth, was found to reduce the need for launches while still meeting delivery schedules of 2 to 6 weeks.

The infrastructure for the insurance of payloads to and from orbit was found to be inadequate, and it was suggested that the lack of statistical models for two-way mass transport would result in high early insurance costs. However, the very different nature of resupply flights from that of current satellite launches, may make the insurance costs much lower than existing launch insurance.

The development of specialized processing equipment for use in space was found to involve significant risk as new processes and new equipment were simultaneously required. It was suggested that the adoption of the dry processes required for space, by commercial fabrication facilities on Earth, would reduce the risk and cost of space equipment development.

Chapter 11
Conclusions & Suggested Further Work

11.1 Conclusions

Space-based microfabrication requires the implementation of semiconductor fabrication processes in a space environment. Sequential application of patterning, deposition, etching, and doping processes to a silicon wafer can be used to produce many different types of electronic devices, on Earth or in space.

While the near-Earth space environment offers several advantages such as low particle counts, native vacuum, atomic oxygen, and microgravity, it also poses difficulties for conventional processing. Alternatives to several Earth-based processes must be developed in order for such processing to be feasible. In addition, in order to maintain the inherently clean environment of space, non-contact wafer transport within the fabrication facility was shown to be practical.

A wafer handling scheme based upon electromagnetic levitation was developed. Numerical simulations indicated that wafer handling in such a system was possible at power levels suitable for a space-based facility. Use of such a system could reduce mechanical contact between wafers and transport equipment, resulting in less wafer damage and particle scatter than mechanical grips.

A detailed process flow model was developed in order to provide information on consumable use, energy use, and process times. Comparison with published results indicated that the model was in general agreement with industry averages.

Alternative processes were developed for space-based microfabrication. These dry processes were found to be compatible with a vacuum, microgravity environment and not only eliminated the problems associated with processes

involving liquids, but also resulted in significant energy savings and reductions in consumable mass. Numerical models of a dry lithographic process using an inorganic resist and a dry cleaning process incorporating a combination of plasma etching and ion milling were added to the process flow model.

Comparisons of simulation results between three reference process flow models indicated that space-based semiconductor fabrication used much less material and energy per processed wafer and that processing cycle times were faster than equivalent Earth-based fabrication.

Extension of the reference process flows, derived for a 12 level CMOS device, to other devices allowed a series of production cases to be examined. Operating cost per wafer was determined to be a reasonable metric with which to compare economic feasibility of a commercial, space-based microfabrication facility. For a base production case of 5,000 ASIC wafers per month, using a series of key assumptions, it was determined that, as of 1999, Earth-based fabrication was about 50% less expensive than space-based semiconductor fabrication. However, by examining the sensitivities of input parameters such as process equipment cost (which is changing significantly with time), transport mass, and transportation cost, it was found that optimizations in the space-based production model could be made. These optimizations indicated that space-based fabrication costs could be decreased to 58% that of an advanced, future Earth-based facility when trends of increasing process equipment costs and decreasing orbital transport costs are considered.

Transport cost to and from orbit was found to be a critical factor in determining the economic viability of a space-based microfabrication facility. After a review of the existing transportation infrastructure, an asynchronous mode transport scheme was proposed in which finished wafers were transported from the orbital facility to Earth in small return capsules. Transport cost and payload models for the

asynchronous transport mode highlighted the requirement for lightweight return capsules with large payload ability.

A space-based manufacturing facility does not operate in isolation, but requires a support infrastructure in order to function. A review of the existing space transportation infrastructure indicated that present and proposed launch vehicles were not directly suited to the frequent, two-way mass flow of raw materials and finished goods required for a space semiconductor fabrication facility. In addition, examination of the MTBF of typical semiconductor processing equipment indicated that service flights to supply either manned or robotic maintenance requirements would be necessary in order to keep the facility operating. Insurance was found to be a key part of space transportation and an assessment of insurance underwriters methods indicated that insurance costs would be high for initial shipments until a statistical database of material launches and returns was developed.

It was proposed that the development cost of space-based processing equipment could be reduced if the dry processes required for space, such as thermal lithography and dry cleaning, would become the standard on Earth in commercial fabrication facilities. It is possible that factors such as better process control plus water and energy savings may be compelling, even on Earth. If such processes are implemented in commercial facilities, then much of the development cost for space-qualified versions of the equipment is eliminated.

In summary, this thesis has examined the feasibility of fabricating silicon semiconductor devices in orbit on a commercial basis and concludes that while the processing is technically feasible, it is difficult to compete economically with Earth-based facilities today. However, it is found that space-based semiconductor fabrication can be economically favourable provided that the processes are carefully optimized and the cost of transportation to and from orbit is reduced.

11.2 Suggested Further Work

This thesis has touched upon many areas in which there is little or no information available. These areas must be further developed in order to fully determine the feasibility, both technical and economic, of space-based semiconductor fabrication.

11.2.1 Process Modeling and Experimentation

The process flow modeling of this thesis is the first modestly detailed comparison of the wet earth, dry earth, and dry space processes. These models need to be confirmed with more detailed modeling and experimentation. For example, only two process flows (a 3 level device and 12 level CMOS) have been simulated. While the consistency of the results indicate that these process flows can be reasonably extrapolated to additional levels, complete 20 and 30 level process flows should be fully simulated.

In addition, several methodologies in the dry processes have been proposed that need experimental verification. For example, it has been assumed that in a vacuum environment, without the need for continuous pumping, many processes like sputtering can be done with just the required pressure of gases (such as argon), rather than maintaining a continuous flow of gases. This needs to be experimentally confirmed.

Furthermore, the potential savings in equipment mass and power has been only briefly studied. Conservative models of space-based equipment were derived through the method of functional decomposition. Future work should include a detailed redesign of several process tools (such as a CVD system, a plasma etch system, a sputter system, and an ion implantation system) to study the savings in mass, volume, cost and power.

11.2.2 Electromagnetic Wafer Handling System

The scope of this thesis was limited to a first-pass feasibility analysis. However, many of the ideas presented need to be demonstrated and refined. One such idea is the electromagnetic wafer levitation system. It is suggested that a single solenoid prototype be constructed and a set of experiments performed to determine the correlation between actual forces and predicted forces on the wafer. Further development would result in a circular array solenoid actuator that could serve as a robotic end effector and the eventual implementation of a recto-linear solenoid array.

In connection with the electromagnetic wafer handling system, the author is exploring the use of lasers to assist with the chemical vapour deposition of tungsten silicide for the eddy current loops on the backside of wafers. These conductors are required by the proposed electromagnetic wafer transport system and are not easily fabricated by conventional means. The use of laser CVD is expected to result in a rapid, direct-write process to form these large conductors.

11.2.3 New Processes

Several dry processes have been developed and presented. The thermal lithography process using inorganic resists was based upon available literature. However, current work at Simon Fraser University is extending the range of available inorganic resists and lowering the exposure thresholds. It is suggested that future work on these resists include developing dry etching processes and eventual testing in a vacuum environment.

The dry cleaning processes, plasma etching and ion milling, are well known separately. However, work needs to be done to ensure that the combination is able to effectively clean organics and particles from wafers and is compatible with a vacuum environment.

The issue of chemical mechanical polishing was neglected in the 12 level CMOS model, as it was not one of the process steps. However, CMP is a common process in commercial facilities and must be replicated in space for multi-level metal devices. An alternative to CMP, based on photoablation, was described. Work on developing this process, or other dry alternatives, is required.

Copper is used as top level conductors in many high-end devices. However, the liquid electroplating process commonly used is incompatible with the space environment. An alternative process, based upon use of a charged copper vapour, was described. Work on developing this process, or other dry alternatives, is required.

11.2.4 Experimental Verification of Vacuum Processing

Once alternative, dry processes are developed, a demonstration of the process flow is needed. As it is difficult to obtain the resources to demonstrate the processes in space, it is suggested that the processes be demonstrated in a large, Earth-based vacuum chamber, such as that employed to test space hardware. Such facilities are available with Boeing in Washington State or with the Canadian Space Agency. An initial prototype test could involve placing modified current equipment (with the vacuum systems and controls removed) in such facilities and determining operational needs for a single process. Eventually, a full process flow of one level could be tested in such a facility. In such a test, a single wafer could be processed through all of the major steps (patterning, deposition, etching, doping) within the vacuum environment. The only factor of the space environment that could not be simulated would be the microgravity, which is not expected to alter the processing. The possibility of such testing is being investigated. The analysis of this thesis has supplied the preliminary indication of advantages that justifies the continuation of this work.

11.2.5 Commercialization

From a business perspective, successful development of the processes and hardware leading to commercialization requires that a consortium be formed that brings together at least the two elements of: knowledge of the semiconductor fabrication business, and knowledge of space utilization[153]. As the development of a commercial, space-based semiconductor fabrication facility has an inherent risk in the development of new processes and equipment and a long time period requiring major expenditures before revenue production[154], it is envisioned that such a consortium would likely be comprised of several, large multi-national companies from the aerospace, semiconductor, and electronics sectors.

Pending successful testing in a large, vacuum chamber, it is suggested that the next step would be the development by the consortium of space-qualified, prototype processing equipment to allow demonstration in a space facility such as the Space Shuttle or the International Space Station.

11.2.6 Return Capsules

Finally, it was found that for frequent, two-way mass transport to space to be effective, a lightweight return capsule was required. It is suggested that such a return capsule is a requirement for many types of space manufacturing and that the conceptual design of such a capsule be undertaken. Work required to support such development would include determining the allowable stress levels for silicon wafers and finished goods packaging requirements.

References

[1] “Global Semiconductor Sales to Decline 1.8 Percent in 1998; Strong Growth of 17-19 Percent Forecast for 1999-2001”, Semiconductor Industry Association, http://www.semichips.org/news/pr060398.htm (July 28/99)

[2] Pieter Burggraaf, “Vacuum ‘Cluster’ Tools: Rethinking the Fab”, *Semiconductor International*, November 1992, pp. 71-73

[3] Peter Maroulis, John Langan, Andrew Johnson, et. al., “PFCs and the Semiconductor Industry,: A Closer Look”, *Semiconductor International*, November 1994, pp. 107-110

[4] Charles R. Tilford, J. Patrick Looney, “Vacuum Measurement: The BASIC’s”, *Semiconductor International*, May 1994, pp. 72-76

[5] Peter Singer, “1995: Looking Down the Road to Quarter-Micron Production”, *Semiconductor International*, January 1995, pp. 47-52

[6] Nick McKiddie, “Some ‘No-Panic’ Help for Wafer-Start Surges”, *Semiconductor International*, June 1995, pp. 115-120

[7] Peter Singer, “CVD Technology Trends”, *Semiconductor International*, February 1995, pp. 55-62

[8] “Plasma Cookbook”, Trion Technology, http://www.triontech.com/cookbook.html (March 19, 2000)

[9] Applied Materials Inc., “Where Speed and Availability Make the Difference to Productivity” advertisement for Endura VHP PVD System, *Semiconductor International*, April 1995, p. 21

[10] “Technical Data: The PAS 5500 Family of Steppers”, *Semiconductor International*, September 1994, p. 112

[11] Stephen A. Campbell, “The Science and Engineering of Microelectronic Fabrication”, Oxford University Press, New York, 1996, p. 206

[12] Stephen A. Campbell, “The Science and Engineering of Microelectronic Fabrication”, Oxford University Press, New York, 1996, p. 203

[13] M.V. Sarunic, G.H. Chapman, Y. Tu, "BiIn: a Sensitive Bimetallic Thermal Resist", submitted to *SPIE Microlithography*, Santa Clara, CA, February 2001

[14] Stephen A. Campbell, “The Science and Engineering of Microelectronic Fabrication”, Oxford University Press, New York, 1996, p. 98

[15] Ian Iscoff, “Are Ion Implanters the Newest Clean Machines?”, *Semiconductor International*, October 1994, p. 65

[16] Stephen A. Campbell, “The Science and Engineering of Microelectronic Fabrication”, Oxford University Press, New York, 1996, p. 102.

[17] Jeff Davis, Mitchell Weiss, “Addressing Automated Materials Handling in an Existing Wafer Fab”, *Semiconductor International*, June 1995, pp. 125-128

[18] “Theory and Fabrication of Integrated Circuits: RCA Clean”, University of Illinois at Urbana-Champaign, Department of Electrical and Computer Engineering, http://www.ece.uiuc.edu/ece344/new/appendices/rca.html (October 9/00)

[19] Peter H. Singer, “Trends in Wafer Cleaning”, *Semiconductor International*, December 1992, pp. 37-39

[20] Ron Iscoff, “The Greening of the Fab”, *Semiconductor International*, December 1994, pp. 67-72

[21] Stephen A. Campbell, “The Science and Engineering of Microelectronic Fabrication”, Oxford University Press, New York, 1996, p. 344

[22] Robert K. Waits, “Controlling Your Vacuum Process: Effective Use of a QMA”, *Semiconductor International*, May 1994, pp. 79-84

[23] W. Scot Ruska, “An Introduction to the Manufacture of Integrated Circuits”, McGraw-Hill, 1987, p. 108.

[24] R. Geiger, “VLSI Design Techniques for Analog and Digital Circuits”, McGraw-Hill, 1990

[25] Marcel J. Lopez, Samuel C. Wood, “Systems of Multiple Cluster Tools: Configuration and Performance Under Perfect Reliability”, *IEEE Transactions on Semiconductor Manufacturing*, Vol. 11, No. 3, August 1998, pp. 465-474

[26] R. S. Srinivasan, "Modeling and Performance Analysis of Cluster Tools Using Petri Nets", *IEEE Transactions on Semiconductor Manufacturing*, Vol. 11, No. 3, August 1998, p. 394

[27] Srilakshmi Venkatesh, Rob Devenport, Pattie Foxhoven, Jaim Nulman, "A Steady-State Throughput Analysis of Cluster Tools: Dual-Blade Versus Single-Blade Robots", *IEEE Transactions on Semiconductor Processing*, Vol. 10, No. 4, November 1997, p. 419

[28] Samuel C. Wood, "Simple Performance Models for Integrated Processing Tools", *IEEE Transactions on Semiconductor Manufacturing*, Vol. 9, No. 3, August 1996, p. 320

[29] Terry L. Perkinson, Ronald S. Gyurcsik, Peter K. McLarty, "Single-Wafer Cluster Tool Performance: An Analysis of the Effects of Redundant Chambers and Revisitation Sequences on Throughput", *IEEE Transactions on Semiconductor Manufacturing*, Vol. 9. No. 3., August 1996, p. 400

[30] Xaview Pucel, "SEMI, JESSI, SEMATECH Drive Minienvironment Standards", *Semiconductor International*, April 1994, pp. 69-74

[31] "International Technology Roadmap for Semiconductors: 1999 Edition", Semiconductor Industry Association, 1999, Table 1a, http://public.itrs.net/Files/1999_SIA_Roadmap/ORTC.pdf (October 15, 2000)

[32] "International Technology Roadmap for Semiconductors: 1999 Edition", Semiconductor Industry Association, 1999, Table 4a, http://public.itrs.net/Files/1999_SIA_Roadmap/ORTC.pdf (October 15, 2000)

[33] "International Technology Roadmap for Semiconductors: 1999 Edition", Semiconductor Industry Association, 1999, Table 5a, http://public.itrs.net/Files/1999_SIA_Roadmap/ORTC.pdf (October 15, 2000)

[34] Jeff Johnson, Glenn H. Chapman, Nick Pfeiffer, Joe Hopkins, "Feasibility of Commercial Space-Based Microchip Fabrication", *AIAA Space 2000 Conference*, AIAA-2000-5164, Long Beach, CA, September 2000

[35] "Intel Microprocessor Quick Reference Guide", Intel Corporation, http://www.intel.com/pressroom/kits/processors/quickrefyr.htm, (October 10, 2000)

[36] "FACE-OFF: Emulation vs silicon prototyping", *Computer Design*, April 1995, http://www.computer-design.com/Editorial/1995/04/ASIC/emulation.html (October 15, 2000)

[37] "International Technology Roadmap for Semiconductors: 1998 Update", Semiconductor Industry Association, 1998, Table 2

[38] SI Staff, "Selecting a Product: The Task at Hand", *Semiconductor International*, March 1992, pp. 7-8

[39] "About Dominion Semiconductor", Dominion Semiconductor, http://www.dominionsc.com/about.htm (January 16, 2000)

[40] Peter Singer, "Intel, Motorola, Philips Win Top 1995 Fab of the Year Honors", *Semiconductor International*, May 1995, pp. 48-52

[41] Betty Newboe, "Top Fabs of 1992", *Semiconductor International*, April 1992, pp. 50-53

[42] Ron Iscoff, "SI Honors Top Fabs of 1994", *Semiconductor International*, April 1994, pp. 77-80

[43] "Coping with the High Cost of Wafer Fabs", *Semiconductor International*, March 1995, p. 45

[44] John C. Gregory, "Space Processing of Semiconductor Materials with Fast Atomic Oxygen", *CONF 950110*, American Institute of Physics, 1995, p. 314

[45] M. Desai, "Vacuum and Flow Field Results from the Wake Shield Facility Flight Experiment", *CONF 950110*, American Institute of Physics, 1995, pp. 323-330

[46] John P. W. Stark, "The Space Environment and Its Effects on Spacecraft Design", *Spacecraft Systems Engineering*, Peter W. Fortescue and John P.W. Stark (eds.), John Wiley and Sons, West Sussex, England, 1991, p. 21

[47] Lenwood G. Clark, John DiBattista, "LDEF/Shuttle Capabilities for Environmental Testing in Space", *The Industrialization of Space*, Vol 36, Part 1, Ed. Richard A. Van Patten, American Astronautical Society, 1977, pp. 297-308

[48] John P. W. Stark, "The Space Environment and Its Effects on Spacecraft Design", *Spacecraft Systems Engineering*, Peter W. Fortescue and John P.W. Stark (eds.), John Wiley and Sons, West Sussex, England, 1991, p. 23

[49] Glenn Chapman, Nick Pfeiffer, Jeffrey A. Johnson, “Synergy of Combining Microfabrication Technologies in Orbit”, *Spacebound 2000 Conference Proceedings*, Canadian Space Agency, May 2000

[50] Robert J. Naumann, “Materials Processing in Space: A Strategy for Commercialization”, *The Industrialization of Space*, Vol 36, Part 1, Ed. Richard A. Van Patten, American Astronautical Society, 1977, pp. 349-362

[51] Francis C. Wessling, “A Survey of Research Results of the Consortium for Materials Development in Space”, *CONF 950110*, Amercian Institute of Physics, 1995, pp. 341-351

[52] A. Ignatiev, “Thin Film Microelectronics Materials Production in the Vacuum of Space”, *CONF 970115*, American Institute of Physics, 1997, pp. 685-689

[53] A. Ignatiev, “Thin Film Growth in the Ultra-Vacuum of Space: The Second Flight of the Wake Shield Facility”, *CONF 960109*, American Institute of Physics, 1996, pp. 83-87

[54] C. Horton, “III-Vcompound Semiconductor Film Growth in Low Earth Orbit on the Wake Shield Facility”, *CONF 950110*, American Institute of Physics, 1995, pp. 305-311

[55] S. M. Rossnagel , “Sputter Deposition for Semiconductor Manufacturing”, *IBM Journal of Research Development*, Vol. 43, No. 1/2, 1999, http://www.research.ibm.com/journal/rd/431/rossnagel.html, (October 15, 2000)

[56] John Mikulsky, “Chemically Clean Air: An Emerging Issue in the Fab Environment”, *Semiconductor International*, September 1996, pp. 115-122

[57] Klaus C. Wiemer, James R. Burnett, “The Fab of the Future: Concept and Reality”, *Semiconductor International*, July 1992, pp. 92-96

[58] John C. Gregory, Ganesh N. Raikar, Jon B. Cross, Mark A. Hoffbauer, “Space Processing of Semiconductor Materials with Fast Atomic Oxygen”, *CONF 950110*, American Institute of Physics, 1995, pp. 313-322

[59] Gelbart, D., Karasyuk, V.A., “UV thermoresists: sub-100-nm imaging without proximity effects”, *Emerging Lithographic Techniques III, Proc. SPIE*, Vol. 3676, 1999, pp. 786-793

[60] Glenn Chapman, “Exploration of Inorganic Thermal and Photoablative Photoresist for Overcoming Semiconductor Microfabrication Barriers”, grant application to Advanced Systems Institute, B.C., 1999

[61] G.H. Chapman, M.V. Sarunic, Y. Tu, "A Prototype Laser Activated Bimetallic Thermal Resist for Microfabrication", accepted by SPIE Photonics West, *Laser Applications in Microelectronics and Optoelectronics Applications*, San Josa, CA, January 2001

[62] “International Technology Roadmap for Semiconductors: 1999 Edition”, Semiconductor Industry Association, 1999, Table 72a, http://public.itrs.net/Files/1999_SIA_Roadmap/ESH.pdf (October 15, 2000)

[63] Stephen A. Campbell, “The Science and Engineering of Microelectronic Fabrication”, Oxford University Press, New York, 1996, p. 259

[64] Brett A Peters, Taho Yang, “Integrated Facility Layout and Material Handling System Design in Semiconductor Fabrication Facilities”, *IEEE Transactions on Semiconductor Manufacturing*, Vol. 10, No. 3, August 1997, p. 361

[65] “ISS Mission Modules”, Boeing Space Systems, http://www.boeing.com/defense-space/space/spacestation/mission_modules/first_element_launch.html (October 15, 2000)

[66] H. Bloom, “A Baseline of Logistic and Power Requirements for Full-Scale Manufacturing of Metallic Materials in Earth Orbit”, *The Industrialization of Space*, Vol 36, Part 1, Ed. Richard A. Van Patten, American Astronautical Society, 1977, pp. 277-295

[67] personal email from Bill Bartholet, Associate Technical Fellow - Radiation Effects on Electronics, Boeing Phantom Works - Physics Technology, Seattle, Washington , U.S.A., December 4, 2000

[68] Nick Pfeiffer, Glenn H. Chapman, “Silicon Wafer Transport in a High Vacuum, Microgravity Environment”, *Spacebound 2000 Conference Proceedings*, Canadian Space Agency, May 2000

[69] Robert L. Hammel, Donald M. Waltz, “A Road Map to Space Products”, *The Industrialization of Space*, Vol 36, Part 1, Ed. Richard A. Van Patten, American Astronautics Society, 1977, pp. 363-390

[70] Shiaw-Jong Steve Chen, Ilene J. Busch-Vishniac, “A Magnetically Levitated, Automated Contact Analytical Probe Tool”, *IEEE Transactions on Semiconductor Manufacturing*, Vol. 8, No. 1, February 1995, pp. 72-78

[71] Pieter Burggraaf, “Lithography News: Mag-Lev Stage Planned for XLS Stepper”, *Semiconductor International*, April 1995, p. 38

[72] WanjunWang, Margaret Lamb, Ilene J. Busch-Vishniac, “An Automated Loading and Unloading System for Maglev Wafer Transport Path”, *IEEE Transactions on Semiconductor Manufacturing*, Vol. 6., No. 3, August 1993, pp. 276-279

[73] Samuel C. Wood, “Cost and Cycle Time Performance of Fabs Based on Integrated Single-Wafer Processing”, *IEEE Transactions on Semiconductor Manufacturing*, Vol. 10., No. 1, February 1997, pp. 98-111

[74] William H. Hayt, Jr., “Engineering Electromagnetics”, Fourth Edition, McGraw-Hill, New York, 1981, p. 313

[75] David Halliday, Robert Resnick, “Fundamentals of Physics”, Second Edition, John Wiley and Sons, New York, 1981, p. 539

[76] David Halliday, Robert Resnick, “Fundamentals of Physics”, Second Edition, John Wiley and Sons, New York, 1981, p. 576

[77] David Halliday, Robert Resnick, “Fundamentals of Physics”, Second Edition, John Wiley and Sons, New York, 1981, p. 558

[78] David Halliday, Robert Resnick, “Fundamentals of Physics”, Second Edition, John Wiley and Sons, New York, 1981, p. 567

[79] Glenn Harrison Chapman, “Production and Testing of Pico Ohm Resistance Joints Between Superconductors”, Master of Science Thesis, Queen’s University, Kingston, Ontario, 1975, p. 220

[80] Larry K. Forbes, Stuart Crozier, David M. Doddrell, “Rapid Computation of Static Fields Produced by Thick Circular Solenoids”, *IEEE Transactions on Magnetics*, Vol. 33, No. 5, September 1997, pp. 4405-4410

[81] A. Kip, “Fundamentals of Magnetism”, 2nd Ed., McGraw-Hill, New York, 1969, pp. 325-372

[82] David Halliday, Robert Resnick, "Fundamentals of Physics", Second Edition, John Wiley and Sons, New York, 1981, p. 558

[83] William H. Hayt, Jr., "Engineering Electromagnetics", Fourth Edition, McGraw-Hill, New York, 1981, p. 509

[84] Ferdinand P. Beer, E. Russell Johnston, Jr., "Vector Mechanics for Engineers: Statics and Dynamics", Fourth Edition, McGraw-Hill, New York, 1984, p. 64

[85] David Halliday, Robert Resnick, "Fundamentals of Physics", Second Edition, John Wiley and Sons, New York, 1981, p. 62

[86] J.H. Yi, K.H. Park, S.H. Kim, Y.K. Kwak, M. Abdelfatah, I. Busch-Vishniac, "Force Control for Magnetic Levitation System Using Flux Density Measurement", *Proceedings of the 34th IEEE Conference on Decision and Control*, Vol. 3, New Orleans, 1995, pp. 2153-2158

[87] Ingolf Groning, Stefan Butz, Gerhard Henneberger, "Design of a microcontroller-based state control for a magnetic levitation transport system", *IECON '98, Proceedings of the 24th Annual Conference of the IEEE Industrial Electronics Society*, Aachen, Germany, 1998, pp. 1657-1662

[88] S.W. Park, M.A. Brdys, "Identification and Control of Jumping Ring System Using Dynamic Neural Networks", *1998 IEEE International Conference on Neural Networks Proceedings*, IEEE World Congress on Computational Intelligence, Vol 2., Anchorage, Alaska, USA, 1998, pp. 958-962

[89] Yoshio Kawamura, Tatsuharu Yamamoto, Natsuki Yokoyama, Yoshifumi Mawamoto, "A Wafer-Handling Interface Under Processing Ambient Conditions for a Single-Wafer Cluster Tool", *IEEE Transactions of Semiconductor Manufacturing*, Vol. 11, No. 1, February 1998, pp. 13-19

[90] Charles E. Bryson, III, "The Problem of the 'Easy' Vacuum Specification", *Semiconductor International*, August 1994, pp. 90-92

[91] R. DeJule, "Vacuum Pump Designs to Meet Process Requirements", *Semiconductor International*, October 1996, pp. 125-133

[92] Don Fried, Philip Lessard, "Improve Your Sputter Process by Better Water Vapor Pumping", *Semiconductor International*, August 1994, p. 95

[93] Peter Singer, "New Advances in Turbomolecular Pumps", *Semiconductor International*, October 1994, pp. 77-80

[94] Peter Singer, "Vacuum Pumping in Etch and CVD", *Semiconductor International*, September 1995, p. 74

[95] Hablanian, "Design and Performance of Turbine-type High-vacuum Pumps", *Semiconductor International*, June 1995, pp. 177-184

[96] "Vacuum Technology: Its Foundations, Formulae and Tables", Product and Vacuum Technology Reference Book, Leybold-Heraeus Inc., San Jose, CA, p. 39

[97] "Vacuum Technology: Its Foundations, Formulae and Tables", Product and Vacuum Technology Reference Book, Leybold-Heraeus Inc. San Jose, CA, p. 40

[98] "Vacuum Technology: Its Foundations, Formulae and Tables", Product and Vacuum Technology Reference Book, Leybold-Heraeus Inc. San Jose, CA, p. 44

[99] David Halliday, Robert Resnick, "Fundamentals of Physics", Second Edition, John Wiley and Sons, New York, 1981, p. 375

[100] Christopher Pilcher, "Standard CMOS Process", http://www.iue.tuwien.ac.at/diss/pichler/diss/node150.html (April 5, 2000)

[101] Robert C. Leachman, David A. Hodges, "Benchmarking Semiconductor Manufacturing", *IEEE Transactions on Semiconductor Manufacturing*, Vol. 9, No. 2, May 1996, pp. 158-169

[102] "International Technology Roadmap for Semiconductors: 1999 Edition", Semiconductor Industry Association, 1999, Table 70a, http://public.itrs.net/Files/1999_SIA_Roadmap/ESH.pdf (October 15, 2000)

[103] P.H. Singer, "Trends in Wafer Cleaning", *Semiconductor International*, December 1992, p. 37

[104] H. Wakamatsu, "Introduction of Ultra Pure Water Close System into Semiconductor Plant", *Oki Technical Review 160*, Vol. 63, January 1998, p. 45

[105] Peter Burggraaf, "Coping with the High Cost of Wafer Fabs", *Semiconductor International*, March 1995, pp. 45-50

[106] D. Lammers, "Contenders crowd lithography arena", *EETimes*, December 06, 1999, Issue: 1090, http://www.techweb.com/se/directlink.cgi?EET19991206S0003 (October 15, 2000)

[107] D. Gelbart, V. A. Karasyuk, "UV thermoresists: sub-100-nm imaging without proximity effects", *Proceedings SPIE Emerging Lithographic Technologies III*, v 3676, 1999, pp. 786-793

[108] S.W. Pang, "Aluminum oxides as imaging materials for 193 nm excimer laser lithography", *Journal of Vacuum Science Technology*, B 7 (6), Nov/Dec 1989, American Vacuum Society, pp. 1624-1627

[109] D.L. Dance, D.W. Jimenez, "Application of Cost-of-Ownership", *Semiconductor International*, September 1994, p. 6-7

[110] Pieter Burggraaf, "Applying Cost Modeling to Stepper Lithography", *Semiconductor International*, February 1994, pp. 41-44

[111] Werner Rust, Mike Lodoen, "Cost-of-Ownership: Use and Misuse", *Semiconductor International*, November 1995, p. 110

[112] Ruth DeJule, "Next-Generation Lithography Tools: The Choices Narrow", *Semiconductor International*, March 1999, http://209.67.253.149/semiconductor/issues/issues/1999/mar99/docs/feature1.asp, (October 15, 2000)

[113] "Solar Array System Trades - Present and Future", AIAA Conference, January 1999, personal email from Tom Kessler, Solar Orbit Transfer Vehicle Program, Boeing Phantom Works, Seal Beach, California, U.S.A., June 28, 2000

[114] Donald A. Hicks, "Evolving Complexity and Cost Dynamics in the Semiconductor Industry", *IEEE Transactions on Semiconductor Manufacturing*, Vol. 9, No. 3, August 1996, p. 294

[115] Hans ten Cate, Charles Murphy, "Space Transportation and the Global Space Commerce Market: Issues and Indicators", *AIAA Defense and Civil Space Programs Conference*, October 28, 1998, p. 14

[116] "LEO Commercial Market Projections", Office of the Associate Administrator for Commercial Space Transportation, Federal Aviation Administration, U.S. Department of Transportation, July 25, 1997

[117] Donald D. Smith, submission to Western Commercial Launch Strategy to Committee on Science, U.S. House of Representatives, June 12, 1996, http://143.231.86.196/science/dsmith.htm, (October 15, 2000)

[118] Journey Air Freight International Inc., Dorval, PQ, Canada, quotation to Technocarb Equipment Ltd., Abbotsford, B.C., Canada for air freight from Italy to Canada, April 17, 2000

[119] "Four Case Studies of High-Tech Water Exploitation and Corporate Welfare in the Southwest" describing water use at Intel plant in New Mexico, www.igc.apc.org/svtc/execsum.htm (October 28, 2000)

[120] London Metal Exchange, May 26, 2000

[121] Ron Wilson, Brian Fuller, "Hidden mask costs roil fine-geometry ASIC's", *EETimes*, Issue: 1054, March 29, 1999, http://www.techweb.com/se/directlink.cgi?EET19990329S0003, (October 28, 2000)

[122] John Kanz, Danny Lam, "Wafer Fab Profit Opportunities and Costs: Looking outside the box at facilities lifecycle cost-of-ownership", *Semiconductor International* July 1998, http://www.semiconductor.net/semiconductor/issues/Issues/1998/jul98 /docs/feature3.asp, (October 5/00)

[123] "International Technology Roadmap for Semiconductors: 1997 Edition" Semiconductor Industry Association, 1997, p 114

[124] "Goals and Objectives: Advanced Space Transportation", NASA, http://www.aero-space.nasa.gov/goals/sp.htm, (October 8/00)

[125] Daniel S. Goldin, "NASA Administrator Daniel S. Goldin's remarks in his keynote address at the Space Frontier Foundation's conference", *Space Frontier Conference VIII - Launching the Space Millennium*, http://space-frontier.org/MEDIA_ROOM/OtherVoices/1999/19990924-goldin.html, (October 15, 2000)

[126] "International Technology Roadmap for Semiconductors: 1999 Edition", Semiconductor Industry Association, 1999, p. 7, http://public.itrs.net/Files/1999_SIA_Roadmap/ORTC.pdf (October 15, 2000)

[127] Hans ten Cate, Charles Murphy, “Space Transportation and the Global Space Commerce Market: Issues and Indicators”, *AIAA Defense and Civil Space Programs Conference*, October 28, 1998, p. 5

[128] Hans ten Cate, Charles Murphy, “Space Transportation and the Global Space Commerce Market: Issues and Indicators”, *AIAA Defense and Civil Space Programs Conference*, October 28, 1998, p. 7

[129] “Satellite Networks”, http://www.ethoseurope.org/ethos/Techterm.nsf/All/SATELLITE+NETWORKS, (September 2, 2000)

[130] Hans ten Cate, Charles Murphy, “Space Transportation and the Global Space Commerce Market: Issues and Indicators”, *AIAA Defense and Civil Space Programs Conference*, October 28, 1998, p. 14

[131] “1998 Worldwide Space Launches”, NASA, http://www.hq.nasa.gov/osf/1998/launch98.html, (September 2, 2000)

[132] Hans ten Cate, Charles Murphy, “Space Transportation and the Global Space Commerce Market: Issues and Indicators”, *AIAA Defense and Civil Space Programs Conference*, October 28, 1998, p. 21

[133] Tim Beardsley, “The Way to Go in Space”, *Scientific American*, 1999, http://www.sciam.com/1999/0299issue/0299beardsley.html, (October 28, 2000)

[134] Gerard K. O’Neill, Henry H. Kolm, “Mass Driver for Lunar Transport and as Reaction Engine”, *The Industrialization of Space*, Vol 36, Part 1, Ed. Richard A. Van Patten, 1977, pp. 191-208

[135] Hans ten Cate, Charles Murphy, “Space Transportation and the Global Space Commerce Market: Issues and Indicators”, *AIAA Defense and Civil Space Programs Conference*, October 28, 1998, p. 36

[136] “Pegasus Launch Vehicle”, Orbital Sciences Corporation, http://www.orbital.com/LaunchVehicles/Pegasus/pegasus.htm, (September 2, 2000)

[137] Hans ten Cate, Charles Murphy, “Space Transportation and the Global Space Commerce Market: Issues and Indicators”, *AIAA Defense and Civil Space Programs Conference*, October 28, 1998, p. 40

[138] Hans ten Cate, Charles Murphy, “Space Transportation and the Global Space Commerce Market: Issues and Indicators”, *AIAA Defense and Civil Space Programs Conference*, October 28, 1998, p. 37

[139] “Written Statement of Kistler Aerospace Corporation Before the Subcommittee on Space and Aeronautics”, House Committee on Science, October 13, 1999, http://www.house.gov/science/mueller_101399.htm, (October 15, 2000)

[140] “K-1 VEHICLE PAYLOAD USER’S GUIDE”, Kistler Aerospace, Kirkland, Washington, USA, http://www.kistleraerospace.com/payload/index.htm, (September 2, 2000)

[141] Hans ten Cate, Charles Murphy, “Space Transportation and the Global Space Commerce Market: Issues and Indicators”, *AIAA Defense and Civil Space Programs Conference*, October 28, 1998, p. 31

[142] “1998 Worldwide Space Launches”, NASA, http://www.hq.nasa.gov/osf/1998/launch98.html, (September 2, 2000)

[143] “1999 Worldwide Space Launches”, NASA, http://www.hq.nasa.gov/osf/1999/launch99.html, (September 2, 2000)

[144] “2000 Worldwide Space Launches”, NASA, http://www.hq.nasa.gov/osf/2000/launch00.html, (September 2, 2000)

[145] Robert Unger, “Optimize Ion Implantation Through Improved Vacuum Technique”, *Semiconductor International*, March 1996, p. 91

[146] “MTBF and MTTF Calculation”, Relex Software Corporation, http://www.i-mtbf.com (September 16, 2000)

[147] Judy Erkanat, Dylan McGrath , “The Fab Line”, *Electronic News*, July 21, 1997, http://www.electronicnews.com/enews/Issue/1997/07211997/fab072197.asp, (September 16, 2000)

[148] “Ergospeed II Specifications”, INFAB, Inc., http://www.infab.com/1244/content.htm, (September 16, 2000)

[149] “Industry News”, *Micro Magazine*, April 1999, http://www.micromagazine.com/archive/99/04/300mm.html, (September 16, 2000)

[150] Ed Muzio, Phil Seidel, Mark Mason, John Canning, Gil Shelden, "Lithography Cost of Ownership Analysis", Revision Number 4.0, December 1999, International SEMATECH Lithography Co., p. 62, http://www.sematech.org/public/resources/coo/finalr4.pdf, (September 16, 2000)

[151] Charla Griffy-Brown, Karl Knapp, John Humphreys , "The Cape York Spaceport: Lessons in Sustainable Strategic Advantage for Developing Commercial Space Ventures", Center for Technology Management, Griffith University, Queensland, Australia, http://www.gbhap-us.com/fulltext/free/S960040F793.htm, (September 16, 2000)

[152] Jerome Simonoff, "Financing of Space Business", *Heaven and Earth: Civilian Uses of Near-Earth Space*, D. Dallmeyer and K. Tsipis (eds.), Kluwer Academic Publishers, Netherlands, 1997, pp. 69-82

[153] Tony Overfelt, John Watkins, "Programmatic and Economic Challenges for Commercial Space Processing", *CONF 970115*, American Institute of Physics, 1997, pp. 691-696

[154] P. Schwartz, N. Cumming, l. Halvers, R. Sprague, "Business Decision-making for the Commercialization of Space", *Heaven and Earth: Civilian Uses of Near-Earth Space*, D. Dallmeyer and K. Tsipis (eds.), Kluwer Academic Publishers, Netherlands, 1997, pp. 57-67